DE GRUYTER

Li Jianjun, Ou Yuxiang

FLAME RETARDANTS

POLYMER COMBUSTION AND MECHANISMS
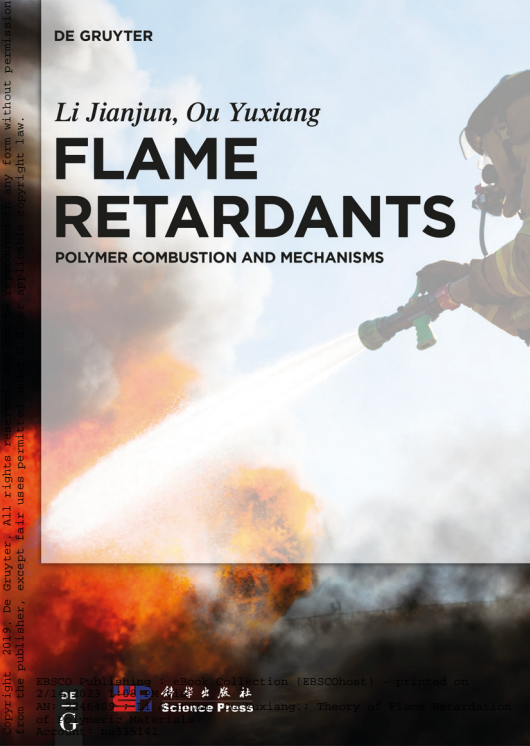
Li Jianjun, Ou Yuxiang
Theory of Flame Retardation of Polymeric Materials

Also of interest

Shape Memory Polymers
Kalita, Hemjyoti, 2018
ISBN 978-3-11-056932-2, e-ISBN 978-3-11-057017-5

Polymer Engineering
Tylkowski, Bartosz; Wieszczycka, Karolina; Jastrzab, Renata, 2017
ISBN 978-3-11-046828-1, e-ISBN 978-3-11-046974-5

Magneto-Active Polymers
Fabrication, characterisation, modelling and simulation at the micro-and macro-scale
Pelteret, Steinmann, 2019
ISBN 978-3-11-041951-1, e-ISBN 978-3-11-041857-6
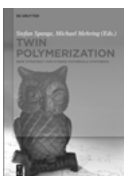
Twin Polymerization
New Strategy for Hybrid Materials Synthesis
Spange, Mehring, 2019
ISBN 978-3-11-050067-7, e-ISBN 978-3-11-049936-0

Nanomaterials in Joining
Charitidis, Constantinos A. (Ed.), 2015
ISBN 978-3-11-033960-4, e-ISBN 978-3-11-033972-7

Li Jianjun, Ou Yuxiang

Theory of Flame Retardation of Polymeric Materials

—

DE GRUYTER   科学出版社

Authors
Dr. Li Jianjun
Kingfa Science & Technology Co., Ltd. (China)
No. 33 Kefeng Road, Science Town
510663, Guangzhou, Guangdong Province
Guandong Bloomachine Co. Ltd. (China)
Sanxia Industry Zone, Heng Li Town
523460, Dongguan, Guangdong Province
China

Prof. Ou Yuxiang
Beijing Institute of Technology
Dept. of Chemical Engineering
100081 Beijing
China

Preface

Flame retardant is one of the basic strategies for disaster prevention and mitigation and also a major initiative in environmental protection and improving the quality of life. Nearly for half a century, scientific experiments and practical experience have shown that the benefits brought forward by flame retardant (in particular in the aspect of ensuring personal safety) to the society cannot be underestimated. Continuously improved safety performance of consumer goods is the due commitment that manufacturers ought to make for consumers and is also a sign of social civilization and progress. For example, the EU has made "fire safety" as one of the six necessary prerequisites for commodity circulation in the markets. In recent years, China has also provided great importance to the application and development of flame retardant technology and issued a number of regulations on flame retardant enforced by the country, such as "Combustion Performance Requirements and Signs for Flame Retardant Materials and Components in Public Places" (GB20286-2006), and so on. Currently, the severe fire disaster situation, strict flame retardant and environmental protection regulations have also promoted the sustainable development of flame-retardant science.

For nearly 50 years, the research and development, production and application of flame-retardant materials in China have drawn attention from the relevant international counterparts. In terms of the annual average growth rate of production capacity, flame-retardant materials have been far ahead in four global markets of the same. In terms of total production capacity of flame retardants, in 2008, Chinese global market share has accounted for 10%. However, flame-retardant industry is still facing very urgent and arduous tasks in the aspects of transformation of economic development mode and updating products species. Nowadays, with the growth of environmental requirements, the development direction of flame retardants and flame retardant materials should be transferred from mainly halogen-oriented family to (low) nontoxic, low-smoke, low or high polymerization directions. Therefore, new designs of new green molecular structures and new material formulations are required. Workmanship in production processes needs to be adjusted and more in-depth studies of flame-retardant mechanism are also required. These aspects require certain theoretical guide and references which is the first purpose of compiling the book.

Second, for more than 10 years, the authors and their team have published 12 translations and over 300 papers on flame retardant. In addition, most of the academic colleagues of the authors have published valuable and prospective books. Moreover, numerous domestic journals about flame retardant have been published. The above works covered flame-retardant mechanism but scattered in various materials. In the beginning of 21st century, academic books and papers in the field of international flame retardant were published one after another. During 2003–2011, Dr. Weil, New York Polytechnic University, and Dr. Levchik, Supresta LLC – IP from the United States, coauthored at least 12 comprehensive, systematic,

and forward-looking feature reviews, covering the flame-retardant polyolefin, flame-retardant polystyrene (PS) and high impact polystyrene(HIPS), flame-retardant polyamide(PA), flame-retardant thermoplastic polyester, flame-retardant polycarbonate(PC), flame-retardant polyurethane(PU), flame-retardant unsaturated polyester, flame-retardant epoxy resin, smoke suppression of Polyvinyl chloride(PVC), flame-retardant textiles and flame-retardant coatings, and other important aspects. As for books on flame retardant, five English books were published from 2009 to 2011, namely, Hall and Kandola, editors of *Retardancy of Polymetric Materials* (2010); Wilkie and Morgan, editors of the *Fire Retardancy of Polymetric Materials* (2010); Weil and Levchik, editors of *Flame Retardants for Plastics and Textiles* (2009); Merlani, editor of *Flame Retardants: Functions, Properties and Safety* (2010); and Mittal, editor of *Thermally Stable and Flame Retardant Polymer Nanocomposites* (2011). To understand the state of the art and the prospect of production, research and development of global flame retardants and flame-retardant materials, these works have not only provided informative information for researchers in the area of flame retardant but also contained world-famous scholars' recent contributions for the theory of flame retardant. These novel theories are also distributed in various books. Many literatures have provided innovative and abundant information to the authors, whether within the country or abroad. Thus, it has been possible for the authors to systematically organize and deepen the materials, with their experience, in the process of scientific research, teaching, research and development, production and application, and to share with colleagues benefit the readers.

Third, so far, there are few comprehensive and systematic books about the flame retardancy theory both in China and the rest of the word. When the authors exchanged experience with R&D staff, production technicians and academic researchers on the research and production, as well as writing papers, they all thought that the flame-retardant theory is very helpful in terms of opening their thoughts for R&D, improving production processes and the quality of the papers. So, the authors were preparing to write this book for years, which may be beneficial to many aspects mentioned above and may fill a vacancy of numerous publications on flame retardant from both home and abroad as well.

The book has adopted the latest data and materials to complete a comprehensive content. Characterized by a certain depth in the theory and a relative high starting point, the book is also clear and concise as well. Hopefully, it can cater for people with different tastes and provide readers guide and references on flame-retardant reaction processes study, designed by molecular structures and formulations of flame-retardant materials.

On the occasion of publishing this book, first, the authors would like to thank all the authors who provided detailed referential literatures to help finish the book, without whom, the book would not have been finished. Special thanks also go to a number of doctoral students of Ou Yuxiang, whose research findings enriched this book. The authors also thank Science Press for its great kindness and help,

especially the executive editor and associated personnel who worked with them to publish the book smoothly through harmonious and close cooperation. Finally, sincere thanks are extended to Dr. Ye Nanbiao, Dr. Li Wenda, Dr. Tang Lei, Dr. Peng Li and Dr. Su Yujun of Kingfa Sci. and Tech. Co., Ltd. for their valuable help, which undoubtedly improved the quality of this book.

The authors spent several years to compose the book, several times revised and updated the manuscripts and reviewed the book repeatedly. In particular, the authors constantly supplemented new materials to enrich and update the contents and tried to minimize mistakes as well. But due to the limitations of the authors' academic levels and time, the flaws and omissions in the book are inevitable. So, we welcome criticisms and suggestions from readers.

<div align="right">

Li Jianjun, Ou Yuxiang
March, 2018, Guangzhou, China

</div>

Contents

About the Authors

Born in Pengxi County, Sichuan Province, in April, 1963, **Li Jianjun** graduated from Beijing Institute of Technology (BIT) and received his Ph.D. degree in engineering in 1995. As a researcher, he enjoys the State Council's special allowance. He was the Representative of Thirteenth Guangzhou Municipal People's Congress, the Vice Chairman, General Manager of Kingfa Scientific and Technological Co., Ltd. He has successive granted titles including "Model Worker of Guangdong Province," "Guangdong Provincial Labor Medal" and "The Labor Model of Guangzhou," and so on and also won two Second National Science and Technology Progress Prizes and various awards for inventions and patents of Science and Technology Progress Award in Guangzhou, Guangdong Province. He was the council member of the of "Chinese Engineering Science;" the editorial board member of magazine "Plastic," Vice Chairman of China Association for Promotion of Private Sci-Tech Enterprises; the incumbent Vice President of China Plastics Processing Industry Association; Chairman of Multifunctional Master Batch Professional Committee; member of the National Technical Committee for Standardization of Plastics; Executive Deputy Director of Modified Plastics Sub-Technical Committee of the National Technical Committee for Standardization; and adjunct professor of Beijing Institute of Technology, Sun Yat-sen University, Southwest University of Science and Technology. He has written and translated six books including *The Plastics of Flame Retardancy of Styrene Plastics, Flame-Retardant Performance Manufacturing and Application, The Test Methods of the Performance of Flame Retardance of Materials, Flame-Retardant Plastics Handbook, The Nanocomposites of Flame Retardant Polymers* and *Plastics Additives Handbook*. What's more, he has published 28 academic papers.

Born in February 1936 in Ji'an, Jiangxi Province, **Ou Yuxiang** graduated from Department of Chemical Engineering of Beijing Industrial Institute (BIT) in 1959. He engaged in physical organic chemistry research in both Britain and the United States during 1979–1982. He was the former Chief Professor of Ph.D. programs of Materials Science of Beijing Institute of Technology, the Chairman of Institute of Flame Retardant of China, and a famous expert in the areas of energetic materials and fire-retardant materials. He has long been committed to the researches of energetic materials and flame-retardant materials and published more than 20 books and over 300 papers, collected the parts of energetic materials and fire-retardant materials in various large-scale encyclopedias and dictionaries and edited relevant proceedings of international conference 7 times. His representative works include *Practical Flame Retardant Technology, Polymer Materials of Flame Retardant, The Test Methods of the Performance of Flame Retardance of Materials, Flame Retardant*, and so on. He was the first inventor to hold the first position in the Progress Award of National Defense Science and Technology, Petrochemical Industry Excellent Book Award and other awards and obtained seven National Invention Patents. As a doctoral tutor, he has polished nearly 30 doctoral students. Since 1992, he has enjoyed special government allowance. He was recommended twice as the effective candidate of The Chinese Academy of Engineering in 2003 and 2005. In 2001, he was also included into the *World's Outstanding Scientists List* by the International Biographical Centre. In June 2007, *China Chemical Industry News* published a special report for his outstanding contribution to Chinese flame-retardant science and technology under the title "The Founder of Chinese Flame Retardant Science."

1 Polymer combustion

Generally speaking, the combustion process of polymers can be divided into five stages (Figure 1.1) [1] in time, which includes thermal decomposition, ignition, propagation, stable combustion and combustion attenuation. At the same time, these five stages can also be separated in space, such as surface-heating area, condensed phase transformation area (decomposition, crosslinking, carbonization) and vapor-phase combustible combustion area. Figure 1.2 shows the unit model of polymer combustion [2].

Due to their characteristics, there will be some special thermal behaviors of polymer during the heating procedure, such as glass transitions, softening, melting, expansion, foaming, shrinkage, etc [3].

In this chapter, we will not only explain the five stages of polymer combustion but also analyze the smoke, toxic and corrosive products produced during the combustion procedure to provide some theoretical foundations for the discussion of the flame-retardation mechanisms of polymers.

1.1 Thermal decomposition

1.1.1 Overview

When the thermoplastics were heated, evaporation and pyrolysis of the solid phase were considered to be confined to a thin layer, namely condensed-phase/vapor-phase interface. Generally, when the polymer is heated, it will be first thermally degraded into pieces or monomers or fragments with low-molecular weight, and the escape rate of the latter is concerned with the mass transfer process [4, 5].

The thermal decomposition of polymers is the first step for the cause and development of combustion, and it is very important for estimating the reaction of materials to fire, synthetizing heat-resistant polymer and recycling waste polymer.

When an external heat source is put on the material, the material temperature gradually rises. An external heat source may be produced directly from the flame (by radiation and convective heat transfer), the hot vapor (by conduction and convection heat transfer) and the hot solid material (by heat conduction). When heated, heating rate of material not only depends on external heat flow rate and temperature difference but also is related to specific heat capacity, thermal conductivity and carbonization, evaporation and other changing latent heat of the material.

Under the intense radiation near the hot objects, the surface of polymer will be heated rapidly, and its temperature rises with the square root of thermal radiation time. Taking polyethylene (PE) as an example, when the radiation intensity is
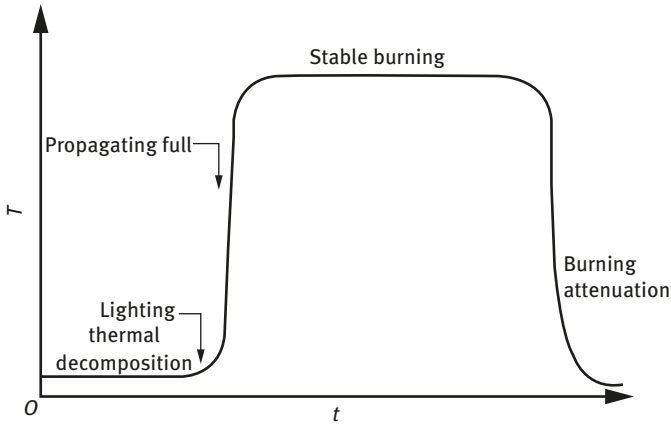
Figure 1.1: Five stages of polymer combustion [1].
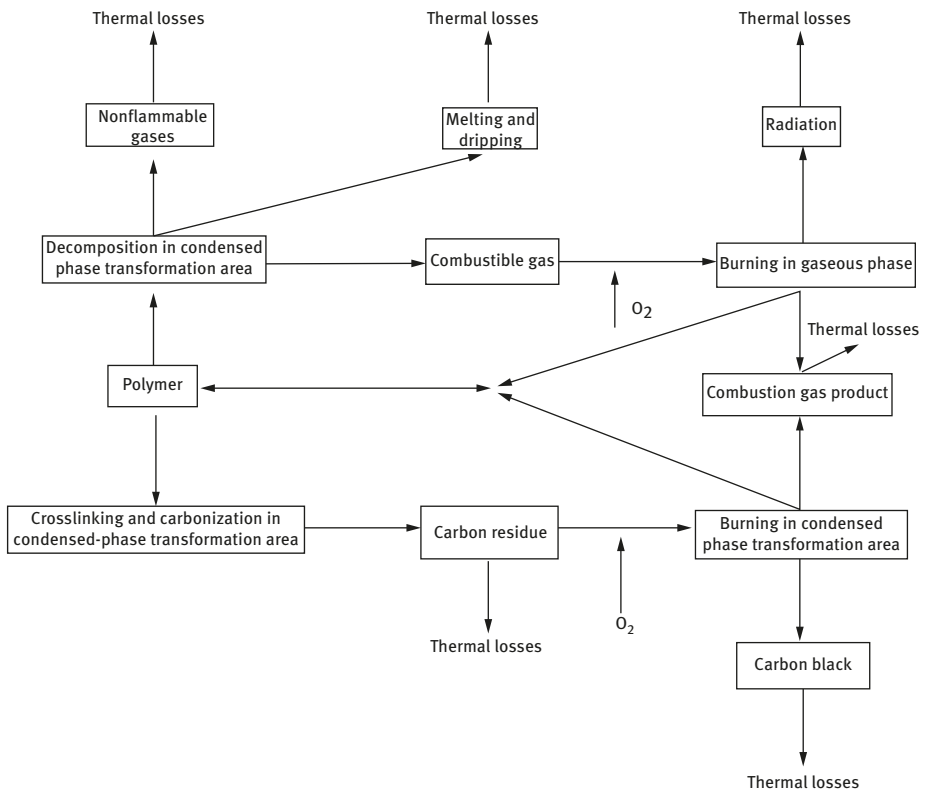
Figure 1.2: Unit model of polymer combustion [2].
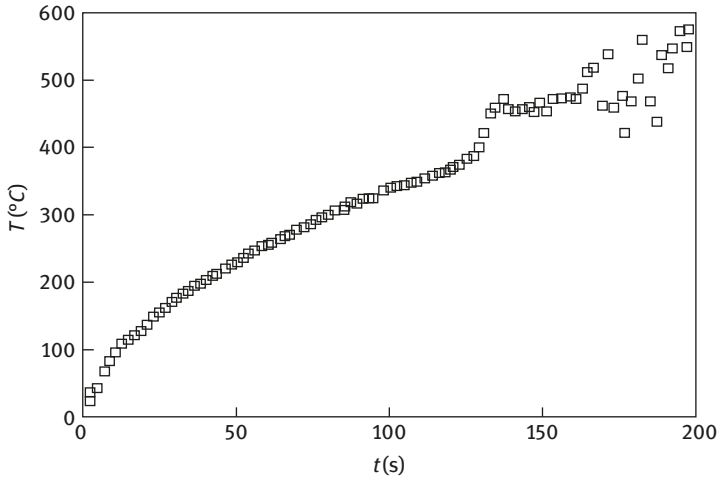
Figure 1.3: Relationship between polyethylene surface temperature and time [6] under a radiation intensity of 36 kW/M^2.

36 kW/M^2 (which is equal to the blackbody temperature of 613 °C), its surface temperature rising based on time is shown in Figure 1.3 [6].

If the radiation intensity is low, the highest surface temperature of polymer would not be enough to ignite polymer, as well as would have low thermal diffusivity and thin thermal layer. Thus, polymer is difficult to be ignited (the ignition temperature of polymethyl methacrylate [PMMA] is 250–350 °C, whereas that of PE is 330–370 °C), and only thermal decomposition will occur [7].

When the temperature of polymer rises up to a certain level, it begins to degrade, and the initial temperature of degradation is usually the temperature of bond rupture that has the worst thermal stability. During this period, polymer could still be intact, but the weakest bond ruptures often change the color and luster of polymers. There are two forms of degradation: nonoxide degradation and oxidative degradation. The former occurs without oxygen, whereas the latter should be heated and degraded with oxygen. Proportion of the most volatile decomposition temperature of the bonds and the instability of bonds in polymer are closely related to the degradation of polymer.

When most bonds rupture due to polymer decomposition, it enables a long chain of 10^4–10^5 carbon atoms to be decomposed into low molecular product. Then, the molecular weight of polymer gets smaller dramatically, polymer itself also begins to change, and this change can lead to a complete loss on its physical integrity or generate new substance with different properties, most of which are compounds with low molecular weight and many of these compound are inflammable materials, which can also volatilize into the vapor phase, thus reducing the total weight of polymer. For example, when thermal decomposition occurs, polyformaldehyde (POM) or PMMA can be decomposed into monomer formaldehyde or methyl methacrylate, respectively.

Only when the weakest bond fracture temperature is much lower than the decomposition temperature of the most bonds in polymer, the processes of degradation and decomposition can be separated. When the decomposition temperature of various bonds of polymer is almost continuous, the two processes become one.

The following characteristics of polymer have important influences on its decomposition: First is the initial decomposition temperature of the chemical bonds, namely the lowest temperature when decomposing. For two polymers with the same specific heat and thermal conductivity, when their surfaces are under intense heat, their decomposition degrees, to a great extent, are related to the initial decomposition temperature. Second, the latent heat of decomposition of each chemical bond (i.e., decomposition heat) is either endothermic or exothermic when decomposed. Obviously, heat releasing can aggravate decomposition, and heat absorption can inhibit decomposition. Third, decomposition model includes the physical state and performance of the products formed by decomposition, the relative content of various products and their phases.

1.1.2 The thermal decomposition temperature and thermal decomposition rate

When we measure the decomposition temperature of polymer under laboratory conditions, the most common is to measure the decomposition temperature range or a specific decomposition temperature (such as the temperature when weight loss is 5%, 10% and 15%). Some decomposition temperature ranges of polymer are shown in Table 1.1 [4, 5]. In addition to high-temperature-resistant polymer

Table 1.1: Some polymer decomposition temperature range (T_d) (°C) [4, 5].

Polymers	T_d (°C)	Polymers	T_d (°C)
PE	335–450	PET	283–306
PP	328–410	PC	420–620
PIB	288–425	PX	420–465
PVC	200–300	LCP	560–567
PVDC	225–275	PA6 and PA66	310–380
PVAL	213–325	POM	222
PVA	250	PTFE	508–538
PVB	300–325	PVF	372–480
PS	285–440	PVDF	400–475
SBP	327–430	CTFE	347–418
PMMA	170–300	CTA	250–310
SAR	250–280	POE	324–363
		POP	270–355

(such as Polytetrafluoroethylene (PTFE)), common polymers' decomposition temperature is between 250 °C and 400 °C.

The thermal decomposition rate of polymer can be expressed by the weight loss rate. Table 1.2 lists the temperature ($T_{50\%}$) when some polymers can lose 50% of its weight due to heat in a vacuum condition for 30 min and the weight loss rate of $m_{350\,°C}$ when temperature is 350 °C [8]. Figure 1.4 is the thermal decomposition temperature curve of some polymers [8], that is, the relation curve of sample weight loss rate and temperature. The slope of this kind of curve is related to the polymer pyrolysis reaction mode. The polymers decomposed from stochastic (random) chain fracture and chain depolymerization (as shown in 1.1.3) have a large thermal decomposition temperature-curve slope. If it is in the process of thermal decomposition, there are cyclization, crosslinking, char formation, etc., the curve slope is small and plateau phase part occurs in the late thermal decomposition (high temperature).

Table 1.2: Thermal weight loss data of some polymers [8].

Polymers	$T_{50\%}$ (°C)	$m_{350°C}$ (%/min)	Polymers	$T_{50\%}$ (°C)	$m_{350°C}$ (%/min)
PTFE	509	2×10^{-5}	PS	320	0.24
PX	432	2×10^{-3}	POP (stereoregular)	313	20
PCTFE	412	1.7×10^{-2}	POP (atactic)	295	5
PBD	407	2.2×10^{-2}	PMS	286	–
PE (branching)	404	8×10^{-3}	PVAL	269	–
PP	387	6.9×10^{-2}	PVA	268	–
PMA	328	10	PVC	260	
PMMA	327	5.2			
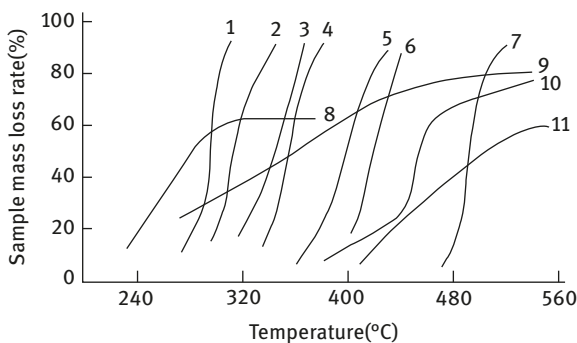
Figure 1.4: Thermal decomposition temperature curve of some polymer. (1) PMS, (2) PMMA, (3) PIB (polyisobutene), (4) PS, (5) PB, (6) PE, (7) PTFE, (8) PVF, (9) PAN, (10) PVDC, (11) third poly vinyl benzene [8].

The degradation of polymers can be divided into primary, secondary and tertiary reaction. Primary reaction refers to the primary decomposition of the original polymer, the formation of volatile products of low molecular weight and intermediates. It is only related to heat transfer, and the secondary and tertiary reactions refer to the crosslinking and repolymerization of primary reaction products, which are also influenced by the heat and mass transfer.

1.1.3 Thermal decomposition modes

Thermal decomposition modes of polymers have several kinds of classification methods. The specific patterns are related to polymer properties and heating conditions.

According to thermal decomposition modes, thermal decomposition of polymer can be divided into kinetics mode, surface degradation and heat or mass transfer control mode.

For thermoplastic polymers and carbonizable polymers, when the sample size is small and heating condition is moderate (such as low heating temperature and rate), its decomposition often happens in kinetics mode. For thermoplastic polymers with a thick layer, if the heat-transfer condition of condensed-phase/vapor-phase interface does not change, the degradation of polymers can be conducted under quasi-steady conditions. When external heating conditions are gradually strengthened, thickness of solid-phase reaction zone is reduced, and the decompose mechanism of the internal heat transfer will be dominant. But carbonizable polymers cannot be carried out under constant conditions, because the char layer severely interferes mass transfer and heat transfer. With the degradation, the propagation rate of solid polymer reaction front is reduced, and the internal and external heat transfer becomes very important [3, 9, 10].

In terms of the way of chain cracking, thermal decomposition of polymer can be divided into random cracking, chain-end cracking, zipper cracking, chain-eliminating cracking, cyclization, carbon, etc. The following sections state the thermal decomposition of polymer in detail according to the classification.

Random cracking
This chain breaking always occurs in weak bond places and also in other places as well. In the process, polymer molecular weight decreases, but the total weight of polymer remains almost constant. When the main chain fractures, it generates a large number of low molecular volatile fuels (monomers and oligomer), as a result, the total weight of polymer falls rapidly. Some polyolefin (such as PP, PE) and polyester (PET) random chain scission would take place [3, 10].

Random chain scission involves C–C bond rupture on the polymer main chain, forming two free radicals. One is primary free radical and the other is secondary or tertiary free radical. Primary free radical will extract a hydrogen atom from the neighboring position to form a more stable secondary or tertiary free radical with the latter conducting further degradation.

All C atoms in polyolefin (such as PE and PP) connect with H atoms; thus, the random chain rupture is probably the main degradation model. Degradation products at the same time include monomers and oligomer. Random chain rupture of thermal cracking of PE is shown in eq. (1.1) [10], including depolymerization, intramolecular hydrogen transfer, β-fracture, etc. Thermal decomposition of PP is more complex than that of PE.

(1.1)
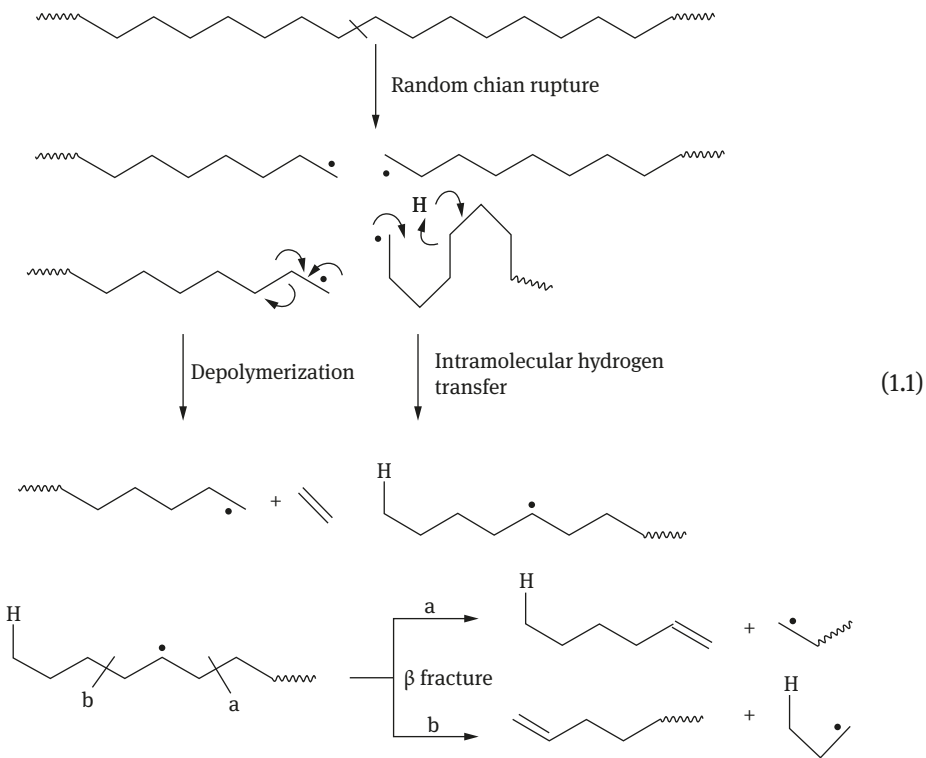
Zipper cracking and chain-end scission

When the hydrogen transfer is restricted, polymers cannot not easily generate random cracking, but generate cracking in the polymer chain end or weak bond, which removes monomer links from the chain one by one, forming volatile products of low molecular weight monomers which evaporates quickly, thus causing a significant reduction in the polymer's molecular weight and total weight [3, 10].

PMMA with methyl and carboxyl, polymetharylonitrile (PMAN) with cyano and methyl, and polymethylstyrene with phenyl and methyl are prone to have this type of cracking and generate a large number of monomers.

Taking PMAN as an example, it has two substituents on C atom, so the chain-end cracking will occur, thus forming a large number of monomers (while generating few monomer quantities in the process of polyacrylonitrile (PAN) thermal decomposition due to crosslinking), and generate different kinds of volatile products, such as hydrogen cyanide, propylene, butene, acetonitrile, acrylonitrile, etc. But amount of monomer generated by PMAN thermal degradation decreases with the increasing temperature, and the number of hydrogen cyanide also increases, which means that hydrogen cyanide may belong to the secondary degradation products.

In addition, when thermal decomposition of polystyrene (PS) happens, zipper cracking is a very important process and can be expressed by eq. (1.2), that is to create carbon free radicals at the first step and then to fracture through C–C key fracture of β to generate styrene monomers.

$$(1.2)$$
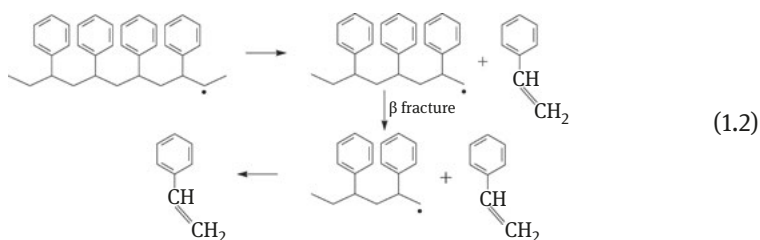
Still, PA6 and PA66 are heterochain polymers; for example, when conducting zipper cracking, PA6 generates caprone monomers (eq. (1.3)) [10].

$$(1.3)$$
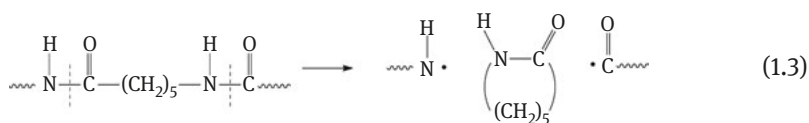
One of the differences among random cracking, chain-end cracking and zipper cracking is the products; products of the former are monomers and oligomers, while the latter are monomers only.

Chain-eliminating cracking
This is a kind of rupture reaction on side radical of chain, and the side-chain eliminating generates small molecular products (not monomers). With the implementation of elimination reaction, the main chain ruptures finally, the molecular weight and the total weight of polymer drop quickly. Thermal decomposition of polyvinyl

chloride (PVC) (HCl), polyvinyl alcohol (PVA) (dehydration), and poly (methyl *tert*-butyl acrylate and methacrylic) belongs to elimination reaction.

For example, the most famous PVC HCl reaction can be shown by eq. (1.4) [10]; it is the auto-accelerated reaction [11], and the generated conjugated dienes can have further cyclization and aromatization.

$$\tag{1.4}$$
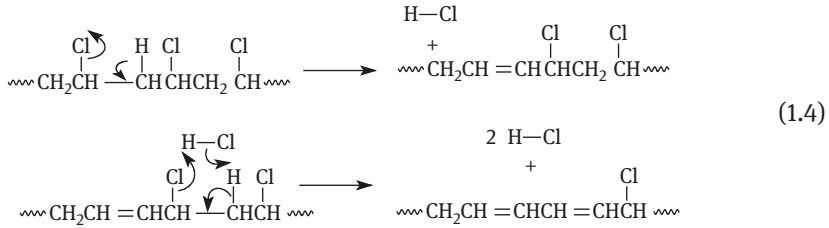
Cyclization reaction

Cyclization in the process of polymer thermal decomposition which means that linear polymer transfers into a ladder polymer. A well-known example is PAN cyclization thermal decomposition shown in eq. (1.5) [12].

$$\tag{1.5}$$
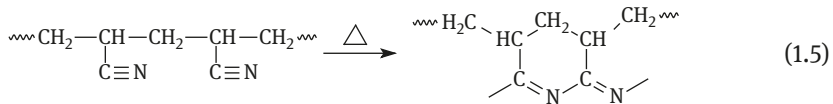
It is a secondary reaction, which decomposes primary products by heat, such as Diels–Alder cyclization reaction which conjugates double-bond compound formed by HCl, see eq. (1.6) [10].

$$\tag{1.6}$$
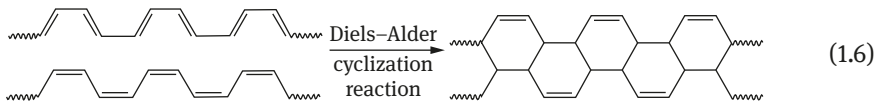
Crosslinking reaction (crossing–linking)

When polymer thermal decomposition occurs, macromolecular structures will connect, forming a network and bulk structure. Reaction (1.7) represents the crosslinked polyolefin thermal decomposition products of PVC [3].

$$(1.7)$$

Cyclization and crosslinking promotes the formation of char and is helpful for the smoke suppression and flame retardancy.

1.1.4 The complexity of thermal decomposition

Thermal decomposition of polymer is a very complex process. Sometimes, several thermal decomposition modes will exist. Therefore, it is difficult to describe the thermal decomposition of all aspects by a single mode. For example, thermal decomposition mechanism of PVC was proposed following several modes, but some conclusions and ideas are still under the research, discussion and debates [13].

Molecular mechanism

The auto-accelerated PVC decomposition due to the reaction of PVC structural unit and HCl is shown in eq. (1.8).

$$(1.8)$$

But this mechanism does not include the formation of free radicals or polymer groups. Therefore, it does not involve the chain transfer. It cannot explain the formation of polynoid during the chain transfer reaction [13].

Mechanism of Amer–Shapiro

Amer and Shapiro proposed three steps of thermal decomposition mechanism of PVC. The first step is the reaction of free radical (a) or 1,2-bimolecular elimination and (b) formation of *cis* double bonds. See reaction (1.9).

$$(1.9)$$
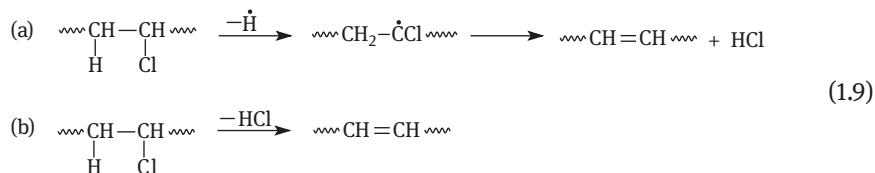
The second and third step is the so-called six-molecular synergistic mechanism, which will eliminate the HCl. See eq. (1.10)

$$(1.10)$$
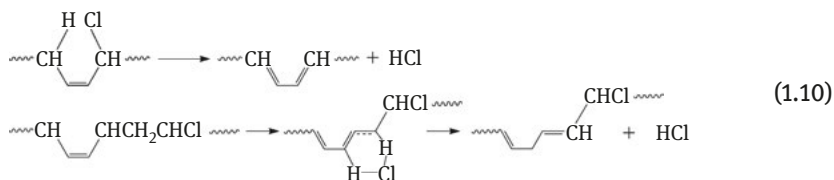
Free radical mechanism

Winker has proposed the thermal decomposition of PVC as follows [15] (see eq. (1.11)):

$$(1.11)$$
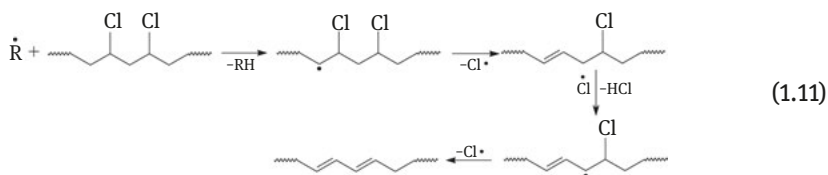
It is considered that [16] the free radical mechanism of thermal decomposition of PVC can explain the process of chain transfer, and this process can lead to auto-acceleration of thermal decomposition.

The mechanism of ion

Ion-pair mode

Equation (1.12) can express the PVC thermal decomposition mechanism of ion pairs, which is proposed by Starnes [16]:

$$\text{∿CH}=\text{CH}-\text{CHCl}-\text{CH}_2\text{∿} \;\; \rightleftharpoons \;\; \text{∿CH}=\text{CH}-\overset{\oplus}{\underset{}{\text{CH}}}\overset{\text{Cl}^{\ominus}}{}-\text{CH}_2\text{∿} \;\xrightarrow{-\text{HCl}}\; \text{∿(CH}=\text{CH})_2\text{∿} \qquad (1.12)$$
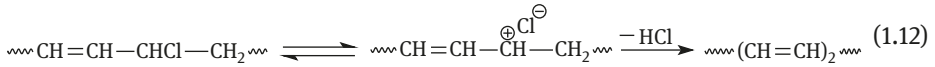
Ion pair forms on α-site of double bonds, thus causing conjugated chain growth.

Quasi-ion mode

It can be expressed by eq. (1.13) [17]:

$$\qquad (1.13)$$
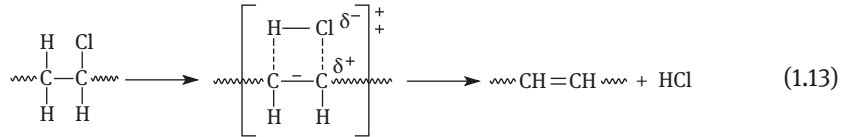
According to the quasi-ion mode, removing HCl from PVC is a process of catalyzing or synergism by the ion pair [16].

Ion-pair mode cannot explain why oxygen can accelerate the process of removing HCl from PVC and the prediction kinetics data which according to the mechanism did not fit with the experiment results [18].

1.1.5 The thermal decomposition mode

At present, only for some simple polymers, such as PMMA, PE and PS, their thermal decomposition modes have been studied in detail, but not yet for the application. Now, the mechanism analysis about synthetic polymers' thermal decomposition is based on the one-step reaction, and there is a distance from the decomposition in reality. Besides, one-dimensional thermal cracking of a small amount of polymer under rapid heating conditions cannot be applied to a large number of polymers.

Modeling to study the chemical reaction of thermal decomposition of the polymers and the transfer process are very difficult; even a series of simplified application of the results is limited. A simulation study is conducted on the relationship between the thermal decomposition kinetics of polymer, thickness of reaction surface, temperature, reaction zone and the heating conditions. The results have been used to elucidate the mechanism of interaction of internal and external heat transfer and transport processes and chemical reactions. Moreover, there are reports that have used the one-dimensional model to predict the influence of bubble within polymer melt layer on the steady-state transfer of volatile products during pyrolysis.

In order to apply the polymer thermal decomposition data for flame-retardant polymer science and combustion of waste polymer, reactor design, reliable mechanism and kinetic constants of thermal decomposition need to be studied thoroughly. Through the determination and the establishment process of heat and mass-transfer

model of comprehensive treatment about the experiments, it will be helpful to deepen understanding of polymer pyrolysis.

1.1.6 Thermal decomposition products

Many factors contribute to polymer decomposition products, such as composition, decomposition temperature, heating rate, thermal decomposition effect (endothermic or exothermic) and release rate of volatile products [4, 5].

The decomposition can generate two kinds of substances: one is polymer chain residues, which still have the certain chain integrity structure, and the other is the polymer fragments (including small-molecule vapors, liquid and solid products). They are very susceptible to oxidation. When intensely heated in oxygen, the char residue will glow, but the combustion generally occurs only within the vapor phase near the residue, and gaseous substance and fine solid powder take part in combustion. The common combustible gas generated from thermal decomposition includes methane, ethane, ethylene, formaldehyde, acetone, carbon monoxide, etc. The common noncombustible vapors are carbon dioxide, hydrogen chloride, hydrogen bromide, water vapor, etc.; liquid products are organic compounds with high molecular weight polymer and partial decomposition of the solid product is, generally, char residue, carbon or ash. In addition, other solid particles or polymer fragments can be suspended in the air to form smoke.

In most cases, the ignition and combustion system occur in the vapor phase. If the polymer decomposition does not produce any combustible vapor, it can effectively prevent combustion. But it is almost impossible, because when the vast majority of polymer decomposes, besides generating char-residue solid, it is always accompanied by release of volatile flammable products. For the suppression of combustion, generating nonflammable gas should be favorable, but any vapor release will make the system expand and change the physical and chemical structure so that more surface of system will be exposed to air at high temperature. Moreover, the generated nonflammable gas is toxic and corrosive. The flammability of flammable liquids may be lower than the combustible vapor, because the evaporation of liquid-to-vapor phase consumes latent heat, but the polymer decomposition of solid residue contributes to the overall structure to maintain the original polymer structure integrity and can protect the adjacent polymers from further decomposition, hindering the mixture of the combustible vapor and air.

The volatile low molecular weight organics that are generated by some polymers during thermal decomposition in laboratory devices are shown in Table 1.3 [21].

Thermal decomposition products of polymers in a fluidized bed at high temperature have been studied [22]; some additional polymers' (such as polyolefin, PS) cleavage product is a mixture of monomers, liquid and vaporous fuels and char

Table 1.3: The volatile low molecular weight organics produced by some polymers during thermal decomposition [21].

Polymer	Main products
PE	Methylpentene, hexene-1, *n*-hexane, heptylene-1, *n*-octane, nonylene-1, decene-1
PP	Propylene, isobutene, methyl butene, pentane, methylpentene-2,2-methyl amyl-1, cyclohexane, 2,4-two methylene-1, 2,4,6-three methyl nonylenol-8, methane, ethane, propane, butane, 2-methacrylic, 2-methyl pentane, 4-methyl allyl, 2,4-two methyl allyl-1
PVC	Methyl chloride, benzene, toluene, two dioxanes, xylene, chlorobenzene, naphthalene, chlorobenzene, two vinyl benzene, methyl ethyl cyclopentane
ABS	Benzophenone, acrylonitrile, propylene aldehyde, benzaldehyde, cresol, two methyl benzenes, ethylene, ethyl benzene, ethyl benzene, hydrogen cyanide methyl, isopropyl benzene, α-methyl styrene, β-methyl styrene, phenol, phenyl cyclohexane, α-phenyl-1-propylene, *n*-propyl benzene, styrene propyl benzene, styrene
PMMA	Methyl methacrylate
PMBA	*n*-Ding Ji acrylate
PET	Acetaldehyde, acid, anhydride
PA6, PA66	Benzene, acetonitrile, caprolactam, hydrocarbons containing five and less than five carbons
PU	Cyclohexanone, containing five and less than five carbon hydrocarbons, acetonitrile, acrylonitrile, benzene, benzyl cyanide, naphthalene, pyridine
PF	Toluene, methane, propylene, acetone, propanol, methanol, two cresols

composition, but when it comes to the thermal decomposition of PMMA, it can generate the monomers up to 97%.

Pyrolysis products of several synthetic polymers at the temperature of 550 °C in fluidized bed (quantitative data) are shown in Table 1.4 [23]. Table 1.4 shows that hydrogen, methane, ethane, ethylene, propane, propylene, butane and butene are the major vaporous products of PE and pyrolysis, whereas oil and wax are mainly the aliphatic alkanes and alkenes. PVC, PC and PET pyrolysis generate aromatic oil, whereas PS can get about 60% of the styrene monomers.

1.2 Ignition

1.2.1 Lighting conditions

Polymer ignition refers to light the mixtures of flammable gas and oxidizer near the solid surface. Generally, ignition needs to satisfy the following three conditions:

(1) Must form the mixture of fuel and oxidizer, and the concentration of the fuel must be within the combustion limit.
(2) The vapor temperature should be high enough to cause and accelerate the combustion reaction.
(3) The heating area must be large enough to overcome the heat loss.

Table 1.4: Some pyrolysis products of polymers in fluidized beds at 550 °C [23].

Product	HDPE	LDPE	PP	PS	PVC	PET
Hydrogen	0.31	0.23	0.24	0.01	0.20	0.06
Methane	0.86	1.52	0.44	0.08	0.79	0.41
Ethane	0.90	1.71	0.45	<0.01	0.55	0.02
Ethylene	3.01	5.33	1.48	0.09	0.51	1.27
Propane	0.79	0.84	0.67	<0.01	0.28	0.00
Propylene	2.26	4.80	1.08	0.02	0.92	0.00
Butane	0.35	0.55	0.26	0.00	0.11	0.00
Butene	2.34	6.40	1.95	0.02	0.92	0.00
CO_2	0.00	0.00	0.00	0.00	0.00	24.28
CO	0.00	0.00	0.00	0.00	0.00	21.49
Hydrogen chloride	0.00	0.00	0.00	0.00	31.70	0.00
Oily substance	36.8	17.8	31.5	59.0	22.1	23.5
Wax	29.9	35.4	38.3	12.4	0.0	15.9
Carbon	0.0	0.0	0.0	0.0	13.5	12.8

For ignition, the temperature of mixture on the solid surface plays a critical role. The heat transfers by the degradation of polymers surface and/or the ignited source of vapor phase can raise the temperature of the mixed vapor to ignition temperature. Ignition can also be caused by the hot air flow.

When materials are ignited, the surface temperature reaches a critical value, and there is a lag period. If the heat used to ignite is supplied by radiation heat, then heat radiation and heating area are reduced, and the lag phase is prolonged. But the radiation heat intensity cannot be lower than a certain value, that is, a minimum value of 160 kW/m^2 s [25].

1.2.2 Ignition and spontaneous combustion

Ignition of polymer can be divided into the induced ignition and spontaneous combustion. Combustible vapor may be ignited under enough oxygen or oxidizer or external ignition source. Then, the material begins to burn. The corresponding temperature is called the ignition temperature, that is, the temperature of the combustible vapor decomposed by the polymer that can be ignited by a flame or spark. It is usually higher than the initial decomposition temperature. But when without an external source of ignition because of the chemical reaction (decomposition) of the polymer matrix itself, spontaneous combustion occurs. The corresponding polymer temperature is called spontaneous combustion temperature which is usually higher than the ignition temperature (although there are exceptions), because the self-

Table 1.5: Ignition and spontaneous combustion temperature of some polymers (ºC) [5, 26].

Polymers	Ignition Temperature	Spontaneous combustion temperature	Polymers	Ignition temperature	Spontaneous combustion temperature
PE	341–357	349	PES	560	560
PP (fiber)		570	PTFE		530
PVC	391	454	CN	141	141
PVCA	320–340	435–557	CA	305	475
PVDC	532	532	CTA (fiber)		540
PS	345–360	488–496	EC	291	296
SAN	366	454	RPUF	310	416
ABS		466	PR (glass fiber laminate)	520–540	571–580
SMMA	329	485	MF (glass fiber laminate)	475–500	623–645
PMMA	280–300	450–462	Polyester (glass fiber laminate)	346–399	483–488
Acrylic fiber		560	SI (glass fiber laminate)	490–527	550–564
PC	375–467	477–580	Wool	200	
PA	421	424	Wood	220–264	260–416
PA66 (fiber)		532	Cotton	230–266	254
PEI	520	535			

maintained thermal decomposition requires more energy than external force-maintained process.

Ignition temperature of some polymers (underspecified conditions) and spontaneous combustion temperature are shown in Table 1.5 [5, 26].

When oxygen concentration of the external environment increases, spontaneous combustion of polymers decreases (see Table 1.6) [27].

For spontaneous combustion, getting reproducible results is difficult (though some kinds of fires are caused by spontaneous combustion). Therefore, the research on combustion, with the small fire ignited by polymer, is more feasible, but it has some relation with the ignition and ignition-source type (matches, cigarettes, and thermoelectric wire), sample size (1–10 cm) and ambient temperature.

For open systems, spontaneous combustion and ignition designed by human have no distinction. Generally, the human pilot is because of some devices in the vapor phase of high-temperature region (flame, spark, glow wire). The spontaneous combustion is caused by the thermal radiation, heat flow and thermal surface. Local heat caused by accidental fires often is ignited; the heat radiation is the main heat-transfer model.

Table 1.6: Spontaneous combustion temperature of polymers under 10.3 MP oxygen pressure [27].

Polymers	Spontaneous temperature (°C)	Polymers	Spontaneous temperature (°C)
PTFE	434	PET	181
TFE/PFPVE	424	POM	178
PCTFE	388	PE	176
PET	385	PP	174
HFP/TFE	378	ECTFE	171
PES	373	PVF	222
PPO/PS	348	TFE/PFMVE	355
PI (contains 15% graphite fiber)	343	VF/HFP	302–322
PEEK	305	SIR	262
PC	286	GR-M	258
PPS	285	TFE/PL	254
PVDF	268	IB/IP	208
PA66	259	PUR	181
ABS	243	BD/AN	173
ETFE	243	EPDM	159
PVC	239		

1.2.3 The performance of ignition

The performance of ignition is not the inherent attribute of polymer; it is connected to the ignition conditions. The ranking of the ignition of some polymers will change with the test methods.

When the ignition source exists, and the combustible substance generated from the polymer pyrolysis rises to the surface of the polymer, and when the temperature of the combustible reaches the critical value, the combustible substance will be ignited. When the polymer is ignited by the experimental small fire, it will be connected to the critical surface temperature of the ignited polymer. Once ignited, part of the combustion heat will fed back to the adjacent unburned polymer surface, and the polymer will continue its pyrolysis and repeat the process of ignition, thus making the flame spread along the surface of the polymer.

The performance of ignition demonstrates the complexity of the polymer, the difficulty level of being ignited, particularly being ignited by flamelet or sparkle. Ignition is the initial stage of combustion.

The performance of ignition can be regarded as the degree of difficulty when polymer itself or its pyrolysis product is ignited under certain temperature, pressure, and oxygen concentration. The lower the spontaneous combustion temperature of the polymer, the easier the occurrence and spread of fire disaster, whereas if

Table 1.7: The performance of ignition of some material measured by USF ignition experiment (the time needed for ignition per second) [4, 5].

Material	Heat flow (kw/m^2)		
	58	**81**	**105**
PMMA (3.2 nm)	115	33	31
PS (3.2 nm)	108	35	31
Rigid polymelamine urea acid ester foam plastics (12.7 nm)	Nonignition	Nonignition	56
PVC (3.2 nm)	269	95	78
Linoleum (3.2 nm)	59	54	12
Wool carpet (foam rubber lining)	26	9	6
Polyester carpet flame retardant viscose (resin lining)	79	42	28
Nylon fabric	22	16	7
Bafta	10	6	3
Nylon carpet (foam rubber lining)	29	17	13
Flame-retardant wool fabric	104	62	15
Flame-retardant wool/nylon fabric	20	16	8
Acrylic class carpet (fiber lining)	38	15	9
Flame retardant viscose fabric	12	9	5

Table 1.8: The performance of ignition of some materials measured by cone calorimeter method (the time needed for ignition per second) [4, 5].

Material	Heat flow (kw/m^2)		
	25	**50**	**75**
Flaming ABS	120	34	17
Antiflaming ABS	111	38	17
Flaming HIPS	304	106	25
Antiflaming HIPS	205	52	24
Flaming PC|ABS alloy	267	53	28
Antiflaming PC|ABS alloy	189	49	75
Flaming UPT	Unignition	159	79
Antiflaming UPT	119	42	–
Flaming XLPE	162	63	37
Antiflaming XLPE	86	37	–

the spontaneous combustion temperature of the polymer is higher, the situation will be the opposite. The performance of ignition of some polymer is showed in Tables 1.7 [4, 5] and 1.8 [4, 5].

The temperature makes the polymer decomposed as heating in air can be an indictor to measure the igniting temperature, because at the same time, many small molecule combustibles have escaped from the polymer. Vapor-phase inhibitors and

some gaseous products due to the polymer pyrolysis may influence the igniting temperature of the polymer, because they can reduce the oxygen concentration in vapor and the combustible concentration. When the polymer is ignited, the loss of weight in nitrogen can demonstrate the rate of the combustible generation from the polymer. In this case, the oxygen concentration in the flame tends to be zero.

When the polymer is ignited under thermal condition, it is the combined result of heat flow and time. As to the given polymer, the bigger is the heat flow, the less the time it needs to be ignited. In the polymer with good thermal insulation, the surface can be ignited quickly due to less internal heat circulation.

Most of the big fire is caused by small fire; there is an induction period before the polymer is ignited (including smoldering); then, the temperature continues to rise until it gets burnt (usually at 800 °C–1000 °C). Finally, the fire will decay due to the exhaustion of fuel.

1.2.4 The factors causing ignition

Source of ignition
The stronger the source power of ignition is, the faster the developing rate and spread of ignition are. Soft fire or a combustion cigarette can cause smoldering. It will last for a long time before it turns into combustion. The rate of combustion is quite slow. Open flame can cause combustion directly, and then, it can spread and develop quickly.

The direction of heat transferring
For ignition, the process for heat transferring is quite important. When polymer is ignited, convective heat transferring and radiative transferring are seen above the fire in all directions. At this scenario, the flame propagation will promote the development of the combustion. When the surface of the polymer come close to the cracking zone or the flame zone and is heated, the polymer will decompose into many flammable products. The flame on the surface of the polymer ignited by small fire is outside the combustible zone, so the essence of the flame propagation is the process of the repeating of the ignition. When the release of the heat is more than the heat lost in the process of the combustion, continuous ignition happens. The prevention of continuous ignition will help to stop the spread of the flame.

The thermal inertia of the polymers
The thermal inertia of the polymers (Q_1) is the product of its thermal conductivity (K), density (P) and specific heat capacity (c), that is $Q_1 = KPc$. When the polymer is ignited, the time related to its combustion is connected to its Q_1. The lower the Q_1 of the insulating polymer is, the higher will be the Q_1 of the thermal-conductive

polymer. For example, it is easier to ignite the bits of wood with small fire, but it is difficult to ignite a wood brick; the foams with combustible component (the polyurethane (PU) foams) burn more quickly than solid body with the same material. It is all because of the fact that the lower the Q_1 of the polymer, the easier for heat to accumulate on the surface, thus making it easier for the ignition, which means less time needed to reach the igniting temperature.

The component of the polymer

The chemical component and existence of fire retardants will influence the decomposition temperature and the species and weight of the flammable pyrolysis products when it is ignited. Thus, it is also closely related to the ignition temperature of the polymer. When the natural polymers (timber, cotton and paper) are compared with synthetic polymer (PP and PVC), the former is easier to be ignited and produce combustible products. But the influence of physical condition on the ignition temperature can not be ignored. Sometimes, such physical factor may outweigh its chemical components.

Kinetics control factors

The process of the ignition of the polymer has something to do with the time that the combustible products rest on the surface of the polymer and the induction time of the vapor-phase combustion reaction. If the later is shorter than the former, then the control factors for ignition are solid-phase decomposition rate and heat-transfer process. However if the former is shorter than the later, then ignition will not happen, and the controlling factor for ignition is vapor-phase combustion reaction rate.

   The ignition of the polymer is the primary phase of the combustion of the material, and it is also the critical stage for the development of combustion. There are many factors causing the ignition, and the change of these factors can promote or stop combustion. However, ignition is one of the indicators for the flammability. The shortened igniting time does not mean the worse flammability of the overall material. The igniting time of some flame-retardant polymer is less than some nonflame retardant polymer, because some flame-retardant polymer is easier to give off the combustion during pyrolysis.

1.2.5 Ignition model

Researchers have previously done modeling work on the ignition caused by thermal radiation [29, 30]. For example, for the non-charring polymers and non-exothermic surface reactions, the one-dimensional equation of solid-phase energy and the

mass and energy of the vapor phase can simulate the conduction mechanism of solid surface radiation heating of the adjacent vapor layer, but this can only be used to the predict ignition when the surface temperature of the solid is quite high. In addition, this can easily be interrupted by some occasional factors. For example, diffused flame is easily produced in the ignition of some vapors, and it magnifies the radiant heat flux and will increase the surface temperature and crack material flow, thus reducing ignition time. In addition, the delayed ignition time will be shortened if the ignition, when it happened, approach the surface of the inflammable substance. The vapor absorption of the radiation energy will greatly influence the ignition and the delay of ignition time.

For the ignition caused by hot air, simple quantitative solid thermal model [25,28] has been put forward. This model can prove that the delayed ignition time is the function of igniting temperature, but there are exceptions when the igniting temperature is low. Some boundary-based models have pointed out that ignition is the controlled mechanism for vapor-phase reaction. As the airflow rate decreased, the delayed ignition time increased [31], and the delayed ignition time is controlled by the decomposition rate of the solid phase (with low flow) or the combustion of vapor phase (with high flow).

1.3 Combustion propagation and the spread of combustion

1.3.1 Overview

When the combustible is ignited, exothermic reaction will happen both in vapor phase and condensed phase to produce combustion and heat the unburned combustible. To spread combustion, the combustion zone should provide enough heat for the unburned combustible for degradation. At the same time, some proper condition should be gained by the vapor phase. In fact, the spread of the combustion is not only influenced by the degradation mechanism of the solid combustible but also controlled by many other factors [4, 5].

The spread of combustion means the development of combustion along the surface of the polymer. Because the spread of combustion is a surface phenomenon, the decisive factors are the combustible vapors produced on the polymer surface, or the flammable vapor formed in the inner part of the polymer, and it has the ability to release to the surface of the polymer. The spread of combustion must be achieved when the temperature of the polymer surface can be raised to the combustion temperature, which is caused by the hot flux of forward-spreading flame. Therefore, the ignition of the polymer is directly linked to the spread of the flame. The surface of the insulating material can be ignited at a higher rate, so that it can get higher combustion-spreading rate.

Under specific conditions, the spreading speed is the moving forward speed of combustion front. The higher the combustion rate, the easier it is for the nearby combustible to be affected and cause the larger combustion. Sometimes, the polymer that can spread combustion is not only of high risk, but the loss caused by affected polymers combustion can also be really heavy. Thus, the rate for the spreading of the combustion of the polymer is an important factor that can not be ignored in the fire-retardance technology.

1.3.2 The spreading direction of combustion

The spreading of combustion of solid combustible can be divided into two categories: syntropic spreading and reversed spreading [32]. If the direction of oxidant flow is same as the direction of the spreading of the combustion, it will be called syntropic spreading combustion, otherwise it is called reversed spreading combustion. For the syntropic spreading combustion, the flame is on the surface of the burned combustible, and the heat transfer to the surface of the unburned combustible is quite intense, which will rate up the spreading of combustion. On a large scale, this process seems to be controlled only by the heat transfer. When the rate of combustion is low and the combustible stays in laminar airflow, the heat transfer of unburned combustible is mainly preceded by convection. When the fire is enlarged, the heat transferring of the turbulence flow is mainly preceded by the way of radiation. For the reversed spreading combustion, the heat transferring of unburned combustible is quite difficult, because the pyrolysis front and the combustion front are in the same area, but the amount of heat passed from vapor phase or solid phase to the unburned combustible is quite low, so its combustion is easily controllable. When the rate of counterblast is comparatively low while the oxygen concentration is quiet high, the combustion is mainly controlled by the heat transferring. But when the counterblast rate is high while the oxygen concentration is low, the combustion is mainly controlled by the chemical kinetics [28].

1.3.3 The heat conversion model of combustion propagation

If the polymer is ignited and the ignition can last, the combustion will develop and spread along the surface. The prerequisite of combustion spread entails sufficient heat being fed back to the polymer of the flame front, making the latter pyrolysis and providing combustibles.

Figure 1.5 illustrates the heat conversion model for maintaining the combustion after the polymer is lighted [33]. When QC≥QH+QP+QI+QD, the combustion flame of polymer will spread. The factors such as polymer's specific heat, heat conductivity
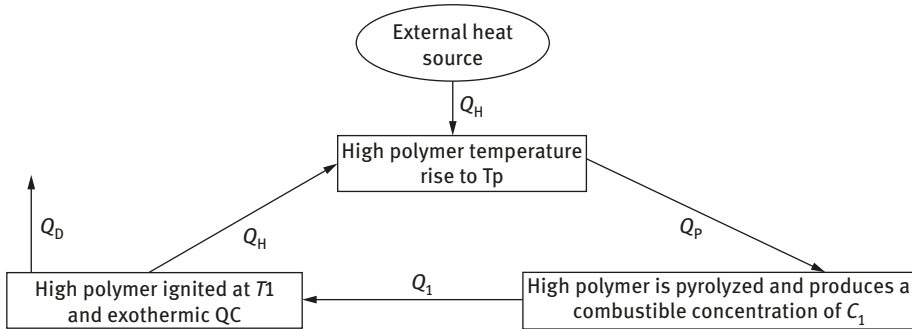
Figure 1.5: The heat conversion model when polymer ignites and maintains combustion. Q_H is the heat needed for the splitting of polymer to reach the temperature T_P; Q_P is the decomposition heat for the combustible vapor concentration caused from splitting to reach the concentration needed for combustion limit C_1; Q_1 is the temperature T_1 needed for the combustible vapor to be ignited; Q_C is the heat of combustion; Q_D is the lost heat.

coefficient, decomposition temperature, decomposition heat, light, flashing point and enthalpy of combustion will influence the combustion process. The combustion products of polymer are relevant to its geometry, property and oxygen supply. When the polymer in its common form is ignited, the combustion products will contain carbon monoxide and carbide particle due to the lack of oxygen, the latter will be one of the main reasons for the formation of fog and the low visibility around the comburent.

1.3.4 The factors affecting combustion propagation

During the ignition, the accumulated heat inside the system increases the temperature of the polymer through conduction, convection and radiation to spread and expand the combustion. The following properties of polymer are related to combustion:

(1) The difficulty of igniting the polymer: The easier the polymer will be ignited, the greater will be the contribution for the combustion development.
(2) The combustion heat of polymer: The more heat the polymer produces in the process of combustion, the faster the combustion development will be.
(3) The exposure of polymer: The polymer whose surface is mostly exposed to the flame is easy to spread the combustion.
(4) The amount of the polymer: Only some adequate substances that exist inside the system can threaten the expansion of combustion.
(5) Wind direction.
(6) Ventilation and oxygen supply.
(7) Combustion direction.

First and the second point are decided by the properties of the polymer. Therefore, the remaining points will be discussed in the following.

The exposure of combustible

A good amount of energy is required for the adjacent combustible to propagate combustion, thus making it enter into combustion phase. It is easy to get burnt when the nearby substances are on the initial combustion surface whereas hard to be burned when inside the combustion. Thus, the combustion propagation is usually regarded as a surface phenomenon. When most of the surface of the polymer is exposed to the highly heated environment, the rate of surface combustion can be regarded as the actual measurement of combustion propagation [4, 5].

The thickness of combustible

If the thickness of the combustible is thinner than the thermal diffuse layer, it is regarded as thin layer. The properties of thin-layer combustible are relatively homogeneous. For the transfer of heat to unburned surface, thickness exerts little influence in thin layer. But it will be significantly influenced in thick layer. In thick layer, the combustion propagation is the consumption of solid combustible in combustion area. With the increase of oxygen concentration and air velocity, the rate of pyrolysis and combustion will accelerate for combustion propagation in the same direction [28].

Wind direction

Combustion propagation can be divided into two cases: downwind and upwind. Apparently, the former is faster than the latter. The airflows hinder the passing of heat to the polymer in front of the flame, when the propagation is against the wind, which reduces the rate of polymer pyrolysis and makes the concentration of combustible gas at the top surface hard to reach the lower flammability limit. The case of downwind is adverse.

The orientation of combustible

Generally, combustion propagation and the direction of solid combustible are closely related [32]. The upward combustion propagation is faster than the downward one due to the heat transfer from the hot combustible gas to the unburned substance; the enhancement of natural convection and the enduringness of three kinds of heat transfer such as radiation, convection and transmission. The former is a delayed flame propagation process due to natural convection.

The horizontal combustion propagation is also slow as well because the combustible in front of the flame can only be heated by heat conduction vapor phase
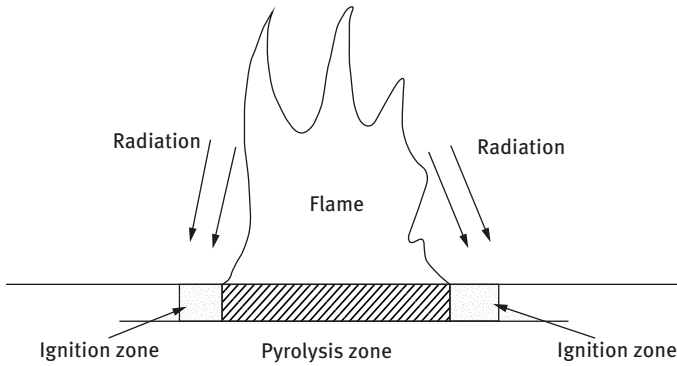
Figure 1.6: The horizontal combustion propagation [1].
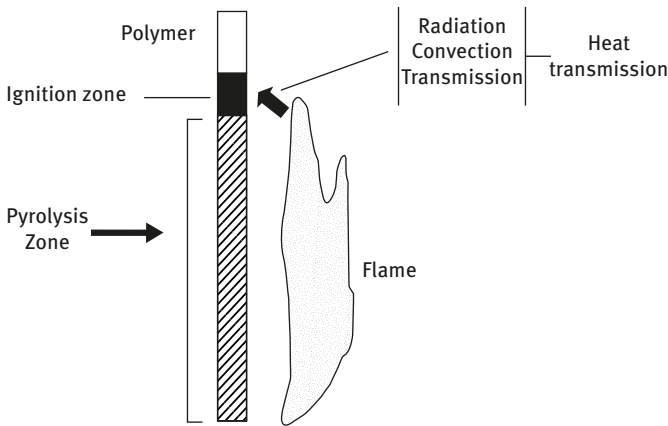
Figure 1.7: The vertical combustion propagation [1].

and downward heat radiation [1]. Figures 1.6 and 1.7 show the horizontal combustion propagation and the vertical combustion propagation, respectively [1].

Oxygen supply

In general, combustion can be spread faster when heat is intense or oxygen is sufficient (such as ventilation). But sometimes excessive ventilation may remove heat and slow down the spread of combustion. In addition, the melting or charring of polymers can also directly consume energy, thus reducing the rate of forming a fire.

In the early phase of combustion development, combustion can only be propagated inside the ignited substance. But when the flame reaches 1–2 m, the radiant heat can ignite the polymer even staying a few meters away. When the fire spreads to

the ceilings, the radiant heat flux increased dramatically against other objects in the room, resulting in flash burning with extreme high rate of propagation. In the phase of combustion development, external heat flow should reach 20–60 kW/m to maintain the combustion, with the sample of 10 cm to 1 m, and the ambient temperature up to 400–600 °C, higher than ignition temperature, with required proper ventilation.

1.3.5 Combustion propagation coefficient of materials

In summary, combustion propagation is not only dependent on the properties of the materials but also is related to a series of external conditions. Therefore, the measurement of combustion propagation coefficients should be conducted under strict requirement conditions. Moreover, different measuring method could obtain different results. Table 1.9 [4] shows some combustion propagation coefficients of different materials under the standard of ASTME-84. (The relative value of untreated red oak is 100.)

Table 1.9: Combustion propagation coefficients of different materials under the rule of ASTME-84 [4].

Materials	Coefficients	Materials	Coefficients
Red oak (untreated)	100	Basswood (treated)	25–35
Red oak (treated)	20–50	Velveteen (treated)	25
Oak (treated)	35	Yellow pine (treated)	25
Aspen wood (treated)	30	Bai Congmu (treated)	20
Box-wood (treated)	25	China fir (treated)	15–25
Birch (treated)	15–30	Rose wood (treated)	20
Lauan (treated)	15–20	Plastic	10–>200
Soft maple (treated)	20–30	Reinforced plastic	15–>200

1.3.6 Combustion propagation model

For combustion propagation, a lot of models have been built [34,35], of which some describe the combustion propagation rate and its relationship with ambient conditions and fuel performance; most of them are based on heat-transfer mechanism. Some complex mathematical models can describe the balance of vapor and solid fuel. Recently, some two-dimensional models about the weather have been published [28]. Those equations described the conservation of momentum, energy and mass of the vapor phase.

The mathematical model of combustion process can help people understand the chemical and physical mechanism of combustion propagation, and they can be used to explain the experimental results. Although mathematical model is a

powerful tool which can estimate materials' reaction in fire, it should consider all physical and chemical processes related to combustion, and they can be simplified.

1.4 The full and stable combustion

1.4.1 Overview

When a certain critical point of the combustion was reached (as shown in Figure 1.1), the heat released from the combustion of polymers can raise the decomposition products of polymers temperature, making the vapor expand; thus, the heat transfer will be increased through the convection, conduction and the radiation. For some polymers, it is the appropriate time to enter the phase of full and stable combustion. Once the combustion enters this stage, it can not be subdued.

The combustion of polymer can be charred in two ways: combustion and smoldering. If the heat is enough to cause the pyrolysis of the polymer into combustible and ignite it, then combustion is possible. But when the heat and temperature are lower than the critical value, then smoldering is possible.

The combustibles after being lighted and burned properly will be in a steady-state combustion. According to the combustion directions (vertically or horizontally), the combustion process can be classified into wall combustion and pool combustion. Combustion is a complicated chemical and physical process. During combustion process, the interaction between fuel flow and its surroundings is generally nonlinear and irregular, making quantitative estimation difficult. In an enclosed space, one of the pivotal problems lies in the heat transfer and mass transfer between the fuel and its surroundings.

For the combustion in an enclosed space, two environmental factors can be decisive for the combustion behaviors. The first one is the heat of flame (from the top of the combustion combustible) and the other is the external heat (from the hot vapor, hot surface and the flame of other combustible). The former is closely related to the ventilation and the oxygen supply, whereas the latter is obviously influenced by the geometry of the enclosed space, ventilation and the surface of the material [9].

1.4.2 Combustion key points

Heat and mass transfer

Polymer combustion relates to heat transfer, pyrolysis in the condensed phase, diffusion of pyrolysis products in the condensed phase and the vapor phase, mixing with air to form an oxidation reaction and a series of chain reaction in the vapor phase. Figure 1.8 [33] is an element state model of polymers in general combustion process.
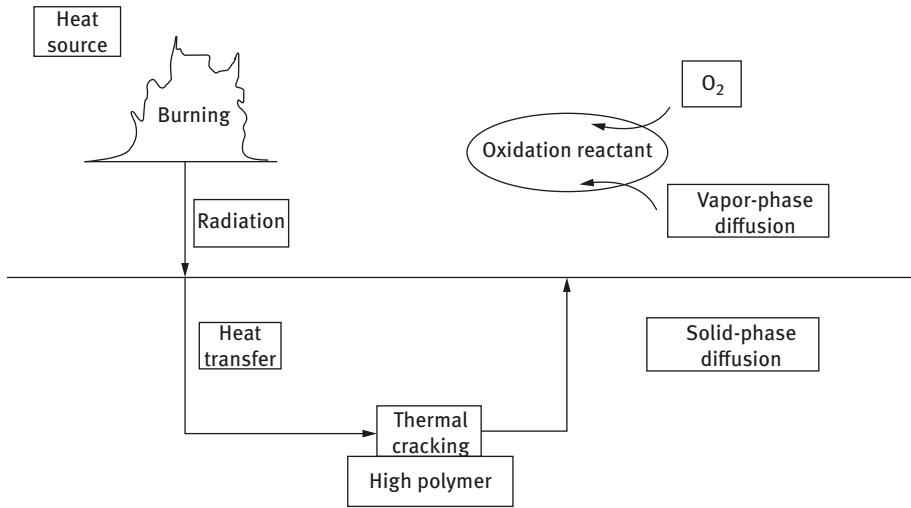
Figure 1.8: The element state model of polymer in the process of combustion [33].

When polymer is burned, a part of the thermal energy is absorbed by the polymer itself used for the pyrolysis, and the combustible pyrolysis volatile products enter into the vapor phase as fuel to sustain combustion. It is obvious that the combustion rate of the polymer is decided by the heat, polymer cleavage and the phase transition. The rate of polymer cleavage increases with the rise of temperature but depends more on the properties of the polymers [4, 5].

Features

In the full combustion phase (the main stage of combustion), external heat flux is often greater than 50 kW/m^2. Hence, the sample size needs to reach 1–5 m and the environment temperature should be more than 600 ℃, higher than spontaneous combustion temperature with low ventilation. In the small fire test, simulation of these conditions is generally not easy. The state of polymer will be different in small combustion test compared with the big combustion test. However presently, people have taken a great step in the aspect of predicting large fire behavior on the basis of the results of small-scale test due to the development of combustion-testing technology.

In full combustion phase, the environment temperature is higher than that of most of the ignition temperature of the polymer. In the current scenario, all exposed surfaces of the polymer reach ignition temperature, and combustion spreads very fast in the whole space and the flame almost covers all combustible surfaces. In other words, combustion takes place in all combustible surfaces, and the surface of material is almost exposed completely to the flame.

In full combustion phase, the degree of polymer ignition has no practical impact on combustion, but the flammability of the surface of polymer still affects the

combustion. The degree of combustion is related to the heat of combustion, the exposure degree and the amount of material. The higher the heat of combustion of material, the more the amount of material; the larger the exposed surface, the stronger the combustion.

Chemical reaction

The state of combustion varies with polymers of different molecular structures. For instance, the surface temperature of PS, PE, expanded polystyrene (EPS)and the epoxy resin during pyrolysis increases along with the heat supply. However, the surface temperature of PMMA remains almost constant, whereas its surface structure changes and specific surface area of PMMA increases as well.

When the PMMA is the combustion in various mixtures of different oxygen and nitrogen composition, the vapor compositions of different burning zones are different. However, all zones have enough oxygen with more oxygen in the high-temperature zones. When PMMA and PS are in combustion process, the surface temperature of the condensed phase and the temperature of areas (the pyrolysis area) close to the surface are the same, meaning that the rate of combustion is constant under critical condition.

The combustion of pyrolysis products of polymer is based on free radical chain reaction, including the following four steps (see eqs. (1.14)–(1.17)) [36]:

$$(1)\ \text{Chain initiation} \quad RH \rightarrow RH^* \text{ or } R\cdot + H\cdot \tag{1.14}$$

$$(2)\ \text{Chain transfer} \quad R\cdot + O_2 \rightarrow ROO\cdot \tag{1.15}$$

$$RH + ROO\cdot \rightarrow ROOH + R\cdot$$

$$(3)\ \text{Chain branching} \quad ROOH \rightarrow RO\cdot + \cdot OH \tag{1.16}$$

$$2ROOH \rightarrow ROO\cdot + RO\cdot + H_2O$$

$$(4)\ \text{Chain termination} \quad 2R\cdot \rightarrow R-R \tag{1.17}$$

$$R\cdot + \cdot OH \rightarrow ROH$$

$$2RO\cdot \rightarrow ROOR$$

$$2ROO\cdot \rightarrow ROOR + O_2$$
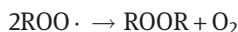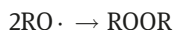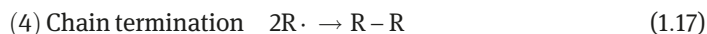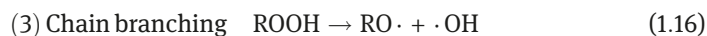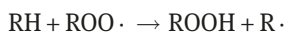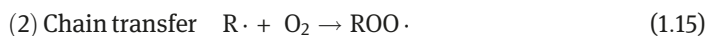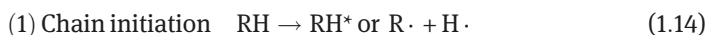
1.4.3 Smolder

Smolder is one of the most hazardous combustion modes, because it can produce a large amount of CO, and char and combustible volatiles too. Smolder involves condensed phase pyrolysis and the oxidation of condensed phase and char. Meanwhile, the oxidation of some components in smolder can accelerate the heat release

rate, which is a remarkable contribution and cannot be ignored in the process of transforming smolder into combustion [28].

Smolder spreading in the opposite direction of oxygen flow is reversible smolder. Both oxidation and pyrolysis exist at this moment and both get enhanced with the rise of temperature. Smolder that spreads in the same direction of oxygen flow is forward smolder. The degradation of condensed phase is mainly pyrolysis and oxygen is almost consumed by the oxidation of carbon, which accelerates the smolder and affects the heat-transfer rate of the original polymer and the pyrolysis rate of condensed phase.

The different configuration between reversible smolder and forward smoldering also leads to different controllable mechanism. The forward smolder is supported by the oxidation of carbon; however, reversible smolder is controlled by solid oxidation degradation. In addition, forward smolder can be easily converted to sustained combustion. Single reversible smoldering and single forward smoldering are easier to test or simulate, but forward smolder of multidimensional structure can further reflect dangers of fire in the real situation.

The spreading of oxygen from the material surface to original solid fuel and char residue layer can accelerate the exothermic reaction of solid fuel and the oxidation of char layer. The former supports reversible smolder, whereas the latter supports forward smolder.

Now, almost all the ignitions and the smolders are found in one-dimension system, but the ignition and smolder research should focus on the exothermic reaction process of condensed phase, a shift from smolder to combustion, artificial ignition and multidimensional model.

1.4.4 Flashover

The acceleration of combustion rate and the spreading of combustion to the second-fuel combustion increase the thermal layer temperature rapidly, and the heat of other combustibles will also increase because of the spreading of the thermal layer in the enclosed space. As a result, all fuels burned inside the enclosed space have been ignited, releasing a large amount of heat instantly. Then, complete combustion comes up in a short period, which is known as flashover (as shown in Figure 1.9, solid line) [9, 37].

Without enough oxygen, the hot vapor layer sinks quickly to the combustion zone. If this occurs, little amount of oxygen enters into the combustion area and the combustion comes to an end. Dashed lines in Figure 1.9 indicate this situation. That is to say, the combustion can only last to point *A* rather than flashing point *B*. With deficient oxygen, the combustibles still pyrolyze at a relatively high rate. If some air flow is added caused by some changes, the heat-release rate will improve, which makes flashover possible.
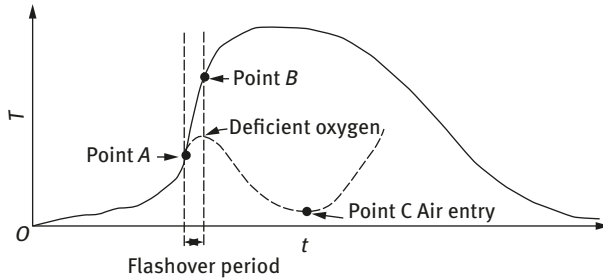
Figure 1.9: The relationship between developing time and temperature of close fires in burning process. Solid line indicates a flash and dashed lines indicate oxygen-deficient combustion. Point B is the flashing point.

Table 1.10: Flashover performance of some polymers measured by USF method [4].

Polymers	Flashover high (cm)	Flashover time (s)	Polymers	Flashover high (cm)	Flashover time (s)
PE	66 ± 0	115 ± 20	PA610	56 ± 20	77 ± 10
PS	20 ± 10	160 ± 37	RPUF	8 ± 3	92 ± 4
PMMA	46 ± 0	61 ± 18	FPUF	66 ± 3	44 ± 10
ABS	18 ± 5	127 ± 32	EPS	8 ± 5	203 ± 10
PC	15 ± 8	97 ± 13	PVC	No	No
PA6	66 ± 0	55 ± 7	MPPO	No	No
PA66	66 ± 0	95 ± 37	PPS	No	No

Flashover performance of some polymers measured by University of San Francisco (USF) method is shown in Table 1.10 [4].

1.4.5 Combustion model

Development of polymer combustion is difficult to predict. This is not only because the combustion process of the chemistry and physics is complicated but also because it is linked to geometry in enclosed space and many other factors, which are very changeable.

In addition, the combustion of polymer in an enclosed space can change the space environment, which in turn alters the combustion. Thus, the development of the combustion becomes more complicated.

Although it is difficult to predict the general rule of the combustion in an enclosed space, a reasonable engineering assessment of combustion development inside the building is possible through relevant test data and approximate engineering models.

Some engineering models can be used to simulate enclosed space combustion. At present, there are three kinds of deterministic models for the physical and chemical principles of combustion design: computational fluid dynamics model (CFD), two zone model (TZD use) and mobile phone model (hand-calculation model [HCD]).

(1) *CFD*: It is widely used in engineering calculation. It is about the division of involved scope multiple small volumes, the conservation of mass, momentum and energy that are applied to each small volume. When we apply CFD to combustion process (currently, only a few CFD programing classes are used in combustion process), the supply rate of fuel will be derived to calculate the release rate and, combined with a variety of assumptions, to estimate the combustion of products. By now, some researches have been published: by introducing the propagation, fuel hydrolysis and combustion development into CFD code, an attempt has been made to correlate between combustion process and environment conditions [38]. Such researches are still ongoing.

The use of CFD computing devices requires large capacity equipment and many professionals. Moreover, applying CFD in safety engineering is not practical, but molding is very useful to solve some of the design issues, and sometimes, it is the only way.

(2) *TZD*: It divides the enclosed space involved into two areas – hot area at the top and cold area at the bottom, and then it solves the conservation equations of mass and energy. In general, the regional model can describe the products of the combustible in pyrolysis (when the mass is lost), whereas heat-release rate describes the product of the fuel weight loss rate and comburent. But the products of the combustible pyrolysis and heat release rate are closely related to ventilation. For the given fuel, with good ventilation during combustion, its heat release rate and products of pyrolysis are steady but change with time, especially in poor ventilation. The TZD has been published in literatures. Some of them simulated the combustion in a single room, and others simulated in several rooms (connected to each other with a door or mechanical ventilation).

In recent years, TZD has been adopted for fire safety design by an increasing number of people. But we should be fully aware of the assumptions and its limitations and be familiar with combustion kinetics and kinetics in enclosed space.

(3) *HCD*: It can also be used to analyze some basic combustion process, including some simple empirical methods that are used to calculate the flame height, mass flow rate, the flame temperature and rate, interior overpressure and other fire parameters. Some are suitable for the combustion process, whereas others are suitable for the evaluation of environmental effects of combustion and are also suitable for heat-transfer process. This method is available in [9] for interested readers.

Nowadays, a range of different models have been used to estimate environmental consequences caused by the combustion in an enclosed space, but most of the models need to input the combustible properties, namely the heat release

rate and combustion products. But only a few methods can predict both and they are all under research without any application in engineering.

1.5 Combustion decay

When the heat of the combustion on the surface of the polymer decreases, the pyrolysis rate of polymer reduces, lowering the concentration of combustible on the surface to a certain limit which the combustion cannot maintain. It continues to diminish till it extinguish. The lack of fuel and oxygen, of course, are also important factors which cause the attenuation and extinguishment.

Attenuation and extinguishment vary with the polymer properties. Therefore, some polymers are easy to extinguish by fire, whereas others are very difficult. Self-extinguishing can be measured by limiting oxygen index (LOI). The higher the oxygen index is, the easier the combustion is to extinguish, and vice versa. That is to say, the combustion of polymer with low oxygen index often lasts for a long time in the fire.

The LOI of polymer is closely linked to the degree of amortization and charring rate, which, to a certain degree, can be quantitatively calculated [33].

Polymers with a lot of aromatic groups in the main chain, such as phenol resin, polyphonic oxide, polycarbonate, aromatic polyamide, polystyrene, etc., have higher LOI than aliphatic hydrocarbon polymer. This is mainly because this kind of polymer can form aromatic char by the condensation and generate little vaporous products. The LOI of charcoals itself is up to 65%, and the char layer it forms can cover the surface of polymer in the combustion and extinguish the fire. In general, polymers with low char yield have less than 20% LOI, while those with 40–50% char yield have more than 30% LOI. The LOIs of some polymers are shown in Table 1.11 [39–41].

Some vapor-phase reactions (capture combustion-needed free radicals and dilute combustible vapor, etc.) and condensed-phase reactions (form protective layer of mass transfer and heat transfer as well as absorb heat, etc.) caused by adding flame retardant into polymer can help to extinguish the combustion.

1.6 The smoke of combustion

Flame retardancy and smoke suppression are equally important requirements for the flame-retardant polymer materials, but they are often contradictory. Polymers, which can be decomposed into monomers during pyrolysis and burnt completely, generally produce less smoke. To realize the "flame retardant" and "smoke suppression" at the same time, or to achieve a balance between them, is one of the main contents of formula design for the flame-retardant polymer materials [42, 43].

Smoke is visible and nonglowing suspension, formed by fine particles dispersing in the air, and the solid particles are the result of the incomplete combustion or

Table 1.11: LOI (%) of some polymers [39–41].

Polymers	LOI (%)	Polymers	LOI (%)
PE	17	CTFE	83–95
PP	17	ETFE	30
PBD	18	ECTFE	60
CPE	21	CA	17
PVC	45	CB	19
PVA	22	CAB	18
PVDC	60	PR	18
PS	18	EP	18
SAN	18	Unsaturated polyester resin	20
ABS	18	ALK	29
PMMA	17	PP (fiber)	18
Acrylic resin	17	Acrylic fiber	18
PET	21	Modified acrylic fiber	26
PBT	22	Wool (fiber)	23
PC	24	PA (fiber)	20
POM	17	CA (fiber)	18
PPO	30	CTA (fiber)	18
PA6	23	Cotton (fiber)	18
PA6/6	21	Viscose fiber	19
PA6/10	25	Polyester	21
PA6/12	25	PBD (rubber)	18
PI	25	SBR	18
PAI	43	PCR	26
PEI	47	CSPER	25
PBI	40	SIR	26
PSU	30	NR	17
PES	37	Wood	22
PTFE	95	Cardboard	24
PVF	23	Fiberboard	22
PDF	44	Plywood	25
EEP	95		

sublimation of polymer. Smoke is one of the most severe risks in the fire. Because visibility allows people to evacuate from the ablaze building as well as help fire-fighters find place of fire and extinguish it in time, the smoke greatly reduces visibility and leads to choking.

Admittedly, the amount of smoke in the pyrolysis or combustion of polymer is not the nature of the polymer, but it is connected to combustion conditions (such as the combustion of enthalpy, oxidant supply, sample geometry, combustion or smolder, etc.) and conditions (such as temperature, ventilation, etc.). Undoubtedly, the molecular structure of the polymer is one of the important factors that affects the amount of smoke.

Polymers of polyene structure, or with aromatic side chain, usually generate a lot of smoke. This is because the combustion of polyene chain can form graphite particles through cyclization and condensation, and the polymer with aromatic side chains (such as PS) is easy to produce with conjugated double bonds of unsaturated hydrocarbons. The latter can be further cyclized and condensed into char. Polymers with aliphatic hydrocarbons in the main chain, especially those polymers which are easily decomposed into monomers in the presence of oxygen and thermal cracking in the backbone, such as POM, PMMA, PA6, etc., can be burned more fully; thus, the amount of smoke produced is low. In addition, the polymer with benzene on the backbone results in dispersion of higher amount of smoke [44].

Some polymers with high thermal stability and high charring yield usually generate little smoke as they form char in condensed phase and reduce volatile products. For example, PC and PSF both are the polymers with high amount of aromatic ring on the backbone, but the char yield of PSF was 2 times that of PC, the thermal stability of PSF is better than PC and PSF-specific optical density given by smoke box method is only 30% of PC.

Halogen-containing polymers generate high amount of smoke, and PVC is a typical example of this. The amount of smoke produced is almost the highest in all commonly used plastics; so, many studies of smoke suppression are directed at PVC. However, the amount of raw smoke is not always related to the content of halogen in polymers. Some polymers with high content of halogen do not emit high amount of smoke because of their special molecular structure and thermal cracking. For example, the chlorine content of PVDC is 1.3 times that of PVC, but the maximum specific optical density measured by the smoke-box method is only about 1/7 of the latter. This is because the HCl structure is formed after removal of PHCl by thermal cracking, and the carbon chain [44] is left after PVDC pyrolysis.

It should be pointed out that some flame-retardant polymers have a high amount of smoke. For example, some of the flame retardants in the vapor phase can inhibit the oxidation and promote the smoke generation, whereas some types of flame retardants (such as ATH, MH, etc.) and intumescent flame retardants simultaneously have flame retardancy and smoke suppression function. With a certain amount of zinc borate instead of Sb_2O_3 in the halogen antimony system, the generation of smoke gets suppressed without much retardancy deterioration.

Smoking properties are often measured by smoke density or optical density. The density of smoke produced by decomposition or combustion of a polymer under a given condition measured the extent to which it is obscured by light or vision. Smoke amounts in burning polymers and smoldering polymers are different. For polymers, the greater the density and the faster the growing of smoke density of the smoke, the shorter time would be left for evacuation and outfire. However, the specific optical density measured by optical density meter (smoke density) does not necessarily reflect the extent of visual shielding, because sooty particle size and their distribution

in the atmosphere affect the light absorption, and decrease of people's vision is mainly because of the shading effect of smoke, and simulative effect on human eyes. The smoke density of polymer combustion is related to a series of factors, such as combustion rate and ventilation intensity, which is inversely proportional to the ventilation intensity. The maximum specific optical density (D_m) of some polymers determined by National Institute of Standards and Technology (NBS) smoke-box method and the time required to reach D_{16} are shown in Table 1.12 [4, 26].

Table 1.12: D_m of some polymer and time required to D_{16} (NBS) [4, 26].

Polymers	Thickness (mm)	D_m		Time required to D_{16} (min)	
		Smoldering	Combustion	Smoldering	Combustion
PE	3.18		85	2.74	0.91
PP	6.35		119	3.00	4.18
PTFE		0	53		11
TFE-VDF	1.80	75	109	2.5	1.2
PVF	0.05	1	4		
Unfilled hard PVC	6.35	470	535	2.1	0.6
PVC fabric	0.66	261	198	1.4	0.3
PS	6.35	395	780	4.00	0.63
SA	6.35	389	249	4.13	1.11
ABS	6.35	780	780	2.98	0.57
PMMA	6.35	190	140	6.5	2.3
Polyacetal	3.18		6		
PA fabric	1.27	6	16		15.0
PAA sheet	1.60	7	14		
PSU	6.35	111	370	12.61	1.89
PC	6.35	48	324	10.88	1.95
PR	3.18	137	55	5	5.5
UP	3.18	780	780	2.66	0.59
Rigid PU foam (polyether)	50.8	221	113	0.35	0.22
Rigid PU foam (polyester)		161	70	0.43	0.20
PU rubber (polyether)		57	210	4.3	2.1
PU rubber (polyester)		131	230	4.0	1.5
Red oak	19.8	660	117	7.1	7.8
Fir wood	12.7	378	145	4.6	4.3

1.7 The toxic substances generated during combustion

Toxic substances refer to the materials that may destroy human tissues or interfere in function of organs. The toxic vapors generated in the course of combustion of polymers can cause chocking or even death, threatening the life security. The substances generated during the combustion relate to a range of factors, including the composition of the polymer, oxygen supply, temperature and heating rate, endothermic or exothermic reaction, the releasing rate of combustible volatiles, etc. The vaporous products of combustion of carbonaceous polymer are mainly CO and CO_2 (it is considered that CO_2 is nontoxic, but it can reduce the concentration of oxygen in the air and harm human health when inhaled too much). When the polymers containing carbon, hydrogen and oxygen burn, its vaporous products contain aliphatic and aromatic hydrocarbon (such as butane and benzene), ketone (such as acetone), aldehyde (such as formaldehyde and acrolein), acid (such as acetic acid), ester (such as ethyl acetate), etc. Many polymers containing other elements besides carbon, hydrogen and oxygen generate vaporous products in the process of combustion, such as SO_2 and H_2S (polymer-containing sulfur), NH_3, HCN, NO_3 (polymer-containing nitrogen) and HX (polymer-containing halogen). Some of the above products have severe corrosion. The toxic vapors produced in the combustion under different conditions are shown in Figure 1.10 [1].

CO is the most common toxic vapor in fire, which is produced by the incomplete combustion of materials. It is easily generated in the following situations:

(1) Insufficient heat supply in the vapor phase (e.g., smoldering).
(2) The flame is quenched (e.g., polymers contain halogen chemical component or excessive ventilation extinguishes the flame).
(3) Polymer with thermal stable structure (e.g., aromatics chemical component): Because these chemical components can stay longer in flames, it produces much CO in good ventilation conditions and produces even more under limited ventilation conditions.
(4) Insufficient oxygen supply: When ventilation is poor in fire, a lot of radiant heats makes polymer pyrolysis, whereas it cannot burn completely for lack of oxygen.

However, it is difficult to simulate poor ventilated combustion in small-scale experiments. Smoldering generates the highest amount of toxicants, but its combustion rate is much lower than combustion.

Large-scale fire test data show CO and a large amount of HCH is generated in toxic vapors when reducing the intensity of ventilation.

Generally, it is difficult to estimate the density of toxicant in the combustion of polymers accurately. It is true in both small-scale combustion tests and the experiments simulating real fire cases, let alone in real fire scenes.

Identification and analysis of all toxicant are difficult. The current science level also cannot predict the comprehensive hazard of the mixture of

```
        ┌──────────┐
        │   High   │
        │ polymer  │
        └──────────┘
             │ Heat
             ↓
        ┌──────────┐   Smoldering   ┌─────────────────────────┐
        │ Cracking │───────────────→│ Combustion products are │
        └──────────┘                │ rich in organic matter  │
             │                      │ and incomplete oxidation│
             │ Ignite               │ produces                │
             ↓                      └─────────────────────────┘
  ┌────────────────────────┐  Adequate ventilation  ┌─────────────────────────┐
  │ Bright burning (large  │───────────────────────→│ Most of the combustion  │
  │ heat flow, fast        │                        │ products are CO₂ and H₂O│
  │ pyrolysis of polymers) │                        │ (also SO₂, NO₂, acrolein│
  └────────────────────────┘                        │ and formaldehyde)       │
             │                                       └─────────────────────────┘
             │ Limited ventilation
             ↓
  ┌────────────────────────────────┐
  │ Combustion products are rich in│
  │ CO, smoke, organic matter and  │
  │ HCN (such as organic compounds │
  │ containing N)                  │
  └────────────────────────────────┘
```

Figure 1.10: The toxic vapors produced in the course of combustion of polymer.

diversified toxicants with different concentrations on human bodies. We usually observe the overall effects of the mixture of toxic vapors dispersed by materials in the course of combustion on animals, and its result can be expressed by the time and density, which can have a certain effect, such as the necessary time or density of toxicants for the death of half the amount of all animals (LC_{50}).

To analyze the danger of combusting exhaust vapors, we must know the combustion rate and the toxicant yield. Steady-state tube furnace test can measure the relationship between the amount of toxicant generated in a particular polymer and combustion conditions. A more complete test program related to the toxicity of fire vapors has been developed. The toxicants generated by some polymers in air combustion are shown in Table 1.13.

1.8 Corrosive combustion products

In general, all organic polymers will produce corrosive vaporous products in the process of pyrolysis and combustion. Even the pyrolysis or combustion products of wood, wool and cotton have corrosive effect on metal. PVC and polymers

Table 1.13: Main toxicants products generated by some polymers in air combustion (measured by infrared spectroscopy) [49].

Polymers	Toxicants combustion products/polymer (mg/g)								
	CO_2	CO	SO_2	N_2O	NH_3	HCN	CH_4	C_2H_4	C_2H_2
PE	502	195					65	187	10
PS	590	207					7	16	6
PA66	563	194			4	26	39	82	7
PAAM	783	173			32	21	20	13	4
PAN	630	132				59	8		
Acrylic fiber	1400	170				95			
Polyphenylene sulfide	892	219	451						
PU	625	160				1	17	37	6
RPUF	1400	210				8			
EPR	961	228				3	33	5	6
UFR	980	80				2			
UFF	1350	41				15			
MFR	702	190		27	136	59			
deodar	1397	66					2	1	
Wool	1260	180				54			

containing halogen flame retardants can produce highly corrosive hydrogen halides during pyrolysis. However, the materials with high halogen content are not equal to high corrosion. The corrosivity of combustion products of some polymers is shown in Table 1.14.

1.9 Flame retardation patterns

Flame retardation patterns can be divided into physical and chemical patterns and can also be divided into condensed and vapor phase, but this classification is parallel, for example, condensed phase char and intumescent type can be considered as chemical type. The following are classified by physical and chemical patterns [1, 36, 51, 52].

1.9.1 Physical model

(1) Cooling, such as endothermic reactions, can cool a burned polymer.
(2) The coating can be used as a mass-transfer and heat-transfer barrier, which prevents heat and oxygen from passing to polymer and prevents the combustible vapor escaping from vapor phase.
(3) Dilution of the released water vapor and CO_2 can dilute the free radicals and fuel concentrations in the combustion zone.

Table 1.14: Corrosion of the combustion products of some polymers measured by cone calorimeter (50 kW/m^2).

Material	The average loss for 24 h/metal	Material	The average loss for 24 h/metal (45,000 for probe)
XLPO elastomer (metal hydroxide filler)	3	XLPO copolymer (inorganic filler)	8
HDPE/CPE	23	XLPO copolymer (containing alumina trihydrate filler)	1
CPE (filler)	10	EVA (inorganic filler)	6
EVA (containing alumina trihydrate filler)	2	PO (inorganic filler)	7
PPO/PS	2	XLPE copolymer (chloride additive)	26
PI	1	Polyvinylidene fluoride two PVDF	31
PI/PSI	3	PVC	70
PP (expansion type)	3	PA66	23
PO copolymer (inorganic filler)	3	XLPE copolymer (brominated additive)	6

1.9.2 Chemical mode

(1) The vapor-phase reaction interferes with the free radical reaction in the combustion zone and makes the concentration of free radical drop below the critical value of combustion.
(2) Condensed phase reaction.

The cross-linking, grafting, aromatization and catalytic dehydration char layer forming contribute to the formation of char layer, such as by the removal of polymer side bonds, formation of double bonds and finally formation of a multi-aromatic ring carbon layers.

Forming intumescent protective layer: By adding intumescent flame retardant or foaming agent into polymer, and through certain chemical reaction, the surface polymer can form intumescent-type mass-transfer and heat-transfer barrier.

Condensed-phase and vapor-phase flame retardance have long been recognized as two main flame-retardant modes. The former mainly contributes to the charring of materials, whereas the latter mainly slows down the chain oxidation reactions in flame.

However, some new flame-retardant mechanisms have been proposed in recent years, especially those based on physical principles. This mechanism has led to a better understanding of flame retardancy. In fact, in many cases, the realization of flame retardant is often the result of the combined action of several flame-retardant modes, and it is difficult to attribute it to the effect of a single flame-retardant mechanism.

Flame retardancy is a complicated process, and the flame retardant of condensed phase can not be completely separated from that of vapor phase. The condensed-phase flame retardant on one hand can alter the reaction equilibrium by reducing volatile pyrolysis products, and on the other hand, the material may form a char layer with low thermal conductivity at the burning zone boundary due to the polymer rheology state change by gas produced by pyrolysis. Therefore, the flame retardant in the condensed phase will directly affect the combustion process in the vapor phase. The vapor-phase flame retardant can reduce the degree of vaporification of polymers and inhibit the combustion of polymer pyrolysis products and can also reduce the heat release of combustion and increase the radiation heat loss due to the increase of char layer formation.

The objective of flame retardation of polymeric materials is to make polymers difficult to ignite (such as extending ignition time), to slow the spread of combustion, to reduce the rate of combustion heat releasing and to make attenuation or self-extinguishment of combustion easier. But the problem now is that the above-mentioned tests of properties of flame-retardant polymers are mainly small scale. A number of predicative mode have been developed, which enable scientists to make a big step forward to roughly predict the behaviors of flame-retardant polymers in real fire cases through the results of some small-scale or large-scale experiments. It has become possible for some certain polymers to conduct above-related analysis and has also made a success to some extent. However, it is hard and even impossible to compare the flame resistance of polymers in different combustion tests and predict the flame resistance accurately in different fire cases because the performances of polymers vary in different fire situations. Furthermore, the size of text sample is crucial to the results of combustion test, especially when the number of sample is large. Moreover, polymers and their added components are extremely diverse and varied, and the pyrolysis ways of polymers are quite different, which make flame retardant more complex. Therefore, flame-retardant method cannot be copied from one polymer to another.

References

[1]   Hull T R, Stec A A. Polymer and Fire [A]. Hull T R. Kondola B K. Fire Retardancy of Polymer, New Strategies and Mechanisms[M]. Cambridge (UK): Royal Society of Chemistry, 2009. 1–4.
[2]   Ou Yuxiang, Flame Retardant Plastics Handbook [M]. Beijing: National Defence Industry Press. 2008. 5–6.

[3] Zhang Jun, Ji Kuijiang, Xia Yanzhi. Polymerization of Combustion [M]. Beijing: Chemical Industry Press, 2005.1–28.

[4] Hilado C J. Flammability Handbook for Plastics (5th edition) [M]. Lancaster (UK): Technomic Publishing Co. Inc, 2000. 1–63

[5] Ou Yuxiang, Practical Flame Retardant[M]. Beijing: Chemical Industry Press, 2003.5–10.

[6] Hopkins D, Quintiere J G. Material Fire Properties and Predictions for Thermoplastics [J]. Fire Safety Journal, 1996, 26(3): 241–268

[7] Milles N. Plastics [M]. Amsterdam (Netherland): Elsevier Publisher, 2005. 302–306.

[8] Lin Shangan, Lu Yun, Liang Zhaoxi, Polymer Chemistry[M] Beijing, Science Press. 1987.703.706

[9] Karlsson B. The Combustion Process and Enclosure Fires [A]. Troitzsch J. Plastics Flammability Handbook (3rdedtion) [M]. Munnich (Germany); Hanser Publishers, 2004.33–46.

[10] wilkie C A, mckinney M A. Thermal properties of thermoplastics [A]. Troitzsch J Plastics Flammability Handbook (3rd edition) [M]. Munnich (Germany); Hanser Publishers, 2004.58–76.

[11] Jamieson J,Macnill J C, Degradation of Polymer Mixtures, IV. Blends of Poly(vinyl acetate) with Poly(vinyl chloride) and Other Chlorine-Containing Polymers [J],Journal of Polymer Science, 1974,12(2);387–400.

[12] Fried J. Polymer Science and Technology(2rd edition)[M]. Upper Saddle River(NJ, USA); Prentice Hall 2003, 268.

[13] Wypych G, PVC Degradation and Stabilization [M], Tronton(Canada); Chemtee Publishers, 2008, 98–103.

[14] Winkler D E, Mechanism of Poly(vinyl chloride) Degradation and Stabilization [J]. Journal of Polymer Science, 1959,35(128);3–16.

[15] Starnes W H. Structural and Mechanistic Aspects of the Thermal Degradation of poly(vinyl chloride) [J], Progress in Polymer Science, 2002.27(10):2133–2170.

[16] Hoang T V,Guyot A. PolaronMechanism in the Thermal Degradation of poly(vinyl chloride) [J], Polymer Degradation and Stability,1991.32(1);93–103.

[17] Troitskii B B, TroitsKaya L S, Mathematical Mode of the Initial Stage ofthe Thermal Degradation of Poly(vinyl chloride) [J], European Polymer Journal,1995,31(6);533–539.

[18] Li Jianjun, Huang Xianbo, Cai Tongming, Flame Retardant Styrene Plastic [M]. Beijing: Science Press, 2003.261.

[19] Scott D S, Czernik S R, Piskorz J, et al. Fast Pyrolysis of Plastic Wastes [J],Energy Fuels,1990,4 (4);407–411.

[20] Williams P T, Williams E A, Recycling Plastic Waste Pyrolysis [J].Journal of the Institute of Energy. 1998,71(487):81–93

[21] Kashiwagi T, Radiative Ignition Mechanism of Solid Fuels [J], Fire Safety Journal,1981,3:185.

[22] Akita K, Ignition of Polymers and Flame propagation on polymer Surface[A].Jellinek H H G. Aspects of Degradation and Stabilization of Polymers [M], Amsterdam (Netherland); Elsevier Scientific Publication 1978:500–525.

[23] Wang Yongqiang, Flame Materials and Application technology [M], Beijing: Chemical Industry Press, 2004:50–70.

[24] Hshieh F Y, Stoltzfus J M,Beeson H D, AutoignitionTemperature of Selected Polymers at Elevated Oxygen Pressure and Their Heart of Combustion [J],Fire and Materials, 1996,20(60);301–303.

[25] Blasi C D. The Combustion Process [A]. Troitzsch j. Plastics Flammability handbook (3rd edition) [M], Munnich (Germany);Hanser Publishers,2004,47–58.

[26] kashiwagi T A, Radiative Ignition model of a Solid Fuel [J]. Combustion Science and technology, 1974,146(80):225.

[27] Kindelan M, Williams F A,Vapor-Phase Ignition of a Solid with in-Depth Absorption of Radiation [J], Combustion Science and technology, 1974,146(8);225.

[28] kashiwagi T, Kotia G G, Sunmmerfeild M, Experimental Study Ignition and Subsequent Flame Spread of a solid Fuel in a Hot Oxidizing Vapor Steam[J],Combustion and Flame, 1975, 24:357–364.

[29] Fernandez-Pello A C, Hirano T, Controlling Mechanism of Flame Spread [J], Combustion Science and Technology,1983,32:1.

[30] Ou Yuxiang, Chen Yu, Wang Xiaomei, Flame Retardant Polymer Materials[M], Beijing National Defense Press, 2001, 2–35.

[31] Williams F A, Mechanisms of Fire Spread [A], Proceedings of the 16th international Symposium on Combustion [C], Pittsburgh(USA);the Combustion Institute, 1976, 1281–1294.

[32] Sirignano W A, A Critical Discussion of Theories of Flame Spread Across Solid and Liquid Fuels [J], Combustion Science and Technology, 1972,6:95–105.

[33] Ou Yuxiang, Performance, Manufacture and Application of Flame Retardant[M], Beijing: Chemical Industry Press, 2006,22–39.

[34] Karlsson B, Quintiere J G. Enclosure Fire Dynamics [M]. Boca Raton(FL,USA): CRCPress,1999,81–138.

[35] Rubin P A.SOFIL-Simulation of Fires in Enclosures[A], Proceedings of the 5th international Symposium on Fire Safety Science [C], Melbourne (Australia); International Associational for Fire Safety Science, 1997-03-3/7.

[36] Ou Yuxiang, Li Jianjun, Testing Methods of Flame Retardant Performance of Materials [M]. Beijing: Chemical Industry Press, 2007,18–19.

[37] Dong Mingyan, Analysis of Utilization of Polymer Materials [M],Beijing: Chemical Industry Press, 1997,27.

[38] Editors. Characterization and Failure Analysis of Plastic(3rd Printing) [C]. Materials Park (OH, USA);ASM International, 2005,129.

[39] Innes J D, Cox A W, Smoke: Test Standards, Mechanism, Suppressants [J]. Journal of Fire Sciences, 1997,15(3):227–239.

[40] Green J, Mechanism for Flame Retardancy and Smoke Suppressants. A Review[J]. Journal of Fire Sciences, 1996,14(6):426–442.

[41] Ou Yuxiang, Fire Retardant[M]. Beijing: Weapon Industry Press, 1997, 129–130.

[42] Xue enjue, Zeng Minxiu, Flame Retardan Science and Application[M], Beijing: National Defence Idustry Press, 1998,39.

[43] Weil E D, Levchik S V. Flame Retardants for Plastics and Textiles [M]. Munich (Germany): Hanser publishers. 2009,241–252.

[44] Lewin Menachem, Weil Edward. Mechanism and Modes of Action in Flame Retardancy of Polymers[A]. Price D Fire Retardant Materials[M], Cambridges(UK); WoodheadPublishing Ltd,2001,31–57.

2 Flame retardation mechanism of halogenated flame retardants

Halogenated (brominated and chlorinated) flame retardants (FRs) contain either single halogen FR or halogen/antimony synergistic combination, but the latter is dominant in actual applications. Halogenated FRs have been widely used for decades. Systematic and in-depth researches have been done on the flame-retardation mechanism and a large number of papers have also been published. Further details can be found especially in literatures [1–4]. Even today, this kind of mechanism still has not been fully understood, but experts2 in FR area have formed a consistent view that halogenated FRs mainly work in gas phase. Furthermore, increasingly growing evidences have been found in FR behaviors in condensed phase.

2.1 Flame retardation mechanism of single halogen FRs

Halogenated FRs work mainly through gas phase. It can restrain gas-phase chain reaction, and its decomposition products can be used as inert substances to dilute fuel concentration and serve as a cover to function a so-called blanketing effect. This kind of FR, of course, also has certain FR effects in condensed phase.

2.1.1 Flame retardation mechanism in gas phase

It is well known that some substances which can react with oxygen in the atmosphere will be produced in the course of thermal cracking of polymers, forming H_2–O_2 system, and combustion propagation is progressing through branched chain reaction [(2.1) and (2.2)] and exothermic reaction (2.3) [5].

$$H\cdot + O_2 \longrightarrow \ \cdot OH + \cdot O \qquad (2.1)$$

$$O\cdot + H_2 \longrightarrow \ \cdot OH + \cdot H \qquad (2.2)$$

$$OH\cdot + CO \longrightarrow \ CO_2 + H\cdot \qquad (2.3)$$
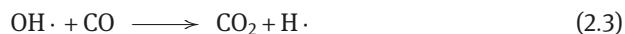
To reduce or terminate burning, the above chain-branching reactions should be prevented. The flame retardancy of halogenated FRs was at first realized by inhibiting chain-branching reaction in gas phase. For halogenated FRs with no hydrogen, X· is usually liberated when heated. If they contain hydrogen, HX is released first in thermal decomposition. These are separately shown in reactions (2.4) and (2.5) [1].

$$MX \longrightarrow M\cdot + X\cdot \tag{2.4}$$

$$MX \longrightarrow H\cdot M + X'\cdot \tag{2.5}$$

M· or M'· in the above reaction shows the rest of FR after releasing X· or HX. In addition, X· produced in reaction (2.4) also reacts with fuel to generate HX (eq. (2.6))

$$RH + X\cdot \longrightarrow HX + R\cdot \tag{2.6}$$

HX can really influence chain branching. It captures highly reactive H· and OH·, producing low activity X· to mitigate or stop burning [eqs. (2.7) and (2.8)] [6].

$$H\cdot + HX \longrightarrow H_2 + X\cdot \tag{2.7}$$

$$OH\cdot + HX \longrightarrow H_2O + X\cdot \tag{2.8}$$
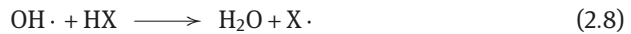
Reaction velocity of H· with HX is twice as that of HX with OH·[6]. H_2/OH ratio in flame front is high, so the reaction of H· with HX (2.7) might be the main FR reaction, and competition between this reaction and the one of H· with O_2 is a decisive factor for FR efficiency. In reaction of H· with O_2, two free radicals are formed by consuming one H·. Moreover, for reaction of H· with HX, consumption of an H· helps to form a low-activity X· which is able, in turns, to produce stable halogen molecules by itself.

Reaction (2.7) in which H· combines with HX to give H_2 and X· is a reversible reaction. There is a balance between positive reaction and adverse reaction. The equilibrium constant of (2.7) for HCl or HBr is shown in formulas (2.9) and (2.10) [7].

$$K_{HCl} = 0.583\exp(1097/RT) \tag{2.9}$$

$$K_{HBr} = 0.374\exp(16760/RT) \tag{2.10}$$

When temperature tends to be high, the above equilibrium constants are reduced greatly; so, the FR efficiency of halogen derivatives declines in fire. That is to say, temperature has a strong impact on the FR efficiency of halogen-containing compounds. When temperature is between 1200 and 1300 °C or higher in fire zone, bromine can act as an oxidizer and is able to catalyze chain reactions in gas phase, showing no FR effects. Calculation shows that reaction of H· with HX goes mainly toward positive side with temperature range between 230 and 1230 °C, and K_{HBr} is far larger than K_{HCl}. Around ignition temperature of polymers, both bromide and chloride have high flame retardancy.

Reactions (2.1) and (2.2) increase the concentration of free radicals in gas phase, whereas reaction (2.3) gives off a lot of heat to increase the temperature in gas phase.

Based on mass spectrometry analysis obtained from CH_4/O_2 mixture in low-temperature fire, addition of halides into the mixture helps to detect HX in early

combustion products and increases the concentration of H_2 [8]. It is proved that on burning, reaction (2.7) goes rapidly and competes with chain-branching reaction (2.1) in an effective manner in front flame area. Furthermore, the measured flame retardancy is higher than the expected based on the reaction balance.

In addition, X· produced by reactions (2.7) and (2.8) can react with combustible gases and volatile products, such as RH, generated from polymer thermolysis to form HX; thus, flame resistance is processing in a catalytic way (eq. 2.11) [9].

$$X \cdot + RH \longrightarrow HX + R \cdot \qquad (2.11)$$

Researchers have not yet drawn a consistent conclusion for reaction of OH· with HX (2.8) [10]. But for the combustion and explosion of styrene/O_2 mixture in low pressure, production of OH· can be delayed when there is HBr.

In high-temperature flame area, there is a balance between H·, OH· and O·; reducing the concentration of any one of the three may inhibit the chain-branching reaction.

The reason for a low flame retardancy of fluorides is that reaction of HF with H· [see reaction (2.7)] is difficult to happen because of high activation energy, whereas a low flame retardancy of iodides is because of the difficulty to produce HI when RH reacts with I·, and R· can combine with I· to form RI (2.12) [11].

$$R \cdot + I \cdot \longrightarrow RI \qquad (2.12)$$

The FR efficiency of chlorides is lower than bromides. This is because of the fact that reaction of HCl with H· [reaction (2.7)] is close to hot neutral, which is also likely to go in the reverse direction, namely to regenerate H·.

The mechanism of halogenated FRs is based on the breakage of C–X bonds. The thermal stability of C–X bonds is C–F>C–Cl>C–Br>C–I, and the corresponding bond energy and initial degradation temperature of bonds are shown in Table 2.1 [3].

Table 2.1: Bond energy and initial degradation temperature of bonds [3].

Bond	Bond energy (kJ/mol)	Initial degradation temperature (°C)
C_{aliph}–F	443–450	>500
C_{arom}–Cl	419	>500
C_{aliph}–Cl	339–352	370–380
$C_{benzilic}$–Br	214	150
C_{aliph}–Br	285–293	290
C_{arom}–Br	335	360
C_{aliph}–I	222–235	180
C_{aliph}–C_{aliph}	330–370	400
C_{aliph}–H	390–436	>500
C_{aliph}–H	469	>500

Halogenated FR's efficiency relates to strength of C–X bonds. C–I bond energy is too low, and iodides cannot be used as FRs. Although fluorine derivatives are quite stable, thus unfavorable to quench free radicals from fire, they are not suitable for being FRs. But some fluorides are suitable for X/Sb synergistic systems [12]. In addition, bond strength and stability of aliphatic halogen derivatives are relatively lower, and they are easier to decompose. In general, HX molecules can be generated at lower temperature for aliphatic compounds; thus, their FR efficiency is higher than that of the corresponding aromatic derivatives (see Figure 2.1) [4]. However, the thermal stability of aromatic bromides is higher than that of the aliphatic, but the light stability is the opposite. Bromide's FR efficiency is better than that of chlorides. This is mainly because C–Br bond energy is relatively low, and in the process of burning, bromides generate Br· and HBr at the right time. Meanwhile, although HCl can be generated in a larger temperature range, in the front of flame their, concentration tends to be relatively lower. Some highly volatile FRs may be gasified to provide halogens for flame before their decomposition.
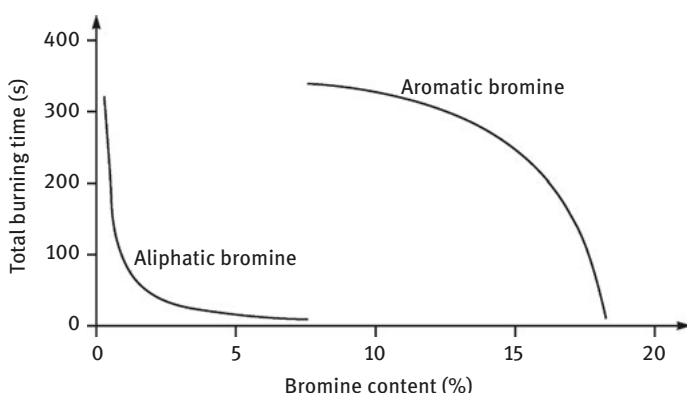
Figure 2.1: Comparison of flame retardancy between aliphatic and aromatic bromides in polypropylene (PP) [4].

Recently, it was found that the flame retardancy of NH_4Br is very good for PP, and in this case, the limiting oxygen index (LOI) produced by unit of bromine, namely LOI/Br (mass ratio), is as high as 1.24. For aliphatic bromides, this value is only 0.6 [13]. This is possibly because of the fact that the necessary decomposition energy of NH_4Br into NH_3 and HBr is far lower than C–Br bond dissociation energy.

Derivation of vapor flame retardancy of halides is mainly that they capture free radicals which transmit thermal oxidation in flame. Researchers sometimes used FR volume required to extinguish *n*-heptane/air flame to characterize the efficiency of FRs [14].

The flame retardancy of halides has some relations with burning conditions (such as external heat flux) of flame-retarded materials [15].

For chlorides and bromides, however, when they are used in flame retard some polymers, the efficiency of Br is about 1.7–2.0 times than that of Cl. For example, comparing the FR efficiency of tetrahalogenated phthalic anhydride for polyester, 13% of bromine is equivalent to 22% of chlorine. Similar patterns can also be found when this anhydride is used to flame retard PP, polystyrene (PS) and polyacrylonitrile (PAN). In addition, comparing NH_4Cl to NH_4Br for flame-retarding cellulose, the FR efficiency of bromine is higher than chlorine about 70% [16].

When halides are used to flame retard polymers, the structures and performances of FRs and polymers have an important effect on FR efficiency. For example, when ratio of chlorine to carbon is 0.1 (mass) in the flame-retarded polymers, LOI of polyester with chlorinated FR is quite different from that of chlorinated polyester, of which the former is 23% and the latter is 29% [1].

For copolymer of bromoethylene and methyl methacrylate, bromoethylene's influence on LOI is not important; however for copolymer of bromoethylene and acrylonitrile or styrene, bromoethylene has a great effect on LOI. In addition, researches showed that almost all of the bromine content in materials will be transferred into gas phase on combustion. According to statistics, when flame temperature ranges from 850 to 1150 °C, halogenated FRs have a good inhibition effect on chain reactions of combustion. This effect of halogens containing in polymer molecules is better than that of mechanically incorporated halides in polymers.

Some researches suggested that after addition of a small amount of halogenated FRs into polymers, the flame propagation speed will be reduced one order of magnitude, and the necessary threshold energy for igniting material can also be greatly increased [1].

2.1.2 Development of flame retardation mechanism in gas phase

Today, the widely accepted flame retardation mechanism in gas phase is the interruption mechanism of combustion chain reactions. It is generally believed that the flame retardancy of halogenated FRs mainly depends on the reaction of released HX from FRs with free radicals formed in combustion, that is, the following equilibrium reaction.

$$H\cdot + HX \rightleftharpoons H_2 + X\cdot \qquad (2.11)$$
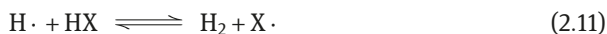
But from 200 to 1200 °C, the balance of (2.11) is quite related to temperature. The efficiency of HBr for capturing hydrogen radical greatly decreases with temperature higher than 700 °C. Moreover, at $T > 700$ °C, the halogenated FRs display little FR action.

However, the aforementioned conclusion widely accepted has not been verified by experiments; so, relevant discussions are still needed. First, the FR functions of

halogenated FRs should not just be chemical reactions of cleaning the free radicals. There are some physical effects. For example, heat of decomposition and heat of vaporization of FRs as well as halogen molecule concentration in flame are all related to flame retardancy, whereas these factors have little connection with temperature [17]. Therefore, relevant experiments have become a necessity. They should demonstrate whether the flame retardancy of halogenated FRs will decrease with the increase of temperature, and the relationship between decreasing amplitude of efficiency and the variation of temperature needs to be understood. The synergistic effect between bromine and chlorine is another related topic. The best FR efficiency can be realized with the presence of antimony trioxide (AO), and mass ratio of Br/Cl in FR system is 1:1 [18]. Lewin stated a possible explanation that bromine radicals and chlorine radicals can probably combine into active polar Br–Cl molecules in flame, which can react with hydrogen radicals more rapidly, producing additional HX molecules. Therefore, the ability of capturing hydrogen radicals is enhanced [19]. However, this is just a hypothesis and further supported experiments are still required.

It is also pointed out that except the pattern of gas phase, there is another pattern about the action of brominated FRs. For example, the synergistic effects can be found in polyacrylonitrile with ammonium polyphosphate (APP) and hexabromocyclododecane (HBCD), but the pattern of gas phase does not exist in this formulation [20]. This is also true for brominated phosphate. In accordance with this, we can speculate whether HBr released from flame-retarded polymer pyrolysis can be served as foaming agent to promote the inflation of carbon layer. Thus, here comes a question: whether HBr is a foaming agent and not a free radical capturing agent or is both foaming agent and free radical capturing agent to play the roles in other brominated FR system?

There remain some points which need to be further studied: first, whether NH_4Br in polymers shows better FR efficiency than other aliphatic and aromatic brominated FRs; second, whether this is the result from synergistic effects between bromine and nitrogen; third, whether NH_4Br can release HBr before polymer pyrolysis due to the lower decomposition temperature of NH_4Br than other bromine derivatives [21].

2.1.3 Flame retardation mechanism in condensed phase

One of the methods to distinguish between gas phase and condensed phase is to measure LOI of FR materials in O_2/N_2 and N_2O/N_2, respectively. In the case of gas phase, LOI of flame-retarded materials in N_2O/N_2 hardly changes with the variation of FR's loading, whereas LOI's change history is a different picture in O_2/N_2 and a maximum record often can be observed. One reason for this phenomenon is that in gas pattern, O_2 in O_2/N_2 system is mainly used in branching

reaction $O_2 + H\cdot \rightarrow OH\cdot + O\cdot$, but N_2O in N_2O/N_2 is mainly used in nonbranching reaction $N_2O + H\cdot \rightarrow OH\cdot + N_2$. Clearly, the best fire-retarding effect is inhibiting the abovementioned branching reaction, whereas the nonbranching reaction, which involves N_2O, has little effect on flame retardancy in gas phase.

Recent researches have shown that halogenated FRs also have fire-retarding effects in condensed phase [1]. Some halogen compounds release halogens and hydrogen halides, and the remainders in condensed phase become coke residue through cyclization and condensation. The residue formed can act as protective barrier of fire proof, preventing the material below to be oxidatively cracked. Besides, some halogen compounds might change the reaction mechanism in flame and in anterior flame zone, promoting the formation of char and increasing the loss of radiant heat.

For example, some halogen free radicals released from halogenated FRs can form a double bond with some polymer chains (see reaction (2.12)).

$$X\cdot + -CH_2 - CH_2 - \xrightarrow{-HX} -H\overset{\centerdot}{C} - CH_2 - \xrightarrow{-H\cdot} -CH = CH - \qquad (2.12)$$

Double bond can cause crosslinking or char-forming by aromatization. Halides react with hydrogen on aromatic rings, and the formed aromatic compounds further react with other aromatic rings to give polyaromatics which are precursors of graphite carbon, whereas the char-forming is a very typical condensed-phase reaction [1].

Aliphatic brominated FRs have a different mechanism from charring flame-retardation mechanism in condensed phase. Bromine radicals in polymer melts can induce the bond cleavage on territory carbon at polymer chains (2.13) [22, 23].
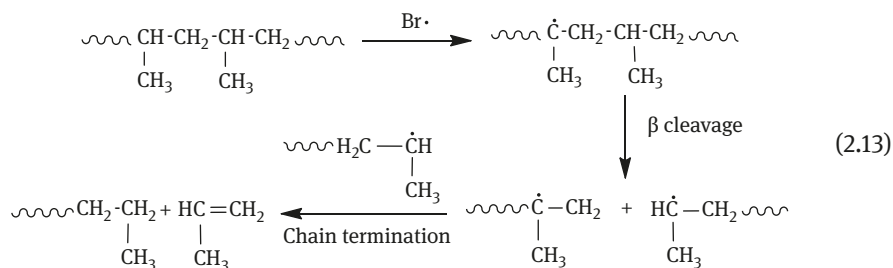
This bond rupture makes polymer melts drop quickly, lowering the temperature of the melts to their self-extinguishing point. Incorporation of a very small amount (0.01–0.5%) of polytetrafluoroethylene (PTFE) onto polymers with halogenated FRs can effectively inhibit the fusant from dropping. The reason is that under polymer processing temperature (200–300 °C), PTFE particles will soften, and the extrusion screw shear force will stretch the softening particles to microfiber. The fiber's length is as 5 times as that of the original particles. When polymer burns, the microfiber in the fusant retracts, thus forming a kind of network structure and inhibiting the fusant from dropping.

The LOIs respectively measured by polyethylene/chlorinated paraffin (PE/CP) in O_2/N_2 and N_2O/O_2 illustrate that FR actions in this system probably proceed in condensed phase [24, 25]. Adding a lot of Cl_2 or HCl into O_2/N_2 does not affect the LOI of PE/CP system. What is more, the LOI of PE/30% CP in O_2/N_2 is 22%. If CP from which a certain amount of HCl was removed at high processing temperature was used for PE, LOI of PE/30% CP (in O_2/N_2) still remains to be 22% [3]. All of these illustrate further the condensed phase FR effects of PE/PC. But FR functions of CP to PP mainly occur in gas phase. For PP/CP (30%), its LOI is 28%, and after abstracting part of HCl from CP, the LOI of PP/CP (30%) decreases to 22% [3].

The difference of flame-retardation mechanism between PE/CP and PP/CP is because of the fact that CP causes PE crosslinking at high temperature, whereas PP induces chain fracture. For example, keeping PE/CP (30%) or PP/CP (30%) in N_2 at 260 °C for a certain time, crosslinking occurs in the former, whereas the relative molecular mass of the latter falls from nearly 10^5 to about 10^4 [3]. In addition, CP can also change the composition of volatile products released from PE (PP)/CP at a high temperature.

In fact, the FR performances of any FR are often a result from combined actions of several kinds of flame retardation mechanisms.

2.2 Flame retardation mechanism of halogen/antimony synergistic system

2.2.1 Overview

To improve the efficiency of FRs, halogen derivatives are usually used with synergistic agents altogether. A number of synergistic agents are available among which the most important one is Sb_2O_3 (Sb_2O_3 itself is of no FR effect). The action modes of various synergistic agents are quite different, among which are capture mechanism of free radicals, flame retardation mechanism in condensed phase, expansion effects, and physical actions. Moreover, the synergistic efficiency (SE) of different agents varies greatly.

The so-called synergistic system refers to a FR system containing two (one is a FR, the other is an agent possessing synergistic functions) or more than two components; however, the system's FR effects are better than the sum of FR effects determined by all of the single components. To compare different synergistic systems, the term "synergistic efficiency" was introduced. SE is defined as FR efficiency (EFF) ratio on certain loadings of synergistic system to single FR (without synergistic agent), and EFF is defined as the increase of LOI of flame-retarded matrix (loadings are within a certain range) by unit mass of FR elements. In most cases, SE value is calculated according to the results of synergistic system with optimum FR efficiency.

SE values of two synergistic systems: Aromatic bromide/Sb_2O_3 and aliphatic bromide/Sb_2O_3 are, respectively, 2.2 and 4.3. SE value of polystyrene with aliphatic chloride/Sb_2O_3 is 2.2 (calculated value) [1]. Formulations based on halogen/antimony systems are widely used in all kinds of polymers, such as cellulose, polyester, polyamide, polyolefin, polyurethane, polyacrylonitrile, polystyrene, etc.

X/Sb synergistic system also has FR actions in both gas phase and condensed phase, but the former is generally the priority.

2.2.2 Flame retardation chemical mechanism of X/Sb synergistic system in gas phase

Synergistic FR effects of antimonides to halides were found when using CP/Sb_2O_3 to treat cellulose. These kinds of effects were observed later in FR by involving a series of polymers. Gas activator of X/Sb system was originally considered to be SbOX released from the flame-retarded polymers when heated; so, the atom ratio of X to Sb of X/Sb system was 1:l when used. Later, it was found that when the atom ratio was increased to 2:1 or even 3:1, the FR efficiency improved [26].

Chemical flame retardation mechanism of X/Sb system in gas phase is based on (1) insulation of oxygen owing to high density vapor of SbX_3 and $Sb_nO_mX_p$; (2) inhibition of chain oxidation reactions (chemical inhibition from X and physical inhibition of wall effect) [27]; (3) increase of X's lifetime by $Sb_nO_mX_p$ intermediates, and free radical reactions interfering combustion propagation [28].

Most of Sb is evaporated or transferred to charcoal when X/Sb flame-retarded materials are burning.

The action modes of halogen/antimony synergistic system are mainly based on mechanism in gas phase. In general, on thermal cracking of flame-retarded polymers with this system, HX is first released from decomposition of halogen-containing compound itself or its reactions with Sb_2O_3 or with polymer. Then, HX reacts with Sb_2O_3 to form SbX_3 and SbOX. Although in the first stage, the thermal cracking generates a certain amount of SbX_3, mass loss of material also indicates that some other antimony compounds (antimony oxyhalides) with low volatility are also formed, probably by halogenation of Sb_2O_3. In this process, gaseous SbX_3 escapes to gas phase, whereas SbOX (a strong Lewis acid) remains in condensed phase, promoting the cleavage of C–X bond.

Speaking further, halogenation of Sb_2O_3 gives a series of compounds $Sb_nO_mX_p$ (with higher X content) which can heat disproportionate into $Sb_xO_yX_z$ (with lower X content) and volatile SbX_3. This disproportionation is related to temperature, and relative stability and chemical reactivity of $Sb_nO_mX_p$. Some Lewis acids are catalysts of dehalogenation process [29].

FR effects of SbX_3 are mainly derived from two functions: first, providing HX in early stage of combustion; second, forming a cloud composed of fine particles of

solid SbO in center of combustion zone. Flame retardancy of SbO has nothing to do with HX. For example, single Ph_3Sb has good FR actions for epoxy resin. The reason is that Ph_3Sb with low volatility is susceptible to oxidation, forming SbO in gas phase and playing FR roles [30]. In addition, SbO is so stable in flame that it can catalyze combination of H·, O·, HO· and other free radicals.

Referring to literature [1–4], chemical reactions of X/Sb system in gas phase may be summarized in eqs. (2.14)–(2.38). At high temperatures, Sb_2O_3 reacts with HX generated by the decomposition of halogenated FRs, giving SbX_3 and SbOX [(2.14) and (2.15)].

$$Sb_2O_3(s) + 6HX \longrightarrow 2SbX_3 + 3H_2O \tag{2.14}$$

$$Sb_2O_3(s) + 2HX \xrightarrow{250°C} 2SbOX(s) + H_2O \tag{2.15}$$
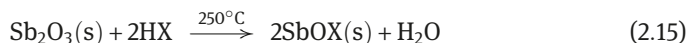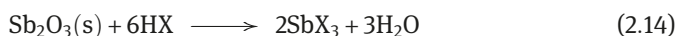
The generated SbOX further decomposes to SbX_3 and antimony oxyhalides [(2.16)–(2.18)].

$$5SbOX(s) \xrightarrow{245\sim280°C} Sb_4O_5X_2(s) + SbX_3(g) \tag{2.16}$$

$$4Sb_4O_5X_2(s) \xrightarrow{410\sim475°C} 5Sb_3O_4X(s) + SbX_3(g) \tag{2.17}$$

$$3Sb_3O_4X(s) \xrightarrow{475\sim565°C} 4Sb_2O_3(s) + SbX_3(g) \tag{2.18}$$
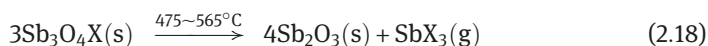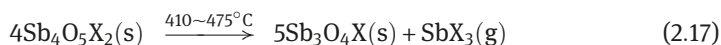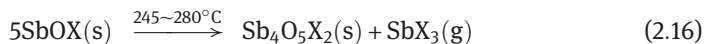
In addition, in higher temperature, solid Sb_3O_3 can be gasified (2.19).

$$Sb_2O_3(s) \xrightarrow{>650°C} Sb_2O_3(g) \tag{2.19}$$
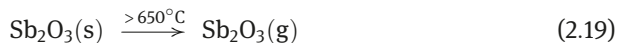
SbX_3 generated in the above reactions can capture active free radicals, change reactive modes and restrain combustion reactions in gas phase [(2.20)–(2.26)].

$$SbX_3 + H· \longrightarrow HX + SbX_2· \tag{2.20}$$

$$SbX_3 \longrightarrow X· + SbX_2· \tag{2.21}$$

$$SbX_3 + CH_3· \longrightarrow CH_3X + SbX_2· \tag{2.22}$$

$$SbX_2· + H· \longrightarrow SbX· + HX \tag{2.23}$$

$$SbX_2· + CH_3· \longrightarrow CH_3X + SbX· \tag{2.24}$$

$$SbX· + H· \longrightarrow Sb + HX \tag{2.25}$$

$$SbX· + CH_3· \longrightarrow Sb + CH_3X \tag{2.26}$$
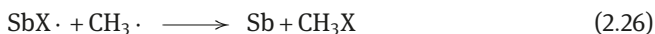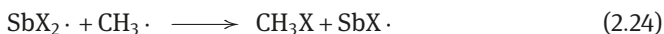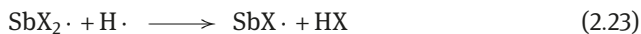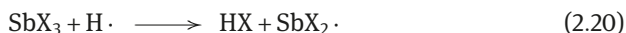
At the same time, the decomposition of SbX_3 can slowly release X· which can combine with active free radicals (such as H·) in gas phase and keep the time of quenching flame longer. This means that the life of radical scavengers is extended in combustion zone, increasing the probability of combustion reaction inhibition [(2.27)–(2.32)].

$$X \cdot + CH_3 \cdot \longrightarrow CH_3X \tag{2.27}$$

$$X \cdot + H \cdot \longrightarrow HX \tag{2.28}$$

$$X \cdot + HO_2 \cdot \longrightarrow HX + O_2 \tag{2.29}$$

$$HX \cdot + H \cdot \longrightarrow H_2 + X \cdot \tag{2.30}$$

$$X \cdot + X \cdot + M \cdot \longrightarrow X_2M \quad (\text{M is a material absorbing energy}) \tag{2.31}$$

$$X_2 + CH_3 \cdot \longrightarrow CH_3X + X \cdot \tag{2.32}$$
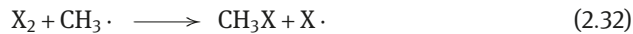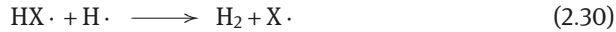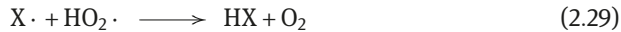
Finally, O· can react with antimony to form SbO in combustion reaction zone, and SbO can capture H· and OH· in gas phase. This also helps to stop combustion and makes flame self-extinguished [(2.33)–(2.38)].

$$Sb + O \cdot + M \longrightarrow SbO \cdot + M \tag{2.33}$$

$$Sb + O \cdot \longrightarrow SbO \tag{2.34}$$

$$SbO \cdot + 2H \cdot + M \longrightarrow SbO \cdot + H_2 + M \tag{2.35}$$

$$SbO \cdot + H \cdot \longrightarrow SbOH \tag{2.36}$$

$$SbOH + H \cdot \longrightarrow SbO + H_2 \tag{2.37}$$

$$SbOH + OH \cdot \longrightarrow SbO \cdot + H_2O \tag{2.38}$$
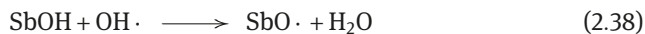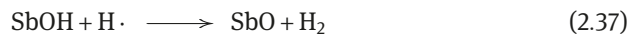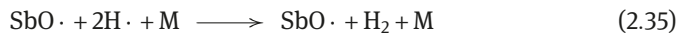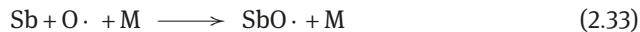
As for Br/Sb system, for example, polymer flame retarded with $DBDPO/Sb_2O_3$ generates mainly $Sb_8O_{11}Br_2$ on intensively heating or burning; however, $Sb_4O_5Br_2$ has not been detected in combustion products. This may be because of the fact that when $Sb_8O_{11}Br_2$ is brominated into $Sb_4O_5Br_2$, it rapidly eliminates $SbBr_3$ by hot disproportionation reaction [31].

The flame retardancy of SbX_3 in gas phase has already been acknowledged. For example, when SbX_3 was added into CH_4/O_2 combust, only Sb and SbO were found in flame, and Sb_2O_3 was discovered in the front-flame zone. SbX_3 has not been detected in flame [3] because it has the above reactions.

As for Cl/Sb system, regardless of whether HCl is released upon heating, $Sb_8O_{11}Cl_2$ is primarily generated on the approximate polymer combustion conditions, and $Sb_8O_{11}Cl_2$ further transforms to $Sb_4O_5Cl_2$ at high temperature. Thus, $Sb_4O_5Cl_2$ is the main antimony oxychloride. Then, $Sb_4O_5Cl_2$ becomes $SbCl_3$ by hot disproportionation or direct complete oxidation with low velocity. SbOCl is so active at high temperature that it is difficult to confirm its existence [3].

Figure 2.2 shows LOI curves [3] of $PP/CP/Sb_2O_3$ in O_2/N_2 and in N_2O/N_2. Curves prove that this ternary system mainly retards flame in gas phase. Maximum value appears in O_2/N_2 curve when the ternary system contains a certain
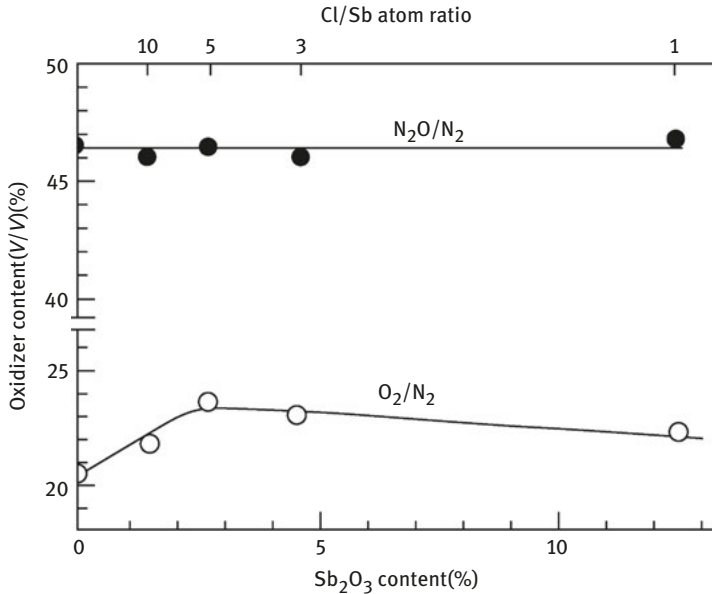
Figure 2.2: LOI curves of PP/CP/Sb$_2$O$_3$ ternary system [3].

amount of Sb$_2$O$_3$, whereas the LOI curve in N$_2$O/N$_2$ is unchanged with Sb$_2$O$_3$ loading.

Synergism of X/Sb system involves reactions of antimony compounds (such as Sb$_2$O$_3$) with halogenated compounds or with their decomposition products (such as HX). Therefore, the synergism of this system relates to X/Sb atom ratio and the degree of decomposition of halogenated compounds.

Physical modes

In addition to chemistry actions, functions of X/Sb system in gas phase have physical roles and may include at least the following [1]:

(1) SbX$_3$ vapor with high density can stay in the combustion zone for a long time and play the roles of dilution and coverage ("blanket" effect). The insulation against oxygen of "blanket" effect is very effective in suppressing pyrolysis and combustion of materials, because gas-phase ignition usually occurs in combust–air mixture adjacent condensed phase. Velocity of oxygen into condensed phase may affect polymer thermal cracking rate. Velocity of oxygen into material and diffusion rate in material reduce possibilities of material cracking and combustion decrease. There is no doubt that a number of halogenated compounds and noncombustible gases released from material's cracking can hinder oxygen penetration to the interior materials and inhibit further thermal

cracking of materials. For example, the rate of isothermal cleavage of cellulose in the presence of air is one order of magnitude higher than under vacuum. And as for viscose fiber, cleavage rate in the presence of air decreases linearly with fiber orientation degree. This may be because polymer orientation shortens the gap between chains, and the chains arrange more closely. So, the rate of oxygen getting into polymer or/and diffusing in polymer reduces and the cracking velocity decreases.

(2) Decomposition of SbX_3 is an endothermic reaction. This can effectively reduce the temperature and decomposition speed of the flame-retarded materials.

(3) The surface effect of liquid and solid SbX_3 microparticles can reduce the flame energy.

In some cases, the physical modes of X/Sb system in gas phase can estimate FR loading necessary for flame suppression. The physical modes and free-radical capture theory might replenish with each other, but it is quite difficult to identify the respective contribution of these two modes to flame retarding. This often depends on structures and performances of flame-retarded materials and FRs, flame parameters and conditions, as well as sample size and other factors.

2.2.3 Flame retardation mechanism of X/M synergistic system in condensed phase

Although X/M system has been widely used, the flame retardation mechanism is still not fully understood. However, it is possible that X/Sb system also has condensed-phase FR functions in addition to gas phase ones [32]. It is known that several systems containing Sb_2O_3 possess flame retardancy in condensed phase. For example, adding Sb_2O_3 into cellulose fabric treated with chloride can lower charring temperature. When using X/Sb system for cellulose, $SbCl_3$ formed in situ reacts with cellulose. This changes thermal decomposition route of cellulose and forms solid or liquid particles containing antimony, and the particle surface provides sites for absorbing energy. All described above may attribute to condensed-phase actions. Adding Sb_2O_3 into polyolefin treated with aliphatic chlorinated compounds [dechlorane (DCRP)] significantly improves degree of char forming [1]. Moreover, in some polymers containing X/Sb, char formation is improved and the functions in condensed phase enhanced with the increase of Sb loading. Direct evidences of condensed-phase mechanism of X/Sb system have not been reported. But some evidences of condensed-phase mechanism of X/Bi system [3] might be used for X/Sb system. This is described below.

Separately measuring LOI of ternary system of PP/CP/bismuth carbonate (BC) in O_2/N_2 and in N_2O/N_2, the obtained two curves are shown in Figure 2.3 [32]. Both show a maximum of LOI, and both Cl/Bi atom ratio and BC loading corresponding to these two maximum points are the same. This simplifies that the action modes
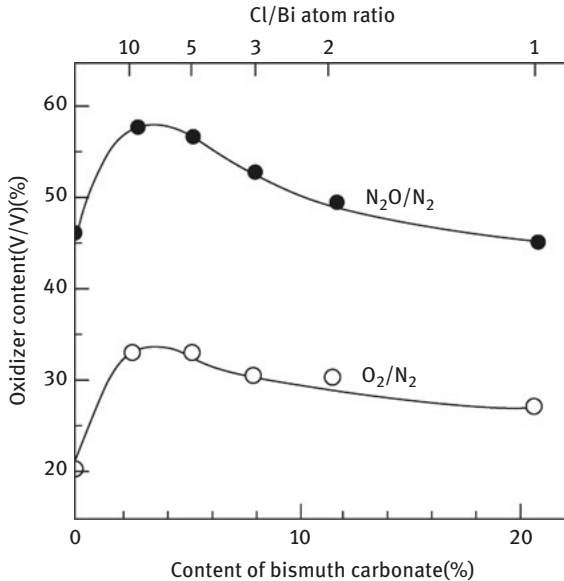
Figure 2.3: LOI curves of PP/CP/BC [3].

of Cl/Bi synergistic system may be mainly carried out in condensed phase. In addition, in the system with maximum LOI, PP pyrolysis rate is also low [33]. What's more, the efficiency of increasing LOI of $BiCl_3$ for PP is less than ternary system of PP/CP/BC. This is also evident that PP/CP/Bi possesses condensed-phase effects.

In addition, $BiCl_3$ or BiOCl has similar effects to BC for PP/CP system [34]. Therefore, condensed-phase flame retardancy of PP/CP/BC may be better than gas-phase flame retardancy of $BiCl_3$ released from the system. In fact, FR efficiency of $BiCl_3$ in gas phase is only slightly better than HCl, whereas Cl–Bi synergistism in PP/CP/BC system is very obvious, showing that there must exist condensed-phase flame retardancy. What is more, as for PP/CP system, the synergistic effects of BC are more effective than Sb_2O_3 [29]. According to reports [35], flame retardation of $SbCl_3$ is better than $BiCl_3$ in gas phase; thus, high effects of PP/CP/BC should be partly from condensed phase.

PP/CP/BC's condensed-phase FR actions may be due to the weakening of PP's heat cracking, because $BiCl_3$ released from the system can catalyze condensation of CP with PP (by double bond addition at end bond), thus reducing unsaturation of end bonds and evaporation rate of PP. In addition, bismuth may also stabilize PP's cracking [3].

The results obtained by PP/CP/BC might also be applied to other metals or metal compounds which can improve PP's LOI.

2.3 Suitable Sb/X atom ratio in X/Sb system

In 1930, people found the synergistic effects between halogenated FRs (such as CP) and Sb_2O_3. This important achievement was regarded as an epoch-making milestone in FR technology. It has laid the foundation of modern FR chemistry. Today, X/Sb synergism is still an active subject in the field of FR technology, and the suitable ratio of Sb/X is on the focus.

Taking flame-retarded PP for an example, three topics will be discussed below: (1) relationship between Sb/X ratio and FR performances (oxygen index, ignition time, etc.); (2) principles of selecting suitable Sb/X ratio and (3) effects of FR's chemical structure on suitable Sb/X ratio [36, 37].

2.3.1 Relationship between oxygen index and Sb/X atom ratio

When different brominated FRs and Sb_2O_3 are for PP, the relationship between PP's LOI and bromine content is shown in Figure 2.4. Every system has an optimal Sb/X ratio. 2,3-Dibromopropyl pentabromophenyl ether containing alkyl bromine can endow PP with comparatively high LOI (29%), whereas the LOI of PP with tetrabromophthalic anhydride containing only aromatic bromine is up to at most 24%. As for improving PP's LOI, the efficiency of bromine from 2,3-dibromopropyl pentabromophenyl ether/Sb_2O_3 is 2 times as good as the 1 time from tetrabromophthalic anhydride/Sb_2O_3. At the same time, FR efficiency is not always proportional to FR's total loading and is quite relevant to FR's chemical structures in the presence of Sb_2O_3 (see Figure 2.4).
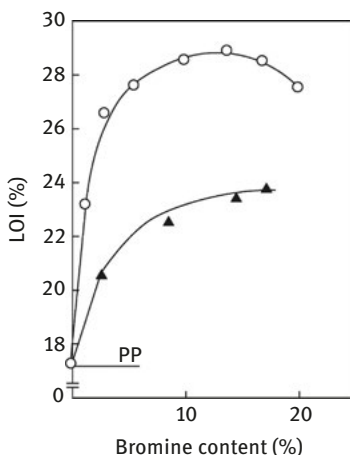
Figure 2.4: Relationship between LOI and bromine content of PP/brominated FR/Sb_2O_3 [36]O – 2,3-Dibromopropyl pentabromophenyl ether (atom ratio of Sb/Br 0.23); ▲ – tetrabromophthalic anhydride (atom ratio of Sb/Br 0.27).

As for PP/2,3-dibromopropyl pentabromophenyl ether/Sb_2O_3, when FR's loading is 9% or 23% and Sb/Br ratio is 1/4, the flame-retarded PP will reach the highest LOI (see Figure 2.5) and the shortest self-extinguishing time. It is reasonable to judge the flame retardancy by self-extinguishing time for materials with LOI within a certain range. For this type of materials, when FR's loading is less than 3%, the self-extinguishing time changes obviously with the change of FR's loading. LOI is suitable for flame-resistance evaluation of systems with high efficiency. Materials passing UL94V-0 test and having different LOI usually show variable ignition.
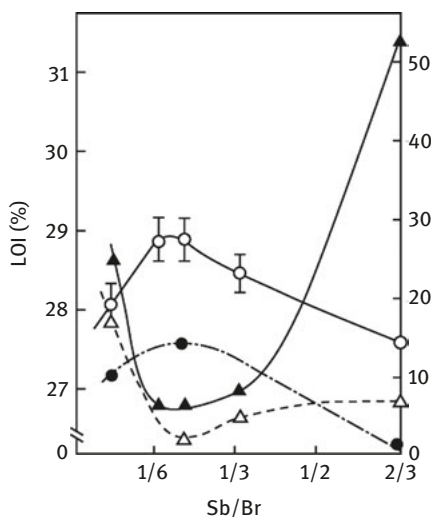
Figure 2.5: LOI of PP/2,3-dibromopropyl pentabromophenyl ether/Sb_2O_3 with different atom ratio of Sb/Br [37] Δ – 4.5% (mass) FR loading; ● – 9% (mass) FR loading; O – 23% (mass) FR loading.

Some experimental results have shown that PP with 2,3-dibromopropyl pentabromophenyl ether containing mixed bromine will reach a relatively high LOI at a low heat flux intensity. PP with decabromodiphenyl oxide (DBDPO) containing a single aromatic bromine has a relatively low LOI, and its combustion could be suppressed at high heat flux. Therefore, it may be better to use two kinds of brominated FRs (with alkyl bromine and without alkyl bromine) for PP FR formulations [36].

2.3.2 Relationship between ignition time and Sb/X atom ratio

Figure 2.6 is the relationship between Sb/Br ratio and ignition time, when 9% of different brominated FRs [pentabromotoluene, pentabromophenylpropyl ether, tri (2,3-dibromopropyl)isocyanurate] and Sb_2O_3 are used for PP. On addition of brominated FRs and Sb_2O_3 into PP, if FRs decompose and react with Sb_2O_3, the ignition time will be shortened. For example, the ignition time of neat PP is 28 s, whereas
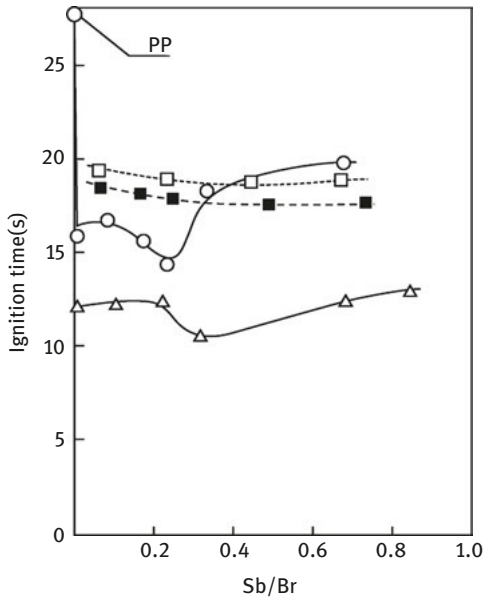
Figure 2.6: Relationship between ignition time and Sb/Br atom ratio of flame-retarded PP (FR's total loading 9%) [36] □ – pentabromobenzene; ■ – pentabromophenyl propyl ether; ○ – dibromopropyl pentabromophenyl ether; Δ – tri(2,3-dibromopropyl)isocyanurate.

for the above flame-retarded PP, it is 10–20 s. As for FRs containing aliphatic bromine, when Sb/Br ratio is 1/4.5–1/3, the ignition time appears minimum value. In addition, PP/tetrabromo bisphenol A bis(2,3-dibromo-propyl) ether/Sb$_2$O$_3$ possesses best LOI at Sb/Br ratio of 1/4. For FRs containing aromatic bromine (no aliphatic one), the relationship curve between ignition time and Sb/Br ratio does not have the lowest point, and LOI of aromatic brominated PP is lower than that of aliphatic brominated PP (at the same bromine content in PP). Therefore, the synergistic effects between Sb$_2$O$_3$ and brominated FRs are related to the structure of FRs, and the better synergism between brominated FRs with alkyl bromine and Sb$_2$O$_3$ may be because of the generation of acid HSbBr$_4$.

2.3.3 Relationship between heat release rate and chemical structure of brominated FRs

Due to heat release rate (HRR), aromatic bromides are better than aliphatic/aromatic mixed or aliphatic ones. The HRR of PP flame retarded by aromatic bromide and Sb$_2$O$_3$ (under burning at 500 °C) is far less than that of PP by aliphatic one. When aliphatic bromide/Sb$_2$O$_3$ is used for PP and bromine content is about 20%, the HRR of flame-retarded PP is equivalent to half of that of neat PP; when aromatic

bromide/Sb_2O_3 is used, 10% of bromine content in PP can achieve the same effect. Obviously, for PP/mixed or aliphatic bromides/Sb_2O_3 system, HRR is not so satisfactory; but its LOI is pretty well [37].

In short, when PP is flame retarded with Sb_2O_3, and halogenated FRs with different chemical structures, better performances are obtained at different Sb/X ratio, because different FRs have different SE with Sb_2O_3. For enhancing LOI, the synergism of general aliphatic or mixed bromine with Sb_2O_3 is better than aromatic bromine. PP flame retarded with 2,3-dibromopropyl pentabromophenyl ether/Sb_2O_3 has the highest LOI and the shortest self-extinguishing time at Sb/Br ratio of 1/4. PP with aliphatic brominated FR/Sb_2O_3 shows the shortest ignition time at Sb/Br ratio of 1/4.5–1/3.

2.4 Synergism between halogenated FRs and nanocomposites

2.4.1 Synergism with PP nanocomposites

Melting PP-g-MA and blending it with nano-organic clay (MMT), DBDPO and AO, nanocomposites with delamination–exfoliation mixed structures (confirmed by X-ray diffraction and transmission electron microscopy) are obtained. DBDPO can also be replaced by CPs. But if compatibility between PP and organic clay is poor, CP can not be well dispersed in PP containing DBDPO/AO.

The mechanical properties (yield stress, elongation at break and storage modulus) of the above PP-g-MA/MMT/DBDPO–AO nanocomposites are listed in Table 2.2 [38, 39]. PP-g-MA containing 5% of MMT compares with a single PP-g-MA, the yield stress increases by 19%, the storage modulus increases by 100% and the elongation at break decreases only by 1%. Adding some DBDPO into PP-g-MA can also improve the storage modulus but the degree is not as large as MMT. On adding DBDPO and AO into PP-g-MA/MMT (5%), some mechanical properties are not affected, but the yield stress increases and the degree is similar to that of MMT. Of course, DBDPO/AO can improve flame retardancy of composites. That is to say, adding halogenated FR and antimony synergist into nanocomposites can not only improve flame

Table 2.2: Mechanical properties of PP-g-MA/MMT/DBDPO/AO nanocomposites [39].

Sample	Yield stress (MPa)	Elongation at break (%)	Storage modulus (MPa)
PP-g-MA	16.9	5.4	462
PP-g-MA/MMT/DBDPO (22%)	15.1	4.2	628
PP-g-MA/MMT (5%)	20.1	4.2	955
PP-g-MA/MMT (5%)/DBDPO (22%)/AO (6%)	23.3	3.8	950

retardancy but also maintain or optimize mechanical properties. This means that they are compatible with each other.

2.4.2 Synergism with ABS nanocomposites

Heat release rate (HRR) curves of ABS, ABS/MMT, ABS/DBDPO/AO and ABS/MMT/DBDPO/AO [38, 40] are shown in Figure 2.7. As can be seen from the chart, the PHRR of polymer/organic clay nanocomposites is far lower than that of the original polymers. Adding DBDPO into composites further decreases PHRR. AO addition has even larger effects on decreasing peak heat release rate (PHRR). This means that there is a synergistic effect between organoclay and halogenated FR. In the halogenated flame-retarded polymers, replacing part of FRs by MMT and reducing the loading of halogenated FRs will not only impart the material satisfactory flame retardancy and excellent mechanical properties but also reduce the negative effects brought by halogenated FRs (such as smokiness, toxicity, corrosivity). For example, as for PHRR, ABS is 1078 kW/m^2, ABS/MMT (5%) 720 kW/m^2, ABS/MMT (5%)/DBDPO (18%) 350 kW/m^2 and ABS/MMT (5%)/DBDPO (15%)/AO (3%) 235 kW/m^2.
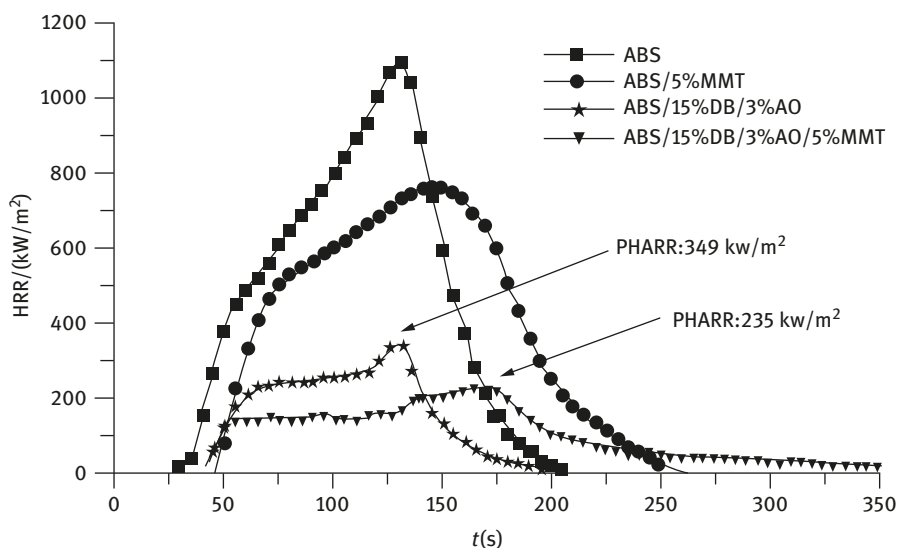
Figure 2.7: HRR curves of ABS, ABS/MMT (5%), ABS/DBDPO (15%)/AO (3%) and ABS/MMT (5%)/DBDPO (15%) /AO (3%) [40] (cone calorimeter, heat flux 50 kW/m^2).

Addition of 5% MMT into flame-retarded ABS by DBDPO or DBDPO/AO increases LOI only by about 0.5%, but addition of 5% of MMT into DBDPO flame-retarded ABS (no antimony, etc.) will help the material pass the UL94 V-0 FR grade (see Table 2.3) [40].

Table 2.3: Influences of MMT on ABS/Br and ABS/Br/Sb systems [40].

Sample	LOI (%)	UL 94
ABS	18.7	Combustion
ABS/MMT (5%)	21.5	Combustion
ABS/DBDPO (18%)	22	Combustion
ABS/MMT (5%)/DBDPO (18%)	22.6	V-0
ABS/DBDPO (15%)/AO (3%)	27	V-0
ABS/MMT (5%)/DBDPO (15%)/AO (3%)	27.5	V-0

2.4.3 Synergism with PBT nanocomposites

In Br/Sb flame-retarded reinforced PBT containing 9% of DBDPO and 4.5% of Sb_2O_3, addition of 1% of organoclay (multiple modifier) and 0.3–0.5% of alkali metal salts will make the material self-extinguishable, producing no droplet, passing UL 94 V-0 grade and getting satisfactory impact strength (see Table 2.4) [38, 41]. This shows that there is a good synergistic effect between Br/Sb and organoclay in PBT. Organoclay disperses well in PBT and the composite shows exfoliation structure.

Table 2.4: Formulations and performances of reinforced PBT with Br/Sb and organoclay.

Formulation (%)	1	2	3	4	5
PBT	55.0	55.1	55.0	55.2	55.2
Glass fiber	30.0	30.0	30.0	30.0	30.0
DBDPO	9.0	9.0	9.0	9.0	9.0
Sb_2O_3	4.5	4.5	4.5	4.5	4.5
Modified MMT[1]	1.0	1.0	1.0	1.0	1.0
Potassium oleate	0.5	0.4	0.5	0.3	0.3
Performance					
UL 94	V-0 (no drop)	V-0 (no drop)	V-0 (no drop)	V-0 (no drop)	V-0 (no drop)
Impact strength (kJ/m^2)	25.9	25.8	22.5	32.2	29.0

[1]MMT used for different samples were modified by different modifiers

2.4.4 Reaction mechanism between nanocomposites and halogenated FRs

As mentioned before, halogenated FRs suspend combustion process in gas phase via inhibition of free radical chain reactions. When antimonides (such as AO) are used as synergistic agent of halogenated FRs, SbX3 is formed to further slow down or prevent flame radical chain reactions and to enhance flame retardancy of halogenated FRs. If bromide/AO is compounded with nanocomposites, AO can react with NaBr [42] (NaBr is an impurity of organic clay, because in clay modification process,

sodium ions have not been completely substituted by ammonium ions) and LS^-H^+ to produce $SbBr_3$ (2.39). LS^-H^+ is formed by thermal decomposition of organoclay modified with ammonium salts (2.40). LS^-H^+ dispersed in clay layers of polymer matrices may have catalytic effect (2.39).

$$3LS^-H^+ + 6NaBr + Sb_2O_3 \xrightarrow{\Delta} 3LS^-Na^+ + 2SbBr_3 + 3H_2O \qquad (2.39)$$

$$(2.40)$$
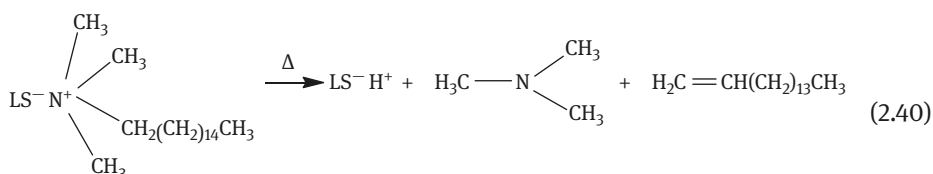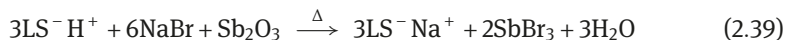
When bromide/AO is added into PA, three main processes take place [43, 44]: (1) formation of termination agent for free radicals chain reactions, that is, $SbBr_3$; (2) promotion of char formation through dehydrogenation reaction and (3) formation of HBr as a barrier between gas phase and condensed phase. Although bromide/AO is a very effective FR, it will promote degradation of PA chain, producing combustible monomer and its analogs (2.41) [43,44]. LS^-H^+ formed in reaction (2.40) has catalytic effects on thermal degradation of PA (2.42). Compounding bromide/AO and PA6/MMT nanomaterials, $SbBr_3$ can react with $-NH_3^+Br^-$ forming antimony complex (2.43). This is one of the reasons that Br/Sb_2O_3 can play roles in condensed phase [42].

$$(2.41)$$

$$(2.42)$$

$$x SbBr_3 + y - NH_4^+Br^- \longrightarrow x SbBr_3 \cdot y NH_4Br \qquad (2.43)$$
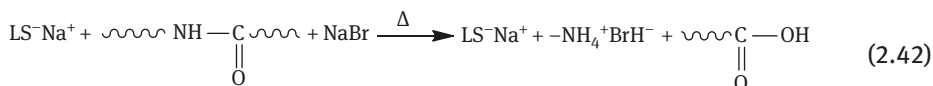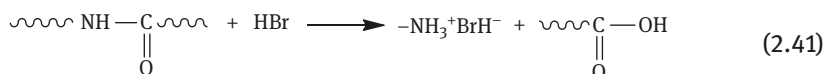
The thermal decomposition reaction of PA/MMT/bromide/AO nanocomposites will be slowed down because of the barrier effects of nanodispersion clay layer. Synergistic effects between MMT and bromide/AO will change the flame retardancy of PA. Flame retardancy of nanocomposites measured by conventional methods (such as UL94 vertical burning) shows that compatibility and synergistic effects exist among bromide/AO/MMT/polymer matrix. For example, the flame retardancy of PP and ABS FR nanocomposites are improved because of the effects mentioned above.

References

[1]   Ou Yuxiang, Li Jianjun. *Flame Retardant*[M].Beijing: ChemicalIndustry Press,2006: 3–26.

[2]   Lewin Menachem, Weil Edward. Mechanisms and modes of action in flame retardancy of polymers[A]//Price D. Fire Resistant Materials[M]. Cambridge: Woodhead Publishing Ltd., 2000: 1-40.

[3]   Bocchini S, Camino G. Halogen-containing flame retardant [A]//Wilkie C A, Morgan A B. Fire Retardancy of Polymeric Materials. 2nd Edition[M]. Boca Raton: CRC Press, 2009: 75–85.

[4]   Levchik S V. Introduction to flame retardancy and polymer flammability[A]//Morgan A B, Wilkie C A. Flame Retardant Polymer Nanocomposites[M]. New York: John Wiley and Sons, Inc., 2007: 7–11.

[5]   Hu Yuan,Song Lei, Long Fei. et al. *Introduction to fire chemistry[M]*.Beijing: ChemicalIndustry Press,2007:70

[6]   Bovynies S, Przygocki W. Polymer combustion processes. 3. flame retardants for polymeric materials[J]. Program Rubber Plastic Technology, 2001, 17, 127–148.

[7]   Funt J, Magill J H. Estimation of the fire behavior of polymers[J]. Journal of Fire and Flammability. 1975, 6: 28–36.

[8]   Wilson W E, O'Donovan J T, Fristro R M. Flame inhibition by halogen compounds[A]//Proceedings of the 12th Symposium (International) on Combustion[C]. Pittsburgh: The Combustion Institute, 1969: 929–942.

[9]   Day M J, Stamp D V, Thompson K, et al. Inhibition of Hydrogen-Air and Hydrogen-Nitrous Oxide flames by Halogen compounds[A]//Proceedings of the 13th Symposium (International) on Combustion [C]. Pittsburgh: The Combustion Institute, 1971: 705–712.

[10]   Pownall C, Simmons R F. Some observation on the near flame limit [A]//Proceedings of the 13th Symposium (International) on Combustion[C]. Pittsburgh: The Combustion Institute, 1971: 585–592.

[11]   Noto T, Babushok V, Burgess D R, et al. Effect of halogenated flame inhibitors on Cl-C_2 Organic flames[A]//Proceedings of the 26th Symposium (International) on Combustion[C]. Pittsburgh: The Combustion Institute, 1996: 1377–1383.

[12]   Roma P, Camino G, Luda M P. Mechanistic studies on fire retardant action of fluorinated additives in ABS[J]. Fire and Material, 1997, 21(4): 199–204.

[13]   Lewin M, Guttmann H, Sarsour N. A novel system for the application of bromine in flame-retarding polymers[A]//Nelson G L. Fire and Polymers[C]. Washington: ACS Symposium Series 425, 1990: 130–134.

[14]   John W. Lyons. The Chemistry and Uses of Fire-Retardants[M]. New York: Wiley Interscience, 1970: 16.

[15]   Larson E R. Some effects of various unsaturated polyester resin components upon FR-agent efficiency[J]. Journal of Fire and Flammability/Fire Retardant Chemistry, 1975, 2: 209–223.

[16]   Lewin M, Flame Retarding of Fibers[A]//Lewin M, Sello S B. Handbook of Fiber Science and Technology. Chemical Processing of Fibers and Fabrics, Vol. 2,Part B[M]. New York: Marcel Dekker Inc.,1984: 1–141.

[17]   Ou Yuxiang. *Practical Flame Retardant Technology* [M]. Beijing: Chemical Industry Press, 2003:49–50.

[18]   Li Jianjun, Huang Xianbo, Cai Tongmin. *Flame Retardant,Styrene Plastic Series* [M]. Beijing: Science Press,2003: 140–141.

[19]   Lewin Menachem. Flame Retardance of Polymers: The Use of Intumescence[M]. London: The Royal Society of Chemistry, 1998: 1.

[20] Ballisteri A, Montaudo G, Puglisi C, et al. Intumescent flame retardants for polymer. I. The poly (acrylonitrile)-ammonium polyphosphate-hexabromocyclododecane system[J]. Journal of Applied Polymer Science, 1983, 28(5): 1743–1750.

[21] Lewin M. Unsolved problems and unanswered questions in flame retardance of polymers[J]. Polymer Degradation and Stability, 2005, 88: 13–19.

[22] Kaspersma J H. FR mechanism aspects of bromine and phosphorus compounds[A]// Proceedings of the 13th Conference on Recent Advances in Flame Retardancy of Polymeric Materials[C]. Stamford: Stamford CT, 2002.

[23] Prins A M, Doumer C, Kaspersma J G. Low wire and V-2 performance of brominated flame retardants in polypropylene[A]//Proceedings of the Flame Retardants 2000[C]. London: Interscience Communication, 2000: 77–85.

[24] Fenimore C P, Martin F J. Flammability of polymers[J]. Combustion and Flame, 1966, 10: 135–139.

[25] Fenimore C P, Jones G W. Modes of inhibiting polymer flammability[J]. Combustion and Flame, 1966, 10: 295–301.

[26] Coppick S. Metallic Oxide-chlorinated. fundamentals of process[A]//Little R W. Flameproofing Textile Fabrics[M]. New York: Reinhold Publishing Company, 1947: 239–248.

[27] Thiery P. Fireproofing: Chemistry, Technology and Applications[M]. Amsterdam: Elsevier Pub. Co., 1970.

[28] Lindemann R F. Flame retardants for polystyrenes[J]. Journal of Industrial and Engineering Chemistry, 1969, 61(5): 70–75.

[29] Camino G. Mechanism of fire retardancy in chloroparaffin-polymer mixtures[A]//Grassie N. Developments in Polymer Degradation, Vol. 7[M]. London: Elsevier Applied Sciences, 1987: 221–269.

[30] Martin F J, Price K R. Flammability of Epoxy Resins[J]. Journal of Applied Polymer Science, 1968, 12 (1): 143–158.

[31] Bertelli G, Costa L, Fenza S, et al. Thermal behavior of bromine-metal fire retardant systems [J]. Polymer Degradation and Stability, 1988, 20(3–4): 295–314.

[32] Wang Yongqiang, *Flame Retardant Materials and Application Technology* [M]. Beijing: Chemical Industry Press,2004: 17–18.

[33] Costa L, Camino G, Luda M P. Effect of the metal on the mechanism of fire retardance in chloroparaffin-metal compound-polypropylene mixtures [J]. Polymer Degradation and Stability, 1986, 14(2): 113–123.

[34] Costa L, Camino G, Luda M P. Mechanism of condensed phase action in fire retardant bismuth compound chloroparaffin-polypropylene mixtures. Part I. The role of bismuth trichloride and oxychloride [J]. Polymer Degradation and Stability, 1986, 14(2):159–164.

[35] Leamlonth G S, Thwaite D G. Flammability of plastics. IV. An apparatus for investigating the quenching action of metal halides and other materials on premixed flames[J]. British Polymer Journal, 1970, 2:249–253.

[36] Ou Yuxiang, Li Xing, Cui Yunpeng. Suitable Sb/X Ratio in Flame Retarded PP [J]. New Materials for Chemical Industry, 1999, 27(12): 26–29.

[37] Ou, Yuxiang,Cheng Yu, Wang Xiaomei, *Flame Retardant Polymer Materials* [M]. Beijing: National Defence Industry Press,2001: 38–42.

[38] Yuan H, Lei S. Nanocomposite with halogan and nonintumescent phosphorus flame retardants additives[A]//Morgan A B, Wilkie C A. Flame Retardant Polymer Nanocomposites [M]. Hoboken: John Wiley and Sons, Inc., 2007: 204–225.

[39] Zanetti M, Camino G, Canavese D, et al. Fire retardant halogen-antimony-clay synergism in polypropylene layered silicate nanocomposites[J]. Chemistry of Materials, 2002, 14(1): 189–193.

[40] Wang S F, Hu Y, Zong R W, et al. Preparation and characterization of flame retardant ABS/montmorillonite nanocomposite[J]. Applied Clay Science, 2004, 25(1–2): 49–55.

[41] Breitenfellner F, Kainmuelle T. Flame-retarding, reinforced moulding material based on thermoplastic polyesters and the use thereof[P]. US Patent: US4546126. 1985, 10–08.

[42] Hu Y, Wang S F, Ling Z H, et al. Preparation and combustion properties of flame retardant ABS/montmorillonite nanocomposite[J]. Macromolecular Materials and Engineering, 2003, 288(3): 272–276.

[43] Levchik S V, Weil E D, Lewin M. Thermal decomposition of aliphatic nylons[J]. Polymer International, 1999, 48(7): 539–557.

[44] Levchik S V, Weil E D, Combustion and fire retardancy of aliphatic nylons[J]. Polymer International, 2000, 49(10): 1033–1073.

3 The flame-retardation mechanism of organic phosphorus flame retardants

Currently, most of the organic phosphorus flame retardants improved their properties of retardation of combustion mainly in condensed phase, including flame suppression, the heat consumption of melt flow, the surface barrier produced by phosphoric acid, carbon catalyzed by acids, thermal insulation and oxygen insulation for carbon layers, etc. Besides, a lot of phosphorus compounds have flame-retardant function both in condensed and gas phase [1]. For a specific system of phosphorus retardation of combustion, the performance proportion of its retardation of combustions in condensed and gas phase is related to a range of factors, such as (1) the types and structures of the polymers, (2) elemental phosphorus or phosphorus in the compound, (3) the valence state of the phosphorus in the compound, (4) the elements and groups, etc., that are surround with phosphorus. Chemical and physical action modes are present in both the condensed and gas phase. All actions are affected by the interference, synergism, antagonism and additional actions of other additives in the system. The flame-retardation mechanism of organic phosphorus compounds has been summarized in some monographs [2–4].

3.1 The flame-retardation mode in condensed phase

No matter whether it is flame-retardant thermoplasticity or thermosetting polymers, the main function of phosphorus flame retardants is not in gas phase but in the condensed phase. High performance of phosphorus flame retardants cannot be achieved only in gas phase. The performance of phosphorus flame retardants in condensed phase mainly lies in two aspects: one is to reduce the formation of combustible products, and the other one is to promote carbonization. In some cases, it can also enhance coherence and strength of the carbon layer. In phosphorus flame-retardant systems, most of the phosphori remain in the carbon layers. In some polymers, such as polystyrene(PS), the phosphorus compounds can change the generation rate of combustible gaseous products and, thus, can change the combustions of high polymers [5].

The efficiency of phosphorus flame retardants in different polymers is often related to their dehydration and carbonization, both of which are related to the fact that whether the polymers contain oxygen or not. For example, the oxygen-containing cellulose can improve considerable flame-retardant properties if 2% P is provided [6]. But oxygen-free polymers, such as polyolefins and polystyrenes, are not easy to be carbonized; thus, phosphorus flame retardants are not effective to them. However, polymers without reactive functional groups can form oxygen-containing groups or double bonds when organic phosphorus flame retardants combust with them on their

surfaces. The heterocyclic compounds, if formed, can be a part of intumescent carbon layers. In order to effectively improve the carbonization of phosphorus flame retardants, an important way is to add extra carbonization agents into the polymer. Some high molecular weight carbonization agents are not only helpful to improve flame-retardant properties but also helpful to improve the thermomechanical properties of materials, whereas some only have flame-retardant properties [4].

The interaction between phosphorus compounds and polymer without –OH group is discussed. Sometimes, phosphorus compounds are first oxidized; so when flame retardants made by phosphorus compounds are used in oxygen-free polymers, most phosphori in the system may be evaporated due to the formation of oxide compounds (such as P_2O_5 or other compounds) during thermal cracking of phosphorus compounds [7].

In terms of flame retardation mechanism in condensed phase, we must pay attention to improve the interactions between flame retardants and high polymers. It usually happens when the temperature is lower than the decomposition temperatures of flame retardants and polymers. The main reactions are dehydration and cross-linking (promoting into carbonization). For example, such interactions exist between celluloses, synthetic polymers and flame retardants [8].

A typical example of phosphorus flame retardants in the condensed phase is the flame-retardant properties of phosphoric acids and/or organic phosphates as well as inorganic phosphates to celluloses [9]. When there are such flame retardants (containing P–O–C bond), hydroxyl radicals of celluloses are phosphorylated and the thermal degradation routes of celluloses are changed, then it will be very helpful for the celluloses to be carbonized even though they can dehydrate, not depolymerize the celluloses.

3.1.1 The modes of carbonization

Phosphorus flame retardants can increase the char yield, especially for oxygen-containing polymers. In fact, the phosphorus compound is a kind of carbonization promoting agent.

When acting on celluloses, the phosphorus flame retardant will be decomposed into phosphoric acids or anhydrides at high temperature, and the latter one can phosphorylate celluloses and release water. The phosphorylated cellulose can be further converted into carbon. In this case, the functions of phosphorus flame retardants are as follows: (1) generating steam which cannot combust, (2) reducing the amount of combustible materials and (3) the protection role of the carbon layer. The flame-retardant efficiency would be higher if the carbon layer has oxidation resistance. But even the transitional carbon layer also has a certain effect on flame-retardant property. Even though the carbon layer is oxidized (usually happening by

smoldering), but the presence of phosphorus compounds can prevent carbon from being oxidized into carbon dioxide, thus reducing the heat released during the process of oxidation [4].

When the phosphorus flame retardant acts on celluloses, its retardation of combustion in condensed phase may contain two dehydration carbonization mechanisms: first, the cellulose is subsequently decomposed into carbon by esterification reaction with acids (see eq. (3.1)); second, carbonium ions catalyze and disproportionate the cellulose to dehydrate into carbon (see eq. (3.2)) [3].

$$R_2CH - CHR'OH + ZOH(acid) \rightarrow R_2CH - CHR'OZ + H_2O \rightarrow R_2C = CHR' + ZOH \quad (3.1)$$

Z is an acyl free radical

$$R_2CH - CHR'OH \rightarrow R_2CH - CHR'OH_2{}^+ + H_2O \rightarrow R_2C = CHR' + H^+ \quad (3.2)$$
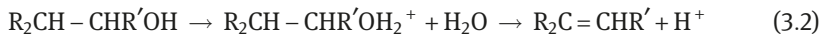
However, the retardation of combustion of the cellulose mainly lies in reaction (3.1). The flame-retardant efficiency of phosphides is related to fine structures of polymers (cellulose). For example, the temperature of polymers in amorphous regions is lower than crystalline regions, and the former one sometimes decomposed before the decomposition of phosphate flame retardant, which reduces the efficiency of the flame retardant. Strong acids can hydrolyze the crystalline region of celluloses to deteriorate fire retardation performance [3].

Cross-linking can promote carbonization during the thermal cracking of the cellulose; thus, it can reduce the combustibility of polymers in many cases (but there are exceptions). For example, the char yield of PS with cross-linking after thermal cracking can reach 47% [10], but the char yield of PS without cross-linking is almost zero. Some organometallic compounds can promote carbonization of polymers into carbon by cross-linking.

Cross-linking can stabilize the structures of celluloses because of additional covalent bonds formed between polymer chains (stronger than hydrogen bond), but a low degree of cross-linking will reduce the thermal stability of celluloses due to the increased distance between individual chain segments and, thereby, weakening and breaking the hydrogen bonds. For example, the increase of formaldehyde cross-linking can improve the limited oxygen index(LOI) of cotton fibers to some extent [3].

Since the −OH radicals of neighboring chain segments in celluloses can form oxygen bridges bonds, celluloses can form char rapidly and automatically by cross-linking. Celluloses lose weight due to anhydration, and the formed carbon layer can improve the thermal cracking temperature.

The flame-retardant performances of phosphorylated polyvinyl alcohol and ethylene-vinyl alcohol copolymers are higher than those without being phosphorylated. It is because dehydration, cross-linking and carbonization happen to phosphorylation system in condensed phase (see reaction (3.3)) [11].

(3.3)

P represents polymer
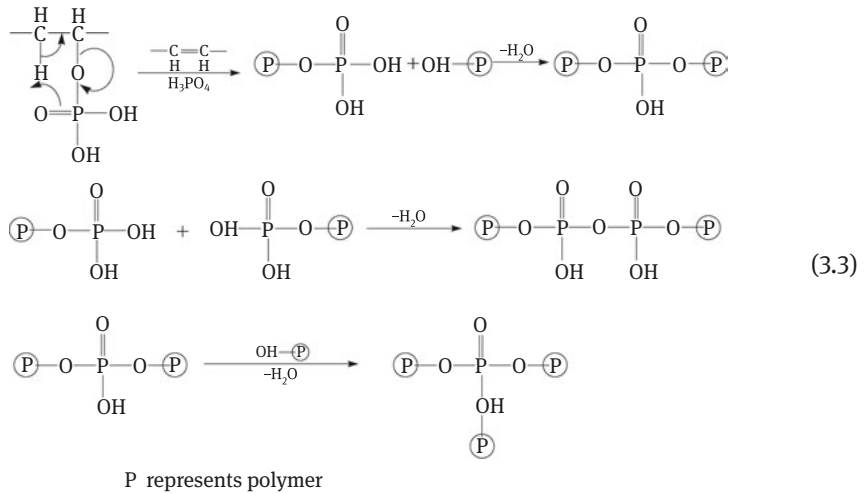
Introducing phosphori into polymers (such as PS and polymethyl methacrylate, PMMA) by copolymerizing with phosphorus-containing monomers can greatly improve the flame-retardant properties and the rate of char yield of the polymers after reactions [12]. As most of the phosphori remain in the carbon layer, they follow condensed-phase flame retardation mechanism. In addition, the copolymers formed by acrylonitrile and phosphorus-containing monomers have obvious P–N synergy effects [13].

Copolymers produced by copolymerizations of PMMA and reactive phosphates have flame-retardant properties both in gas and condensed phase (carbonization). The flame-retardation mechanism of the latter happens due to the production of phosphoric acids when the system is heated. Then, phosphoric acids react with methyl acrylate to form methacrylic anhydride, which decarboxylates into carbon (see eq. (3.4)) [14].

(3.4)
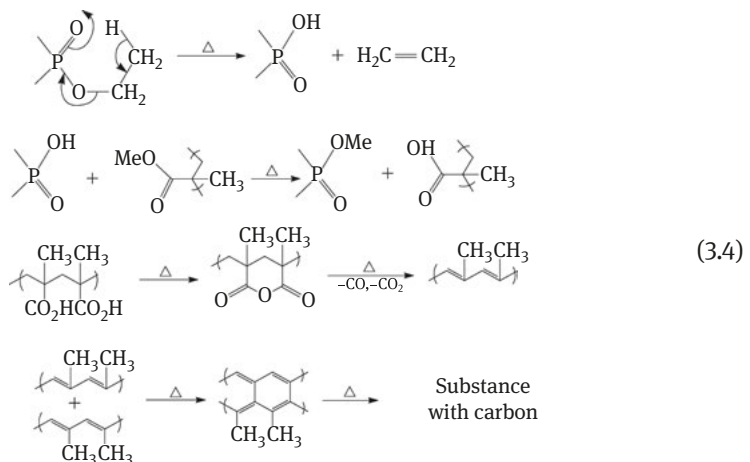
The products formed by copolymerization of polyacrylonitrile (PAN) with phosphorus-containing monomer can improve their flame-retardant properties in condensed phase. When the PAN is heated, the intramolecular cyclization will happen (phosphorus-containing acids can accelerate this cyclization as the nucleophilic center generated by thermal cracking of the side chain), thereby reducing the generation of volatile products (including monomers) and increasing char yield (see Section 3.4.1, "Phosphorus–nitrogen synergy effect") [15–16].

In rigid polyurethane foams, the phosphorus compound can promote char yield. The carbon layers become better flame-retardant barriers because most of phosphori remain there. Furthermore, the phosphorus flame retardants in the polyfoam also perform a flame retardation mechanism in gas phase besides carbonization. On the contrary, in flexible polyurethane foams, the situation is different. The main function of phosphorus flame retardants in soft polyurethane foams is not carbonization. It can only form a little carbon, insufficient to become a fire barrier [4].

In polyethylene terephthalate (PET) and PMMA, phosphorus flame retardants can increase the residual contents after the combustion and delay the release of volatile combustible products. It is because the PET and PMMA have acid esterification cross-linking reactions, thereby promoting char yielding [17,18]. When red phosphorus is applied on PA6, LOI and NOI (N_2O-measured index) are very similar to the relation curve of flame-retardant amount; thus, red phosphorus is likely to follow condensed-phase flame-retardation mechanism. Infrared spectrum shows that when PA6 is heated on fire with red phosphorus as flame retardant, it is oxidized to phosphoric acids, whereas PA6 molecules combine with phosphoric acids via alkyl esters [3, 19].

Though char yield of phosphorus flame retardants in PA is not high, some heteropoly acids can further improve the char yield and provide materials with the flame-retardant level as high as UL94V-0. Some experiments indicate that if the concentration of ammonium polyphosphates in PA6 is high enough, it can form intumescent char layer. One type of cross-linking coating with P–N bond also helps to protect char layer, therefore improves the flame retardancy. [3, 4]

For the char-forming polymer polyphenylene, it can rearrange into polythene cross-linked by the methylene, the latter can be dehydrated and dehydrogenated by the phosphate to be carbonized. The phosphorylation of rearranged phenols may be the first step of carbonization [4].

3.1.2 The coating effect mode

Phosphorus coating also suppresses smoldering combustion of carbon. The mechanism is probably that the surface of carbon layer is covered with polyphosphoric acid (for physical protection) and passivation of oxidized carbon active center. For example, even though the concentration of phosphorus is as low as 0.1%, the graphite carbon's oxidation by free oxygen is hard to find. Furthermore, hydrophilic

groups within phosphoric acids and structural units with P=O bonds may bond with reaction site on the material surface with tendency of being oxidized [3]. For example, the structural units with P=O bonds can bond with reaction site of graphite carbon, which are sensitive to oxidation [3]. Recent studies indicate that phosphorus flame retardants can reduce the permeability of the carbon layer to improve its barrier function. It is still unknown that whether it is caused by surface coating or by the change of the carbon layer structure [20]. It also proposes that phosphoric acids on the surface of the material can hinder volatilization of the combustible from hydrocarbon polymers which utilizing ammonium polyphosphate (APP) as flame retardant [21].

3.1.3 The modes of suppressing free radicals in condensed phase

It has been shown that some of the nonvolatile phosphorus flame retardants in condensed phase can suppress free radicals, which act as anti-oxidation agents [22]. Electron spin resonance spectroscopy also points out that phosphate flame retardants with aromatic group can scavenge the peroxy radical and alkyl radical on the surface of polymers, but its mechanism is unknown.

3.1.4 The modes based on the fillers' surface effect in condensed-phase modes

There are two types of surface effects in flame-retardant system: first, phosphorus compounds (such as alkyl radicals' acidic phosphoric acid esters) which can perform as a kind of surfactant. It can improve the dispersion of solid flame retardants (such as alumina trihydrate), resulting better flame-retardant efficiency; second, the surfactant can promote and increase char yield.

For example, some alkoxy titanate coupling agents and alkoxy zirconium-coupling agents, containing alkyl acid pyrophosphate anion, can improve the flame retardation of polypropylene with inorganic fillers. However, different fillers have different suitable surfactant concentrations [3, 4].

3.2 Flame-retardant modes in gas phase

3.2.1 Chemical effect modes

Volatile phosphorus compounds are effective flame retardants to suppress flames. For example, triphenyl phosphate and triphenyl phosphine oxide can dissociate into smaller molecules or free radicals, which can reduce the concentration of hydrogen free radicals in flame zone to extinguish the flame (see reaction (3.5)) [2].

$$
\begin{aligned}
R_3PO &\longrightarrow PO\cdot + P\cdot + P_2 \\
H\cdot + PO\cdot + M &\longrightarrow HPO + M \\
HO\cdot \ + PO\cdot &\longrightarrow HPO + \cdot O\cdot \\
HPO + H\cdot &\longrightarrow H_2 + PO\cdot \\
P_2 + \cdot O\cdot &\longrightarrow P\cdot + PO\cdot \\
P\cdot + OH\cdot &\longrightarrow PO\cdot + H
\end{aligned}
\tag{3.5}
$$
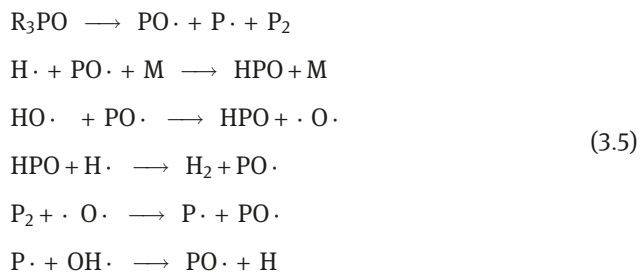
The flame retardation mechanism of phosphorus flame-retardant systems in gas phase (eq. (3.5)) is proposed according to the flame-retardant properties of triphenyl phosphate and triphenylphosphine oxide. The main features of these reactions are promoting the binding of H· and capturing O·of the phosphorous molecules to reduce the concentration of free radicals that support flame propagation.

The small phosphide molecules mentioned above can inhibit the steps of speed control of flame propagation, namely, chain branching steps. It is similar to flame retardation mechanism of halogen flame retardants in gas phase. Volatile phosphorus flame retardants, such as trialkyl phosphate and trialkylphosphine oxide, also have such function to reduce concentration of free radical in flame zone. Some experimental studies have provided the evidences of chemical flame-retardant effects of phosphine oxide in gas phase [3, 4].

3.2.2 The physical effect mode

The flame retardancy can also be achieved by physical effect mode in gas phase, for example, based on some factors of specific heat, vaporization heat, endothermic dissociation in gas phase, etc. The modes the flame retardancy in gas phase are all physical effect modes. For phosphorus flame retardants, they can at least make contributions in terms of vaporization heat and specific heat in gas phase [4]. The relation curve between the amount of flame retardants used and LOI, and NOI containing rigid polyurethane foam plastics with trimethyl phosphine oxide are vastly different [23]. For modified PA, when phosphine oxide is used as reactive flame retardant, its fire retardation is carried on by flame-retardant mechanism in gas phase, although it can slightly improve the char yield of the materials.

For flame retardants acting on wool fabrics and wool polyester fabrics, the flame retardancy of volatile phosphonium salt is better than that of reactive phosphine oxide with low volatility, which indicates that flame retardants in gas phase produces better result in these situations [24]. The relative efficiency of flame retardants in both gas and condensed phase is related to polymer matrix, as well as relative tendency of carbon and volatile combustible products formed.

For the blend of polyphenylene oxide(PPO) and high impact polystyrene(HIPS), the main effect of triaryl phosphate seems to be performed in gaseous phase. In this blend, PPO forms a protective carbon layer with some phosphates reserve in the carbon layer. Besides, the triaryl phosphate also has an obvious function to suppress the combustion of combustible products that are produced by thermal cracking of PS in gas phase [25].

Some diphosphine phosphates and oligomer phosphates act on polycarbonate/ acrylonitrile butadiene styrene (PC/ABS) and HIPS, and the flame-retardant UL94 level of PC/ABS and HIPS is associated with volatility of phosphorus flame retardant. The higher the volatility of phosphorus compounds, the higher the level of UL94 of flame-retardant materials can be achieved. This shows that flame retardancy is mainly related to the gas phase [26].

If we dissolve in PCL_3 and then react it with molecular oxygen, which can phosphorylate Thus, PE with excellent flame retardancy can be obtained. If the degree of phosphorylation of PE is higher than 10% (molar fraction), the crystalline of PE goes down and the properties of physics and machinery get worse. In this case, the flame-retardant properties of PE are partly derived from flame retardancy in gas phase [2].

3.3 Polymer structure parameters affecting the efficiency of phosphorus flame retardants

Besides bond strength and intermolecular forces, some factors (such as rigidity, resonance stability, aromatic, crystallinity and orientation of bond) also play an important role in polymer thermal cracking and combustion. According to the parameters which are related to the combustion process, such as the amount of production of combustible gases and carbon, the universal dynamics model of dissociations of polymer can be achieved [27].

The degree of polymerization (DP) is quite related to the thermal cracking rate of polymers and the amount of carbonization. For example, thermal cracking rate of pure fiber in vacuum is inversely proportional to the square root of DP, while its degree of cross-linking is proportional to the amount of carbonization. LOI increases as the amount of carbonization increases (see Van Krevelen equation [28]), except some polymer blends.

Furthermore, the cross-linking can increase the dynamic viscosity of polymer in combustion, thus reducing the speed of combustible gaseous products generated by thermal cracking of polymer flow into the flame.

Thermal cracking of polymer blends and flame retardancy depend on the components type of the blend. For example, cotton fiber has a differential scanning calorimetry (DSC) exothermic peak at 350 °C, which is caused by the

decomposition of levoglucosan monomers formed. However, when a small amount of cotton wool is added into cotton fiber, the exothermic peak disappears at once. This is because the glucan is formed by crystalline fibers, while amino-derivative produced by thermal cracking of wool (225 ℃) can swell crystallization [3].

In addition, after adding 18% of wool into cotton fiber, its activation energy of thermal cracking decreases from 220 (cotton) to 103 kJ/mol (blend fibers). But the addition of wool to cotton fibers can increase the amount of carbonization (higher than expected). This is due to the abovementioned swelling, which increases low-order area of cotton fibers. The increased amount of carbonization does not mean the improvement of flame retardancy in that case. In fact, the flame retardancy of cotton/wool blend fibers is lower than that of cotton [29], because under the same conditions, combustible gaseous products increase. Cotton/Polyester blend fibers also have similar phenomenon [30].

Some physical factors, such as increasing specific heat and evaporation heat, absorption of heat and dissociation in gas phase, can make contribution to the performance of phosphorus flame retardants. Especially for some additive easy-volatile phosphorus flame retardants, it is more important for the above factors (especially in gas phase) to play a role (e.g., the tris-phosphates (dichloropropyl) used in polyurethane flexible foam).

3.4 Phosphorus flame retardants and their interaction with others

3.4.1 Phosphorus–nitrogen synergy Effect

Some nitrogen chemicals can enhance the function of flame retardancy of phosphorus compounds to celluloses; one such reason is that the phosphorus compounds react with nitrogen to form PN bond intermediates. In-situ formed PN bonds can improve the reactivity of cellulose carboxyl and phosphorylation and further improve char yield. Thus, some of the phosphorus–ammonia compounds are taken as phosphorylation agent better than phosphorus compounds [2]. The other reason is that nitrogen can delay volatilization loss of phosphorus compounds in condensed phase. Furthermore, nitrogen in phosphorus–nitrogen system can enhance the oxidation of phosphorus compounds and can release inert gases including ammonia. But the flame retardancy of ammonia is related to both aspects of chemistry and physics.

Many studies focus on phosphorus–nitrogen synergy effects [2, 31–33]. It is believed that this collaboration is not a common phenomenon, but it is related to the

type of nitrogen compounds and the polymers. For example, the flame retardancy of phosphamidon in PA is worse than that of phosphorus of the same quantity. If phosphates with nitrogen and the mixture of cyclic phosphonates as flame retardant in ethylene-vinyl acetate copolymer(EVA) are used, and the ratio of two components in the mixture is suitable, the carbonization rate of EVA increases. The formation of P–NH bonds in carbon is helpful for carbonization and more phosphori remains in carbonization layer.

Phosphorus (tributyl phosphate [TBP]) and nitrogen flame retardants (guanidine carbonate, GC) act on cotton fibers as an example to illustrate the possible flame-retardation mechanism of P/N system [31].

When cotton fibers in P/N flame-retardant system combust, their surfaces can form carbon layers, which is a complex compound composed of P, N and O, among which the P/N/O high polymers bear heat resistance of a high level. When the single phosphate (e.g., TBP) is used as flame retardant in cotton fibers, TBP will be decomposed at high temperature forming acidic phosphate and alkene by *cis*-form and elimination actions [34] which is similar to carboxylic ester. The phosphate can be further turned into polyphosphoric acid. Besides, in the process of thermal decomposition, TBP can be volatilized into combustible products (see reaction 3.6) [31]. Alkene formed in the process of thermal decomposition of TBP is a kind of combustible product. But the formed acidic phosphate can phosphorylate the cotton fiber, catalyze the dehydration and form the polyphosphoric acids. This is the flame retardation mechanism of phosphate acting on cotton fiber.

However, the phosphate is not effective in terms of forming the polyphosphoric acids to coat the cotton fiber to reduce its flame retardancy. However, the situation is different when phosphates and nitrogen flame retardants are used together because these two compounds can have synergistic effect with each other. The nitrogen flame retardant is decomposed into NH_3 that can catalyze the thermal decomposition of phosphates (such as TBP) to form acidic phosphates (see eq. 3.7) [31]. It can phosphorylate the cotton fiber and can form polyphosphoric acids. Equation (3.8) [31] shows the reaction pathways of the product of P/N/O polymer (as a product to protect carbon layers) in the P/N system at a high temperature. First, the organic acids and alkalis form organic salts. Then, the P/N system generates phosphamide and water. This is an endothermic reaction and the generated water can also help flame retardancy; thus, this step can provide high flame-retardant efficiency. The other two reactions are phosphates and acid phosphates, respectively, which react with NH_3 to form phosphoramide. Phosphoramide formed in the above three steps can be converted into

P/N/O polymer, which could be polyphosphamide or polyphosphazene. They can cover cotton fibers to achieve flame retardancy.

It is known that several kinds of nitrogenous compounds (such as urea, GC, melamine, etc.) can be used in cotton fibers to have synergistic flame retardation effect with phosphates (such as TBP, triallyl phosphate, etc.). The phosphorylation of cotton fiber and its dehydration to form a P/NO polymer protection layer are important to flame retardation performance, which is verified by Attenuated total reflectance-Fourier transform infrared spectrometry (ATR-FTIR) and X-ray photoelectron spectroscopy (XPS).

(3.6)
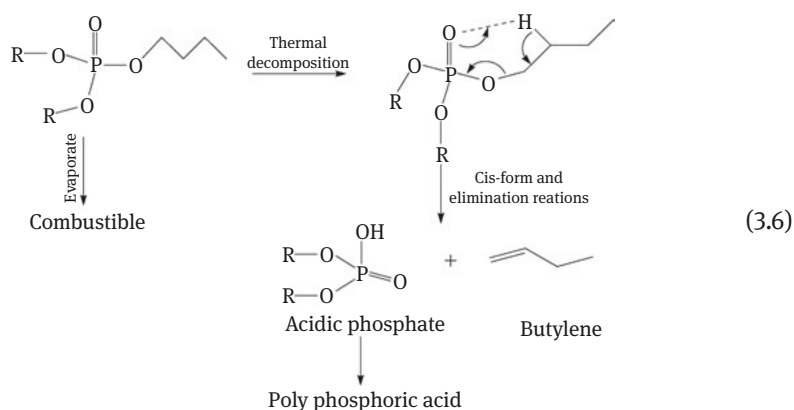
Thermal decomposition mechanism of phosphate, urea, GC, and melamine formaldehyde resin is shown.

(3.7)
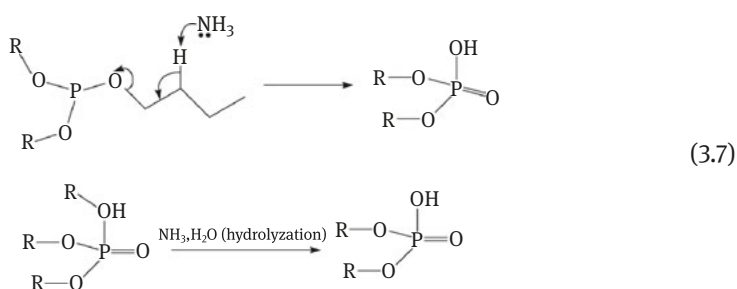
The mechanism of the production of the acid phosphate by P/N system:

$$(3.8)$$

Poly phosphorus
amide polyphosphate
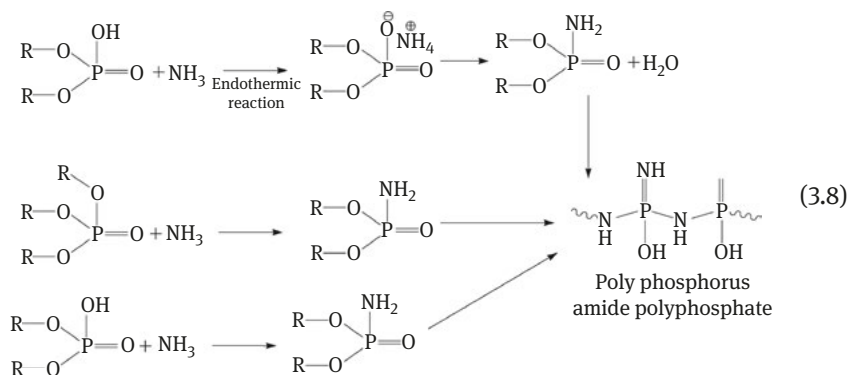
Production mechanism of P/N/O polymer [31].

Synergism effect of P/N flame-retardant system in polyacrylonitrile

The copolymer formed by copolymerization of the flame-retardant aluminum diethyl phosphonate (ADEP) containing P and N and acrylonitrile monomer (AN) according to reaction (3.9). It shows a higher LOI (see Table 3.1) and char yield [31] due to the synergistic effect of these two flame-retardant elements.

$$(3.9)$$
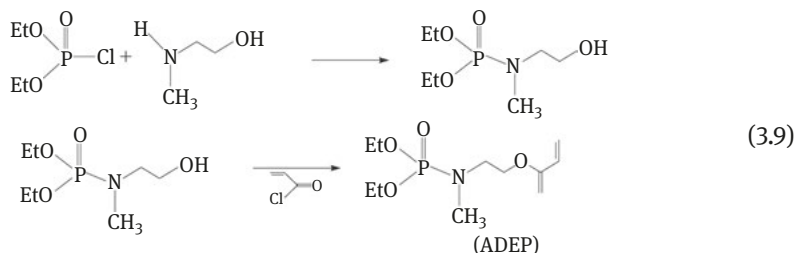
(ADEP)

Table 3.1: LOI in the copolymer of AN and ADEP [33].

The molar ratios of ADEP and AN in copolymers	P contents in the copolymers (%)	LOI (%)
1.0:0.0	0.00	19.7
0.99:0.01	0.54	21.1
0.974:0.026	1.40	22.8
0.97:0.03	1.62	24.7
0.96:0.04	2.18	25.0
0.95:0.05	2.70	26.4

Table 3.1 shows that the phosphorus content of the copolymer, which copolymerized by 0.05 mol ADPE and 0.95 mol AN copolymer, is only 2.7% and the LOI value can be up to 26.4%. The LOI value is 6.7% higher than a single PAN (19.7%) and every 1% of P content can increase LOI by about 2.5%. Phosphorus contents in the copolymer are almost linear relationship with the LOI value. Furthermore, the copolymer with phosphorus content is just about 0.54%, and when its temperature rises up to 700 °C, its char yield in N_2 can increase by at least 15% higher than that in the single PAN and by at least 6% in the air. All these are related to the PN synergistic flame retardancy in the copolymer, because at that situation, it is easier to form P/N/O polymer carbon layer flame retardancy in condensed phase with higher thermal stability. For AN/ADPE copolymer, the phosphate groups can be dissociated into acidic phosphoric acid groups according to reaction (3.10), and the latter can lead to cyclization of PAN (see reaction (3.11)) [33, 35].

$$(3.10)$$

$$(3.11)$$
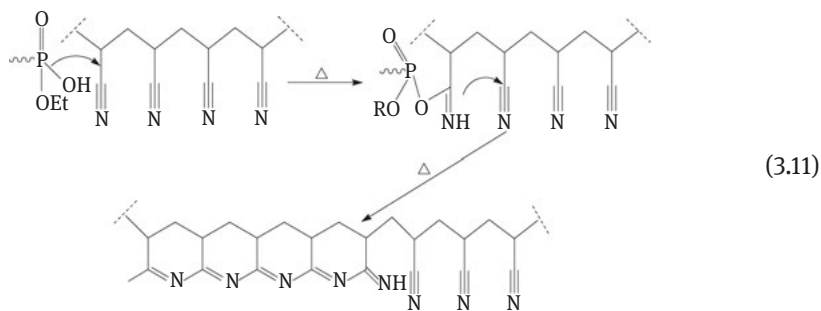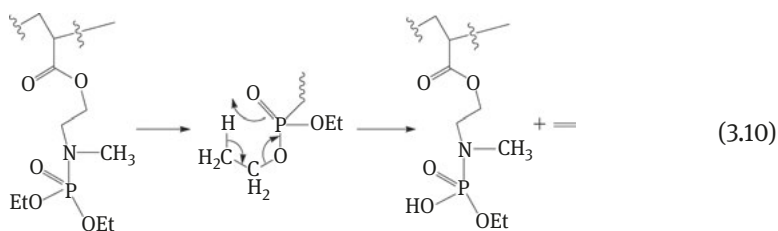
In addition, AN/ADPE copolymer has flame-retardant effect in gas phase when capturing free radicals of PO, PO_2, P_2O_4, etc.

3.4.2 The phosphorus–halogen synergism

Similar to the PN synergistic system, the synergistic mechanism of P–X system has been studied [36, 37]. Organic phosphorus compounds containing X can form phosphorus halides and halogen oxides when heated and X may also enhance flame

retardancy of phosphorus in gas phase, but credible evidences have not been obtained yet. There is another possibility; even though a flame-retardant molecule contains both halogen and phosphorus or a flame-retardant system contains both halides and phosphides, the phosphorus and halogen will play their roles of flame-retardant effects, respectively.

No final conclusion until now has been obtained about the phosphorus–halogen synergistic effect. Researchers propose that halogen–phosphorus synergism is similar to halogen–antimony synergism, but for the view of the formation of phosphorus halide and phosphorus oxide halide, it is impossible from the perspective of bond energy. It is not beneficial to use the phosphate and halogenated hydrocarbon to form phosphorus halide and phosphorus oxide halide in the aspect of bond energy. No evidence shows that flame-retardant materials containing phosphorus can form PCl_3 and $POCl_3$ in the process of combustion [4]. However, when flame retardants contain phosphorus and halogen, they may improve synergistic effects [38]. For example, when the compound of ammonium polyphosphate and hexabromocyclododecane acts on PAN, it has bromine–phosphorus synergistic effect, whose synergistic efficiency is 1.55. LOI and NOI results prove that in the system, bromine derivatives do not function as radical scavengers in gas phase but as a char-foaming agent [10]. Furthermore, in the flexible polyether polyurethane-foamed plastics containing bromine and phosphorus, bromine is also found to improve the char yield [39]. When bromine and phosphorus atoms are contained in a same molecule, bromine–phosphorus synergism becomes more obvious. For example, when a phosphate-containing bromine, whose bromine atom and phosphorus atom ratio (the ratio of the amount of substance) is 7:3, acts on PC-PET, its synergistic efficiency rises up to 1.58. While a phosphate-containing bromine, whose bromine atom and phosphorus atom ratio (the ratio of the amount of substance) is 6:1, acts on PC and its alloy, the obvious synergistic effect can also be observed. In addition, a bromine–phosphorus system that acts on PC-PET can form a lot of carbon foams in the process of thermal cracking or combustion. It shows that the bromine in the flame-retardant ingredients is at least partly used as the foaming agent in the intumescence process. That is to say, bromine–phosphorus flame-retardant ingredients not only have the function to capture radicals in gas phase but also have the ability of intumescence of carbonization [4].

For some oxygenated high polymers (such as PA6 and PET), halogen–phosphorus synergistic effect is notable. For example, when bromine–phosphorus system acts on PET, the amount of flame retardants will be significantly reduced than using regular bromine–antimony system [3]. When the flame retardant acts on PBT, PS, HIPS and ABS, they all have bromine–phosphorus synergisms. For example, dialkyl group-4-hydroxyl radical-3,5-dibromo benzyl phosphate acts on ABS, compared with the bromide or phosphide retardant with similar structure. Bromo-phosphorus retardant derivatives have better flame-retardant properties, which are obviously attributed to bromine–phosphorus synergies [41]. Furthermore, when the tribromophenyl

methacrylic acid ester and triphenyl phosphate act on polyurethane, and the Br/P (molar ratio) in flame retardant is 2.0, the best synergistic effect can be achieved [42]. Bromo-phosphorus synergy cannot be regarded as a general rule. Current situation is more likely to be halogen–phosphorus addition, or even phosphorus–halogen antagonism according to the observations that have been done.

When the flame retardants containing halogens and phosphori and antimony oxide are used together, there is no synergism or adduct effect among halogen, phosphorus, halogen and antimony, but antagonism may be possible. For example, when flame retardants containing halogens and phosphori act on polyethylene, adding antimonous oxide cannot improve flame-retardant efficiency. Experiments have found that in this case, during the combustion of polyethylene, antimony is not gasified. This shows that since the gasification of antimony is hindered by phosphorus, it suppressed halogen–antimony synergism, which result in deterioration of the flame retardancy efficiency. It was suggested that antimony oxide is converted to antimony phosphate which is nonvolatile.

The interactions of the halogen and the phosphorus in flame-retardant system depend not only on the types of polymers but also the structures of phosphorus and halogen flame retardants.

3.4.3 Interactions between phosphorus flame-retardant system with the inorganic fillers

The flame propagation speed of unsaturated polyesters with alumina trihydrate and methyl dimethyl phosphonate shows that there are synergistic effects between them [43]. The addition of titanium dioxide into APP and resin-containing nitrogen (a intumescent flame retardant) can not only increase the char yield but also form denser and more continuous carbon layer, thus significantly improving the flame retardancy of PP. In contrast, tin dioxide can result in multihole and pieces on carbon layer, thus reducing char yield. The titanium dioxide synergistic effect is considered to be a contribution for physical "bridging" effect [44].

If aluminum hydroxide is added into the materials that contain phosphorus compounds, the aluminum phosphate will be formed. It can improve the quality of carbon layers and extend the residual time of volatile-dissociated products in carbon layers, thus improving the flame retardancy of the material.

3.4.4 Interactions among phosphorus flame retardants

Using two or more phosphorus flame retardants in the same system sometimes can also improve the flame-retardancy effect. For example, phosphonium bromide (PH_4Br or R_4PBr) or phosphine oxide and ammonium polyphosphate used together

as flame retardant in polypropylene or polystyrene sometimes can achieve "phosphorus–phosphorus" synergism. It is inferred that this effect is probably caused by the coexistence of two or more effective phosphorus flame retardants both in gas and condensed phase [45].

3.5 Flame retardant mechanism of aromatic phosphate acting on PC/ABS

References [46] and [47] reviewed this topic. Some new types of phosphorus flame-retardant systems are upstarts in the field of flame retardancy. The understanding on mechanism of flame retardancy acting on polymers is insufficient, some of which are still in dispute. Some are not confirmed by sufficient and convincing evidences but further researches are afoot [46, 47]. The following part summarizes the mechanism of organic phosphorus flame retardants acting on PC/ABS. However, to explain the mechanism of flame retardancy, the mechanism of thermal decomposition of PC initially will be discussed.

3.5.1 Thermal decomposition mechanism of PC

Bisphenol type-A PC (hereinafter refers to PC of this kind), with high degrees of thermostability, will not decompose below 250 °C and its decomposition temperature in air is over 310 °C.

Carbonic acid ester groups rearranged into carboxyls and their secondary reactions

When heated PC in a sealed tube, most carbonic acid ester groups have been destroyed in the early phase of thermal decomposition of PC. One of the outcomes of thermal decomposition is that carbonic acid ester groups can be rearranged into a side-chain carboxyl, which is adjacent to the main-chain ether bond of PC to form 2-phenoxy benzoic acid structure. The side-chain carboxyl could be further decomposed into carbon dioxide and water, simultaneously turn itself into secondary products (such as xanthone cyclic structure or anthraquinone compounds) (see eq. (3.12)) [47]. However, the linear structure of PC is still intact.

Although the formation of xanthone cyclic structure is not the main process of PC's thermal decomposition, the water and the hydroxy compounds produced by reaction (3.12) and the subsequent reaction (3.13) are important for PC's further thermal decomposition. Dissociation of mass spectra provides the evidence of rearrangement of carbonic acid ester groups into carboxyls. Some mass spectra can be classified into the category of xanthone cyclic structure or anthraquinone compounds.

$$(3.12)$$
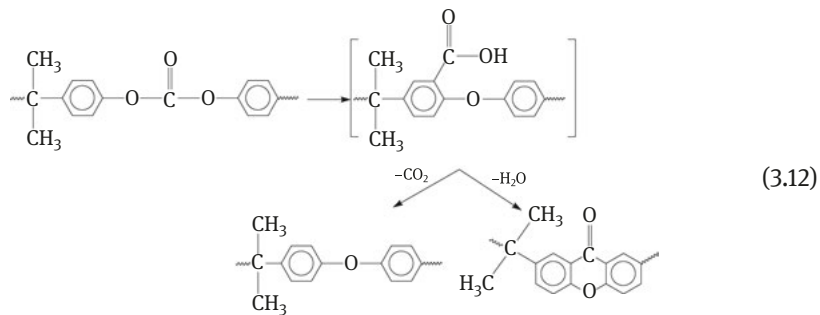
2-Phenoxybenzoic acid's intermediate structure for med by reaction (3.12) can also attack PC and cross-link with it and produce hydroxy compounds in the further decompositions (see reaction (3.13)) [47].

$$(3.13)$$
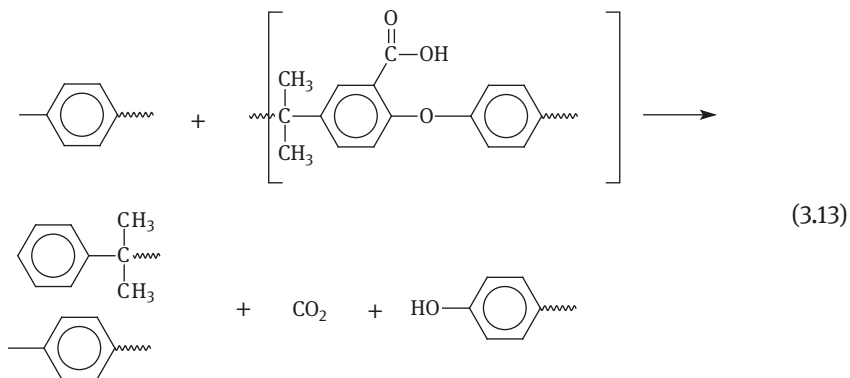
Both reactions (3.12) and (3.13) produce volatile products. The branching of PC will be generated by reactions (3.12) and (3.13) regardless of the fact that whether volatile products are excluded from the system or not. If the hydroxyl-containing compounds (such as water and phenol) are excluded from the system, the breaking of bonds will be suppressed, whereas the above PC's branching will only result in a gel reaction. However, if the volatile products like hydroxyls are kept within the system, the PC's bond breaking will be the main reaction and the gels will not occur. Dynamics research proved that PC's bond breaking in closed system does not comply with random free radical mode.

Effects of hydroxy compounds and PC

The water released during reaction (3.12) and steams in PC promote PC's bond breaking when PC is heated strongly. It will result in the formation of phenolic compounds and carbon dioxide (see reaction (3.14)) [47]. Researchers suggest that reaction (3.14) is one of the main reasons for PC's bond breaking.

$$\text{~~} \bigcirc \text{—O—} \overset{\overset{\displaystyle O}{\|}}{C} \text{—O—} \bigcirc \text{~~} \xrightarrow{-H_2O} \text{~~} \bigcirc \text{—OH} + CO_2 + HO \text{—} \bigcirc \text{~~} \qquad (3.14)$$
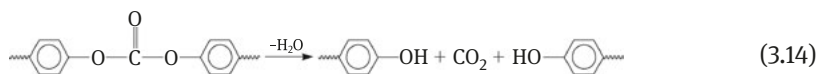
PC's thermal decomposition generates free phenols, bisphenol A (BPA) and small fragments, where phenol bonds' end group is counterproductive to the stability of carbonate ester chains because they initiate the carbonate ester bond's transfer reaction, breaking polymer's chains into small fragments (see reaction (3.15)) [48].

$$\text{~~} \bigcirc \text{—O—} \overset{\overset{\displaystyle O}{\|}}{C} \text{—O—} \bigcirc \text{~~} + \bigcirc \text{—OH} \longrightarrow \text{~~} \bigcirc \text{—O—} \overset{\overset{\displaystyle O}{\|}}{C} \text{—O—} \bigcirc + HO \text{—} \bigcirc \text{~~} \qquad (3.15)$$
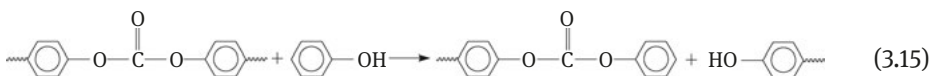
The reactive activation energy of PC bond's break reaction is only 112 kJ/mol, which demonstrates that the molecular mechanism dominates its bond breaking. Reactions 3.14 and 3.15 contribute most to such mechanisms.

Fries rearrangement

Another rearrangement that PC chain may have is Fries rearrangement (see reaction (3.16)) [50, 51]. Many researchers have found that there exist phenolic hydroxyl group and aromatic ester group in the decomposed products of PC, showing the occurrence of the rearrangement, whereas the most convincing proof is the dissociation mass spectrum of volatile fragments formed from the PC thermal cracking.

$$(3.16)$$
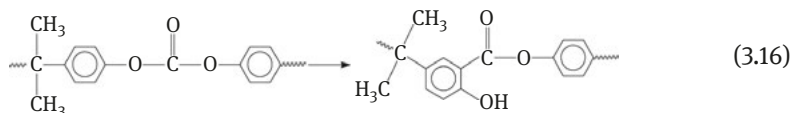
The break of isopropylidene bonds

A small amount of methane was released at the beginning of PC thermal decomposition. With the increasing temperature, the amount of methane released increased. The methane was formed by free radicals from the break of isopropylidene bonds (see reactions (3.17) and (3.18)) [52].

$$(3.17)$$

(3.18)
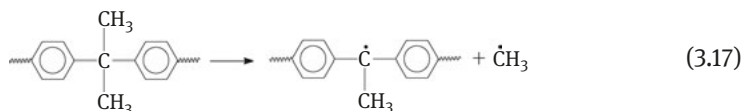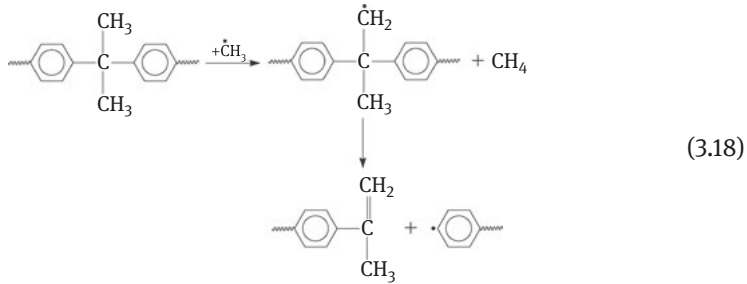
The thermal oxidation of the PC

There is no clear conclusion on the initial assessment that oxygen attacks PC when it was under thermal decomposition in air, but it may be isopropylidene bonds. After the hydrogen is extracted from methyl, it will form unstable radical (I) which will immediately rearrange into a stable radical (II). Then, the oxygen attacks radical (II) quickly and form peroxide. When the temperature is over 300 °C, this peroxide will be decomposed into one active hydroxyl radical and one alkoxyl radical through homolysis. By extracting hydrogen, the hydroxyl radical will form water molecules, whereas the alkoxyl radical will form compounds containing hydroxyls [47]. The formation of water and compound with hydroxyls leads to further degradation of PC (see reactions (3.14) and (3.15)).
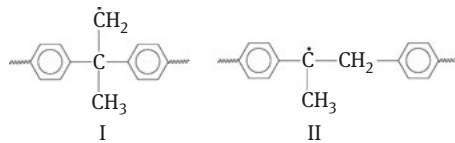
Researchers proposed another oxidation mechanism of PC thermal decomposition, in which methylene radicals were formed at first and then rearranged to relatively stable benzylated radicals. Furthermore, phenol end groups and the oxidative coupling of PC chain may cause the biphenyl cross-linking (see reaction (3.19)), thus forming an insoluble gel fragments, which also have been confirmed by experiments [53].

(3.19)
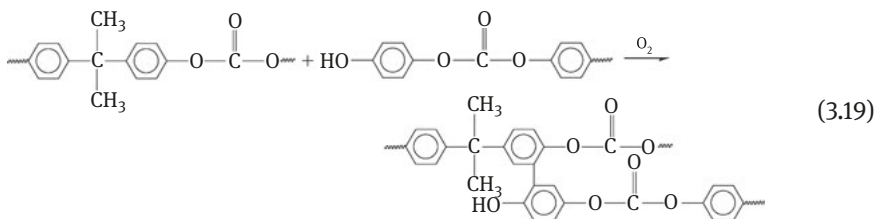
Other thermal decomposition modes
Mass spectroscopic researches of PC and model compounds under mild ionization conditions suggested that the main products of PC's fragmentation are cyclic oligomers. It was suggested that the ionic ester exchange is the predominant process in PC thermal decomposition. The products of methylene formed and the carbon dioxide released in this process form a series of secondary decomposition products. But some researchers disagree with the ion mechanism above [54, 55], and they carried out the experiments under vacuum and showed the outcomes according to the product released from PC's thermal decomposition. The mechanism may be PC bond homolysis rather than hydrolysis or interesterification. But convincing proofs about the ions or radicals mechanisms have not been found yet.

Primary products from thermal decomposition of PC
The most primary products from PC's thermal decomposition are carbon dioxide, BPA, and water. Other products with relatively larger amount include carbon monoxide, methane, phenol, diphenyl carbonate, and 2-(4-hydroxyphenyl)-2-phenyl propane. Besides, it also forms ethyl phenol, isopropenylphenol, and cresol with small amount, which are formed in further decomposition process of BPA. Homolysis of PC chain or 1, 3-migration of carbonic acid ester group can also form carbon dioxide. Combustible gases released in the process of PC thermal decomposition are carbon monoxide and methane, which may be the most important factor for ignition of PC. However as their concentrations are too low, it is very difficult to ignite PC.

All the mechanisms of PC's thermal decomposition and thermal oxidative decomposition discussed above are supported by the volatile products of PC decomposition. Although PC is the kind of polymer with high carbonization capability, there is little research on its solid residue carbon. Only several researchers point out that when the temperature is higher than 440 °C, the carbon formed in the process of PC thermal decomposition has highly cross-linked structures, which contain diaryl ester and unsaturated carbon-bridged bond [56].

3.5.2 The mechanism of flame retardants acting on PC/ABS

Flame retardancy in condensed phase
It is generally agreed that the mechanism of aromatic phosphates acting on PC/ABS mainly related to the function of phosphates that promote the PC in PC/ABS into carbon, namely, the mechanism of flame retardancy in condensed phase [57]. The flame-retardant efficiency is closely related to the proportion of PC and ABS. It has also been found that phosphori gather in condensed phase when the PC/ABS with phosphates retardant is in thermal decomposition and combustion. Results from TGA also show that resorcinol bis(diphenyl phosphate), RDP can protect carbon

layer from oxidation under high temperature. Its synergist effects in condensed phase help PC/ABS to improve carbon yield [58]. In addition, Fries rearrangement may occur in PC thermal decomposition (see reaction (3.16)), and aromatic phosphates can catalyze the rearrangement. What's more, RDP may react with the products in the rearrangement of PC by transesterification (see reaction (3.20)), leading to the enrichment of the phosphorus and cross-linking of PC. All of the above should be attributed to the flame retardancy in condensed phase.

(3.20)
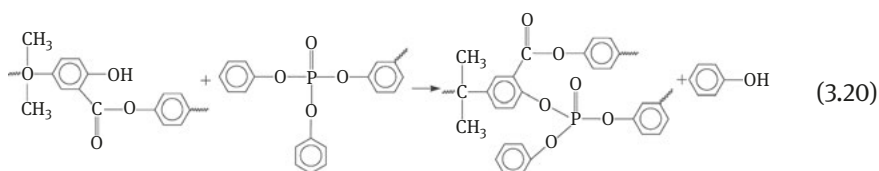
Flame retardancy in gas phase

It has been proved by the experiment that in flame-retardant system, phosphates acting on LOI in PC/ABS and PC in PC/ABS are related with the ratio of ABS, and their rules of variation are rather complex. Besides, aromatic phosphates in PC/ABS will increase the carbon monoxide proportion in combustion products, revealing that the flame retardancy in gas phase does play a role in flame-retardant process. However, their flame-retardant properties in gas phase are still a controversial issue. For example, it has been reported that the flame-retardant efficiency of aromatic phosphates decreases with the increase of molecular weight (oligomerization), indicating that there may be no phosphate in gaseous phase. However, it has also been certified that the flame-retardant efficiency of aromatic phosphates will be improved with the increase of their relative molecular weight.

In general, the reaction can happen both in condensed and gas phase for PC/ABS with phosphates as flame retardants, and their proportion is related to the structure and property of phosphates.

Interaction of phosphates (synergism and antagonism)

When triphenyl phosphate (TPP), RDP and bisphenol A-bis (diphenyl phosphate)BDP with the same phosphorus content acting on the PC/ABS, they show similar flame retardancy in accordance to LOI test even with different PC-to-ABS ratios. However, flame retardancy of RDP and BDP is better than that of TPP measured according to UL94 flame-retardant level. Moreover, aromatic phosphates can effectively increase time to ignition (TTI) and moderately decrease peak heat release rate(PHRR) after the above three flame retardants are tested by cone calorimeter [60]. Overall, the performance of RDP is better than TPP with volatility when utilized in PC/ABS.

An experiment has been conducted by cone calorimeter to get the heat release data of RDP and RDP/TPP (3%) acting on PC/ABS with the heat flux of 35 kW/m^2

and 75 kW/m^2, respectively. The test indicates that PHRR of PC/ABS mixed with RDP/TPP is less than that of the material with one-single RDP when the heat flux is 35 kW/m^2. It is maybe the contribution of TPP flame retardancy in gas phase; when the heat flux is 75 kW/m^2, the situation is totally opposite, that is, the PHRR of the material with RDP is relatively low. Obviously, TPP's flame retardancy in gas phase is no longer important at this moment. Furthermore, TPP may have a negative influence in decreasing PHRR at high temperatures [61]. One possible explanation for this phenomenon is that the flame-retardant properties of some flame retardants in gas phase are reversible. Compounds with phosphorus can generally suppress the flame propagation [62], but they may become combusted catalysts in flames at high temperature. It is clear that TPP's flame retardancy in gas phase has such reversibility that it becomes invalid at high temperature. The above mechanism can also explain the synergistic effects between RDP and BDP with relatively low volatility and TPP with relatively high volatility. RDP or BDP improves flame retardancy in condensed phase that helps carbonization of PC and decreases the fuel supply for combustion, thus lowering the temperature of flame; with the decrease of the flame temperature, the effect of TPP's flame retardancy can be effectively improved. Finally, the flame retardancy of synergistic effect between them can be achieved.

In addition, we can see from the synergisms between RDP and other synergists that the flame retardation mechanism in gas phase does no have synergistic effects on RDP and even sometimes shows antagonistic effects. But some additives have flame retardancy in condensed phase which carbonize PC/ABS and improve the structures of carbon layers, performed by synergism effect [58].

In conclusion, phosphori can gather in condensed phase and prevent the carbon layer from oxidation at high temperatures, which are the main flame-retardant functions of aromatic phosphates. Furthermore, aromatic phosphate can catalyze Fries rearrangement and the isomerization of PC, which contributes to the forming of carbon layers and the blocking of volatilization of polymers.

References

[1]   Ebdon J R, Jones M S. Flame retardants: An overview[A]//Salamone J C. Polymeric Materials Encyclopedia[M]. Boca Raton: CRC Press, 1995: 2397–2411.

[2]   Joseph P, Ebdon J R. Phosphorous-based flame retardants[A]//Wilkie C A, Morgan A B. Fire Retardancy of Polymeric Materials. 2nd Edition[M]. Beca Raton: CRC Press, 2009:119–123.

[3]   Lewin M, Weil E D. Mechanisms and modes of action in flame retardancy of polymers[A]// Horrocks A R, Price D. Fire Retardant Materials[M]. Cambridge: Woodhead Publishing Ltd., 2000: 31–68.

[4]   Ou Yuxiang, Li Jianjun. The Flame Retardants[M].Beijing: Chemical Industry Press,2006: 32–36.

[5]   Price D, Cunliffe L K, Bullett K J, Hull T R, et al. Thermal behavior of covalently bonded phosphate and phosphonate flame retardant polystyrene systems[J]. Polymer Degradation and Stability, 2007,92:1101–1114.

[6]   Lyons J W. The Chemistry and Uses of Fire Retardants[M]. New York: Wiley-Interscience, 1970: 290.

[7]   Brauman S K. Phosphorus fire retardants in polymers. I. General mode of action[J]. Journal of Fire Retardant Chemistry, 1977,4:18–37.

[8]   Lewin M, Basch A. Structure, pyrolysis and flammability of cellulose[A]//Lewin M, Atlas S M, Pearce E M. Flame Retardant Polymeric Materials. Vol.2[M]. New York: Plenum Press, 1978: 1–41

[9]   Kandola B, Horrocks A R, Price D, et al. Flame retardant treatment of cellulose and their influence on the mechanism of cellulose pyrolysis [J]. Journal of Macromolecular Science-Reviews in Macromolecular Chemistry and Physics, 1996,C36:721–794.

[10]   Khanna Y P, Pearce E M, Synergism and flame retardancy[A]//Lewin M, Atlas S, Pearce E M. Flame Retardant Polymeric Materials. Vol. 2[M]. New York: Plenum Press, 1978: 43–61.

[11]   Banks M, Ebdon J, Johnson M. Influence of covalently bound phosphorus-containing groups on the flammability of poly (vinyl alcohol), poly (ethylene-co-vinyl) and low-density polyethylene[J]. Polymer, 1993,34:4547–4556.

[12]   Ebdon J R, Price D, Hunt B J, et al. Flame retardance in some polystyrenes and poly(methyl methacrylate)s with covalently bound phosphorus-containing groups. Initial screening experiments and some laser pyrolysis mechanistic studies[J]. Polymer Degradation and Stability, 2000,69:267–277.

[13]   Banks M, Ebdon J R, Johnson M. The flame-retardant effect of diethylvinyl phosphonate in copolymers with styrene, methyl methacrylate, acrylonitrile and Acrylamide[J]. Polymer, 1994,35:3470–3473.

[14]   Ebdon J R, Hunt B J, Joseph P, et al. Thermal degradation and flame retardance in copolymers of methyl methacrylate with diethyl(methacryloyloxymethyl) phosphonate[J]. Polymer Degradation and Stability, 2000,70:425–436.

[15]   Wyman P, Crook V, Ebdon J, et al. Flame-retarding effects of dialkyl-p-vinylbenzyl phosphonates in copolymers with acrylonitrile[J]. Polymer International, 2006,55:764–771.

[16]   Ebdon J R, Hunt B J, Joseph P, et al. Flame retardance of polyacrylonitriles covalently modified with phosphorus and nitrogen-containing groups[A]//Hull T R, Kandola B K. Fire Retardancy of Polymers: New Startegies and Mechanisms[M]. Cambridge: Royal Society of Chemistry, 2009: 331–340.

[17]   Brauman S K. Phosphorus fire retardance in polymers. IV. Poly(ethylene terephtalate)-ammonium polyposphate, a model system[J]. Journal of Fire Retardant Chemistry, 1980,7:61–8.

[18]   Brown C E, Wilkie C A, Smukalla J, et al. Inhibition by red phosphorus of unimolecular thermal chain-scission in poly(methyl methacrylate), investigation by NMR, FT-IR and laser desorpton/fourier transform mass spectroscopy[J]. Journal of Polymer Science, Part A. Polymer Chemistry, 1986,24:1297–1311.

[19]   Levchik G F, Levchik S V, Camino G, et al. Fire retardant action of red phosphorus in nylon 6 [A]//Paper at 6th European Meeting on Fire Retardancy of Polymeric Materials [C]. Lille, 1997.

[20]   Gibov K M, Shapovalova L N, Zhubanov B A. Movement of destruction products through the carbonized layer upon combustion of polymers [J]. Fire &. Materials, 1986,10:133–135.

[21]   Brauman S. Phosphorus fire retardance in polymers. II. Retardant-polymer substrate interactions [J]. Journal of Fire Retardant Chemistry, 1977,4:38–58.

[22]   Serenkova I A, Shlyapnikove Yu A. Phosphorus containing flame retardants as high temperature antioxidants [A]//Proc. Intl. Symposium on Flame Retardants [C]. Beijing,1989: 156–161.

[23]   Weil E D, Jung A K, Aaronson A M, et al. Recent basic and applied research on phosphorus flame retardants[C]//Proc. 3rd Eur. Conf. on Flamm. and Fire Ret. Technomic Publ., Westport, CT, 1979.

[24] Basch A, Zwilichowski B, Hirschman B, et al. The chemistry of THPC-urea polymers and relationship to flame retardancy in wool and wool-polyester blends, I. Chemistry of THPC-urea polymers [J]. Journal of Polymer Science, Part A. Polymer Chemistry, 1979,17:27–38.

[25] Camahan J, Haaf W, Nelson G, et al. Investigations into the mechanism for phosphorus flame retar-dancy in engineering plastics [A]//Proc. 4th Intl. Conf. Fire Safety [C]. San Fancisco: Product Safety Corp, 1979.

[26] Bright D A, Dashevshy S, Moy P Y, et al. Aromatic oligomeric phosphates: Effect of structure on resin properties [A]//Paper at SPE ANTEC [C]. Atlanta, 1998.

[27] Pearce E M. Some polymer flammability structure relationships [A]//Lewin M, Kirshenbaum G. Recent Advances in Flame Retardancy of Polymeric Materials, Vol. [M]. Norwalk: BCC, 1990:36–40.

[28] Ou Yuxiang, Chenyu, Wang Xiaomei. The Flame-Retardant Polymers Materials [M].Beijing: National Defence Industry Press,2001: 16–17.

[29] Lewin M, Basch A, Shaffer B. Pyrolysis of Polymer Blends [J]. Cellulose Chemistry and Technology, 1990,24:477.

[30] Lewin M. Flame retarding of fibers [A]//Lewin M, Sello S B. Handbook of Fiber Science and Technology. Chemical Processing of Fibers and Fabrics (Vol. 2,Part B) [M]. New York: Mercel Dekker Inc., 1984: 1–141.

[31] Gaan S, Sun G, Hutches K, et al. Flame retardancy of cellulosic fabrics. Interactions between nitrogen-additives and phosphorus-containing flame retardants [A]//Hull T R, Kandola B K. Fire Retardancy of Polymers, New Strategies and Mechanisms [M]. Cambridge: RSC Publishing, 2009: 294–306.

[32] Horrcks A R, Hicks J, Davies P J, et al. Synergistic flame retardant copolymeric polyacrylonitrile fibres containing dispersed phyllosilicate clays and ammonium polyphosphate [A]//Hull T R, Kandola B K. Fire Retardancy of Polymers, New Strategies and Mechanisms [M]. Cambridge: RSC Publishing, 2009: 307–330.

[33] Ebdon J R, Hunt B J, Joseph P et al. Flame retardance of polyacrylonitriles covalently modified with phosphorus- and nitrogen-containing groups[A]//Hull T R, Kandola B K. Fire Retardancy of Polymers, New Strategies and Mechanisms [M]. Cambridge: RSC Publishing, 2009: 331–340.

[34] Higgns C E, Baldwin W H. Interactions between tributyl phosphate, phosphoric acid and water [J]. Journal of Inorganic and Nuclear Chemistry, 1962,24(4):415–427.

[35] Wyman P, Crook V, Ebdon J R, et al. Flame-retarding effects of dialkyl-p-vinylbenzyl phosphonates in Copolymers with acrylonitrile [J]. Polymer International. 2006,55(7):764–771.

[36] Green J. A phosphorus-bromine flame retardant for engineering thermoplastics. A review[J]. Journal of Fire Sciences, 1994,12(4):388–408.

[37] Ballistreri A, Montanudo G, Puglisi C, et al. Intumescent flame retardants for polymers. I. The poly(acrylonilrile)-ammonium polyphosphate-hexabromocyclododecane system [J]. Journal of Applied Polymer Science, 1983,28(5): 1743–1750.

[38] Dombrowski R, Huggard M. Antimony free fire retardants based on halogens. Phosphorus substitution of antimony [A]//Proceedings of the 4th International Symposium Additives [C]. Clear Water Beach: 1996.

[39] Papa A J, Proops W R. Influence of structural effects of halogen and phosphorus polyol mixtures on flame retardant synergy in polyurethane foam [J]. Journal of Applied Polymer Science, 1972,l6 (9):2361–2373.

[40] Yang C P, Lee T-M. Synthesis and properties of 4-hydroxy-3,5-dibromobenzyl phosphonates and their flame-retarding effects on ABS copolymer[J]. Journal of Polymer Science, Part A. Polymer Chemistry, 1989,27:2239–2251.

[41] Guo W. Flame-retardant modification of UV-curable resins with monomers containing bromine and phosphorus [J]. Journal of Polymer Science, Part A. Polymer Chemistry, 1992,30:819–827.

[42] Bonsignore P V, Manhart J H. Alumina trihydrate as a flame retardant and smoke suppressive filler in reinforced polyester plastics [A]//Proceedings of the 29th Annual Conference Reinforced Plastics Composition Institute SPE [C]. 1984.23C:1–8.

[43] Scharf D, Nalepa R, Heflin R, et al. Studies on flame retardant intumescent char, Part I [A]// Proceedings of the International Conference on Fire Safty [C]. 1990.15:306–315.

[44] Savides C, Granzow A, Cannelonngo J F. Phosphine-based flame retardants for polypropylene [J]. Journal of Applied Polymer Science, 1979,23: 2639–2652.

[45] Ou Yuxiang, Zhaoyi, Fei Yanjie. The Thermal Decomposition of PC and the Flame-Retardant Mechanism of PC、PC/ABS [J]. Synthetic Resins and Plastics,2008,25(4):74–79.

[46] Levchik S V, Weil E D. Overview of recent development in the flame retardancy of polycarbonates[J]. Polymer International, 2005,54(7):981–998.

[47] Tagaya H, Katoh K, Kadokawa J, et al. Decompositon of polycarbonate in subcritical and supercritical water[J]. Polymer Degradation and Stability, 1999,64(2):289–292.

[48] Puglisi C, Sturiale L,Montaudo C. Thermal decomposition processes in aromatic polycarbonates investigated by mass spectrometry [J]. Macromolecules, 1999,32 (7):2194–2203.

[49] Oba K, lshida Y, Ito Y, et al. Characterization of branching and/or cross-linking structures in polycarbonate investigated by reactive pyrolysis-gas chromatography in the presence of organic alkali [J]. Macromolecules,2000,33 (32):8173–8183.

[50] Kuroda S I, Terauchi K, Nogami K, et al. Degradation of aromatic polymers. I. Rates of crosslinking and chain scission during thermal degradation of several soluble aromatic polymers[J]. European Polymer Journal, 1989,25(1): 1–7.

[51] Carroccio S, Puglisi C, Montaudo G. Mechanism of thermal oxidation of poly(bisphenol a carbonate)[J]. Macromolecules, 2002,35(11):4297–4305.

[52] Mcneill I C, Rincon A. Degradation studies of some polyesters and polycarbonates.8. Bisphenol a polycarbonate [J]. Polymer Degradation and Stability, 1991,31(1): 163–180.

[53] Mcneill I C, Rincon A. Thermal degradation of polycarbonate. Reaction condition and reaction mechanisms[J]. Polymer Degradation and Stability, 1993,39(1):13–19.

[54] Jang B N, Wilkie C A. A TGA/FTIR and mass spectral study on the thermal degradation of bisphenol a polycarbonate[J]. Polymer Degradation and Stability, 2004,86(3):419–430.

[55] Levchik S V, Bright D A, Alessio G R, et al. New halogen-free fire retardant for engineering plastic applications[J]. Journal of Vinyl Additive Technology, 2001,7(2):98–103.

[56] Murashko E A, Levchik G F, Levchik S V, et al. Fire-retardant action of resorcinol bis(diphenyl phosphate) in PC-ABS blend. II. Reactions in the condensed phase [J]. Journal of Applied Polymer Science, 1999,71(11):1863–1872.

[57] Levchik S V, Bright D A, Moy P Y, et al. New developments in fire retardant non-halogen aromatic phosphates [J]. Journal of Vinyl and Additive Technology, 2000,6(3):123–128.

[58] Levchik S V, Bright D A, Dashevsky S. Specialty Polymer Additives Principles and Application [M]. Oxford: Blackwell Science, 2001:259–269.

[59] Babushok V, Tsang G W. Inhibitor rankings for alkane combustion [J]. Combustion and Flame, 2000,123(4):488–506.

4 Flame retardation mechanism of intumescent flame retardant

The performance of intumescent flame retardant (IFR) mainly comes into play through condensed phase, which means flame-retardant effect can be achieved through delaying or suspending combustion on the basis of carbon mechanism. The following conditions belong to flame retarding in condensed phase: (1) Flame-retardant chemical delays or suspends the thermal decomposition in condensed phase by reducing or preventing the supply of combustible. (2) Porous carbon layer is generated on the surface of flame-retardant materials during burning, which can insulate heat, isolate oxygen and prevent combustible gas in gaseous phase. This is just the flame retardation mechanism of IFR. (3) A large amount of the inorganic filler in flame-retardant material can dilute combustible material and have massive heat capacity to store and conduct heat. Therefore, the material can hardly reach the thermal decomposition temperature. (4) Fire retardant will decompose and absorb heat when heated, which can prevent the material from continued temperature rise. Aluminum hydroxide and magnesium hydroxide, which are widely used in industry, belong to this type of fire retardant.

IFR system is a typical fire retardant, based on flame retardation mechanism of condensed phase. This flame-retardant chemical can stop the combustion at an early stage, because IFR system will form a very thick carbon layer on the surface of material at high temperature, which has high flame retardancy. For example, polyvinyl alcohol and epoxy resin would almost completely decompose in fire of 500 °C (amount to the surface temperature of the flaming polymer); but when phosphori flame-retardant chemical is added into the polymer, which is a kind of IFR, the flammability of the polymer will decrease with a newly formed carbon layer and the oxygen index of epoxy resin will rise to 30 % [1].

In recent years, IFR is the main focus in flame-retardant industry and is recognized as one of the most important approaches to identify halogen-free flame retardant. According to chemical abstract (CA) statistics, in 2007, more than 160 literature and 100 patents were published [2]. Although the flame-retardant mechanism of IFR, especially carbon mechanism, has been studied by many research scholars, it is not fully understood until now. Some relatively clear literature reviews can be found in Refs. [1–7].

4.1 Composition of IFR

4.1.1 The three-component of IFR

The three essential elements for inflation are as follows: (1) inorganic acid or compound (acid source) that can generate acid when heated to 100–250 °C, such as

ammonium polyphosphate (APP); (2) polyhydroxy compound with rich carbon atoms which can dehydrate to carbon source by the effect of acid, such as pentaerythritol (pentaerythritol ester rosin [PER]); (3) amine and amide compounds are used as the gas source which can release volatile products under heat, such as melamine (MA). Besides, water vapor will also produce sparkling effect. Furthermore, amines and amides may also act as a catalyst for carbon generation [1, 2].

Three source materials of IFR are listed as follows [5]:

(1) Acid source: Phosphoric acid, vitriol, boric acid, ammonium phosphate, APP, ammonium sulfate, ammonium halide, urea phosphate, guanidine phosphate, MA polyphosphate and reaction product of nitrogen and P_2O_5.

(2) Carbon source: Triphosphate (Tolyl), alkyl phosphates, alkyl halide phosphate, starch, dextrin, mannitol, pentaerythritol (including dimers and trimers), phenolic resin(PF), PA6, PA6/nanoclay, thermoplastic urethane (TPU) and polyphenyl ether(PPO).

(3) Gas source: Urea, urea–formaldehyde resins, dicyandiamide, MA, and polyvinyl alcohol amine halide.

It is to be noted that researchers usually intermix between "charring agent" and "expansion flame-retardant system" due to lack of detailed information about retardant mechanism. Presently, the porous expansion texture and its insulation effect can only be expanded qualitatively as expansive char layer. Only by in-depth study of expansion characteristics of the coal bed, we could interpret IFR quantificationally.

4.1.2 The conditions that the three components of IFR should satisfy

(1) Thermal stability of the components of IFR must be sufficiently high so that they do not decompose in the polymer-processing temperatures (above 200 °C).

(2) Thermal degradation of polymers should be harmless to the expansion process. Generally, in the process of the thermal degradation of the polymer, a considerable amount of volatile products and carbon residue (connected with the structure of high polymer) are generated. All of the above factors may affect the formation of expansion carbon layer.

(3) IFR should form full-coverage protective carbon layer on the surface of polymer [5].

(4) IFR should not cause the deterioration of physical and chemical properties of polymers. In particular, it should not cause adverse interactions after reacting with other additives (such as stabilizers) [5].

Before the dehydration of acid components of IFR, carbon components must not be decomposed and volatilized. During the formation of porous carbon layer and its

retrogradation and solidification, the gas source should release small bubbles continually. The rate of release from the gas source and the viscosity of the flame-retardant system must be well matched, and it will be influenced by the temperature. Pores in the expansion foam carbon layer are mostly obturator. The diameter of the pores ranges from 20 μm to 50 μm and the wall thickness of the pores ranges from 6 μm to 8 μm. Added ultrafine powder of inert filler with good dispersion (e.g., titanium oxide and silica gel) to the flame-retardant system as nucleating agent could control the bubble volume in the foaming process.

Only a minority of IFR components listed above has practical application and most of them are defined by experiences. Available inorganic acid (acid source) must have a high boiling point and oxidizing ability can not be too strong. As a result, inorganic acid salt is the most common, such as ammonium salts and amide salt of phosphoric acid or organic phosphate ester and organic phosphorus amide. The available carbon source is pentaerythritol, polyurethane, and some epoxy resin. The available gas sources are amine and acid amides, for example, urea, MA, dicyandiamide, and their derivatives. Halide is utilized as the source of gas because they can emit halogenide (HX) upon heating. Now, because of its negative secondary fire effects of chloride (smoke, corrosive and toxic), they have not been used frequently. Because HX is considered as a gaseous phase flame retardant, the IFR containing halide has flame-retardant capacity in both the condensed phase and in the gaseous phase.

To meet the requirements of high flame retarding level, IFR is usually used in a large quantity. At the same time, during the process of expansion of carbon layer, the polymer is likely to cause adverse chemical reaction with components of IFR. In addition, we find that the currently used IFR is unsatisfactory in the matter of water solubility, weather resistance, thermal stability, covering ability and appearance.

4.1.3 Typical IFR

Although the IFR has been widely used in flame-retardant polymers, polyethylene (PE), polypropylene (PP) and polystyrene (PS) are most prevalent. Combustion of these three polymers is difficult to stop because of their production of a large amount of combustible hydrocarbons upon heating.

A mixture of dipentaerythritol and APP (or MA pyrophosphate) is typical IFR, which is most often used in flame-retardant PP, but they are fairly unstable at the processing temperature of PP. The reaction products of P_2O_5, pentaerythritol and MA are more suitable IFR and they can be used for PP. The chemical structure of this product is not quite clear. Add 1% of carbon black into the PP which contains 30% of this kind of IFR, then the flame retardancy of the PP can be reduced

significantly. The flame-retardant efficiency of IFR in PE is far lower than that in PP, perhaps because the thermal properties of IFR and thermal degradation temperature of PE do not match.

IFR, based on APP, has already been applied in PA6 and its mechanism has been studied. The mixtures of APP and nitrogen-containing compounds (e.g., the condensation products produced after urea being replaced by formaldehyde, reaction products between aromatic diisocyanate and pentaerythritol or with MA) have been used as IFR in polymer (particularly polyolefin and PS).

4.1.4 Monomer IFR

The so-called monomer IFR refers to the IFR which contains the ternary compound in one molecular structure. They are better than mixed (two component or three component) IFR. Because the multicomponent must interact effectively, it can produce expanded carbon layer. Experimental results show that IFR should match flame-retardant properties of polymers (such as thermal performance and products formed upon heating). In this way, when components with different chemical structures of IFR play a part in inflaming retarding, the optimum ratio of the components for the different polymers and different amounts of IFR is usually dissimilar on this issue. However, the monomer IFR is relatively simple. But it is necessary for the three sources to match with each other in one molecule; otherwise, other ingredients should be added [1].

Two well-known monomer IFRs are the following compounds (I) and compounds (II) [5].
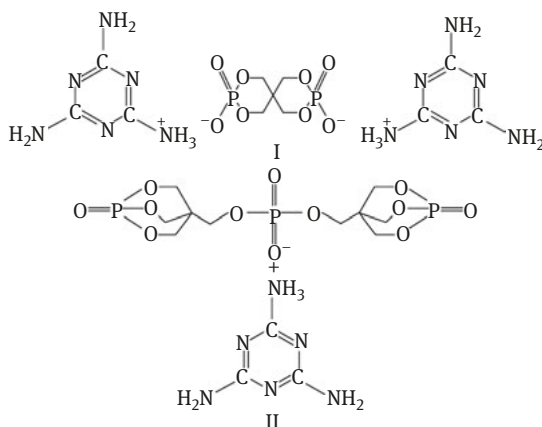
Compound I (3,9-dihydroxy-2,4,8,10-tetraoxa-3,9-diphosphaspiro [5] undecane-3,9-di dioxide MA salt) contains three chemical components needed by IFR in one molecule (acid source is phosphoric acid, carbon source is pentaerythritol

and gas sources is MA). Therefore, it can perform as one type of IFR and can be effectively used in PP and other PO. When it is used combined with three pentaerythritols and flame-retardant PP, it has higher flame-retardant efficiency. This means that the carbon source and gas of (I) did not reach the optimum balance. In fact, the carbon content of (I) is not enough [12]. The carbon source of compound (II) (bis(2,6,7-trioxa-I-phospha-bicyclo[2.2.2]octan-4-hydroxy-methyl) MA phosphate mono salt) of pentaerythritol unit is richer than (I), so it is comparable to the performance of PP flame-retardant mixture (I) and three pentaerythritols [12].

4.1.5 The proportion of three sources of IFR

To further illustrate the relationship between the proportion of three sources in compounds (I) and (II) and their fire resistance, we mix APP, pentaerythritol and MA and get mixed-type IFR to make flame-retardant PP, and when the dosage of IFR is below 30%, the relationship between the flame-retardant PP and limit oxygen index(LOI) has been illustrated (Figure 4.1) [5].
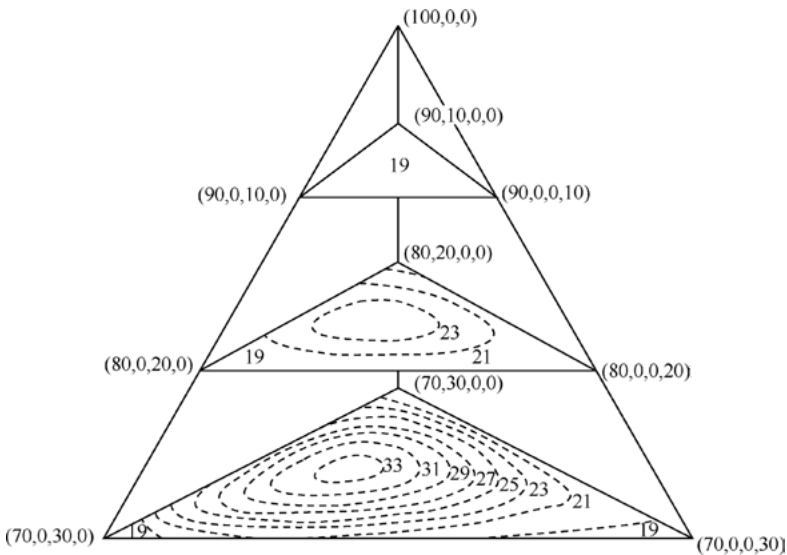
Figure 4.1: Composition of PP/APP/PFR/M and the relationship between PP/APP/PFR/M and LOI.

The total amount of IFR accounts for 10%, 20% or 30% of PP; the digit in the bracket is the mass ratio of the above four components sequentially. The number on the curves is LOI.

Figure 4.1 shows that the composition of flame-retardant PP corresponding to the maximum LOI is not depending on the fact that whether the total amount of IFR is between 20% and 30%. When IFR is used as fire retardant to PP, it is most likely that the actually used consumption is within this range. According to the data in Table 4.1, we can predict that when the three sources of IFR are heating in PP, it is likely to generate the structure of compound (I) or (II) [5]. According to the experimental data [12], if the compound II (wherein the phosphorus atoms: pentaerythritol structure:MA molecule, i.e., P:PER:M is 1:0.7:0.3) replaces I (wherein the ratio is 1:0.5:1) as the IFR flame retardant, the LOI of PP will increase. This is consistent with the data in Figure 4.1 as the maximum LOI value. Because P:PER:M in the graph is 1:0.5:0.3, and the ratio of the compound II is closer to 1:0.5:0.3 than that of compounds (I). It is clear that composition of IFR, which is corresponding to the maximum LOI, is related to flame-retardant polymers and chemical structure.

Table 4.1: Inorganic expansion glass system which may form.

System	Composition and content (mol%)	
Sulfate	K_2SO_4	25
	Na_2SO_4	25
	$ZnSO_4$	50
Phosphate/Sulfate	P_2O_5	36.6
	$ZnSO_4$	19.5
	Na_2O	18.3
	Na_2SO_4	9.7
	K_2SO_4	9.7
	ZnO	6.2
Borate/Carbonate	B_2O_3	86.2
	$LiCO_2$	11.2
	$CaCO_3$	3.6

4.1.6 Inorganic IFR

The organic IFR has several disadvantages such as the generation of harmful substances during combustion. Particularly when the expansion occurs, it is exothermic, because this IFR has limited diathermancy and the carbon layer produced in this process lacks integrity, which has relatively low thermal resistance. Table 4.1 shows that low-melting glass or glass-ceramic (melting point or softening point is lower than 600 °C) can form the inorganic glass system. In this way, they are promising to be used as polymer IFR or smoke suppressant for polymer in the future.

When system in Table 4.1 is used as the IFR, some substance can be decomposed into gaseous products upon heating; some components may be oxidized to be gaseous products, which can be used as a source of foam. Otherwise, we should add foam components. In addition, the gaseous products of thermal decomposition of flame-retardant polymers may also act as foam components. In polyvinyl chloride (PVC), a low-melting glass and glass-ceramic sulfate can form an effective adiabatic expansion of carbon layer [15]. When ammonium pentaborate is combined with conventional FR, it is also a good IFR for TPU.

4.2 Thermal decomposition of IFR components

4.2.1 Thermal decomposition of APP

In modern industry, one of the main components of the IFR is APP. It decomposes in the flame-retardant system according to the following three steps: the first step is thermal decomposition which releases ammonia and generates polyphosphate; the amount of nitrogen in ammonia accounts for approximately 50% of total nitrogen of APP. The second step is that polyphosphoric acid forms a cross-linked structure after dehydration at the temperature from 280 °C to 420 °C. The last step is the degradation of the cross-linked structure at the temperature from 420 °C to 520 °C. The chemical reactions are listed as follows (eq. 4.1) [1]:

$$(4.1)$$
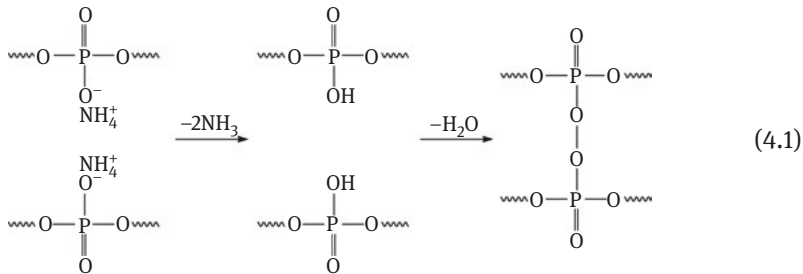
The ammonia released from the reaction mentioned above can prevent the complete degradation of polyphosphate to P_2O_5. In the second stage of decomposition, it will further dehydrate the chemical reactions listed as follows (eq. 4.2) [1]:

$$(4.2)$$
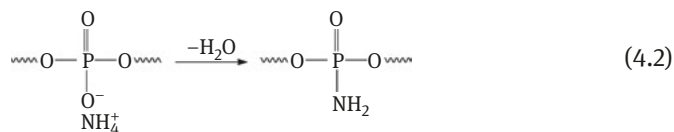
4.2.2 Thermal decomposition of APP/PER

When most of typical IFR is heated, it results in chemical interaction between inorganic acid and polyhydroxy, thus producing the carbon [6]. Charring process of cellulose and inorganic acid has been widely and extensively studied; charring mechanism is related to dehydration of inorganic acids, but its mechanism and agent are related to the structure of carbonizer and flame-retardant polymers [5].

IFR, which is widely used in industry, is the mixture of APP/PER/M. In Reference [6], it is shown that when the mixture of dipentaerythritol and APP is continuously heated, they soften and melt at a temperature of 215 °C and APP begins to decompose; at a temperature of 238 °C, the hydroxyl groups begin esterifying, forming water and producing gas, and the color of the material turns into dark (before the temperature of 238 °C, the material remains clear); at a temperature of 360 °C, the material become jelling and curable.

When the $CH_2OH:P = 6:1$ (molar ratio) in the material, and the temperature is around 500 °C, the carbon layer has the maximum carbon yield.

Reference [5] reports that they have analyzed the release rate of water and ammonia of the mixture of APP/PER upon heating and characteristics of the reaction products by thermal gravimetric analysis and nuclear magnetic resonance (NMR) techniques [31]. The reaction of APP/PER contains two steps of continuous heating. The first step occurs at 210 °C, the phosphate chain fracture and $=P(O)OCH_2$ are formed, which may be caused by alcoholysis or phosphorylation of the APP, but it does not produce gaseous products. The second step is the formation of cyclic phosphate, releasing ammonia and water. The chemical change is shown in eq. 4.3 [5].

$$(4.3)$$
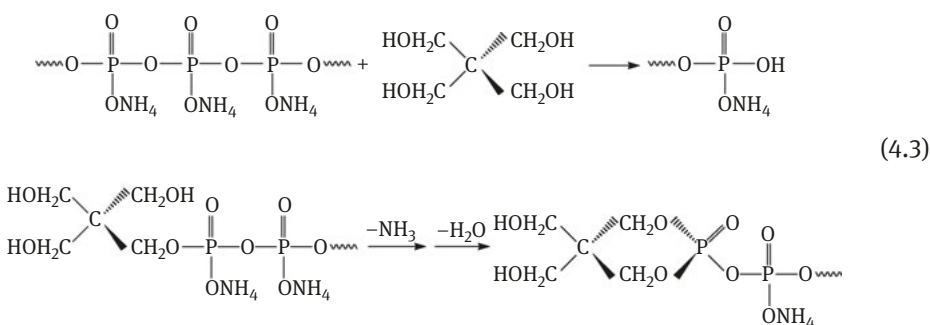
When $-CH_2OH/P$ in the mixture of APP/PER is lower than 2 (molar ratio), the reaction in eq. (4.3) may lead to the formation of diphosphate [5] of PER described below.
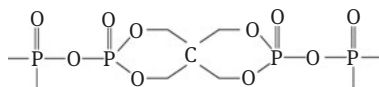
In Ref. [1], the authors make the mixture of APP/PER undergo the isothermal reaction below 200 °C. If the mixture weight remains unchanged, it indicates that the reaction is completed. Under the same condition when APP is added, the weight loss will be very limited. While heating PER only, PER will volatilize merely. Volatiles released by the mixture are made up of the ammonia, water and PER. APP and PER interact and release ammonia and water, the reaction competes with the volatilization of PER. The volatilization of PER will stop after the end of the reaction.

Infrared spectrogram of the APP mixture heating up to 156 °C shows that the 1650 cm^{-1}, 1220–1230 cm^{-1} and 1030–1140 cm^{-1} correspond to the new band of the ester group: (P–OH), (P=O) and (P–O–C).

The 31^P NMR spectrogram at the first stage of APP/PER thermal decomposition is different from the APP; it lacks the signals of parallel middle and terminal group in the polyphosphate chain, which are substituted by the multiplet signals with the center of -2.7δ. This indicates the structure of pentaerythritol phosphate (PEDP).

There are two stages of deaminization and dehydration of the APP/PER mixture and the APP. In the first stage (210 °C), the release rate of ammonia increases with the rise fraction of PER. When the concentration of PER is low, the released water and the ammonia will reach the constant value at the same time. When the amount of the PER increases, a lot of water will be released even after the release of ammonia; the increased water release demonstrates that the ammonia release is because of thermal decomposition of APP and both of them will release water. Heating the sample at 290 °C after the first stage, additional ammonia and water are generated with merely 15% of phosphorus loss.

Alcoholysis is the reaction which is most likely to occur in APP/PER mixture. At 210 °C, the ester bond contains most of the phosphorus atoms. After the alcoholysis of the APP, the cyclic pentaerythritol ester structure will be generated; however, its structure still can not be defined accurately. When the APP/PER is comparatively low, it might be that the bicyclic PEDP is embedded in the APP.

The IFR with rich PER released more water than that released in the complete esterification of the hydroxyl. It may be because of the intermolecular dehydration of the PER and the generation of ester bond. The product PEDP esters or ethers generated in the primary reaction between APP and PER can be expanded when it is further heated.

4.2.3 Thermal decomposition of pentaerythritol diphosphate

Pentaerythritol diphosphate (PEDP) listed below had been adopted as a model compound (the structure may be formed in the primary reaction between APP and PER) to study the probable reaction in the IFR expansion [5].

$$
\begin{array}{c}
\text{HO--P(=O)(O--CH}_2\text{)}_2\text{--C--(CH}_2\text{--O)}_2\text{P(=O)--OH}
\end{array}
$$

(III)
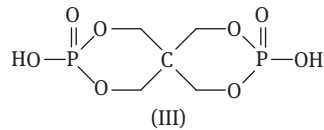
Thermal degradation of the abovementioned model compounds is conducted step by step; each step releases a certain amount of gaseous products and may form P_2O_5 with a high boiling point. The mixture expansion starts from about 300 °C; the most intense expansion occurs at 325 °C. If the temperature is above 325 °C, the expansion tendency disappears, which is mainly because of the limited amount of volatile products generated during thermal degradation. If temperature is further increased to 250 °C, the model compound will be similar to the thermal reaction of APP/PER and phosphate will be generated in the mixture of APP/PER.

If making IFR flame retardation by the model compounds or the APP/PER mixture, the foaming agent should be added, and the latter should provide gaseous products in the expansion range (300–350 °C) of the phosphate structure, in which the amine is quite suitable.

4.2.4 Reaction between each IFR components and the polymer

The multicomponent reaction inside the IFR and its reaction with the flame-retardant polymer attract researchers' attention (detailed as below). According to Ref. [17], if the PP is added into the APP/PER, it will not change the temperature (<400 °C) of IFR etherification and its expansion into carbon as well as the ingredients of hydrocarbons released by PP thermal degradation. But APP affects the thermal degradation of some acid-sensitive polymers significantly (such as polyester and polyurethane), therefore increases the amount of char [5].

In the IFR system, APP may react with other additives and generate active species with terminal base. The char will be formed by interacting with olefin double bond or degrading the PP molecules [18, 19].

As mentioned above, the IFR in high temperature consists of a series of reactions, they should occur at an appropriate rate and in right time. The time and rate of these reactions changes along with the type of the flame-retardant polymers and thermal conditions.

The char-forming reaction between IFR and the polymers is more complex than above decomposition reaction of APP and APP/PER. Taking the PA6/APP system as example, although the thermal decomposition temperature of APP is about 70 °C lower than that of PA6, the thermal decomposition rate of PA6/40% of APP system is lower than that of pure PA6 system because expanded carbon layer can effectively protect the underlying substrate. With the production of app, PA6 of this system forms ester, which releases caprolactam ring and forms foam sputum layer. The chemical reaction is listed as follows (4.4) [20]:

$$
\begin{array}{c}
\text{The chemical structures of reaction (4.4)}
\end{array}
\tag{4.4}
$$

$$
\left[\underset{\underset{\text{ONH}_4}{|}}{\overset{\overset{\text{O}}{\|}}{\text{P}}}-\text{O}\right]_n \xrightarrow{-\text{NH}_3}
\overset{\overset{\text{O}}{\|}}{\underset{\text{OH}}{\text{P}}}-\text{O}-\overset{\overset{\text{O}}{\|}}{\underset{\text{ONH}_4}{\text{P}}}-\text{O}-\overset{\overset{\text{O}}{\|}}{\underset{\text{ONH}_4}{\text{P}}}-\text{O}-\overset{\overset{\text{O}}{\|}}{\underset{\text{OH}}{\text{P}}}-\text{O}\cdots-(\text{CH}_2)_5\overset{\overset{\text{O}}{\|}}{\text{C}}-\text{NH}-(\text{CH}_2)_5\overset{\overset{\text{O}}{\|}}{\text{C}}-\text{NH}\cdots\rightarrow
$$

$$
\text{O}=\text{P}=\text{O}-\left[(\text{CH}_2)_5-\overset{\overset{\text{O}}{\|}}{\text{C}}-\text{NH}\right]_m(\text{CH}_2)_5-\overset{\overset{\text{O}}{\|}}{\text{C}}-\text{NH}_2
$$
$$
\text{O}=\text{P}-\text{ONH}_4
$$
$$
\text{O}=\text{P}-\text{OH}
$$
$$
\text{O}=\text{P}-\text{O}-\left[(\text{CH}_2)_5-\overset{\overset{\text{O}}{\|}}{\text{C}}-\text{NH}\right]_n(\text{CH}_2)_5-\overset{\overset{\text{O}}{\|}}{\text{C}}-\text{NH}_2
$$

$$\xrightarrow{-\text{NH}_3,-\text{H}_3\text{O}}$$

$$
\text{O}=\text{P}-\text{O}-(\text{CH}_2)_5-\overset{\overset{\text{O}}{\|}}{\text{C}}-\text{NH}_2
$$
$$
\text{O}=\text{P}-\text{O}-(\text{CH}_2)_5-\text{C}\equiv\text{N}
$$
$$
\text{O}=\text{P}-\text{O}-(\text{CH}_2)_5-\overset{\overset{\text{O}}{\|}}{\text{C}}-\text{NH}-\overset{\overset{\text{O}}{\|}}{\text{C}}-(\text{CH}_2)_5\cdots
$$
$$
\text{O}=\text{P}-\text{O}-(\text{CH}_2)_5-\overset{\overset{\text{O}}{\|}}{\text{C}}-\text{NH}_2
$$
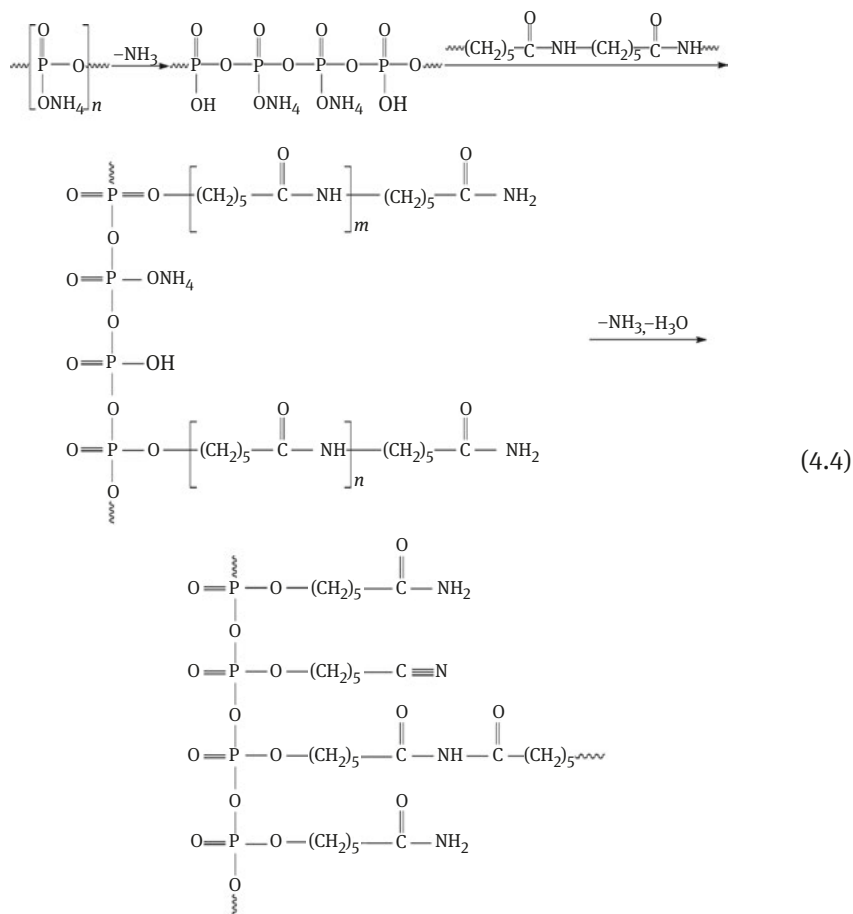
When the PAN and the phosphorus flame-retardant systems containing APP are heated together, PAN will form carbon through cyclization and dehydrogenation. The chemical reaction is as follows (4.5) [21]:

$$(4.5)$$
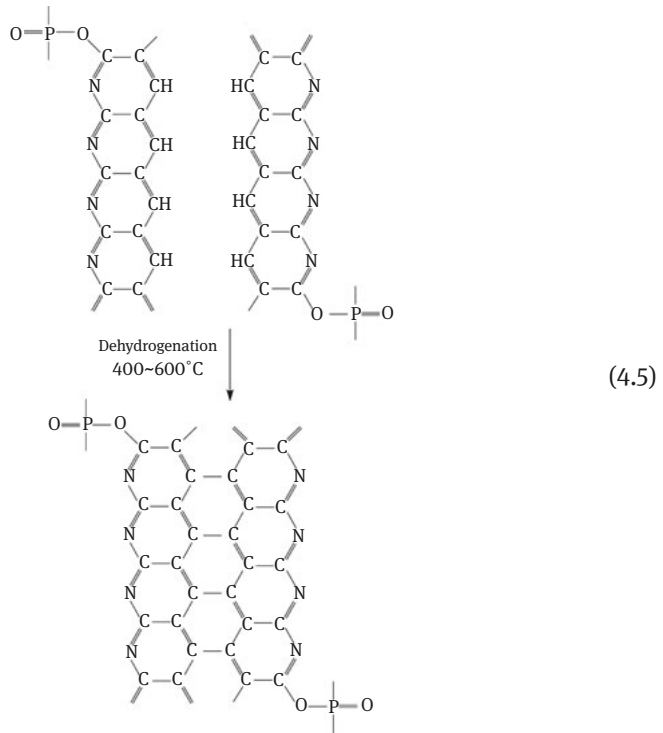
IFR has low smoke and low toxicity without halogen. But the application of the IFR remains limited until now because of the poor water solubility, poor mobility and poor thermal stability of IFR. Besides, it costs a lot due to its large amount of flame retardant (20–30%) and is bad for polymer processing. Thus, it can be possible to develop the high quality of IFR only if we have a deep understanding of the mechanism of expanding and making a detailed study on the chemical and physical process of expansion of the IFR.

4.3 The expansion formation of char of IFR

4.3.1 Char formation process and the chemical reaction

Generally, expanded char layer of IFR can be formed by following interactions: (1) At low temperature (about 150 °C, the concrete temperature depends on the nature of the acid source and other components), the acid source can produce acid which can esterify polyhydric alcohols and acids which is used as dehydrating agent. (2) At the temperature slightly higher than that suitable for the acid releasing, acid will do esterification reaction with polyhydric alcohols (carbon source), and amine

could accelerate the esterification reaction as a catalyst. (3) The system melts before or in the esterification reaction. (4) Water vapor produced in this reaction and the noncombustible gases produced by the gas source made the molten system expand and foam. At the same time, the polyhydric alcohols and ester form inorganic substances and char residue through dehydration and carbonization. (5) At the end of the reaction, the system is gelled and cured and forms porous carbon foam layer finally. The steps above should be done in the following order strictly and in a coordinated way. The whole process is illustrated in Figure 4.2.
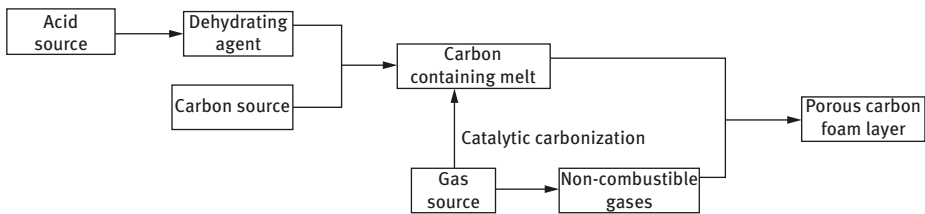
Figure 4.2: Formation process of porous carbon foam layer [1, 22].

When the expansion char layer forms, the rate of gas generation and the growth rate of viscosity of molten polymer as well as the rate of its transition to solid rate should match each other to form stable foam char layer. Otherwise, char layer will collapse and lose its flame-retardant performance. As the flame-retardant polymer system forms foam char layer when heated, the viscosity increases sharply when the molten polymer turns into solid one, and gases generated by foaming agent go into char layer at the same time. If flame-retardant system contains reactive components, their interaction at high temperature will form partly linked and non-melting macromolecules compounds. For example, non-melting solid products generated by the system containing amino benzene sulfonic phthalein amine have partially cross-linked structure in 250–260 °C because of the interaction between terminal amino and secondary nitrogen base. When the temperature rises to 360 °C, the sulfonated phthalein amino groups begin to react with each other, the bond of sulfonated phthalein amino breaks and carbon layer is formed. The main gaseous product of the reaction is of SO_3, whose amount increases with the rise in temperature.

For the system of PP/APP/PER, in the first process of reaction (<280 °C), the acid source in it (APP and its thermal degradation impurity – orthophosphate and phosphoric acid) and carbon source have a chemical reaction and create the mixture of ester. Later, carbonization happened in 280 °C (according to Ref. [23], this process is mainly through the free radical reaction). In the second process of reaction (280–350 °C), the release of gas (e.g., APP releases NH_3) expands char layers. Further increasing the temperature to 430 °C, the intumescent char layers

decompose at higher temperature and no longer have the feature of inflation. Between 280 °C and 430 °C, the thermal conductivity of the carbon layer decreases and isolation performance improves [26].

In addition, Ref. [1] pointed out that when the PP/APP/PER burns, first step is that the APP releases ammonia and water, PER gets phosphorylation and PP gets thermal oxidation. The second step is the dehydration and phosphorylation of the system. The last step is the cross-linking of the network, carbonization and formation of char layer. Nonflammable gaseous products generated by the decomposition of the foaming agent make carbon layer puff and some nonflammable gases enter the gas phase. Studies have pointed out that APP is not only for the formation of carbon layer but also takes part in the chemical reaction of condensed phase. Although the rates of reactions mentioned above are very high and, at different time, the dominant reactions are different, it all depends on relative proportion of each reaction. Phosphorus in IFR generates phosphorus oxide through the combustion of materials, the contribution to oxygen index of the materials is small and the phosphorus content in carbon layer declines, too.

4.3.2 Char formation reaction of the PEDPs

In order to have a better understanding of the chemical reaction among the mixture of APP/PER when they expand into char layer, Ref. [7] has described carbonization process of the model compounds PEDP.

PEDP undergoes five stages of degradation between room temperature and 950 °C. Each stage has released volatile products. The formation of the foam gets to its peak in the second stage of degradation (325 °C); with the further rise of temperature, the formation of foam decreases. When temperature reaches 500 °C, there is no difference in measurement of the curves TGA and DSC, in nitrogen or in air, by PEDP, and its volatilization finished at 750 °C. The first stage –OH condensate and release water and organic matter reduces. This is clearly related to the dissociation of phosphate ester and the formation of a kind of polyphosphate ester and carbon-containing compound. This chemical reaction involves three kinds of reaction mechanism: free radical mechanism, carbonium ion mechanism, and ring CIS elimination mechanism. In free radical mechanism, elimination reaction happens due to the lack of free radical inhibitor in the process of pyrolysis. Carbonium ion mechanism is supported by acid catalysis and kinetic property. If there is no hydrogen atoms on β-carbon (such as PEDP), carboniumion mechanism should be the only mechanism. In transition state of ring CIS elimination mechanism, it also exists. Olefin is the most stable carbon ion in the thermodynamics. If it generates high active carbon ions, it will suffer oxide migration or skeleton rearrangement to produce more stable ions, and when the ring of ionized esters is opened, it will go into the

second pyrolysis reaction. This reaction is going on in line with *cis*-elimination mechanism, which can be seen in the reactions in eq. (4.6) [7].

First step

Second step

(4.6)

Both free radical polymerization and acid catalytic polymerization reaction can generate char from pyrolysis products. For example, the pyrolysis of ester and Diets–Alder reaction after the displacement of δ lead to the formation of aromatic ring structures (4.7).

(4.7)

The above reaction models help to explain the structure of foamed char layer. These reactions maybe take place in an irregular process, competed with other processes. The final products are generated by polymerization, Diets–Alder condensation and the aromatic ring structure. The ester pyrolysis can provide char-forming substance material with quite simple chemical reaction.

Not only the IFR but also the polymer may play a role in char-forming and foaming. For example, volatile products released by PP in the degradation process can also participate in foaming.

Char formation is a complex process, which is related to the polymer structure, additive composition and combustion process. C–C-conjugated double bond, cross-linking bond and aromatic ring lead to char formation. The higher the char content is (in the range of 72–95%), the higher the thermal stability of char will be. When the oxygen index of char is up to 65%, char formation decreases combustibility [1].

4.3.3 Composition and properties of char layer

Products of IFR degradation is one kind of heterogeneous matter [4]; the condensed phase (i.e., porous carbon layer with phosphorus and carbon) is the mixture of solid and liquid phase (acid tar-like substance), and it can capture the gaseous and liquid products of thermal degradation of polymers with required thermal and dynamics performance. In addition, porous char layer of the condensed phase contains pregraphitized high molecular aromatic compounds (combining by polymeric bonding, phosphate base, [two or three] multi-phosphate), and crystalloid IFR subparticles and amorphous phase which covered on crystalline phase. The latter is made up of small molecular aromatic compound, phosphate (easy to hydrolyze), alkyl compound and the polymer chain fragments produced by the degradation of IFR component. The amorphous phase is closely related with protection performance of char layer: its volume must just cover the crystalline phase and should have proper viscosity to make the carbon layer to get desired thermal and dynamic performance, make it easier to withstand the solid particle and gas stress on the char layer.

Flame-retardant efficiency of char layer generated by IFR flame-retardant polymers is also related with plasticity of the char layer under the temperature in its expansion process [27]. Some researches indicated that the rheological and mechanical properties of char layer generated by several IFR flame-retardant polymer could be associated with flame-retardant properties [28, 29]. The chemical reaction in the process of expansion of IFR flame-retardant system can change the heat and dynamic performance of the system. For PP (PP/TPU/APP) utilizing IFR flame retardant at 300–340 °C, the apparent viscosity of the material decreases with time when in presence of stress [27]. Stress is detrimental to entanglement of polymer chain and free radical reaction also makes the length of polymer chain decrease. At 340–390 °C, the apparent viscosity of the system increases with time, because stacked high molecular multi-aromatic compounds linking PP chain and phosphate compound. The high viscosity of the material is beneficial to protect the expansion performance of material in terms of protective properties. If the viscosity of the system is high enough, it can wrap gaseous products generated by material degradation and can also withstand the pressure of captured gas and solid particle. When the temperature is higher than 400 °C, the viscosity of the system declined sharply in the early 200 s period but decreased slightly later. At present, the dual role of temperature and stress led to the degradation of expansion material, results in fracture of multi-aliphatic chain and release of the corresponding products, which makes the material lose its original thermal and dynamic performance and form cracks in char layer, thus results in the loss of protection performance.

Ref. [1] points out that in terms of the PP/APP/PER system, the number of carbon atoms and phosphorus atoms in char layers is corresponding to those in the flame retardant. Polyphosphate chain and certain amount of orthophosphate exist

in carbon layer. If APP in IFR is replaced by diamine pyrophosphoric acid, it will produce pyrophosphate debris instead of orthophosphate fragments [1].

Below 500 °C, carbon–phosphorus ratio on the surface of char layer increased with the increasing temperature, this ratio in the matrix of char layer decreased with the increasing temperature. The oxygen–carbon ratio shows similar tendency which indicates that flame-retardant phosphorus migrated to the surface and then oxidized.

Adding nitrogenous compounds into the IFR polymer-containing phosphorus, the flame-retardant efficiency of phosphorus compound will be enhanced, because phosphorus generated in the char layer may be fixed and difficult to spread. The element analysis and infrared spectrogram pointed out that the char layer generated by some phosphorus and nitrogen IFR has P–N bond on its surface.

In general, no matter whether the polymers are flame retardant or not, they can both form char in the combustion process. In the char-forming process, chemical cleavage, cross-linking, bubble formation and mass-transfer process occurred. Carbon layer formed with combustion often contains disordered polycyclic aromatic compound. When the temperature increases, its orderliness increases, the aromaticity enhances and its crystallinity also increases [3].

The carbon layer generated by IFR is a multiphase system, which contains the solid and liquid, gaseous products generated by material degradation and some carbides of polymers containing aromatic fragments, with the structure of graphite. To protect the underlying material, carbon layer must cover all the surface of the material and should have enough strength [1].

4.3.4 Dynamic viscosity of material in the process of carbonization

In the early period of the expansion, the viscosity of polymer is an important factor in the development of intumescent carbon layer. In particular, degradation of polymer viscosity can affect the morphology of carbon layer, because viscosity restricts the diffusion of gas generated by degradation of the material. The study of the relationship between the viscosity and time of flame-retardant polymer can help us to better understand carbonization [3, 21].

Ref. [27] studied the viscoelastic properties of PP/APP/PU system (Figure 4.3) [27] and showed the external viscosity of the system at different temperatures. At 200–240 °C, the viscosity decreases as the temperature increases, but even within this temperature range, the surface of the material is carbonized. At 240–300 °C, the viscosity decreased slightly, and the material seems to have carbonization and liquefaction at that moment and generate phosphoric acid esters and aromatic compounds [27]. At 300–360 °C, the viscosity is very low and the intumescent protection layer is already formed on the surface of the material at that stage. Most of the materials are liquid, but the liquid phase and the solid phase exist simultaneously; the
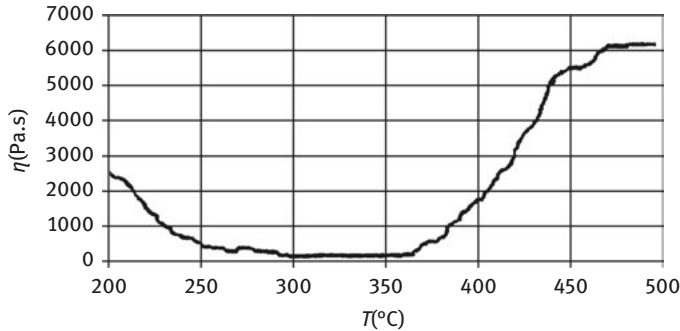
Figure 4.3: Relationship between apparent viscosity and temperature of PP/PU/APP system [27].

viscosity of the material depends on the liquid phase. At 360–450 °C, the viscosity increased dramatically; the polymer has been completely degraded and carbonized. The expandable foam layer consists only of solid particles. At 450–500 °C, the viscosity increases slightly and finally reaches a certain value. At this stage, the char layer begins to degrade and oxidize. In addition, we can also study the relationship between viscosity and time, in order to better evaluate the mechanical properties and thermal stability for protecting the expandable char layer and learn deeply of carbonization process [3]. The flame-retardant efficiency of IFR is related to plasticity of the protective layer it generates.

The relationship between the viscosity and time changes with the temperature of the material. Within the range of 300–400 °C, the external viscosity of the material under stress decreased with the time. In the first 20 min, the external viscosity reduced to 60% of its initial value. This is because of the reduction of the polymer chain's length by stress. On the contrary, at the period of 340–390 °C, the external viscosity of the material increases with the time, because the expansion process happened and generated stacked multi-aromatic compounds (as a link between PP chain and phosphate) [31, 32]. During then, the viscosity of material is high enough to cover the captured gas and withstand the stress from the solid particle and pressure from gas. Over 400 °C, viscosity of the material changes with time under stress. In the first 200 s, the viscosity decreased sharply and then increased slightly. It is believed that with the dual function of high temperature and stress, expansion material becomes thermal decomposition [32]. Although the expansion of the material is good, the viscosity is quite high and almost constant [3].

The study on the viscosity of the system of intumescence is one of the important ways to know the carbonization process. Moreover, the results and chemical constitution of the intumescent protection layer complement with each other. However, the viscosity of the system is measured *in situ*, whereas the study of chemical constitution undergoes after the combustion of the sample.

4.3.5 IFR recognition of HRR curves and TGA curves (char yield)

Heat release rate (HRR) curve of PP/APP/PER IFR system is peculiar to IFR (Figure 4.4) [33]. There are two peaks on the curve; the first peak is generated by the ignition and flame propagation on the surface, whereas the second peak is derived from the destruction of expandable structure and the formation of carbon layers. In the plateau region (HRR value constant) between the two peaks, the material is protected by the expansion layer. The intumescent layer formed by IFR is resistant to high temperature (at least 450–550 °C) and should protect the polymer reach a temperature lower than its thermal degradation temperature. Thus, the high polymer will not be degraded quickly.
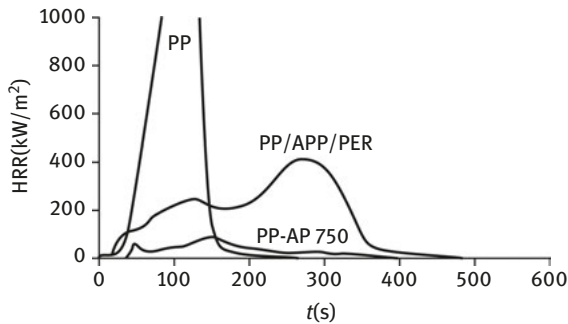
Figure 4.4: PP, PP (70)/APP (20)/PER (10) and PP (70)/AP750 (30) of the HRR curve.

Carbonaceous residues produced by heated IFR retardant polymers change with the flame-retardant polymers and IFR itself, as illustrated in Figure 4.5. For example, the carbon proportion of PP, PP (70)/APP (20)/PER (10) and PP (70)/AP750 (30) (AP750 is APP bonded by the epoxy resin (2-carboxyethyl) isocyanurate trimer diisocyanate compound) are 0%, 18% and 40% at 800 °C, respectively. At 250–800 °C, stability of the PP with IFR is much higher than that of single PP.

4.3.6 Structure of carbon layer

The structure of the foam char layer is related not only to the process of gas generation but also to the viscosity of the relevant semiliquid matrix. The matrix with low viscosity is nearly full of liquid; therefore, the gas is not easily distributed and will diffuse into the flame. Sometimes, the viscosity of the foamed material is critical to the structure and quality of the char layer. In addition, the change of viscosity of char foam layer under stress sometimes results in the loss of protection of carbon layer. If
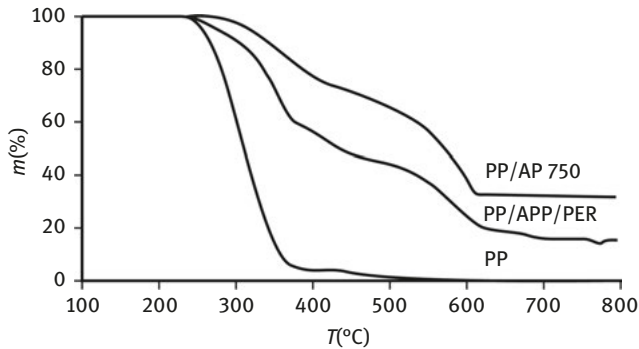
Figure 4.5: PP, PP/APP/PER and PP/AP750 of the TGA curves (as carbon content) [33].

the char layer is very hard, then it is easy to produce and disseminate crack, thus result in rapid degradation of the material. Even if the char layer has a good structure morphology and insulation performance, if the char layer is easily broken by mechanical action, the flame-retardant performance will also be poor [3].

The char layer of IFR system is generated through the half-liquid phase, expansion of the surfaces and production of gas simultaneously [14]. The liquid carbon began to solidify and form solid porous carbon foam layer during expanding process. The gas generated by IFR degradation (in particular the foaming agent) is spread and is captured in the high viscosity of the melt with the development of the expansion process, in the end materials with appropriate properties, and functions are formed [3].

The way of the gas spreading in a semiliquid material has an extremely important effect on the structure and mechanical properties of the formed char layer. For example, epoxy-based expandable material (including APP) the heat-capacity increase sharply for the temperature 100–200 °C, because decomposition of APP releases ammonia (gas) into the gas bubble, which results in the increase of the pressure inside the bubble. But if the APP is shifted to aluminum borate, or manganese dioxide, the heat capacity of the coating does not change significantly with temperature; the process of gas generated by expandable coating is relatively slow, so the structure of formed char layer is formed better [3].

In Figure 4.6, the char layers of two combustion systems including PP/APP/poly acid and PP/APP/polybasic acid/BSil are compared by cone calorimeter. The former shows a lot of fractures, whereas the latter is continuous and compact.

For the condensed-phase flame retardant, the nature of solid phase under burning and steady state is directly related to the fire-retardant efficiency. For example, when MNT is added to PA6/OP1311 (aluminum phosphinate), efficiency of the flame retardation greatly is improved because of the improvement of the char-layer structure (see Figure 4.7) [3]. When the recipe does not contain MNT, char layer will form
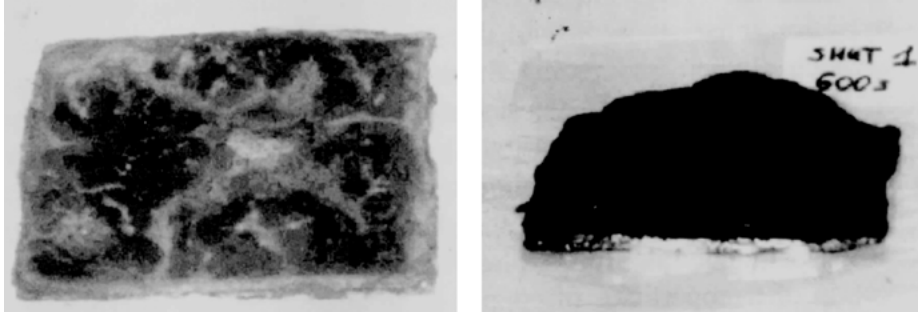
Figure 4.6: BSil (right) and free BSil (left) of the PP/APP/poly acid, carbon layer is measured in cone calorimeter [35].
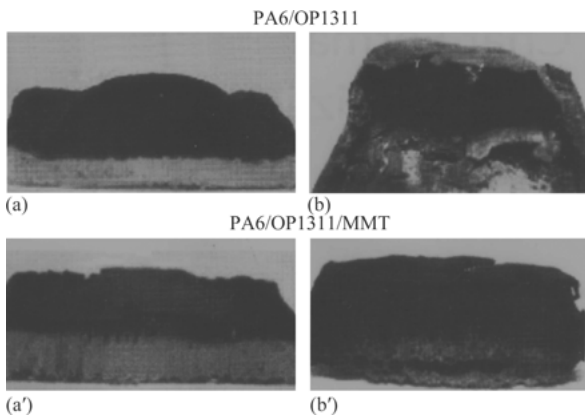
Figure 4.7: PA6/OP1311 (above) and PA6/OP1311/MNT (below) of the combustion residue (char layer) [3]. Left: after ignition and right PHRR time.

a large bubble. Obviously, the char layer containing montmorillonite (MMT) can form better barrier of mass and heat transfer.

Similarly, with a certain amount of well-dispersed carbon nanotubes and polymer nanocomposites, the carbon layer will form with a mesh structure, no large cracks and cover the entire surface [36].

4.3.7 Flame retardancy of carbon layer

When IFR is exposed to strong heat, expandable char layer formed on the surface of the polymer (char-layer density decreases with increasing temperature) is the condensed phase flame retardation which performed as physical barrier of delivering

heat and material transfer between gaseous phase and condensed phase [37]. When IFR utilized in polymers, in the early combustion, the thermal degradation to the gaseous phase of the combustible polymer may be terminated [4]. For example, the LOI of PP, PP (70)/APP (20)/PER (10) and PP (70)/AP750 (30) is 18%, 32% and 38%, respectively. Moreover, PP cannot reach UL94V level, whereas the two PP polymers with IFR have passed UL94V-0 level. For peak heat release rate(PHRR), the above three kinds of materials were 1800 kW/m^2, 400 kW/m^2 and l80 kW/m^2 [33].

IFR directly plays the role in the condensed-phase flame retardancy. For example, oxygen index and N_2O index of PP with APP/PER (3/I) as flame retardant are shown in Figure 4.8, and the flame-retardant effect is independent of all oxidizing agents, which shows that the additive is worked according to condensed-phase flame retardation mechanism.
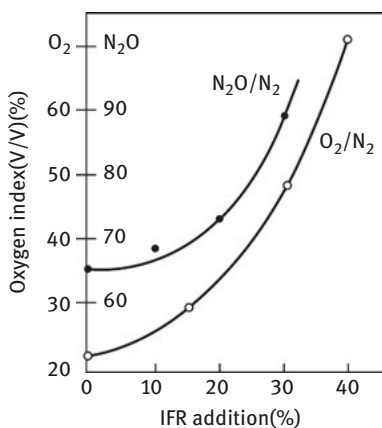
Figure 4.8: PP/APP/PER oxygen index and N_2O index.

In addition, flame retardant of the char layer is not only a barrier for heat and material transfer but also contributes to end the radical reaction chain in the thermal degradation of high polymer because the free radical in carbon layer can react with the gaseous radical. It also helps to mitigate thermal degradation of high polymer protected by carbon layer in the condensed phase. Meanwhile, char layer can be used as a carrier of acidic catalyst which can react with oxidation product formed by oxidative degradation of the polymer [4]

Ref. [1] holds an opinion that the carbonization layer usually contains nitrogen, oxygen, phosphorus and other elements. The carbonization layer on material surface reducing the flammability of material has the following reasons: (1) the carbonization layer makes heat difficult to penetrate through the carbonization layer and enter into the condensed phase, (2) the carbonization layer can prevent oxygen in surrounding medium from diffusing into polymer materials in degradation and (3) the carbonization layer can prevent gaseous or liquid degradation from escaping

from surface. However, the porous structure of carbonization layer also makes gaseous products penetrate through the carbonization layer and permeate through the combustion zone. For the liquid products, pores of carbonization layer can be used as a channel, which leads liquids rise to the surface of material and burn because of the capillary force. The movement of liquids in foam material complies with the Darcy Law, and the burning rate of materials will be influenced by the gasification rate of carbonization layer and the transition rate that gaseous and liquid degradation products of polymer pass through carbonization. The amount of gaseous and liquid degradation products decreases while the amount of carbonization layer increases. The carbonization layer on material surface cannot effectively reduce the flammability of materials when the polymer is of low-melting temperature, low-melting viscosity or is easy to produce liquid products in heat crack.

Here are methods to reduce flammability of materials under carbonization layer: (1) increasing the rate of carbonization, which can reduce the amount of combustible volatile products escaped to the combustion zone. Adding some carbonization promoter into IFR system could get favorable result. For example, potassium hypochlorite, which could help release oxygen when put into epoxy resin, could enhance fire resistance of epoxy resin because of increasing char yield. A quantity of 5% potassium hypochlorite can make oxygen index of epoxy resin reach 23%; the oxygen index of materials will drop sharply when potassium hypochlorite is over 5%. Compounds of tin and cobalt may also promote char conversion and then reduce the combustion velocity of materials. Besides, such metal compounds can also change the composition of volatile products of heat crack. Sulpho can also promote carbonization, but relevant reports do not reach the same opinion about sulpho compounds that these could be used as plastics flame retardant; (2) improving the thermal resistance of carbonization layer and the surface temperature of material, which could help reduce heat of convection, increase radiant heat loss and heat consumption for heating materials; (3) increasing the thickness and decreasing thermal conductivity of carbonization layer; and (4) reducing the permeability of carbonization layer, and increasing the viscosity of liquid degradation products of high polymer, which could decrease its mobility.

IFR may also play a role as flame retardant in vapor phase, because phosphorus–nitrogen–carbon system formed such flame-retardant will produce NO and NH_3 when heated, and a very small amount of NO and NH_3 could lead to the termination of free radical of chain reaction on which burning depends. Furthermore, free radical may collide with particles. Then, it gets the combination and becomes steady molecule and finally interrupts the chain reaction [1].

It is reported in Ref. [1] that the permeability of carbonization layer should be as low as possible to make carbonization layer have good flame retardant. For example, it will produce carbonization layer with a very low permeability when phenol–formaldehyde resin with ammonium phosphate gets hot crack, because the phosphorus compounds in carbonization layer could make Darcy constant several

times lower. The char layer produced by phenol–formaldehyde resin (phenylene-double maleimide), which is disposed by phosphoric acid, as well as polymer gets modified by ammonium phosphate are both of low permeability, thus increase the flame retardancy of polymer. Take epoxy resin composites as an example; its oxygen index could increase from 35% to more than 52% when it is covered by coke laminates treated by phosphorus species. The low permeability of porous carbon layer carbonization layer containing phosphorus may be due to that polyphosphate produced in the heat is of high viscosity and then fills the pores during carbonization.

Some boron compounds can also reduce the permeability of carbonization layer. For polystyrene system, the decreased flammability will partially come from the low permeability of char layer which is formed through the thermal dissociation and cross-linking (cross-linking agent is hexamethylene tetramine) of phenol–formaldehyde containing boron oxide. However, the permeability of this carbonization layer relates with temperature. Below 450 °C, the permeability of carbonization layer will decrease first and then increase with the increasing temperature. Because, at 450 °C, the boron compound is a kind of transparent liquid, and it can cover the pores of carbonization layer and decrease the permeability of carbonization layer, above 450 °C, it will decrease the viscosity of the membrane of compounds containing boron and the coverage of char layer surface goes up, thus increase permeability.

In addition to char yield and char-forming speed, the quality of carbonization layer (as a barrier impeding mass transfer and heat transfer) could be regarded as a quite important factor. If the formed carbonization layer is porous carbon layer, then obturator foramen is better, and the carbonization layer should have no cracks and cavities. For the amount of carbonization layer, the quality is more important than volume.

4.4 Synergist of IFR

4.4.1 Overview

The synergists are something that can accelerate the charring process or improve the quality of char layer of IFR. It can effectively influence many thermoplastic and thermoset high polymers, and usually a little synergist could bring great effect.

Following is a well-known example: adding molecular sieves into IFR could increase flame-retardant efficiency, reduce heat release and inhibit smoke. Moreover, with molecular sieves, phosphorus–carbon structure produced by IFR system is more stable. It is pointed out in other researches that molecular sieves can help form organic phosphate and aluminum phosphate in polymer chains, thereby limit the decomposition of polymers and decrease the amount of the combustible gaseous products entering into flame zone. In addition, molecular sieves are conducive

to form "adherence" structure in polymeric materials, and this "adherence" macromolecular network structure and its interaction with polymer chain could enhance flame retardancy of materials. In fact, aromatic structure in intumescent fire barrier can increase strength of materials and make material surface flexible, and reduce the possibility that material surface cracks in the heat. Thus, the rates that oxygen diffuses into polymer matrix and flammable gaseous generated by degradation of polymers are getting lower [1].

Boron siloxane elastomer is an effective synergist for APP and polyol IFR system, and it will bring remarkable improvement when applied to polyolefin. The dynamic rheology test indicates that the system can generate PER–BSil cross-linked macro-molecular. The APP–BSil reaction could also increase plasticity of intumescent foam carbonization layer produced in the heat. The FTIR test confirms that chemical reaction can occur between boron siloxane elastomer and flame retardant, and DTG test affirms that this reaction can have positive effect on flame-retardant system.

Polyvalent metals affect the oxidation process. For example, compounds of copper, tin, antimony, and cobalt can affect thermal cracking of epoxy resin. With tin compounds, the starting degradation temperature of epoxy resin can be increased from 60 °C to 80 °C, and char yield gets increased as well. When polymers get oxidative degradation at 240–320 °C, tin compounds may greatly extend the induction period of degradation. The compounds of tin and cobalt can also increase the speed of charring process and then decrease combustion rate of materials. Furthermore, such metal compounds can also change the compositions of the volatile products after thermal cracking [1].

There are many other available IFR synergists, such as nanofillers, natural pottery clay, zinc borate, talc, polyhedral oligomeric silsesquioxane (POSS), magnesium oxide, manganese oxide etc [4].

4.4.2 Molecular sieve

According to Refs. [4, 6], the combination of molecular sieve and APP/PER or PY/PER (PY is coke phosphorus) can significantly improve the flame-retardant property of various polymers. For example, when the constant amount of APP/PER comes to 30%, the LOIs of PP, low-density polyethylene (LDPE) and PS are 30%, 24% and 29%, respectively. When 1.5–1% of molecular sieves (4A or 13X) are added, LOIs of the abovementioned matters increase to 45%, 29% and 43%. Moreover, their flame-retardant grade reaches UL94V-0 [4] before and after adding molecular sieves, indicating that molecular sieves have a good synergistic effect on IFR (APP/PER). HRR of materials measured within the cone calorimeter also prove the same [38]. From the curves of LRAM3.5 (I) (ethylene/butyl acrylate River/maleic anhydride copolymer), LRAM3.5/APP/PER (II) (IFR amount of 30%) and LRAM3.5/APP/PER/HRR

4AOID (4A was 1–1.5%), we can see that when the heat flow of cone calorimeter is 50 kW/m^2, 200 s, HRR in (II) and (III) is almost the same. When HRR in (II) and (III) is 300 kW/m^2 and 150 kW/m^2, 600 s and 1.5% 4A is added, HRR value of the high-temperature section (after ignition) decreases to 1/2, which shows that the molecular sieve-containing material under severe thermal oxidation conditions can tolerate longer. Furthermore, the curves of (II) and (III) are similar to the HRR curve. All of them have three peaks: the first peak appears in the process of thermal degradation of IFR, the second one occurs in the process of thermal degradation of residue as well as the formation of expanded char layer and the third one turns up in the process of thermal degradation of the char layer [4].

The function of the carbon molecular sieve is that it can change structure of carbon (stacked-like macromolecular aromatic substance) in char layer and delay the reconstruction of carbon [39–41]. In addition, molecular sieves help char layer to keep much of the aliphatic linking bridges. Besides, the alumina–silica phosphate organic compound generated by the addition of molecular sieve can make char layer steady and reduce P-O-C bond breakage so that a volume of the bulk-shaped macromolecular aromatic composition increases [38]. Furthermore, when introducing molecular sieves, pyridine nitrogen compounds (APP heterocyclic compound by reaction of NH$_3$ with the interpreted generated carbon–carbon double bond) could be detected at any temperature. While the formula is without molecular sieves, pyridine nitrogen compounds [4] can be detected only above 350 °C. The existence of pyridine nitrogen indicates that polycondensation of condensed poly-aromatic has been delayed, which helps to improve the mechanical properties of the char layer and thus improve the flame-retardant properties of the material. Moreover, molecular sieves help to stabilize the phosphorus–carbon structure produced by IFR, because the bridging of polyethylene by the organic phosphite ester or organic aluminum phosphate limits the depolymerization process, which can generate small molecule contributing to the fuel flame. Moreover, participation of molecular sieves also contributes to the formation of adhesions, which is a macromolecular network system, while the bridging polyethylene seems conducive more to improving flame retardancy. In fact, some of the carbon layer generated by polymer/IFR is more brittle. When the bridging polyethylene enters into the carbon layer, aromatic ring system bridges through an aluminum phosphate (ester) or acid phosphate (ester), which empower flexibility to carbon layer so as to have the desired mechanical properties [40]. Encountering a fire, such carbon linked to the generation and propagation can delay the production and transmission of cracks, isolated from heat and oxygen so as to prevent polymers from rapid thermal degradation into small-molecule products.

In recent years, some cheap industrial waste-containing molecular sieve (such as fluidized catalytic cracking catalyst) has also been used as synergist for IFR, and the effect is obvious [4].

4.4.3 Nano-ingredients

According to Ref. [2], nano-ingredients can improve physical and chemical performance of expanding char layer, and Ref. [42] claimed that with a catalytic function, only 0.1–1.0% mass rate nano-ingredients can give a good effect of stabilizing char layer and improve its flowing performance. It can generate active sites of optimal chemical reaction in condensed phase and make char layer with necessary thermatic/dynamic character.

In Ref. [43], organic ameliorated MMT and boron monument siloxane elastomer (as the base carrier of fire retardant and front pottery) were added into IFR with APP as one of the components with 1% mass rate. When using it within flame-retardant PP, its LOI was increased by 2–8% and UL94V-0 can be achieved. The material with these ingredients maintains higher viscosity in high temperature and can control the activity of fire retardant. Furthermore, at early period of material's decomposition, it will generate nanocomposite exfoliate structure and therefore protect the matrix material.

Moreover, boron silicone elastomer makes the char layer more flexible to improve fire-resisting capability of char layer. In addition, boron-silicone elastomer-enwrapped MMT leads to higher surface protection of char layer. According to the test results, no obvious chemical reaction happened between APP, boron silicone elastomer and MMT at a temperature range of 25–350 °C. In IFR with APP and molecular sieve, phosphosilicate produced above 350 °C. Therefore accordingly, boron silicone elastomer can also be generated with APP at a high temperature (e.g., >300 °C). In addition, this kind of compounds improves the flame retardation ability of expanding char layer. For IFR with APP and MMT, aluminum phosphate will be produced.

In IFR, POSS works synergically with phosphate as illustrated in Figure 4.9. When OP950 applied in PET material experiment with the total amount was set as
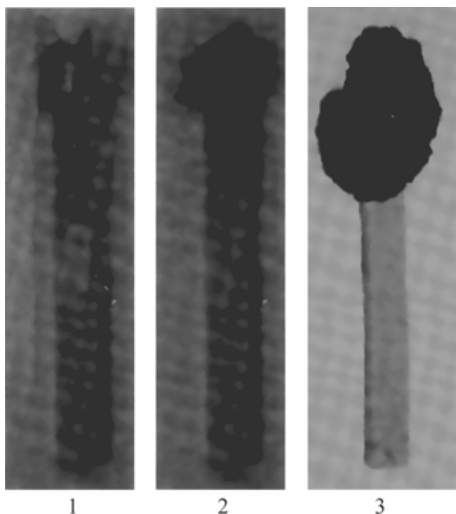
Figure. 4.9: Expansion of material with LOI measurement. (1) single-PET; (2) PET/OP950 (20%); (3) PET/OP950 (18%)/POSS (2%).

10% and 20%, PET's LOI reached to 29% and 35%. But if a few POSS was added into OP950, the PET's LOI raised to 36% (still 10% total amount of OP950/POSS) and 38% (20% total amount of OP950/POSS). The ingredient with POSS owned higher expand rate and then led to higher flame retardation ability. Meanwhile, single-PET, PET/OP950 (20%) and PET/OP950 (18%)/POSS (2%) owned PHRR of 750 kW/m^2, 500 kW/m^2 and 250 kW/m^2. Therefore, POSS could be the expander and synergists of char layer to improve the quality of char layer and protection.

4.5 Improvement of IFR

The methods to improve IFR are as follows: (1) using high polymer (PA, TPU) charring agents to replace normal low molecular polyhydric alcohols charring agents, which could decrease the water solubility and mobility of charring agents and then improve the mechanical performance of char layer; (2) applying high polymer nanocomposites to raise the distortion temperature of fire-retardant polymer and decrease the air permeability to improve the mechanical performance and fire resistance of its char layer and (3) wrapping the acid ingredients (phosphate or borate) with charring agent to make the latter microcapsulative and then gain the internal fire-retardant IFR.

4.5.1 Polymer charring agent

Polyols was usually applied as charring agent for IFR, but the problem of penetration (spreading) and water solubility exists, and its incompatibility with polymers can influence the mechanical performance of fire-retardant polymers. For IFR used in polyolefin, polymer such as TPU and PA6 has been applied as charring agent to avoid or ease those problems. The IFR with TPU as carbon source and APP as acid and gas source have been applied in flame-retardant IPP. Considering the decreasing HRR of flame-retardant PP, polyester TPU works better than polyether TPU. For one polyol, the harder the segment in TPU, the more the HRR decreases. For PP/APP/TPU system, when the total amount of APP/TPU is 40%, the LOI depends on type of polyols and the APP/TPU rate, and polyester polyols can realize higher LOI to PP than polyether polyol can do. The best APP/TPU rate (in quality) depends on polyol's type too but should lie within a range of 1–3. However, PP/APP/TPU system can easily produce molten drop, so it can just pass UL94V-2; only, the APP/TPU amount reaches to 45% if it passes the UL94V-0.

The charring agent PA6 has been applied in PP, for PP/APP/PA6 system; some surface treating agent (such as ethylene-vinyl acetate copolymer) should be added to prevent the transportation of APP in PP and also improve the

compatibility of PA6 and PP. When the total amount of APP/PA6 is 30% (the mass rate of APP /PA6 is 3:1) and the amount of ethylene-vinyl acetate copolymer(EVA) is 5%, LOI of the fire-retardant PP could reach to 28%, fire resistance could pass the UL94V-0 (3.2 mm sampling), and HRR peak value (PHRR) is only 250 kW/m^2 (normally single PP has a value of 1400 kW/m^2). If some other ingredient such as talcum powder is added, higher modulus and better chemical stability will be achieved for PP, which leads to easy process. Talcum powder helps to generate ceramic-like shields and therefore improves the protection performance and the Yang's modulus.

4.5.2 Nanofillers as components of IFR

Lots of researches have pointed out that organically modified MMT can lead to a dramatic PHRR reduction (about 50–70%) of many high polymers, such as PS and PAS. But the improvement of material's LOI and UL94V was too small. This is because in the determination of HRR in a cone calorimeter, the combustion of the sample is conducted in a horizontal direction, whereas the measurements of LOI and UL94V are applied along vertical direction. Moreover, PPCH usually maintains lower viscosity; when melting entropy is generated in combustion, the corresponding material will outflow. However, nanoadditives can improve mechanical performance of high polymers. Thus, the IFR with high polymer charring agents and nanoclay can work competently to ameliorate both fire resistance and mechanical performance. For example, consider EVA-24/APP/PA6-nano (hybridization of PA6 and nano-pottery) and EVA-24/APP/PA6, with a 40% total application of APP/PA6 and a 3:1 mass rate, the former material always maintains higher fracture stress and elongation at break. What is more, the former LOI is 37%, whereas the latter is 32% and if aiming to UL94V-0 authentication, the APP of the former may reach 10–34% and the latter may be 13.5–34%. PHRR of the former would turn to be 240 kW/m^2 and the latter would be 320 kW/m^2. The frangibility of the former char layer was also lower. In Ref. [26], the weight loss curves of EVA-24/APP/PA-nano and EVA-24/APP/PA6 both in N$_2$ (in a radiation gasification equipment) and air (in a cone calorimeter) were compared. According to the four curves, except EVA-24/APP/PA6 curve in air, other curves were similar to each other. This shows that oxygen has an important influence in thermal decomposition of EVA-24/APP/PA6. While for EVA-24/APP/PA-nano, with nanoclay acts as a shield of oxygen spreading and then decreased or eliminated oxygen's influence on material thermal decomposition, the weight loss curves in N$_2$ and in air stay approximately the same. Moreover, nanopottery helps to generate P/C structure or more sticky char layer and slows the mass transfer and the thermal spreading. Furthermore, nanopottery can react with APP and generate aluminum phosphate; the latter can thermally stabilize P/C structure and the heat-resistance temperature will reach 310 °C. When the

temperature continues to rise, with aluminum phosphate's decomposition, the P/C structure will be destroyed. Then, amorphous alumina ceramic with orthophosphate or polyphosphoric acid is produced which can also acts as a shield. No P/C structure but orthophosphate mixture is detected in expanding char layer in EVA-24/APP/PA6 system without nanopottery.

The organic pottery is added into EVA-19 and PA6, and EVA-nano and PA6-nano are obtained; then, the EA-nano/APP/PA6 and EA-nano/APP/PA6-nano are found. When the total amount of IFR is 40%, both LOIs rise to 33–34% and can pass UL94V-0; when the LOIs of EVA/APP/1PA6 and EVA/APP/PA6 with the same formula are 29–34%, UL94V-0 passes too. Moreover, there are two exothermic peaks on the HRR curve of EVA/PP/PA6 system. The first one corresponds to the generation of expanding char layer, whereas the second corresponds to its break. As long as the nanopottery exists in the system, the first peak will be low, but only the existence of EVA-nano can reduce the second peak.

To know more about nano-fire-retardant polymer material, please see Chapter 6.

4.5.3 Microencapsulation of IFR

The microencapsulation discussed here means to wrap acid source, such as APP, with high polymer charring agents, and TPU. Such microencapsulation can lower the water solubility of APP and delay its transportation and penetration in base materials.

Two crafts can be applied for microencapsulation: the interfacial polycondensation and the solvent evaporation. The former can be used for those materials with an average radius of 0.7 μm (fit for microencapsulation materials with lower radius of 5 μm). After the microencapsulation, the material will transform into ball with few aggregations. The latter craft can be used in larger materials and get a higher product yield and easier amplification. The TPU film for wrapping should be flexible enough to transform the particles with no breakage [4].

IFR not only provides the high polymer with necessary fire-retardant performance but also makes other performance, which is acceptable by customers. The application of polymer charring agent is one of the most promising ways for IFR's improvement, which takes both fire-retardant and mechanical performance into consideration. Nanocrystallization of IFR components can get better mechanical performance. These materials are of low inflammability in horizontal combustion experiments but cannot pass UL94V-0 authentication. The application of polymer charring agent and group nanomic process at the same time is likely to be the future direction for the design of effective expansion of fire-retardant polymer material.

4.6 Further understanding of intumescing flame retardation mechanism

Currently, people have little understanding about the high-temperature kinetic of IFR, and the explanation for inflation is qualitative and rough. In this regard, the following questions are needed to be further investigated: (1) It is mainly involved in the relationship between the reaction order and the temperature, during the flame-retardant system, the reaction sensitivity to temperature, reaction order, the influence of the change of the ratio of reaction product properties etc. (2) Function of each composition within expansion-type flame retardant, catalysis and synergistic effect between the components – for example, is APP the catalyst or the base material of expansion of carbon layer? What contribution does APP make? Why this kind of association effect agent (such as MA, our season four alcohol, etc.) greatly improves the flame-retardant effect of APP? How APP network structure contributes to the formation of the char layer? etc.(3) How the char layer network of flame-retardant system is formed? How the precursor of char layer transformed into a carbon layer? In the formation of char precursor, what reaction and physical change happened between the flame-retardant plastic surfaces and formed char layer? What is the structure of char layer, especially the structure of the bubble hole? How to characterize and determine the structure of char layer? How to optimize the flame-retardant formula to improve the quality of the char layer, etc. (4) The fine structure of polymer (such as crystalline, orientation, phase transition, etc.) on condensed-phase flame retardant – it is crucial knowledge to improve the flame-retardant efficiency of expansion-type flame retardant and development of new expansion-type flame retardant. For expansion-type flame-retardant systems, although a lot of literature have been published [52], still many problems remain unsolved. For example, the typical expansion-type flame-retardant system of APP has not yet been fully understood.

In recent years, researchers have made numerous studies on abovementioned fields and obtained valuable achievements. For instance, they have already realized that the premise of char layer is formed at the temperature lower than that of plastic cracking and burning. It is a kind of three-dimensional entity structure, which can further be carbonized and become carbon layer of flame retardant. Moreover, its composition basically retained in the final char layer. The crystallization of char layer is made up of polyaromatic hydrocarbons coated on cell size in the amorphous phase matrix. Through P–O–C bond, amorphous phase is linked to phosphate and system-containing alkyl generated by thermal cracking between flame-retardant plastic and into carbon agent in flame-retardant system. Adding molecular sieve into intumescent char layer system, cell size of both amorphous phase and crystalline phase deceases (10–100 nm) and leads to form closer and more flexible structure. This structure is not easy to break and can organize the combustible gas and free radicals and prevent them

from escaping the char. At the same time, the thermal oxidation resistance of carbon layer is increased; the residue is more stable after the thermal decomposition [45]. In the expansion-type flame-retardant system, add a certain amount of some metal compound catalyst and also meet with added molecular sieve effect [54]. But some deep-seated problems remain to be further investigated and elucidated.

To form a char layer, carbon precursor must reach the surface of the material, namely, it must be able to migrate to the surface of the material; that is to say, carbon precursor layer should be easily moved, and the migration process at least is related to two factors: (1) the difference between the free energy of the surface of the molten plastic and its surface, and the difference between the free energy of the plastic surface and the rich carbon precursor; (2) there must be a driving force on the precursor of char layer; this can be made of temperature gradients and flame retardants in the gas produced by decomposition of foaming agent. Therefore, after a carbon precursor migrating to the surface of flame-retardant polymer, the fire molten plastic and part of the flame retardant into the composition of char layer are reduced. The expansion-type flame-retardant system and other condensed-phase migration phenomenon remain to be investigated. The effect of the foaming agent and the movement of gases in the molten plastic within expansion-type flame-retardant system have been studied and the influence of melting plastic viscosity on bubble motion has been pointed out [55], but the influence of viscosity on char precursor migration is still a subject to study.

With respect to the expansion-type flame-retardant carbon layer structure, it is proven that diameter of bubble hole, mostly closed hole, within carbon layer is 5–50 μm. It is closely related to the composition of the expansion flame retardant, especially the association effect performance of APP, but the bubble pore structure and the relationship between the char layer of fine structure are not well known [56]. Recently, researchers have taken different analysis methods to study the expansion of char layer structure, which are progressing in an effective manner. But the basic properties and structural characteristics of the expansion of char layer, also just have some estimates and sometimes even vague description, need to be further investigated. In fact, the expanded char layer is an extremely complex material, and a lot of parameters, such as volume, quality, density and fracture resistance, elasticity, hardness, toughness, cohesion, coherence, air permeability, thermal conductivity, specific heat, insulation, other fine structure and performance parameters, are used for characterization of its performance. However, there is no feasible way to measure the abovementioned performances. In particular, the appropriate formula has not been invented yet which controls different char layers [22]. The plastic expansion in this area, namely the relationship between structure and properties of the char layer, is still a promising new research field that needs to be further investigated.

References

[1]   Ou Yuxiang, Li Jianjun. Flam Retardant[M].Beijing:Chemical Industry Press, 2006.26–31.

[2]   Bourbigot S, Duquesne S. Intumescence based fire retardants[A]//Wilkie C A, Morgan A B. Fire Retardancy of Polymeric Materials. 2nd Edition[M]. Baca Ration: CRC Press, 2009.129–162.

[3]   Duquesne S, Bourbigot S. Char Formation and Characterization[A]. Wilkie C A, Morgan A B. Fire Retardancy of Polymeric Materials (2nd edition)[M]. Baca Ration: CRC Press, 2009.239–260.

[4]   Bourbigot S, Bras M L, Duquesne S. Recent Advances for Intumescent Polymer[J]. Macromolecular Materials and Engineering, 2004,259:499–511.

[5]   Gamino G, Costal L, Martinasso. Intumescent Fire-Retardant Systems [J]. Polymer Degradation and Stability, 1989,23:359–376.

[6]   Bourbigot S, Duquesne S. Intumescence and Nanocomposites. A Novel Route for Flame-Retarding Polymeric Materials[A]. Morgan A B, Wilkie C A. Flame Retardant Polymer Nanocomposites. Hoboken: John Wiely & Sons Inc., 2007.131–162.

[7]   Camin G, Lomakin S. Intumescent Materials [A]. Horrocks A R, Price D. Fire Retardant Materials [M]. Boca Raton : CRC Press, 2000.318–336.

[8]   Halpern Y, Mott D M, Niswander R H. Fire Retardancy of Thermoplastic Materials by Intumescence [J]. Industrial & Engineering Chemistry Process Design and Development, 1984,23(2):233–238.

[9]   Myers R E, Dickens E D Jr, Licursi E, et al. Ammonium Pentaboraten An Intumescent Flame Retardant for Thermoplastic Polyurethanes [J]. Journal of Fire Sciences, 1985,3(6):432–449.

[10]   Kvoenke W J. Low-Melting Sulfate Glasses and Glass-Ceramics and Their Utility as Fire and Smoke Retarder Additives for PVC [J]. Journal of Materials Science, 1986,21(4):1123–1133.

[11]   Camino G, Costa L, Trossarelli L. Study of the Mechanism of Intumescence in Fire Retardant Polymers．Part I. Thermal Degradation of Ammonium Polyphosphate-Pentaerythritol Mixtures [J]. Polymer Degradation and Stability, 1984,6:243–252.

[12]   Montaudo G, Scamporrino E, Vitalini D. Intumescent Flame Retardants for Polymers. II. The Polypropylene-Ammonium Polyphosphate-Polyurea System [J]. Journal of Polymer Science, Part A．Polymer Chemistry, 1983,21:3361–3371.

[13]   Montaudo G, Scamporrino E, Puglisi C, et al. Intumescent Flame Retardant for Polymers. III. the Polypropylene-Ammonium Polyphosphate-Polyurethane System [J]. Journal of Applied Polymer Science, 1985,30:1449–1460.

[14]   Luo Jieyu, Luo Ximing, Sun Yingcai, et al. Ammonium Polyphosphate and its Application[M]. Beijing:Chemical Industry Press, 2006.276.

[15]   Zhang Jun, Ji Kuijiang, Xia Yanzhi.Polymer Combustion and Flame Retardant Technology[M]. Beijing:Chemical Industry Press, 2005.390–391.

[16]   Ou Yuxiang, Han Yanxie, Li Jianjun. Flame Retardant Plastics Handbook[M].Beijing:National Defense Industry Press, 2009.9–16.

[17]   Le Bras M, Bourbigot S, Delporte C, et al. New Intumescent Formulations of Fire-Retardant Polypropylene.Discussion of the Free Radical Mechanism of the Formation of Carbonaceous Protective [J]. Fire and Materials, 1996,20(4):191–203.

[18]   Bourbigot S, Duquesne S, Leroy J-M. Modeling of Heat Transfer Study of Polypropylene-Based Intumescent Systems During Combustion [J]. Journal of Fire Sciences, 1999,17(1):42–49.

[19]   Bugajny M, Le Bras M, Bourbigot S. Short Communication. New Approach to the Dynamic Properties of an Intumescent Material [J]. Fire and Materials, 1999,23(1):49–51.

[20] Duquesne S, Delobel R, Le Bras M, et al. A Comparative Study of the Mechanism of Action of Ammonium Polyphosphate and Expandable Graphite in Polyurethane [J]. Polymer Degradation and Stability, 2002,77(2):333–344.

[21] Bugajny M, Le Bras M, Bourbigot S, et al. Thermal Behaviour of Ethylene-Propylene Rubber/Polyurethane/Ammonium Polyphosphate Intumescent Formulations. A Kinetic Study [J]. Polymer Degradation and Stability, 1999,64:157–163.

[22] Bourbigot S, Le Bras M, Delobel R, et al. Synergistic Effect of Zeolite in an Intumescence Process: Study of Interactions Between the Polymer and the Additives [J]. Journal of the Chemical Society,Faraday Transactions, 1999,92(18):3435–3444.

[23] Le Bras M., Bourbigot S. Fire Retardant Intumescent Thermoplastics Formulations. Synergy an Synergistic Agents.A Review [A]. Le Bras M, Camino G, Bourbigot S, et al. Fire Retardant of Polymers.The Use of Intumescence [M]. Cambridge (UK): The Royal Society of Chemistry, 1998. 64–75.

[24] Morice L, Bourbigot S, Leroy J M. Heat Transfer Study of Polypropylene-Based Intumescent Systems During Combustion [J]. Journal of Fire Sciences, 1997,15:358–374.

[25] Kashiwagi T, Du F, Winey K I, et al. Flammability Properties of Polymer Nanocomposites with Single-Walled Carbon Nanotubes.Effects of Nanotube Dispersion and Concentration [J]. Polymer, 2005,46(2):471–481.

[26] Yuxiang Ou. Practical Flame Retardant Technology [M]. Beijing: Chemical Industry Press, 2001.81–82.

[27] Bourbigot S, Le Bras M, Delobel R, et al. 4A Zeolite Synergistic Agent in New Flame Retardant Intumescent. Formulations of Polyethylenic Polymers.Study of the Effect of Constituent Monomers [J]. Polymer Degradation and Stability, 1996,54:275–283.

[28] Bourbigot S, Delobel R, Le Bras M. Carbonisation Mechnisms Resulting from Intumescence. Association with the Ammounium Polyphosphate-Pentaerythritol Fire Retardant System[J]. Carbon, 1993,31(8):1219–1230.

[29] Bourbigot S, Le Bras M, Delobel R, et al. Synergistic Effect of Zeolite in an Intumescence Process: Study of the Carbonaceous Structures Using Solid-StatenmR [J]. Journal of the Chemical Society-Faraday Transactions, 1996,92(1):149–158.

[30] Bourbigot S, Le Bras M, Delobel R, et al. Synergistic Effect of Zeolite in an Intumescence Process Study of the Interactions Between the Polymer and the Additives [J]. Journal of the Chemical Society,Faraday Transactions, 1996,92(18):3435–3444.P108

[31] Lewin M. Unsolved Problems and Unanswered Questions in Flame Retardance of Polymers [J]. Polymer Degradation and Stability, 2005.88:13–19.

[32] Marosi G, Marton A, Szep A, et al. Fire Retardancy Effect of Migration in Polypropylene Nanocomposites Induced by Modified interlayer [J]. Polymer Degradation and Stability, 2003,82:379–385.

[33] Marosi G, Keszei S, Marton A, et al. Flame Retardant Mechanisms Facilitation Safety in Transportation [A]. Le Bras M, Wilkie C A, Bourbigot S, et al. Fire Retardancy of Polymers. New Applications of Mineral Fillers [M]. Cambridge (UK): The Royal Society of Chemistry, 2005.347–360.

[34] Bourbigot S, Le Bras M, Delobel R, et al. Synergistic Effect of Zeolite in an Intumescent Process.Study of the Carbonaceous Structures Using Solid State NMR [J]. Journal of the Chemical Society-Faraday Transactions, 1996,92(1):149–158.

[35] Camino G, Costa L, Trossarelli L. Study of the Mechanism of Intumescence in Fire Retardant Polymers.Part VI. Mechanism of Ester Formation in Ammonium Polyphosphate-Pentaerythritol Mixture [J]. Polymer Degradation and Stability, 1985,12(3):213–218.

[36] Lewin M, Endo M. Catalysis of Intumescent Flame Retardancy of Polypropylene by Metallic Compounds [J]. Polymers for Advanced Technologies, 2003,14(1):3–11.

[37] Kashiwagi T. Polymer Combustion and Flammability.Role of the Condensed Phase [A]. Processing of the 25th Symposium Int. Combustyon[C]. Gaither Sburg: Symposium Int. Combust, 1994.25,1423–1437.

[38] Lewin M, Endo M. Intumescent Systems for Flame Retarding of Polypropylene[A]. ACS Symposium Series [C]. 1995,599(Fire and Polymers II).91–116.

5 Flame retardation mechanism of other flame retardants

This chapter discusses the flame retardation mechanism of metal hydroxides, fillers, borates, red phosphorus, polysiloxanes and sulfous and nitrogenous compounds. In addition, we discuss the effect of inorganic flame retardant's surface properties and conditions on flame retardant efficiency, as well as the solubility and migration of FR's in polymers.

5.1 Flame retardation mechanism of metal hydroxides

Some endothermic decomposition compounds [such as aluminum hydroxide (ATH) and magnesium hydroxide (MH)] can cool the flame retarded matrix, reducing the temperature below the degree required to sustain combustion. Moreover, endothermic decomposition can produce water vapor or other non-flammable gases, which can dilute combustibles in the gas phase. The residue formed during thermal decomposition also can act as a protective layer, protecting the matrix underneath from thermal damage.

The molecular structure of ATH and MH has no hydrate water; the water released when heated is generated as a result of the decomposition of hydroxy bonded with the metal. For ATH, the initial temperature for water release is 200 °C, the released water is up to 34% (forming Al_2O_3) and the heat absorption during water release is 1170 kJ/kg. For MH, these values are are 330 °C, 31% (forming MgO) and 1370 kJ/kg, respectively [1]. Obviously, heat absorption and water release constitute flame retardant modes of ATH and MH, but not all of them. Inorganic oxide layer generated by the dehydration of ATH and MH also acts as a good heat insulation layer. However, the newly generated Al_2O_3 can result in smoldering [2]. When the loading rate is low, the flame retardation performance of anhydrous aluminum oxide is at times better than trihydrate alumina, for example, for epoxy resin. Anhydrous aluminum oxide is a catalyst which helps to catalyze char formation. For example, silicon dioxide layer strongly inhibits heat release possibly because of its bad thermal conductivity and the ability to reflect radiation heat. MgO is also a good insulator. MgO formed during water loss by MH can also act as flame retardants. When MH and other additives are used for flame retarding PP, the heat insulating barrier of MgO can be strengthened. Some char forming acrylonitrile copolymers (fiber or fabric) can also improve the flame retardancy of MH in rubber. Certain polycarboxylic acid resins and polysiloxanes have been reported to promote the transformation of ATH and MH to an insulation layer in fires [3].

Thermal analysis shows that the temperature of ATH releasing water is close to the processing temperature of general thermoplastics, but far below than that of

engineering plastics. Thus, ATH is not appropriate for plastics that require higher processing temperature. As the releasing water temperature of MH is higher than 300 °C, it has a wide range of applications.

Endothermic mechanism realizes flame retardancy through three physical processes of cooling, dilution and heat insulation, and the efficiency is much lower than chemical flame retardants.

The main disadvantages of metal hydroxide flame retardants are low efficiency and large loading, which generally accounts for 50%~70% of flame retarding materials to achieve optimum flame retardancy. However, if they are used collaboratively with other efficient flame retardants or as auxiliary smoke suppression agents, the loading rate reduces.

The exact flame retardation mechanism of metal hydroxides is difficult to identify because their efficiency is closely related to the type of polymers, especially the decomposition mechanism of polymers. In polypropylene (PP), 60% loading is required to reach 26% of limiting oxygen index (LOI), whereas in polyamide 6 (PA6), 60% loading can increase LOI to nearly 70% [4]. Moreover, for different flame retardant grades, the effects of metal hydroxides can be different. To pass test of UL94V-0 level, for example, there is a great relationship between the required loading and melt droplet during burning of polymers. Some polymers containing metal hydroxides have a high LOI, however, tend to produce melt droplet during burning. The improved viscosity of melted polymers containing a large quantity of metal hydroxides is beneficial for inhibiting molten drops. In addition, flame retardation efficiency of metal hydroxides also depends on various factors, including particle size and distribution, surface condition, purity and interaction with polymers [4].

5.2 Flame retardation mechanism of fillers

Some natural or synthetic inorganic substances, such as asbestos, talcum powder, molybdenum compounds, alumina and aluminum hydroxide, ammonium salts, and metallic carbides, can be used as flame retardants, mainly acting as fillers. Their flame retardation mechanism includes dilution, accumulation and conduction of heat, cooling, surface effects on polymers, and so on. Fillers can be divided into two categories – active and inert – but this classification is only comparative. Factors that affect the activity or inertia of fillers include temperature, oxidants present in materials and so on. For example, under 900 °C, asbestos in polymers are only inert diluents of low thermal conductivity, but at 900 °C to 1400 °C, asbestos can release crystallization water; above 1400 °C, asbestos can undergo endothermic reactions changing its chemical structure. Some components of asbestos may also react mutually with some thermal degradation products of polymers, making the asbestos in polymers acting as an active filler [1]. When using inorganic fillers as flame retardants for polymers, it is necessary to reduce the negative effects of

fillers on the polymer's properties, to reduce the combustible components produced during the decomposition of the polymer, to improve the thermal physical properties of polymers and to prevent the physical transition of the fillers. It is important to note that some inorganic compounds used as flame retardants act as catalysts for polymerization and polycondensation reactions; moreover, they have catalytic effects on the combustion and decomposition products of polymers, thus contributing to carbonization. The most important mechanism for this is the dehydrogenation cyclization and aromatization of hydrocarbons under the effects of catalyst. Such catalysts include titanium, cobalt and aluminum oxides and aluminum phosphate.

In general, the main factors that affect the flame retardancy of fillers are discussed below [4].

1. Thermal effects

    The thermal effects related to the flame retardation efficiency of hydration fillers are mainly decomposition enthalpy of fillers and the heat capacity of related substances, which can affect the thermal degradation of polymers, as well as the barrier functions of residue formed by decomposition of fillers. Clearly, strong endothermic fillers during decomposition are beneficial for flame retardancy.

2. Thermal stability

    The thermal stability of fillers, similar to polymers, should withstand the processing temperature of polymers; however, this does not imply the higher the temperature the better. The thermal decomposition temperature of fillers should match that of the polymers, so that they can play the role of flame retardancy at the right time.

3. Gas phase interactions

    Although flame retardation effects of some fillers (such as hydrated filler) mainly arise from reactions of condensed phase, dilution cooling and coverage function of inert gases cannot be overlooked. For example, 51% of flame retardation in the case of $Al(OH)_3$ arises from the heat absorption during decomposition, 19% from the decomposition residue (oxide) and 30% from the gaseous decomposition products [4].

4. Interactions between fillers and polymers

    When thermoplastic polymers contain fillers, some affect the thermal degradation behavior of polymers, in turn affecting flame retardancy. For example, metal hydrate fillers release water during decomposition, which helps promote the degradation of PA6 and PA66 (hydrolysis). PA with or without metal-bearing hydrates can release H_2O, CO, CO_2, NH_3 and hydrocarbon during thermal decomposition. However, there is considerable overlap within the thermal degradation of PA6 and $Mg(OH)_2$. PA66 decomposes prior to $Mg(OH)_2$, and hence $Mg(OH)_2$ imposes better flame retardancy on PA6 than that on PA66 [4]. Another example is ethylene-vinyl acetate copolymer (EVA) containing 30% vinyl acetate (VA) with $Mg(OH)_2$, which shows the highest oxygen index reaching an LOI of 46%

compared to 37% with $Al(OH)_3$. In flame-retarded EVA, $Al(OH)_3$ has a delayed water release, whereas $Mg(OH)_2$ has an accelerated water release possibly due to the formation of acetic acid during the reaction of Mg $(OH)_2$ and EVA.

5. Filler conditions

Particle size and distribution and surface conditions of fillers can affect their compatibility with polymers as well as their dispersion in polymers, ultimately affecting flame retardancy properties.

5.3 Flame retardation mechanism of borates

Flame retardant effects of borates can be mainly attributed to the following: formation of glassy inorganic intumescent coatings; promotion of char formation; preventing the escape of volatile combustibles; dehydration at high temperatures, including heat absorption, foaming and diluting the combustibles.

Zinc borate hydrate ($2ZnO \cdot 3B_2O_3 \cdot 3.5H_2O$), an important flame retardant and smoke suppressor releases 13.5% of water and absorbs 503 J/g of heat at temperature ranging between 290 °C and 450 °C [5], which coincides with the decomposition temperature of polyvinyl chloride (PVC) and several other polymers. Zinc borate also displays better thermal stability, and its dehydration temperature is similar to the decomposition temperature of some engineering plastics. During pyrolysis of zinc borate, most of the zinc and boron remains in the char layer.

When zinc borate and halogenated flame retardants are used together, they can perform flame retardancy in both the gas and condensed phase. Zinc borate reacts with hydrogen halide produced by the decomposition of halogen-containing flame retardant polymers or halogenated flame retardants to generate zinc and boron compounds (5.1) [6].

$$2\,ZnO \cdot 3B_2O_3 + 12\,HCl \xrightarrow{\Delta} Zn(OH)Cl + ZnCl_2 + 3BCl_3 + 3HBO_2 + 4H_2O \qquad (5.1)$$

Non-volatile zinc and boron compounds accelerate char formation; volatile boron halides and water vapor can dilute combustibles and lower the temperature by heat absorption. Zinc halides can catalyze crosslinking of some polymers. For example, $ZnCl_2$ prior to its volatilization can catalyze polyethylene terephthalate (PET) and polybutylene terephthalate (PBT) to crosslink and generate char with high aromatic content (5.2). In addition, $ZnCl_2$ catalyzes PVC to crosslink and eliminate HCl in the process. In addition, boron oxides produced by reactions of acids with zinc borate increase the stability of the char layer and inhibit smoldering. Boron halides act as flame suppressants and can capture free radicals as in the case of hydrogen halides. However, when zinc borate woks as flame retardant for PVC, only a small amount of boron converts to volatile boron halides.

$$\text{(5.2)}$$

In a halogen-free system, anhydrous zinc borate helps improve the quality of the char layer, and the flame retardation property of hydrate zinc borate mostly arises from the dehydration mechanism. For instance, in the presence of aluminum hydroxide in flame retardant system, zine borate can form a porous ceramic layer at 550 °C, which functions as a heat and mass transfer barrier. Moreover, boron compounds can delay the oxidation of the graphite structure because boron inactivates certain reaction sites that are important for oxidation on graphite surfaces.

It has been reported [7] that on addition of zinc borate and red phosphorus into PA, both not only work as synergistic flame retardants but also improve the corrosion resistance of the flame retardant system on some metals (such as copper) because zinc borate can capture phosphine produced by red phosphorus.

Recent research has pointed out that a mixture of a small amount of (approximately 10%) zinc borate and ATH (or MH) (approximately 90%) a mixture of melted or sintered at about 700 °C. When used for EVA, this mixture can not only greatly reduce the PHRR value but also delay the time of the second peak of HRR curve. This indicates that the carbonization rate of flame retardant system can be increased with the participation of th zinc borate.

5.4 Flame retardation mechanism of red phosphorus

Red phosphorus is an extremely effective flame retardant which can be used for oxygen-containing polymers such as polyamide (PA), polycarbonate (PC) and polyethylene terephthalate (PET). The flame retardation mechanism of red phosphorus is similar to that of organic phosphorus flame retardants. The formation of phosphoric acid not only covers the surface of the materials but also accelerates dehydration charring and forms a char layer and liquid membrane on the surface, insulating oxygen, volatile combustibles and heat from the internal polymer matrix, thus inhibiting the combustion. Research has shown that phosphorus exposed to fire in PA is oxidized into acid which can esterify PA, producing a char layer possibly coated by polyphosphates. Because red phosphorus directly obtains oxygen from PA during reaction, even if PA was heated in an inert atmosphere, it may still be oxidized. The oxidized phosphorus substances are phosphates as confirmed by IR and NMR. These phosphates are generated as a result of the reaction between PA6 fragments and phosphoric acid generated during the oxidation of red phosphorus. Further indirect evidences of the effects of red phosphorus in the condensed phase include the fact that the LOI curve resembles the nitric oxide curve. This demonstrates that flame retardancy is not affected by the oxidizer but has an effect in the condensed phase.

In addition, red phosphorus may also react with polymers or polymer fragments in the condensed phase, thus reducing the formation of volatile combustibles. Some phosphorus-containing mixtures may also participate in the gas-phase reactions and exhibit flame retardancy. For example, there are several compounds containing phosphorus (phosphorus trichloride and triphenyl phosphine oxide), which are more effective in preventing burning of hydrogen-air mixture than halogen. Table 5.1 compiles a list of possible flame retardation mechanisms of red phosphorus in PET, polymethyl methacrylate (PMMA) and polyacrylonitrile (PAN).

Table 5.1: Possible Flame Retardation Mechanisms of Red Phosphorus in PET, PMMA and PAN.

Flame retarded polymer	Condensed phase	Gas phase
PET	Slowing down PET pyrolysis and forming aromatic residues	–
PMMA	Accelerating formation of cyclic anhydride	–
HDPE	Phosphors-containing acids as combustion inhibitors	Reducing concentration of free radicals
PAN	Accelerating surface carbonization by phosphorus-containing acids	Inhibiting combustion by PO

It seems that flame retardation mechanism and efficiency of red phosphorus is relevant to the flame retarded polymers. For example, on addition of 8% red phosphorus in high-density polyethylene (HDPE), 6% (mass) of the material is lost at 400 °C in air, whereas for pure HDPE, 70% is lost under the same conditions. This implies that red phosphorus can significantly enhance the thermal stability of HDPE. In addition, red phosphorus in PET, the thermal decomposition products contain phosphates and ester crosslinking forms on the surface of polymer, inhibiting the formation of volatiles and pyrolysis products with low molecular weight, increasing the rate of formation of polycyclic aromatic char layer and reducing the release of smoke and toxic gases.

Red phosphorus can control the thermal decomposition of PAN. Phosphates exist in the solid products of the thermal decomposition of flame-retarded PET by phosphorus. P-O bonds with good thermal stability in PET form crosslinked ester on the surface of the polymer. This can inhibit the formation of volatiles and pyrolysis products with low molecular weight, increasing the rate of generation of polycyclic aromatic charcoals [1].

5.5 Flame retardation mechanism of polysiloxane

Polysiloxane is usually associated with one or more synergistic agents as flame retardants. These synergistic agents are organic metal salts (such as magnesium stearate), mixture of ammonium polyphosphate (APP) and pentaerythritol, aluminum hydroxide and so on [10]. They can not only combing with substrate, but also have synergistic effects with polysiloxane. This helps to increase metal infiltration of substrate with polysiloxane, and to promote formation of char layers, further preventing smoke production and flame propagation [1].

Polysiloxane can be bound into a polymer substrate structure with a mechanism similar to partially crosslinked by interpenetrating polymer network (IPN), which can significantly inhibit the mobility of silicon additives, preventing the migration of additives to polymer surface.

In polyolefins with and without fillers, polysiloxane helps in the formation of char layers. This can not only improve LOI but also reduce the speed of flame propagation. The actual flame retardant effects of polysiloxane depend on the binding conditions of polyolefin with flame retardants [1].

Further, the use of polysiloxane in case of PC is very successful, and the following describe its characteristics and flame retardation mechanisms:

Silicon-containing compounds for PC are becoming prominent flame retardants. These compounds have been emerging until the 1980s, and have exhibited excellent flame retardancy (low burning rate, low heat release, anti-dropping), good

processability (high mobility) and satisfactory mechanical properties (particularly low temperature impact strength), especially the environment friendly attributes of low smoke and low CO production. Moreover, they have broad prospects for development.

5.5.1 Features of silicon compounds PC

(1) For flame-retarded PC by organosilicon compounds (mainly polysiloxane flame retardant), thermal deformation temperature is not affected and flame retardancy is likely to reach UL94 V-0 (1.2 mm) or 5VA (2.5 mm) level. The peak heat release rate and average heat release rate decrease considerably, generating little smoke and poisonous corrosive gases.

(2) Silicon-oxygen groups in polymer backbone and organic silicone flame retardant additives can improve moisture resistance and flexibility of materials, and silicon-based flame retardant PC is known for its excellent impact strength. In particular, the impact of low temperature is quite outstanding. Other mechanical properties can also compete with bromine and phosphorus-based flame retardant PC [11].

(3) Silicon in polymer can endow materials with resistance to oxygen free radicals, and the materials used for spaceflight system, reducing degradation and weight loss in low obit.

(4) Some PC flame retarded by organosilicon compounds can be reused by mechanical recycling. After recycling for three times, the mechanical properties, thermal deformation temperature and flame retardancy of PC remain unchanged.

5.5.2 Flame retardation mechanism of organosilicon compounds in PC

In general, silicone-oxygen in PC function performs a flame retardation mechanism of condensed phase, namely through generation of pyrolytic char layer and improving anti-oxygenation of the char layer [12].

Experiments show that combustion residue of side chain methyl phenyl silicone is insoluble crosslinked compounds containing silicon, which is likely to be part of the char layer on the surface of the material. Gas chromatography shows that when compared with neat PCs, silicon-based PCs dehydrate and decarboxylase to a greater extent. This may be caused by the isomerization reaction (5.3) [12], which can accelerate the crosslinking and carbonization of PC. Crosslinking significantly aids the flame retardation of PC.

$$(5.3)$$
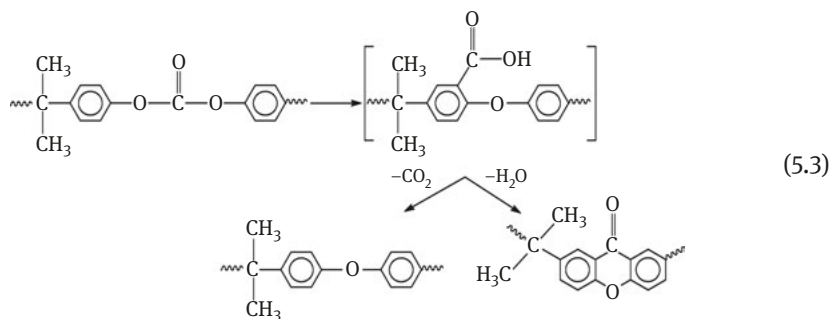
In addition, silicon-containing PCs are more susceptible to Fries rearrangement (5.4) than neat PC [13], which also accelerates the crosslinking and carbonization of PC.

$$(5.4)$$
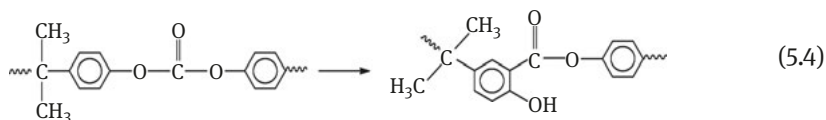
Furthermore, at high temperature PC-containing branched methyl phenyl siloxane may react with silicone-containing phenyl, forming a branched structure containing carbonyl (5.5). Its essence is silicon-containing groups attack hydroxyl generated by Fries rearrangement of PC, forming silicon ether structure containing phenyl with crosslinked carbonization.

$$(5.5)$$
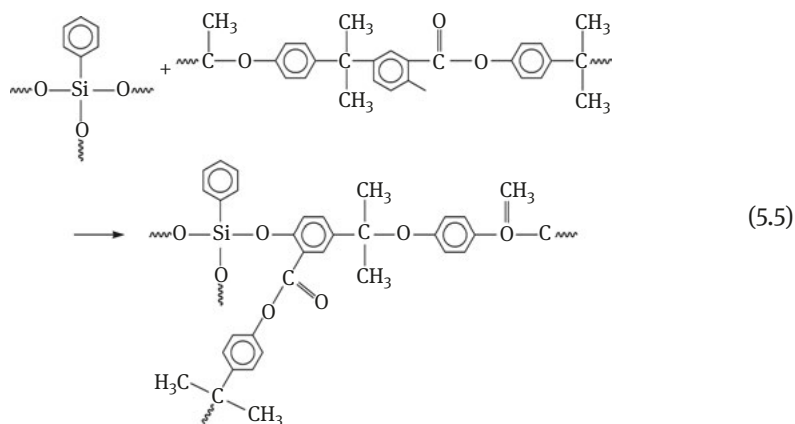
X-ray photoelectron microscope spectra show that, when PC containing siloxane burns, siloxane migrates to the surface and quickly aggregates, forming a functional gradient material with a polysiloxane-enriched layer [15, 16]. In addition,

an inorganic thermal insulation protective layer containing -Si-O- bond and (or) -Si-C- bond can be formed, which are the typical structures of polysiloxane. This layer can not only prevent the spillover of combustion products but also suppress the thermal decomposition of polymers, providing effective flame retardancy, low smoke and low toxicity. The abovementioned migration is due to the difference in viscosity and solubility between siloxane and PC at high temperatures. If silicon-based flame retardants have good compatibility, they can be uniformly dispersed in the matrix resin. The flame-retarded PC remains in a molten state when burning (about 800°). Because the viscosity of liquid silicone flame retardants is lower than that of PC, phase separation is caused, and polysiloxane tends to migrate and gather on the surface of the resin, forming homogeneous flame-retardant char layer [12].

Flame-retardant effects of polysiloxane is related to the enrichment characteristics on its surface, so the compatibility between polysiloxane and matrix resin, and molecular structure of polysiloxane as well as its relative molecular weight are very closely related to the properties of flame-retarded materials.

It is found in recent researches that flame retardant effects can be greatly improved by gradually increasing concentration of flame retardant on surface of molding specimens. In accordance with the abovementioned method, with adding a little polysiloxane in the plastics and made polysiloxane gather on the plastics surface when burning, the best flame retardancy can be realized. X-ray photoelectron spectroscopy (XPS) shows this is caused by the higher concentration of polysiloxane on the surface of molded specimens [12].

Compared with linear polysiloxane, branched chain meth phenyl polysiloxane has higher thermal stability. This is because aryl in branched chain polysiloxane can transform into silicon-containing polycyclic fused ring aromatic compounds with very high flame retardant properties. In addition, the branched chain siloxane can prevent zipper open chain depolymerization of PC.

However, some researchers believe that, because of silicon-based flame retardants for PCs, linear polysiloxane may be better than the branched chain one. The reason is that the aromatic unit and the branched chain structure in polysiloxane have little impact in improving flame retardancy of PC. When PC is burning, linear compounds have high mobility and can easily enrich on the surface of the materials. Furthermore, linear polysiloxane can endow PC with higher impact strength and does not affect the performance of the recycled flame-retarded PC. Additionally, PC is not easy to hydrolyze and exhibits good processability. However, similar to PC-containing branched chain compounds, PC may react with many ends of branched polysiloxane chain and lead to crosslinking, making it difficult to recycle flame-retarded PC. At the same time, too much branch chain is not conducive for efficient processing of PC [11].

Compared with polysiloxane containing aliphatic compounds, polysiloxane containing both aryl and aliphatic compounds is easier to dissolve and disperse in

PC. Moreover, prevention of gelation helps it to well disperse in polymers and substrates. But, in general, aromatic content in linear polysiloxane is not the most important.

5.6 Flame retardation mechanism of sulfur-containing PC compounds

Sulfur-containing compounds unusually used in flame retarded PC are sulfonate and sulfonamide salts. Common structural formulas are shown below [17–20].
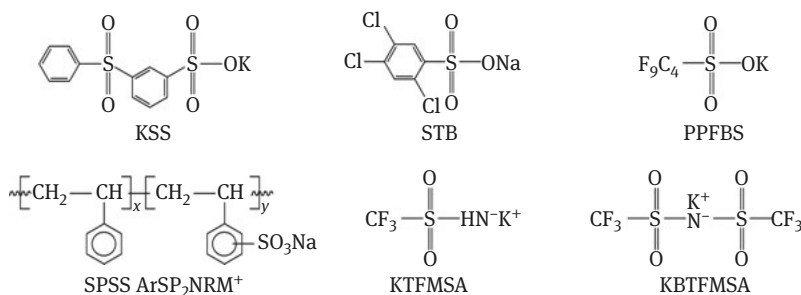
Potassium sulfone benzophenone sulfonate (KSS), sodium trichlorophehyl sulfonate (STB), potassium perfluorobutyl sulfonate (PPFBS), sodium polystyrene sulfonate (SPSS), potassium trifluoromethyl sulfonamide (KTFMSA) and potassium bis (trifluoromethylsulfonyl) amine (KBTFMSA).

The mechanism of sulfur compounds in flame-retarded PC is not very clear. However, they possibly play a role in condensed phase as a result of accelerating carbonization through crosslinking of PC. Some sulfur compounds (such as aromatic sulfonates) are good for isomerization and Fries rearrangement which improves the flame retardancy of sulfur compounds in PC. A previously reported experiment proved this and proposed the following arguments [21]:

(1) Sulfur compounds promote the isomerization of PC and release CO_2 and H_2O, which can dilute combustion products. More importantly, isomerization can promote the crosslinking and carbonization of PC. However, the char yield of pure PC and PC containing very small amounts of sulfonate is almost the same; however, the carbonization rate differs.

(2) They can accelerate Fries rearrangement (5.4) as well as crosslinking and carbonization of PC.

(3) The flame retardancy in the gas phase is not important. Limiting oxygen index measured in O_2 (OI) of flame-retarded PC by aromatic sulfonate and combustion

index measured in N_2O atmosphere (NOI) show similar tendencies. The same is shown even with halogen containing sulfonate [22].

(4) Sulfonates exhibit thermal decomposition between 300 °C and 500 °C, roughly matching the decomposition temperature range of PC.

(5) According to thermocouple measurements, when PC-containing sulfonate burns, the underlying material can maintain relatively low temperature for a long time. However, under the same conditions, PC without sulfonate exhibits relatively high increase in temperature in a short time. The insulating char layer forms on the surface when PC with sulfonate burns. Apparently, this char layer can effectively improve the flame retardancy.

(6) Mass spectrometry has shown that, when sulfonate is added to PC, the type of degradation products of PC does not undergo any changes and no new species are formed. However, the proportions of the products are different.

In general, sulfur compounds (including sulfonates, sulfonamide salts or a mixture of them along with polysiloxane) have high flame retardant efficiency for PC; only 1% or less loading ratevolume can enable flame-retarded PC to achieve an LOI of 35%~40% and UL94 V-0 grade. Other properties of PC are almost the same as those of the substrate. Sulfur compounds mainly act in the condensed phase (by promoting carbonization through crosslinking of PC), and the flame retardant effects in gas phase are insignificant.

5.7 Flame retardation mechanism of nitrogen compounds

Industrial nitrogen compounds used as flame retardants include melamine (MA) and its salts (phosphates, cyanurates, borates, oxalates, phthalates, octamolybdates, etc.). They act simultaneously in the condensed and gas phase. MA and its salts act as flame retardants compared with X-Sb system, organophosphorus compounds and metal hydrates, as shown in Table 5.2 [23].

1. Endotherm
   Sublimation, volatilization, evaporation and decomposition of MA and its salts are endothermic reactions. For example, the heat absorbed during endothermic vaporization of MA is 120 kJ/mol, and heat absorbed in MA decomposition at temperatures ranging between 250 °C and 450 °C is approximately 2000 kJ/mol. MCA absorbs considerable heat when it decomposes into MA and melamine, along with pyrophosphate of MA (DMPY) when it decomposes at temperatures over 250 °C. This clearly reduces the temperature required for combustion.

2. Generation of inert gases
   During the decomposition of MA and its salts, MA vapor, water vapor, N_2, CO_2, NH_3 and other gaseous products are generated, which not only dilute the

Table 5.2: Main Approaches of Some Flame-Retardant Systems.

Flame-retardant method \ Flame-retardant system	MA and its salts	X-Sb system	Organophosphorus compounds	Metal hydrates
Trapping active free radicals	√	√	√	
Interfering with degradation of polymers	√	√	√	
Absorption of heat	√			√
Promoting carbonization	√		√	
Forming an intumescent barrier layer	√		√	
Generating inert gases	√	√		√
Transferring heat by molten drop	√			

concentration of combustible gases and oxygen during combustion but also act as a cover (blanket effect).

3. Promotion of carbonization

   Some MA salts form polycondensate with crosslinking structures when decomposed under high temperature with a high char yield [23, 24]. For example, the char yield of MA phosphate (MP) in air at 700 °C is 30%, melamine polyphosphate (MPP) is 40% and DMPY is 50%. MA and its salts in polymers can affect polymer degradation, affect melting behavior and accelerate carbonization. The char generated at high temperature from plastics flame retarded with MA and/or its salts can withstand thermal oxidation, acting as a good protective layer. In general, for plastics containing MA and its derivatives, there is a quantitative relation between char yield and flame retardancy (such as LOI). The higher the char yield, the better the flame retardancy [25].

4. Formation of an intumescent layer

   As mentioned above, MA and its salts are an important part of intumescent flame retardant (IFR) and are usually compounded with other components to form IFR. When plastics containing IFR are heated or burned, the synergistic effects of triple source form a barrier, hindering mass and heat transfer, effectively improving the flame retardancy.

5. Molten drops and heat transfer

   Some plastics with MA salts can produce molten drops during combustion; the heat is moved quickly from the combustion area and the burning state cannot be maintained, For example, oxalate or phthalate of MA is used as flame retardant for PA6, and only 3%~5% of loading imparts an LOI of 35% to flame-retarded PA (the measured LOI of neat PA under the same conditions is 24%). This is due to contribution from molten drops and heat transfer.

6. Capturing active free radicals

   Some decomposition products of MA and its salts can also capture active free radicals in the gas phase. In addition, collision of active free radicals with an intumescent char layer results in inactive molecules.

5.8 Influences of inorganic flame retardant's surface properties and conditions on flame retardancy

This problem has been addressed in a previous article [26].

Some organic additive flame retardants in plastics (for example, a halogen-containing phosphate in flexible polyurethane foam and brominated epoxy oligomers in high impact polystyrene) are soluble in polymers to a certain extent. However, some inorganic flame retardants are insoluble in polymer substrates, such as alumina trihydrate (ATH), magnesium hydroxide (MH), zinc borate (ZB) and antimony trioxide (ATO). These flame retardants are considered organophobic, and the interface (or without interface) between them and the polymer is extremely complex. The incompatibility between the abovementioned flame retardants and polymers leads to a series of problems, including water leaching, swelling, poor dispersion, deteriorating mechanical properties (such as tensile strength and elongation) of flame-retarded polymers. The abovementioned problems can be resolved if the surface is treated using organic flame retardants using silane, titanate or stearic acid. It is well known that to obtain materials with excellent cost performance, surface modification of the inorganic flame retardants is more economical and efficient. Accordingly, it is necessary to know the surface conditions of inorganic flame retardants. This section is divided into two parts – the surface properties of inorganic flame retardants and the impact of surface conditions of inorganic flame retardants to flame retardant efficiency.

5.8.1 Surface properties

The surface of newly precipitated samples is quite ordered for crystalline inorganic flame retardants, and whole crystals also have an ordered structure to a certain extent. We often pulverize the crystals if the particle size is too large. The surface of the pulverized particles may be quite disorderly, in which changes the chemical properties on its surfaces. High temperature is produced for non-elastic materials. Cracks are often formed in particles during pulverization, and some cracks can be penetrated by gas, excluding large polymer molecules. Nonetheless, some cracks can be penetrated by polymer molecules. Therefore, for non-elastic materials, the surface of pulverized particles and the ordered surface of newly precipitated particles are often different. Of course, in some cases, pulverization does not change the surface conditions of particles.

After pulverization, the particle surfaces are divided into three types:

(1) It has the same surface with initial precipitated particles, i.e., the surface of the original particles is not damaged during pulverization.
(2) It has a surface with cracks that can be penetrated by polymer molecules.
(3) It has a surface with cracks that cannot be penetrated by polymer molecules, but can be penetrated by small molecules.

The surfaces of most so-called "dry" particles and objects exposed to air are not clean and dry, and instead they adsorb water and other substances (such as volatile organic compounds). Organic compounds adsorbed on the surface of additives are usually ignored because the structures of these organic compounds are generally complex and their quantity is small and difficult to analyze. Furthermore, most are removed in the process of mixing. The adsorbed water is not a problem for most flame retardants because small amounts of water combined loosely with flame retardants are usually removed during the process of mixing. However, some flame retardants must be dried before use. The compounders usually allow additives to contain a small amount of loose water but not a relatively large one. The water content should remain constant. It is one of the main reasons that MH should be covered by a hydrophobic surface before selling. Otherwise, the carbonate formed by the adsorbed water and CO_2 on MH surface will absorb more water, deteriorating the surface properties.

Impurities in particles usually exit from the surface of particles, and sometimes, the concentration of such impurities on the surface is even higher than the internal concentration. For some additives, the impurities are fixed in particles, whereas for others impurities migrate inside. For example, for MH, both the inside and the surface may contain chlorides. The chlorides on the surface can be removed by washing with water, while the ones inside migrate to the surface. However, for ATH, there are fixed and soluble sodium-containing impurities both on the inside and on the surface. In general, the former is approximately 0.1% whereas the latter is less than 0.01%. If we clear the soluble alkali of ATH, the fixed alkali does not migrate to the surface. In fact, the fixed alkali in ATH is a part of the crystal structure; even if it is not, the alkali does not migrate to the surface and may concentrate on interface of the crystal; however, because the size of ATH is generally small, most of the crystal interfaces exist inside rather than on the surface.

In addition, the elemental composition of the surface can be different from that of the inside, and does not conform to the theoretically calculated values. Furthermore, heat treatment may change the elemental composition of the surface.

Table 5.3 [26] is based on the surface elemental composition (atomic ratio) of ATH, ZS (zinc stannate), ZB ($2ZnO \cdot 3B_2O_3 \cdot 3.5H_2O$) measured using XPS; the values in parentheses are the theoretical values.

Errors exist between the surface elemental composition of the three flame retardants and the theoretical values listed in Table 5.3. Consider ZS as an example,

Table 5.3: Surface Elemental Composition of ATH, ZS and ZB (Excluding C and H) [26].

Additive	Al	O	Sn	Zn	B
ATH	33.0(25.0)	67.0(75.0)			
ZS		55.9(60.0)	32.4(20.0)	11.7(20.0)	
ZB467		60.1(64.4)		6.9(8.9)	32.9(26.7)

at least on a surface 10 mm long, Zn content is different from the theoretical value. There is no zinc on ZS surface as measured by static secondary ion mass spectrometry (SSIMS). Oxygen content on ATH surface is lower than the theoretical value whereas aluminum content is higher. This is probably because in the process of pulverization a portion of hydroxyl on ATH surface is converted into oxygen and water. Aluminum content in ATH is expected to be 40% whereas the oxygen content should be 60% if hydroxyls are fully converted. Oxygen and aluminum content on the surface of newly precipitated ATH particles measured by XPS correspond to the theoretical values shown in Table 5.3. On the surface, zinc content of ZS and ZB shown in Table 5.3 does not match the theoretical values. This may be caused by variables in the process of production and processing (such as pH value of production liquid, washing method, drying temperature, and so on.).

5.8.2 Influence of surface conditions on flame retardancy

Because of contact with fire, the surface of flame retardant changes first. Regarding the additives acting in the condensed or gas phase, the surface impact and influence vary. For high-loading and low-loading formulations, because of the different total superficial area of flame retardants, the surface impacts of the former are obviously higher than those of the latter.

Influence of specific surface area on flame retardancy

The granularity or the specific surface area of flame retardant plays an important role in the efficiency of flame retardancy (for void-free solid, the granularity is inversely proportional to the specific surface area), which is directly or indirectly related to the specific surface area.

For example, the fine ATH with larger specific surface area can be directly decomposed into Al_2O_3 under 250 °C in a one-step reaction (5.6) [26]:

$$2Al(OH)_3 \rightarrow Al_2O_3 + 3H_2O \tag{5.6}$$

Reaction (5.6) is endothermic and benefits flame retardancy. However, for the coarse grain (grain size >50 μm) ATH with smaller specific surface area, the

increasing hydrostatic pressure in particles contributes to the following two step reaction (5.7) and (5.8) [26]:

$$Al(OH)_3 \rightarrow AlOOH + H_2O \tag{5.7}$$

The second step under 500 °C converts AlOOH into Al_2O_3 (5.8) [26]:

$$2AlOOH \rightarrow Al_2O_3 + H_2O \tag{5.8}$$

The flame retardant efficiency decreases because of the two-step reaction when coarse grain ATH is heated. In some flame retardant tests, the highest temperature that can be withstood by materials is below 500 °C, therefore, the second-step reaction (5.8) is suspended. This phenomenon is first caused by the particle size, and is also indirectly related to the specific surface area. When coarse grain ATH is decomposed, the hydrostatic pressure is the function of the distance through which water molecules released by ATH move on the surface.

In addition, the particle surface may adsorb some components of flame-retardant systems, which can interfere with the activity of these components. Antioxidant is one of these substances. Antioxidant content in some systems can greatly affect the results of some flame-retardant tests. If a majority of antioxidants are adsorbed by additives surface, the effects of antioxidants will be reduced.

Furthermore, when using the same amount of additives, increasing specific surface area can enhance viscosity of the system, deteriorating dispersion of flame retardants. The area with high flame retardant concentration may show better test results, and with lower flame retardant concentration test results will be poor.

The effect of specific surface area to flame retardant efficiency may be related to the reactions of radical reactive groups on the surface. ATH does not exert particle effects (surface effects) to the flame retardancy and it usually affect ignition time instead of flame propagation and other parameters. This is in consistent with the following experimental results: the surface can effectively terminate and hinder some free radical reactions before ignition, delaying the ignition time.

Table 5.4 [26] shows the performance of flame-retarded PP with MH covered with stearate (flame retardant loading of 60%); one MH particle is optimized while the other is not. Obviously, the overall performance of the former (particularly flame retardancy) is far superior to that of the latter.

Influence of surface element composition on flame retardancy

ZS is a product heated by zinc stannate hydrate (ZHS). The flame retardant efficiency and the smoke suppression of intermediates obtained by long-term heating of ZHS at low temperature are much better than those of ZS or ZHS. A mixture of ZS and ZHS does not give satisfactory results, which is possibly due to the different surface elemental composition of the product (the surface is rich in zinc) obtained by slow heating.

Table 5.4: Properties of PP Containing 60% MH (stearate covered).

Performance	Non-optimized grain size	Optimized grain size
LOI/%	25	28
Flame retardant efficiency, UL94 (3.2 mm)	No pass	V-0
MFI (2.16 kg, 230℃) /g·(10 min^{-1})	5	15
Tensile strength / MPa	12.0	12.5
Flexural strength / MPa	29.0	26.0
Flexural modulus / GPa	3.30	2.40
Maximum impact energy / J	0.8	3.6
Maximum impact deformation / mm	5.7	11.4
Maximum impact force / N	200	520

Table 5.5 [26] is the surface elemental composition of ZHS (values in parentheses are theoretical), both baked (heating at lower temperature) and unbaked ZHS. Table 5.6 [26] shows the flame retardant parameters of unbaked ZHS, baked ZHS and ZS acting as the flame retardant on soft PVC.

Table 5.5: Surface Elemental composition (atomic ratio) of baked and unbaked ZHS [26].

Additive	O	Sn	Zn
Unbaked ZHS	66.6(75.0)	25.9(12.5)	7.5(12.5)
Baked ZHS	59.0	28.5	12.6
ZS	55.9(60.0)	32.4(20.0)	11.7(20.0)

Table 5.6: Flame Retardant Parameters of Flame-Retarded Flexible PVC Measured by Cone Calorimeter (heat flow 40 kW·m^{-2}) [26].

Flame retardant	Unbaked ZHS	Baked ZHS	ZS
Ignition time / s	84	86	75
PHRR / kW·m^2	87	78	122
Total smoke production	800	635	1089
Average specific extinction area / m^2·kg^{-1}	229	157	297

The formulation of flexible PVC in Table 5.6 is: PVC (DS7060) 195, DOP 81, ESO 10, ATH 75, brucite 72, clay 75, stabilizer (Irgastabl 17M) 10, and ZHS (or ZS or baked ZHS) 29.

Table 5.6 highlights that compared with unbaked ZHS and ZS, the flexible PVC containing baked ZHS shows the longest ignition time and that PHRR is decreased by 10% and 36%, respectively. The total smoke production reduces by 20% and 42%, and the average specific extinction area reduces by 31% and 47%, respectively.

5.9 Solubility and mobility of additives in polymers

As for this subject, there is a detailed and systematic statement in literature [27].

After adding additives into substrates (typically polymers) additives, chemical and physical properties of polymers during processing and application should not change, and the loss from the substrates should be as little as possible. People always pay attention to chemical losses, but do not have a sufficient realization of physical losses (such as blooming of flame-retarded plastics). In general, from the perspective of plastics, the physical losses of additives are related to the solubility and mobility of additives in polymers. The inherent solubility of additives in polymers decreases (the concentration is lower when reaching equilibrium) and the migration speed increases. Moreover, additives cannot be effectively retained in polymers causing large physical damage.

5.9.1 Solubility

The solubility of additives in polymers is one of the most important characteristics that control the physical state of plastics. Most polymer additives are in a phase-separated state, seldom existing in homogeneous solution state. One of the most effective factors for physical losses of additives is solubility in polymers at processing and application temperatures. Because additives are solids or liquids, they are usually small molecules; however, many recent additives are oligomers or even polymers. In fact, solubilization additives in polymers are mostly small organic molecules in polymer macromolecules. The molar volume of additives is generally much larger than that of crystalline polymer units, and additives cannot enter into crystal polymers. Moreover, they can only dissolve in amorphous polymers [28], and their solubility depends on the interactions and the physical state of both additives and polymers.

Several methods are available to estimate the solubility of additives in polymers such as gas chromatography [29], turbidity method [30], balanced method and extrapolation method [31]. The balance method is adopted in most cases. This method includes stacking up several layers of polymer films separated by additives, and then determining the amount of dissolved additives in an appropriate manner after equilibrium is achieved.

As mentioned above, additives can only dissolve in the amorphous phase of polymers, hence, solubility is inversely proportional to the degree of crystallinity of polymers. At least this is the case when solubility is low. In addition, the solubility of additives in certain polymers is obviously related to chemical structure, heat treatment parameters and density and states of polymers [32].

The solubility of low molecular weight additives in polymers is usually higher than that of high molecular weight additives; decreasing the melting point of additives can increase the solubility. In addition, the solubility of additives increases rapidly with temperature. In general, it is much easier for additives to mix with polymers when temperatures increase, even if they are insoluble at room temperature.

Higher solubility can be achieved when amorphous additives dissolve in amorphous polymers. They may also be miscible even at room temperature, and nearly all additives can enter into rubber phase at the processing temperature.

Some additives can be miscible with the commonly used thermoplastic polymers at the processing temperature. If additives can dissolve in molten polymers, they can be uniformly dispersed in substrates after efficient processing; however their solubility will decrease after they cool down. When the temperature reaches the melting point of polymers, polymers can crystallize. This makes 30%–60% of the polymers no longer serve as the solvent, and exclusion from the crystalline region of the additives increase the concentration of additives in the amorphous phase. At melting point of additives, their solubility in polymers decreases faster than the temperature, resulting in relatively low solubility of additives at room temperature.

In fact, in general, additives cannot achieve equilibrium with polymers. The usually required amount of additives is introduced in plastics at a high processing temperature. During this processing, the system of additives/polymers is first heated to a higher temperature and then rapidly cooled to room temperature. In this process, the following situations may occur [27]:

1. Additives can not only dissolve in high temperature but can also be soluble in solid polymers at room temperature. If the concentration of additives does not exceed the equilibrium solubility in the amorphous phase at room temperature, they will be completely dissolved in the polymer solids. While processing plastics, the additives are in a homogeneous solution and uniformly dispersed in the solute in the amorphous phase at room temperature. At this point, no driving force helps in migrating the additives to the surface of the polymers unless concentration gradient is achieved through surface evaporation or leaching. This condition is the most ideal but cannot always be achieved.

2. Although additives are dissolved in molten polymers at high temperature, they become insoluble when temperature decreases. It is known that a solute can be dissolved in a hot solvent in the equilibrium of single solution, whereas it becomes saturated during the cooling process, leading to solute sedimentation when temperature decreases. The same phenomenon is observed in the solution of additives in molten polymers at high temperature.

That is, when temperature reduces, additives may settle, forming fine particles uniformly dispersed in the substrate.

The viscosity of semi-crystalline polymers typically becomes very high below the melting point of the polymers; additives may not be settled in this scenario but may be dispersed in polymers with a semi-stable state, while also being dispersed on the polymer surface.

3. If the additives have certain solubility in polymers and their concentration in polymers melt is higher than the saturation concentration at room temperature, then most additives disperse in the system in the form of solid particles because additives are dissolved in a balance system at low concentration during cooling. If the free energy of additive particles in polymers is the same as pure additives, the additive particles do not migrate to the polymer surface because of a lack of driving force, unless evaporation or solvent extraction through the surface of the additives generates a concentration gradient.

At times, the loading of additives is increased when plastics exhibit poor performance on application or testing; however, this results in a supersaturated state of additives in polymers at room temperature, even if additives are completely soluble during processing. Such semi-stable conditions result in diffusion of additives to the surface of polymers and deposition on the surface, which is much easier than deposition inside the polymers. This deposition is termed "frosting." Frosting not only damages the additives but also influences the appearance of products.

5.9.2 Diffusion migration

Literature [27] has summarized the diffusion of additives in polymers. The diffusion coefficient of additives in polymers is the key to control the physical loss rate as it relates to the degree of the precipitation and evaporation losses of additives from polymers.

Diffusion is the process of migration of materials along a concentration gradient. The migration flux dm/dt of each molecule in an isotropic medium can be expressed by Fick's first law, see formula (5.9) [27].

$$\frac{\mathrm{d}m}{\mathrm{d}t} = -D\frac{\mathrm{d}c}{\mathrm{d}t} \tag{5.9}$$

D represents the diffusion coefficient of diffusion materials.

Fick's second law shows energy transfer in x-direction, see formula (5.10) [27].

$$\frac{\mathrm{d}c}{\mathrm{d}t} = D\frac{\mathrm{d}^2c}{\mathrm{d}x^2} \tag{5.10}$$

Without considering the volatilization of additives, the known diffusion coefficient can estimate the physical losses of additives.

If the additive concentration in the polymer is low, the diffusion coefficient is independent of the additive concentration . However, at higher concentrations, the diffusion coefficient is related to the concentration of the additive and sometimes no longer follows Fick's law at times. Moreover, when additives migrate slowly, the situation becomes more complex.

Because diffusion is a dynamic process and is more complex than solubility, it is affected by several factors.

Impact of polymer morphology

Most measured diffusion coefficients include large error as the diffusion rate is a complex function of polymer morphology. Although the additives are dissolved in amorphous phase polymers and not crystallization phase polymers, crystallization distorts the migration channels in polymers, decreasing the molecular mobility of amorphous polymers. The crystalline region in polymers is equivalent to a barrier layer that through which diffusion cannot occur. Filler particles play the same role, adding filler particles to polymers can slow down diffusion.

In case of polymer films, additives always diffuse slower on the film plane than on the direction perpendicular to the film plane. This may be because anisotropy exists in a direction vertical to the film to some extent [32].

The orientation of polymers has a significant effect on the diffusion rate of additives, which may cause anisotropy. For example, when additives are diffusing in polymers, the diffusion rate is slower on the direction parallel to orientation than the direction vertical to orientation [32].

Influence of temperature

Diffusion is a thermal acceleration process. The diffusion coefficient can be expressed by the Arrhenius equation, see formula (5.11) [27]

$$D = D_0 \, \exp\left(- \frac{E_D}{RT} \right) \tag{5.11}$$

E_D is the diffusion activation energy, which increases with the increase in molecular weight.

However, the applicability of formula (5.11) is limited in diffusion. The Arrhenius diagram usually bends at a wide range of temperature.

Influence of polymer types

The diffusion of common additives is termed molecular mobility, which requires interaction between polymers and diffusion materials. Therefore, the diffusion of

additives in plastics depends on the relationship between the molecular volume of additives and the free volume of polymers, as well as the thermodynamic interaction between the two. In other words, the diffusion of additive molecules depends on whether the molecules can obtain sufficient energy to transit to polymer free volume and adjacent vacancy, as well as the minimum aperture needed for additives to transit to adjacent holes in the polymer.

At a given temperature, diffusion in polymers with lower glass transition temperature is faster. Considering the effects of crystallinity, additives diffuse much faster in rubber than in semi-crystalline polyolefin. This implies that additives are lost through leaching or blooming.

The effect of the polarity of the polymer on diffusion is usually hard to predict. However, the diffusion rate of some additives is much slower in polymers with high polarity than those with low polarity.

Influence of molecular mass

The diffusion of additives in polymers decreases with increasing molecular weight. The relationship between diffusion coefficient (D) and additive molecular weight (M) can be expressed as $D = KM^{-\alpha}$; the index α is usually between 1.5 and 2.5 [27]. Therefore, D reduces significantly with the increase in M. Hence, using oligomer additives has become a very effective approach to reduce migration.

5.9.3 Losses of additives

If the concentration of additives in polymers is lower than the saturation concentration and if the materials are exposed to air, additives suffer losses owing to evaporation from the surface. However, if additives in polymers are oversaturated or materials are exposed to solvents, additives suffer losses through surface separation or leaching.

Surface escape

A concentration gradient caused by surface escape results in the diffusion of additives along the direction of concentration gradient, namely, diffusion from the inside to the surface. During the application of materials, additives always volatilize [33, 34]. The abovementioned losses include diffusion and volatilization. The escape rate of additives from the surface is proportional to the vapor pressure on the surface, whereas the migration rate of additives is controlled by the diffusion coefficient (D).

The time of consuming a certain amount of additives in polymers depends on its solubility, diffusivity and diffusion coefficient, as well as the shape and size of samples. With fast volatilization and slow diffusion, losses are controlled by

diffusion; whereas with slow volatilization and fast diffusion, losses are controlled by volatilization.

Leach and effusion of solvent

The vapor pressure of most common additives is generally very low. Therefore, air is a poor solvent for additives, whereas almost all organic liquids are good solvents, i.e., water is better than air. Hence, when polymers with additives are exposed to liquids which act as their solvents, they enter into the solvent from the polymer surface and are lost. This rate is much higher than that in air [35].

The process of leaching additives into good solvents is controlled by diffusion. However, if solvents cannot dissolve additives well without enough stirring, the situation becomes more complex. Because the viscosity of liquids is much higher than that of air and the interface between liquids and polymers is much thicker than that between air and polymers, additives diffuse slowly in liquids. If the solubility of additives is poor in liquid, their diffusion loss will also be much smaller than that estimated from the diffusion coefficient, and the loss amount is governed by the diffusion rate. On the contrary, if the liquid is a good solvent of the additives that can penetrate into the polymers, which can lead to increase in diffusion coefficient, it will accelerate losses. Sometimes, the penetration rate of liquids into polymers can be the key element controlling the loss rate of additives.

If the surface of the polymers can form crystallization nucleus without any limitations, then the oversaturated additives will soon separate. Moreover, precipitation rate is controlled by diffusion. As long as polymer additives achieve saturation concentration, volatilization will turn into effusion, even though diffusion remains a rate-determining step.

Approaches of additive losses

Some insoluble-phase separation particle additives migrate slowly in materials with a low loss rate. For polymeric or oligomeric additives, either uniphase or homogeneous phase, as long as they have sufficient chemical stability, their migration loss rate will be quite slow. However, the loss of some additives is quite serious. For such additives, the best way to reduce volatilization losses, blooming or effusion to the minimum is through molecular design. Good additives should be soluble in polymers without precipitation or volatilization on the surface of the polymers.

The relationship between the loss mechanism or loss rate and additive's structure is an attractive topic, and published literature [36] has highlighted this case. Oligomeric structure can remarkably reduce additive volatilization, and the diffusion coefficient is slightly reduced while the loss mechanism remains unchanged. However, the solubility of oligomers in polymers descends, which does not help in reducing additive losses. However, making additives oligomeric is still an effective way to reduce the losses caused by volatilization or bloom. Introducing long alkyl chains into

small molecules can also reduce the volatilization of chemical compounds, which can get stronger with increasing solubility. However, alkyl groups have little influence on diffusion coefficient. This approach is also good to reduce the volatilization loss of additives, but cannot improve blooming and effusion to a great extent.

Another essential way to reduce or eliminate additive losses is through formation of covalent bonds between additives and polymers, thus incorporating additives in the structure of the polymers. Although the technology of copolymerizing additives and polymer monomers during polymerization is popular, it undergoes different synthesis methods, and hence its practical application is limited. Better technologies have now been developed to chemically bond additives into polymers during the processing of polymers, namely reactive extrusion.

Solubility and diffusion coefficient of polymer additives are the key elements that influence the physical losses of these additives (such as blooming). The solubility and migration of polymer additives are associated with their molecule structure, shape, as well as the interaction between them and a series of other factors. Application of oligomeric and polymeric additives or reactive additives is an effective approach to reduce or eliminate the physical losses of polymer additives.

References

[1]   yuxiang Ou, jianjun Li. Fire Retardant[M].Beijing: Chemical Industry Press, 2006:31–39.
[2]   Hull T P, Stec A A. Polymer and Fire [A]//Hull T R, Kandole B K. Fire Retardancy of Polymers, New Strategies and Mechanisms [M]. Cambridge: The Royal Society of Chemistry, 2009.10.
[3]   Huyuan, Songlei, Longzhen. An Introduction to Chemical Fire[M].Beijing: Chemical Industry Press, 2007: 74–75.
[4]   Hornsby P. Fire-Retardant Fillers [A]//Wilkie C A, Morgan A B. Fire Retardancy of Polymeric Materials(2nd edition)[M]. Beca Raton: CRC Press, 2009:163–185.
[5]   Levin M, Weil E D. Mechanism and Modes of Action in Flame Retardancy of Polymers [A]// Price D. Fire Resestant Materials [M]. Cambridge: Woddhead Publishing Ltd., 2001:31–57.
[6]   yuxiang Ou, Fire Retardant[M].Beijing: Weapon Industry Press, 1997:198.
[7]   Bonin Y, LaBlane J. Flame-Retardant. Noncorrosive Polyamide Composition [P]. US Patent, US5466741,1995 -11-14.
[8]   Awad W H. Recent Developments in Silicon-Based Flame Retardants [A]. Wilkie C A, Morgan A B. Fire Retardancy of Polymeric Materials (2nd editon) [M]. Beca Raton (FL, USA): CRC Press, 2009. 187–206.
[9]   Ou Yuxiang, Li Jianjun. Flame Retardant [M]. Beijing: Chemical Industry Press, 2006. 288–294.
[10]   OU Yuxiang, ZHAO Yi, HAN Tingjie. PC Thermal Decomposition Mechanism and PC/ABS Flame Retardant Mechanism[J]. Synthetic Resin and Plastic, 2008. 25(4):74–79.
[11]   Green J. Mechanisms for Flame Retardancy and Smoke Suppression. A review[J]. Green Journal of Fire Sciences, 1996, 14:426–442.
[12]   Hayashida K, Ohtani H, Tsuge S, et al. Flame Retarding Mechanism of Polycarbonate Containing Trifunctional Phenyl-Silicone Additive Studied by Analytical Pyrolysis Techniques [J]. Polymer Bulletin, 2002, 48(6):483–490. (Delete)
[13]   Iji M, Serizawa S. Silicon Derivatives as New Flame Retardants for Aromatic Thermoplastics Used in Electronic Devices [J]. Polymers for Advanced Technologies, 1998, 9(10):593–560.

[14] Iji M, Serizawa S. New Silicon Flame Retardant for Polycarbonate and Its Derivatives [A]. Malaika A S, Golovoy A, Wilkie C. Specialty Polymer Additives Principles and Applications [M]. Oxford (UK): Blackwell Science, 2001. 293–302.

[15] Levchik S V, Weil E D. Overview of Recent Developments in the Flame Retardancy of Polycarbonates [J]. Polymer International, 2005, 54, 981–998.

[16] Wang Jianqi. Research and development of catalytic expansion flame retardant polymer. Research on PC/PPFBS system [A]. Proceedings of the second seminar on flame retardant technology and flame retardant materials [C]. Beijing : National Flame Retardant Laboratory, Beijing Institute of Technology, 2004. 86–96.

[17] Nodera A, Kitayama M. Flame-Retardant Polycarbonate Resin Composition and Molded Article Thereof [P]. Eur Patent Application: EP1369457,2003-12-10.

[18] Boyd S D, Lamanna W M, Klun T P. Flame Retardant Carbonate Polymers and Use Thereof [P]. Eur Patent Application: EP1348005,2003-10-01.

[19] Ou Yuxiang, Zhao Yi, Han Tingjie. Polycarbonate Flame Retarded by Sulfur-containing Compounds and their Flame Retardant Mechanism[J]. Plastic Science and Technology, 2007, 35(10):42–45.

[20] Ballistreri A, Montado G, Scamporrina E, et al. Intumescent Flame Retardants for Polymers.IV. The Polycarbonate-Aromatic Sulfonate System [J]. Journal of Polmer Science, Part A. Polymer Chemistry, 1988,26:2113.

[21] OU Yuxiang, LI Xiangmei. Ecologically Friendly Flame Retardant Polyamide[J].Polymer Materials Science & Engineering, 2010, 26(11):151–155.

[22] Levichik S V, Levichik C F, Balabanovich A I, et al. Mechanistic Study of Combustion Performance and Thermal Decomposition Behavior of Nylon 6 with Added Halgen-Free Fire Retardants [J]. Polymer Degradation and Stability, 1996,5(2-3):217–222.

[23] OU Yuxiang. The Latest Development of None-Halogen Flame-Retardant PA[J]. Polymer Materials Science and Engineering. 2005, 21(3): 1–5.

[24] Ou Yuxiang, Han Tingjie, Zhao Yi. Effect of surface properties and condition of inorganic flame retardants on flame retardant efficiency [J]. Plastics Additives, 2007, (2): 52-54.

[25] H. Zweifel, editor-in-chief. Ou Yuxiang, Li Jianjun. Plastics Additives Handbook[M]. Beijing: Chemical Industry Press, 2005.685–707.

[26] Billingham N C, Calvert P D. [A]. Dawkins J V. Developments in Polymer Characterization Vol.3 [M]. London (UK): Elsevier Applied Science Publishers Ltd., 1982.229–259.

[27] Tseng H S, Lloyd D R, Ward T C. The Solubility of Nonpolar and Slightly Polar Organic Compounds in Low-Density Polyethylene by Inverse Gas Chromatography with Open Tubular Column [J]. Journal of Applied Polymer Science, 1985,30(5):1815–1826.

[28] Frank H P, Frenzel R. Solubility of Additives in Polypropylene. [J]. European Polymer Journal, 1980,16(7):647–649.

[29] Roe R J, Bair H E, Gieniewski C. Solubility and Diffusion Coefficient of Antioxidants in Polyethylene [J]. Journal of Applied Polymer Science, 1974,18(3):843–856.

[30] Moisan J Y. Diffusion des Additifs du Polyethylene III [J]. European Polymer Journal, 1980,16(10):997–1002.

[31] Moisan J Y, Lever R. Diffusion des Additifs du Polyethylene V [J]. European Polymer Journal, 1982,18(5):407–411.

[32] Malik J, Tuan D Q, Spirk E. Lifetime Prediction for HALS-Stabilized LDPE and PP [J]. Polymer Degradation and Stability, 1995,47(1):1–8.

[33] Gedde U W, Viebke J, Leijstrom H, et al. Long-Term Properties of Hot-Water Polyolefin Pipes.A Review [J]. Polymer Engineering & Science, 1994,34(24):1773–1787.

[34] Scott G. Atmospheric Oxidation and Antioxidants(Vol. II)[M]. London (UK): Elsevier, 1993.219–244.

6 Flame retardation mechanism of polymer, inorganic nanocomposite materials

6.1 Introduction

Numerous published studies have reported that polymer/inorganic nanocomposite materials (PIN) may become future flame-retardant materials [1, 2]. Although the exact configuration of PIN is still unclear (including the chemical configuration, nanoparticles, and so on), along with the degree of centralization of nanomaterials in polymers, it is certain that nanofillers perform better than most current fire retardants, specifically in terms of improving the physical performance of the polymer substrate. Of course, before producing satisfactory flame-retardant PIN, more research is needed, especially regarding the mechanism of flame retardants for this type of materials.

The flame retardation mechanism of polymers and inorganic nanocomposites has been researched considerably in recent years, and a summary of the studies can be found in the literature [1–6].

PIN have great potential of flame retardance, however, some of their physical attributes, such as the extremely high viscosity of modulus, makes mass production by conventional plastic extruder difficult. Adding nanofillers into polymers results in a series of physical effects, including the formation of a barrier adhesive layer, reduction of compatibility, migration of additives to the surface and suppression of bubbles in the molten polymer to reduce the flow rate. In addition, chemical properties changes can also be noted, including catalytic polymer decomposition, promoting graphitization of polymer, changing the approach and behavior of decomposition of polymers.

For improving the flame retardancy of PIN, such as extending the time to ignition (TTI) and reducing the peak heat release rate (PHRR), good dispersion of nanofillers in the polymer is a prerequisite (with exceptions), and it is critical that the particles in the polymer are decentralized at the ignition temperature rather than room temperature. Because the compatibilizer may be decomposed at high temperature and deteriorate the dispersion of nanomaterials in polymers. Moreover, The dispersion of the nanoparticles may also change in the partially decomposed polymer at the ignition temperature. Therefore, even if nanofillers are well dispersed at room temperature, it does not necessarily improve flame retardancy.

To produce well dispersed PIN, we need to use bulking agents (such as a surface modified agent) to polarize the surface of the nanofiller and insert it into the polymer chain. Comparing the ion-type polymer (such as PA) and hydrophobic-type crystalline polymer (such as PP), nanofillers are more likely to be dispersed in the former than the latter. Sometimes, we must stem graft the polymer chain (such as grafting the malay coli in the PP chain) to ensure good dispersion of the nanofiller.

As discussed before, the flame retardation mechanism of PIN depends largely on the dispersibility of the nanofiller in the melting and foaming polymer. Under several circumstances, the surface modified agent is easy to decompose, leaving behind the nanofiller. Simultaneously, incompatibility of the system which results in the nanofiller migrating to the surface of the polymer is a problem which needs attention. If the nanofiller is not well dispersed in the polymer, it does not have flame retardant properties.

The inorganic nanofillers that can be used in PIN include [3, 5]: (1) clayb [layered silicate (LS), such as montmorillonoid (MMT)]; (2) carbonic acid nanotubes (CNT) including single-layer and multilayer nanotubes (SWNT, MWNT); (3) layered double hydroxyl compounds (LDH); (4) flake (graphite) oxide (LG, LOG); (5) metal (metal oxide); (6) polyhedral oligomeric silsesquioxane (POSS).

Nanofillers play the following roles in flame retardants [4]: (1) greatly decrease the PHRR (50%~70%) and the mass loss rate (MLR) (40%~60%); (2) strengthen the mass transfer along the heat transfer barrier layer of the organic char; (3) provide the catalyst surface and facilitate char agglutination; (4) improve the polymer membrane structure; (5) improve the polymer ignition temperature near the end of the melting performance; (6) enable the flame retardant to come in close contact with the polymer substrate.

It should be mentioned here that different inorganic nanofillers may have different flame retardancy in different polymers. For example, in the case of PE, PS or EVA polymers that contain MMT, when MMT disperses well and PIN degrades, the relative quantities and types of the released products of cationic modifying MMT and anionic modifying MMT are different. Whereas under the same circumstances, when we change the filler to CNT, irrespective of the dispersion, the degradation products of PIN do not change. In addition, when nanofillers disperse negatively, PIN degradation products remain the same in all cases. It is significant to note that, when LDH is the filler, whether well decentralized or not, the HRR of PIN decreases significantly [7]. This shows that, on varying MMT, CNT and LDH as nanofillers of PIN, the flame retardation mechanism also changes.

6.2 The flame retardation mechanism of the nanocomposite materials of polymer/montmorillonite (layered silicate)

It has been 25 years since 1986 when Toyota produced the first polymer MMT nanocomposite material (PMN), the PA6/MMT nanocomposite material [8]. However, it was not until 1997 that Americans including Gilman researched PMN flame retardant systems, and published a detailed study on PA6/MMT flame retardants [9]. The flame retardation mechanism of PMN is still not fully understood. In recent years, both in books and periodicals, industry experts have made a number of points regarding the flame retardation mechanism of PMN in line with the

experimental results, especially the experimental results from cone calorimeter measurements. The following text will describe and discuss some latest research progress made in the mechanism of flame retardancy of PIN.

6.2.1 The charring and char layer structure of PMN

When PIN is combusting or being heated, the internal MMT particles undergo thermal cracking, and a multilayered char-silicate layer forms on the polymer surface; this layer can be used as an excellent insulation and a barrier to enhance the materials' flame retardant capability, as well as reduce the overflow of volatile gases that occurs during thermal decomposition. In addition, the thermal conductivity of heat-resistant silicate layer is low, which can protect the material from self-regulated heat transfer.

Experiments prove that, when 2% and 6% of PA6/MMT burns, a black flocculent residue is formed which migrates to the surface of the material and forms a protective layer. The residue consists of 80% of MMT and 20% of thermally stable graphite. During the combustion and gasification of PMN, the polymer on the surface of MMT fragmentizes and the exposed MMT is dashed to the surface of the material by the rising bubbles, which only forms a separation layer which is foamy in appearance and not a dense char layer; this results in a foamy layer that cannot function like flame retardants.

High-performance char-silicate layer structure can be studied by scanning electron microscope (SEM), transmission electron microscope (TEM) and X-ray diffraction (XRD). With the combustion of the silicate layer, PE/MMT is formed in the nanocomposite, which has the structure of MMT at the micro level but not at the macro level. This displays a spongy structure, with the latter reassembling a foamy structure when the expansion-type flame retardant polymer material is burning. For some non-char-forming polymers, such as PE, PP and EVA, char-containing silicate layers generated during the combustion of PMN contains 95% of char silicate layers and 5% of char (the thermogravimetric analysis, TGA, measured in the air); however, the small amount of carbon present is quite important to the flame retardation mechanism because it can condense the silicate to form a graphite/clay layer [11, 12].

The ideal structure of the surface protection layer formed during the combustion of PMN (containing MMT particles and char) should be netted with sufficient physical strength, which cannot be damaged or disturbed by increasing bubbles. During the entire combustion time, the protective layer should remain intact. The shocks of the bubbles generated during the combustion of PMN makes MMT particles move away from the areas shocked by bubbles, forming an "island" with a foamy appearance; there is no longer a complete solid protective char layer on the PMN surface, which considerably reduces flame retardancy. Factors affecting the

PMN surface include the initial MMT content, the characteristics of the formed char layer, the melt viscosity of PMN, the diameter to length ratio of MMT, etc. [10].

6.2.2 The char mechanism based on chemical reactions

With polymer cracking, the formation of the char layer is a complex process which includes several steps, such as the formation of double bonds, circularization and aromatization, fusing of the aromatic ring, formation of turbulence char and the formation of graphite [13]. Oxidation of organic molecules has been proposed as the key reaction mechanism [14], with opinions that there are two competing reactions. First, at low temperatures, carbon dioxide is the mechanism of free radical chain reaction, mainly resulting in hydrogen peroxide and oxide. Second, at high temperatures, the hydrogen extraction reaction, namely the oxidation of the hydrogenated species is very likely to happen. At normal combustion conditions, the first reaction is the most dominant. The hot oxidation causes bond cracking, and the polymer follows by gasification. As for PMN, the second reaction is the most dominant, wherein the aromatization of polymer increases while oxidation rate decreases. This indicates that MMT plays a catalytic role in the char forming reaction [15]. Comparing the general mixtures of MMT and polymer, gasification of the polymer is much easier than char formation because in this mixture and layer-shaped MMT structure becomes damaged and powdery, and they do not have a charring catalytic effect [12, 16]. The layered MMT with a nanometer pattern disperses in the polymer substrate with good char-forming catalytic property in PP [17], EVA [18] and PS [19].

MMT has the characteristics of a Lewis acid, and hence, promotes char formation. The Lewis acid characteristics of MMT is due to the distribution of the metal ion in MMT edge (such as Al^{3+}), or siloxane surface multimedia (such as Fe^{2+} and Fe^{3+}) of the wafer, or MMT-layered structure inside the crystalline defects. Such Lewis acid center of MMT can accept electrons from donors with low ionization or from the ethylene monomer. Therefore, as a char forming catalyst, MMT can reduce polymer degradation rate to provide PMN anti-burning the protective barrier; this barrier generated by MMT contains aluminum-silicon materials. According to the thermal combustion of the cone calorimeter, the chemical reaction leading to char formation can be inferred and analyzed as follows.

First, external heat or flame transfers heat to the materials, decomposing the organic MMT and polymer. The MMT layer in some proton catalytic centers focuses on burning surface materials. For polymers in PMN, there is competition between oxidation bond breaking reaction (a volatile part of the carbon dioxide polymer debris) as well as catalytic sodium dehydrogenation and carbon dioxide sodium dehydrogenation reaction. The generated conjugated polyene, through aromatization, crosslinking and catalytic dehydrogenation, forms a layer on the surface of the char, with the latter finally inserting MMT layers as charred MMT combustion residue [20].

Based on the experience, the higher the degree of detachment of MNT in the PMN, the better is the dispersion, and the more conducive it is to form a network during combustion, the more vulnerable it is to form a continuous char layer, resulting in higher flame-retardant efficiency, see Figure 6.1 [4, 21].
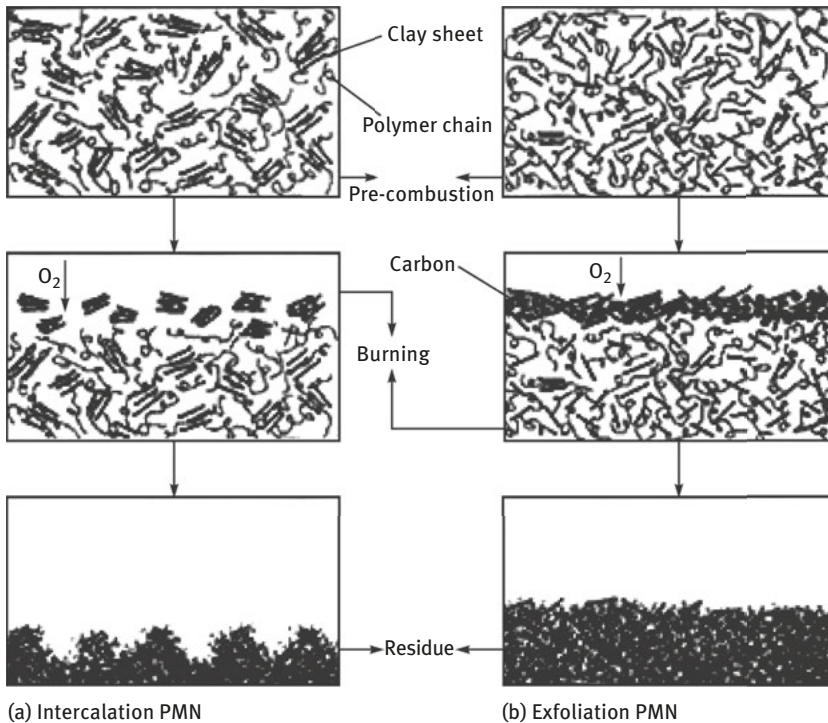

(a) Intercalation PMN   (b) Exfoliation PMN

Figure 6.1: The MNT network facilitates the formation of char layers [4, 21].

6.2.3 The migration enrichment mechanism of MMT in PMN

The mechanism of the migration and enrichment of MMT in PMN [22] is in fact complementary with the chemistry of the char forming mechanism of MMT. According to the theory of migration and enrichment, because of the low surface free energy of MMT, MMT can migrate to the surface of PMN. This hypothesis is based on the theory that the temperature of the organic process of MMT thermal decomposition is lower than that of the general polymer thermal cracking and burning, reducing the surface free energy of MMT, which promotes the decomposition of PMN structure. In this case, MMT migrates to the surface of PMN, which may be caused by the gradient driven at general temperatures or by the bubble

movement of the drive. XPS studies have shown [23] that, as temperature approaches that of polymer decomposition, the MMT of PS/MMT can concentrate on the surface of PMN. Moreover, it is believed that [24] PMN combusts similar to air bubbles, which is a disturbing factor, the decomposition of PMN generates numerous rising bubbles and the molten material flows drive MMT to the surface of the material.

Another flame-retardant mechanism of PMN [25] has also been proposed, with the view that the MMT magnet can capture free radicals. These studies have also reported that MMT content of some PMN (such as PS/MMT) is only 0.1%, the PHRR content can also reduce by approximately 40%. There's no big difference between the result of the PLSN at a high concentration of MMT.

6.2.4 The effects of quaternary ammonium salts used for modifying MMT

In general, alkyl quaternary ammonium salts used for modifying (organic) MMT can decompose at a temperature below 155 °C, namely according to the Hofmann elimination reaction or SN2 nucleophilic substitution reaction, and form a protonation center on the surface of MMT, see eq. (6.1) [1, 26, 27]

$$\overline{\text{MMT}}\ \overset{+}{\text{N}}\underset{\underset{\displaystyle CH_2CH_2R}{\overset{\displaystyle \nearrow CH_2CH_2OH}{\underset{\displaystyle \searrow CH_2CH_2OH}{\overset{\displaystyle CH_3}{}}}}{}\ \longrightarrow\ \overline{\text{MMT}}\ \overset{+}{\text{H}} + H_3C\text{—}N\underset{\displaystyle CH_2CH_2OH}{\overset{\displaystyle \nearrow CH_2CH_2OH}{}}\ + CH_2\text{=}CHR \qquad (6.1)$$
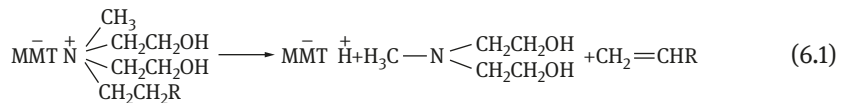
In the late period of the decomposition of all the organic modifier of MMT, the number of protonation centers is related to the cation exchange capacity. After the thermal decomposition of the organic modifier, MMT can be considered as an activated acid clay, with a strong acidity ($-8.2 < H_0 < -5.6$).

In general, the incendiary time of PMN is less than that of the substrate, which indicates that such materials have poor flame retardant capacity during the early burning period. As is evident from the time to ignition measured in many PMN using a cone calorimeter, a universal defect exists in most PMN. This is caused by the thermal decomposition of the organic MMT, as mentioned above the thermal decomposition temperature of those widely used quaternary ammonium salt is relatively low. However, now there are some suppliers of thermally stable MMT modifiers. In the cone calorimeter experiment, what is set on fire is a mixture of air and the flammable gas generated during the thermal decomposition of the polymer material. In other words, the time to ignition of the polymer material depends on the stability of the thermal decomposition of materials. As shown in equation (6.1), PMN containing MMT modified using quaternary ammonium salts can produce combustible olefins at a lower temperature. The cone calorimeter experiment indicated that the PHRR of PMN containing organic MMT appears

in the early period, which is associated with the time to ignition [28]. In addition, olefins can be produced during the extrusion process of PMN when the temperature approaches the thermal decomposition temperature of organic MMT. During sudden drop in temperature with a large number of PMN, olefins may also be produced. In addition, olefins can react with oxygen to generate peroxide radicals, which can widen the polydispersity of polymers through typical free radical reactions. Therefore, the decomposition of organic MMT also affects the thermal degradation of polymers. When molten blending is adopted to produce PMN, the influence of thermal decomposition of organic MMT is very important. Gel permeation chromatography (GPC) studies of the extruded sample of PS/MMT showed that, when there is no nitrogen protection during the extrusion process, low molecular weight PS will be produced [29].

In studies involving PP/MMT, it has been found that MMT (not only the organic MMT) can catalyze the degradation of the polymer matrix [30]. It is believed that adding MMT in PP may catalyze its early decomposition in an oxygen atmosphere. Because the complex crystalline structure and features of the MMT forms some active catalytic centers, such as Bronsted acid center similar to weak acid SiOH and strongly acidic in OH bridge exist in the edges of MMT, the unexchangeable transition metal ions exists in the crystal lattice, the crystal defect point in the MMT layers.

In short, regardless of the situation, for MMT alkyl ammonium salts play an important role in the thermal decomposition and flame retardant behavior of PMN. Significant efforts have been made to develop a new organic modifier with higher thermal stability than the general quaternary ammonium salts, including phosphonium salts (PR_4^+), imidazolinium salts, crown ethers, antimony iodide, tropylium salt, etc.

Flame retardation mechanism is a very complex issue, and most of the present flame retardation mechanisms of PMN are based on the results obtained by material cone thermal scanner experiments, radiation experiments, gasification (hot cracking in N_2 and combusting in the air) and thermal cracking lab analyses. They are mainly based on the mechanism of char formation through chemical reaction and MMT surface enrichment mechanism, however, all are still being investigated. A free radical trapping mechanism has also been proposed, but its experimental evidence remains to be supplemented and improved. However, we know for certain that organic quaternary ammonium salts that are used to modify the surface of MMT have a certain influence on the early pyrolysis and time to ignition of PMN, because they can undergo Hofmann elimination reaction at lower temperatures. Furthermore, MMT (not only the organic MMT) plays a catalytic role in the degradation of the polymer matrix.

The flame retardancy of the polymer/inorganic nanocomposite is surely more significantly improved than a single polymer (this is mainly manifested by the dramatic decline in HRR and MLR), but for improving the time to ignition, oxygen index and

results of UL94 vertical combustion experiment are very limited, and at times even worse. The key to such nanocomposite flame retardants is to form a homogeneous, continuous char layer. The main role of nanoparticles is to facilitate charring (by promoting crosslinking and catalysis), but different polymer and inorganic nanoparticles may have different impacts on the process of char formation. Moreover, inorganic nanoparticles may affect the pyrolysis of polymers, which has certain relevance in flame retardancy. For example, for polymers that are pyrolyzed by the removal of functional groups, the thermal stability of its functional group needs to be related to HRR. In addition, nanoparticles themselves and their induced crosslinking reaction increase the melt viscosity, which is coupled with the "labyrinth" effect. This extends the residence time in the solid phase and increases the lifetime of the combustible group or the occurrence of secondary char reactions, which possibly reduces HRR and MLR. In addition, nanoparticles can restrain the fusing.

It is worth emphasizing that to allow nanoparticles to act, besides adding appropriate volume, inorganic particles should have a large aspect ratio and a higher interface strength between polymers, as well as high viscosity gel characteristics in polymer melt to ensure that nanoparticles are well dispersed and stably decentralized both in composite materials at room temperature and in molten state composites at high temperatures.

6.3 Char formation of nanocomposite PP/MMT

For PP used in nanocomposite PP/MMT, the (partially) use of maleic anhydride grafted PP (PP-g-MA) is required, which is a solubilizer that improves the interface bonding strength of PP and MMT. PP-g-MA/MMT system forms a residue in the thermal cracking gas under a nitrogen atmosphere; Figure 6.2 shows a TEM image [31], displaying the disordered dispersion of MMT layer in the residue.

PP-g-MA can increase the charring ability of the nanocomposite. Figure 6.3 is a TEM image of the thermal cracking residue of three kinds of PP-based materials generated under a nitrogen atmosphere. The first material is a PP/MMT (5%) (a), the second is PP/PP-g-MA (15%)/MMT (2%) (b) and the third is a PP/PP-g-MA (15%)/MMT (5%) (c). According to the Figure, there is no black char layer in (a) residue but only in the residue of MMT. Both (b) and (c) residues exist as a black char layer. The layer of char residue in (c) displays higher quality, fewer cracks and better continuity. Thus, it can be concluded that the addition of PP-g-MA and the amount of MMT is extremely important for the charring of PP-based nanocomposites.

The PP-g-MA in the material can increase the degree of dispersion of MMT in the material system. However, more importantly, it can act directly on the charring of MMT. If PP-g-MA is not added in the PP/MMT system, its flame retardancy is only slightly improved, even with an excellent intercalation system. During thermal
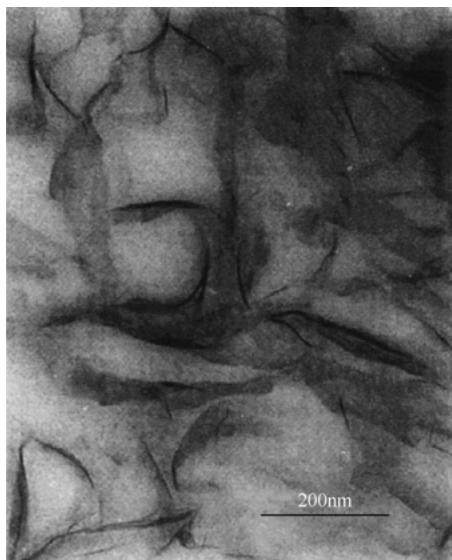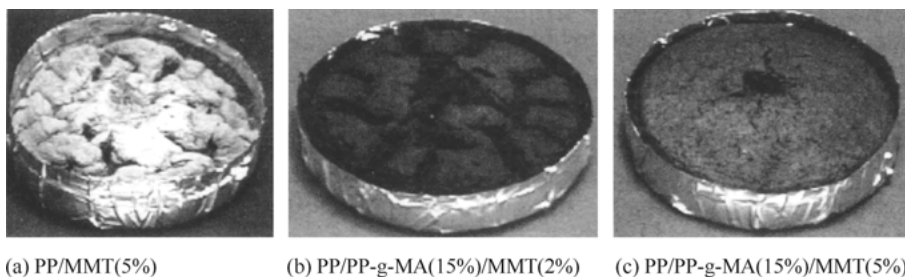
Figure 6.2: Thermal cracking residues of PP-g-MA/MMT nanocomposite (TEM image) [32].

(a) PP/MMT(5%)   (b) PP/PP-g-MA(15%)/MMT(2%)   (c) PP/PP-g-MA(15%)/MMT(5%)

Figure 6.3: Thermal cracking residues of (a), (b) and (c) (TEM image) [31].

cracking and burning, the external components of the char layer of the polymer containing MMT (nanodispersion) may migrate, reunite and gather. This is a complex dynamic process involving the decomposition of the polymer and surface modifiers, as well as migration and rupture of the bubble.

Generating a homogeneous continuous char layer on the surface of the materials is the key to improve the flame resistance of materials (lower HRR and MLR). As for PP/inorganic nanosystems, the types of clay also affect the quality of the char layer. Figure 6.4 [31, 32] compares the MLR of PP nanocomposite of three inorganic nanoparticles (general MMT, synthetic hectorite and synthetic fluorinated mica), all composed of PP (8.4%)/PP-g-MA (7.7%)/inorganic nanoparticles (7.7%), while the fluorine-containing synthetic mica is the lowest. However, materials containing

general MMT or synthetic hectorite are almost the same. Of course, the performance of all these three kinds is far worse than the PP/PP-g-MA systems. Correspondingly, the residue of PP/PP-g-MA/synthetic fluorinated mica, which contains the lowest MLR, has the most uniform and continuous char layer during thermal cracking in nitrogen or burning in air (Figure 6.5) [33].
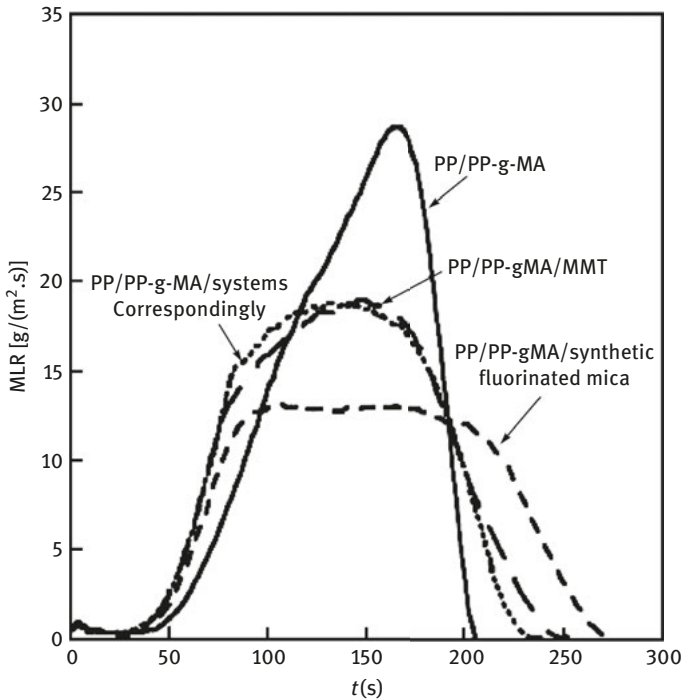

Figure 6.4: The MLR value of PP nanocomposites (composition mentioned in the text) of three different kinds of inorganic particles (thermal cracking in nitrogen) [31, 32].

(a) Imvite   (b) Synthetic hectorite   (c) Synthetic fluorinated mica
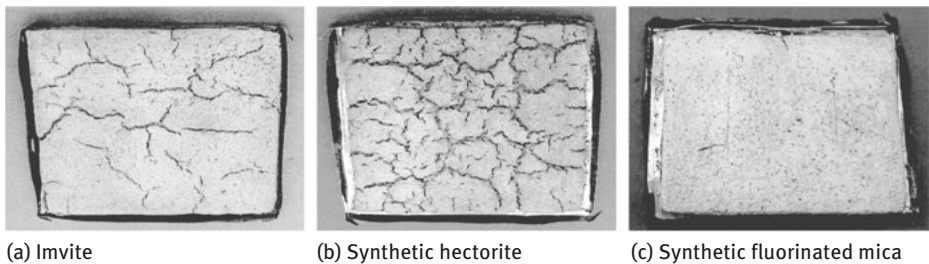
Figure 6.5: The residue of the three PP nanocomposites shown in Figure 6.4 (containing different inorganic particles; composition mentioned in the text) when cracked in a nitrogen atmosphere (TEM image) [33].

In addition, surface modification agents and modification methods of MMT are closely related to the char quality of the PP nanocomposite. Moreover, reasonable modification of MMT tends to favor the formation of a continuous char layer, and delay the time to ignition of the material.

6.4 The charring of PS/MMT nanocomposite materials

Although polystyrene (PS) is extremely difficult to char when burning itself, clay char layers can be formed when PS/MMT nanosystems undergo combustion or thermal cracking (Figure 6.6) [31, 33]. Figure 6.6 shows a TEM image of the residue produced during the thermal cracking of PS/MMT (5%) and PS for 240 s under N_2 (radiation gasification unit, see Chapter 8). The comparison between them can fully explain the fact that nanodispersed MMT in PS can significantly improve the charring of the PS.
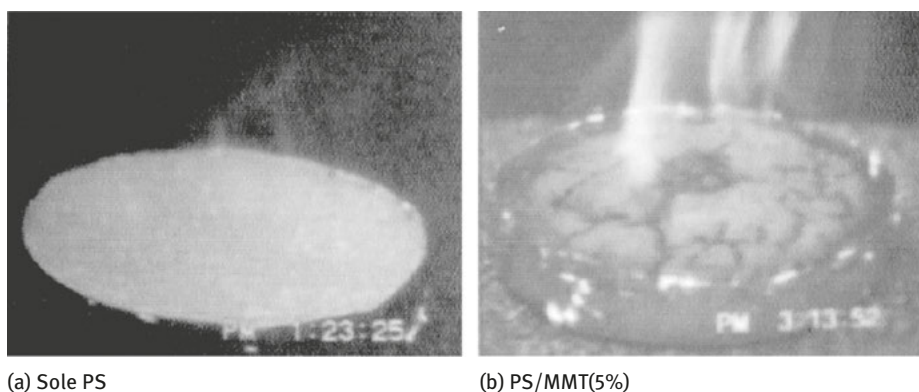

(a) Sole PS   (b) PS/MMT(5%)

Figure 6.6: TEM photocurve of the residue produced by the thermal cracking of PS (a) and PS/MMT (5%) (b) for 240 s in a nitrogen atmosphere [31, 33].

MMT can function as the charring agent of PS and other polymers that are difficult to char because of the "restrict" and "coking" effect of the matrix polymer generated by clay. In addition, the PHRR of the PS/MMT system (5%) decreased by 75%, whereas the total heat release amount (THR) did not decrease noticeably. During the process of thermal cracking (or combustion), the remaining char of PS and clay can form a heat insulation layer which can effectively reduce the heat conduction and the rate of thermal decomposition of the material.

Single PS, PS/Na$^+$ MMT (10% of the micron-sized dispersed in PS) and PS/MMT (10%) nanocomposites (intercalated and exfoliated) undergo thermal cracking in a

radiation gasification apparatus under N_2 for 82 s, 95 s, 200 s, 400 s and 1150 s. These five timeperiods correspond to the five different stages of thermal cracking. For PS/MMT nanosystems, at 82 s, the material begins to cracking; at 95 s, MLR reaches the maximum value (correspondingly HRR also reaches the maximum); at 200 s, the initial stationary phase for thermal cracking is achieved (thermal cracking platform, MLR is of a stable value); at 400 s, the final phase of thermal cracking (MLR began to decrease) ensures, and the thermal cracking ends at 1150 s while the corresponding MLR is close to zero and the residual clay platelets are left. For a single PS and PS/Na$^+$ MMT (micron dispersion), thermal cracking conditions are very different compared to the PS/MMT nanosystems. However, the conditions of the former two are relatively similar. After 200 s, the two MLRs continue to increase (nanosystems enter the thermal cracking phase at 200 s); at approximately 400 s, MLR rapidly declines to zero, and there is no thermal cracking quality loss for the remaining residue. Figure 6.7 [31, 33] is the MLR curve of the abovementioned three materials.
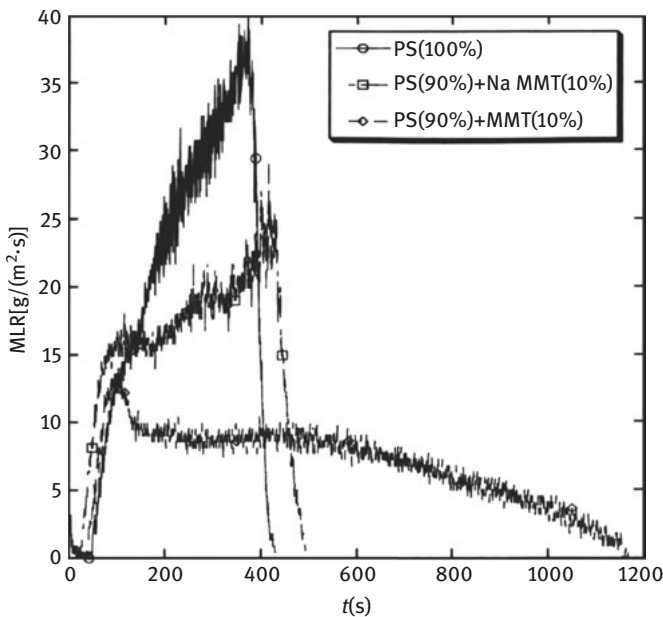

Figure 6.7: MLR curve of PS, PS/Na$^+$ MMT (micron dispersion).and PS/MMT (nanodispersion) [31, 33].

Fifteen thermal cracking residue samples in the upper, middle and lower part of the test specimens at the abovementioned five timeperiods can be obtained. For ease of comparison, we obtained three samples from raw materials (PS/MMT

nanocomposites) that have not undergone thermal cracking in the upper, middle and lower parts, with the total number of samples reaching 18. The interlayer distance of 18 samples (d (001)) was measured by XRD. In the case of upper-layer samples, the interlayer distances of the residue produced 82 s, 95 s, 200 s, 400 s and 1150 s is the same at 1.3 nm. For middle-layer samples, the interlayer distance of the residue produced at 200 s, 400 s and 1150 s is the same at 1.3 nm. For lower layer samples, the interlayer distances of the residue produced at 400 s and 1150 s is the same at 1.3 nm. The interlayer distances of the sample without thermal cracking and other residues is 3.27 nm. This shows that the extent of the thermal cracking of upper layer material is greater than that of the middle and lower layer. Furthermore, for the upper layer material, interlayer distances of the residue, after thermal cracking for 82 s, never increase with the increasing time of thermal cracking, maintaining at 1.3 nm (measured by XRD) [31].

As is evident from the XRD pattern and TEM images, as the time of thermal cracking increases, the clay char layer increasingly deepens into the specimen, and the char layer becomes increasingly thicker. However, after thermal cracking for a period of time, the char layer structure does not change with the thermal cracking time.

Figure 6.8 [31] is a TEM image of PS/MMT nanocomposites before and after the thermal cracking and shows the distribution of MMT layers.
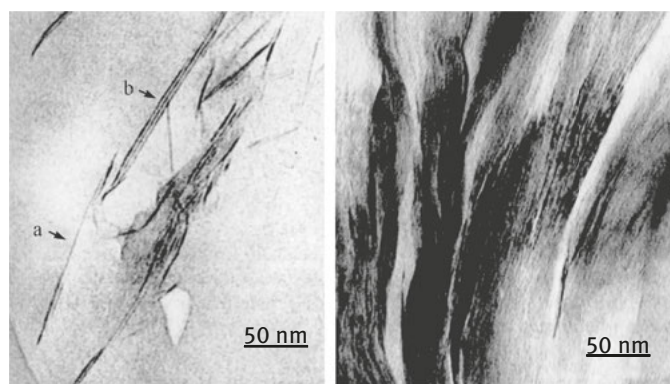
(a) Before thermal cracking   (b) After thermal cracking

Figure 6.8: TEM images of the nanocomposite of PS/MMT (10%) before and after thermal cracking [31].

The PS/MMT nanocomposites were placed in a radiation gasification unit and burned in air for different timeperiods, i.e., 95 s, 200 s, 400 s and 1050 s. The average amount of residues for the four samples was (28.7% ± 6.2%) of the original

sample (determined by TGA), such that the amount of materials burned was 71.3% of the original sample. The residue was a clay char layer, wherein the density of the clay was 2.1 g/cm^3 and the char density was only 1.0 g/cm^3; thus, the ratio of volume of clay to carbonaceous material is approximately 1:1. If the specimen is placed in nitrogen and undergoes thermal cracking, the average amount of residue for the same four samples was (17.5% ± 6.8%) of the original sample, which means that the residue weight for thermal cracking was 10% lower than that of combustion. This difference in the residue weight shows that the clay char layer contains two carbonaceous materials: one could gasify through heating in nitrogen, and the other could only be eliminated through thermo-oxidative degradation in air and under harsh conditions. The mass ratio of the two abovementioned materials was 1.5:1. The main difference between them arises from the different thermal stability.

6.5 The thermal stability and flame retardant of PU/MMT nanocomposites

6.5.1 Thermal stability

The thermogravimetric curve and differential thermogravimetric curve of polyurethane elastomers and its montmorillonite nanocomposites in nitrogen (heating rate is 10^- °C/min) are shown in Figure 6.9 and Figure 6.10, respectively [34]. The PU and PU/MMT in the figure are obtained through the two-step method, and the polyol is a bifunctional group with a calculated value M_n of 4000; the isocyanate here is MDI; MMT here refers to modified 2-hydroxyethyl quaternary ammonium salt; the content of MMT in PU/MMT is 2.5%.
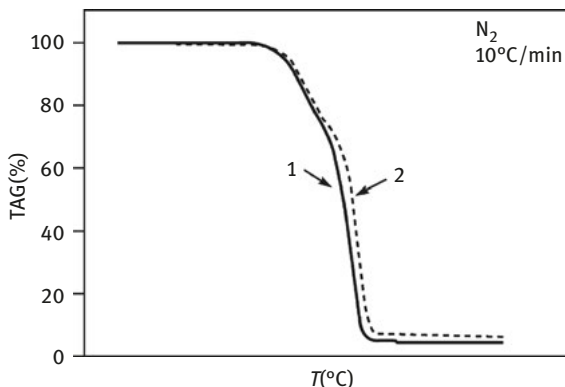

Figure 6.9: TAG carves of PU and PU/MMT [34] (1 refers to PU, 2 refers to PU/MMT).
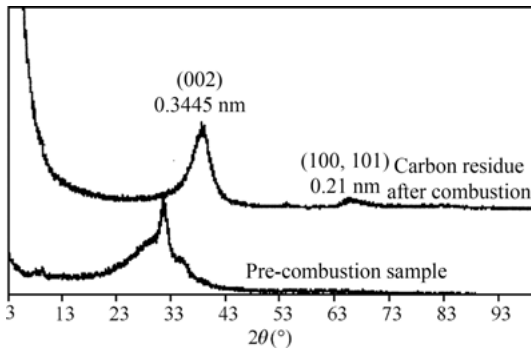
Figure 6.10: DTG carves of PU and PU/MMT [34] (1 refers to PU, 2 refers to PU/MMT).

Figures 6.9 and 6.10 show that the thermogravimetric curves of PU and PU/MMT proceed in two phases; the two peak temperatures of PU are 311 °C and 380 °C, respectively; and the corresponding temperature of PU/MMT are 322 °C and 390 °C, respectively, which is nearly 10 °C higher than that of PU.

On the basis of abovementioned results, the thermal stability of PU/MMT could be generally induced as follows. However, differences exist in reported data because different researchers use various PU/MMT with different compositions and preparation methods.

1. When the amount of MMT in PU/MMT is under 5%, the initial decomposition temperature of PU/MMT, T_i, namely the temperature of the intersection point of the extrapolated baseline and the tangent line of the maximum slope of TGA curve, is similar to or slightly higher than that of PU (see Table 6.1 [35], Figure 6.9 and Figure 6.10), because what decomposes now is the relatively free molecular chain that does not enter the interlamination of MMT. This implies that only the PU molecular chain decomposes, with minimal impact on MMT. When the amount of MMT increases, the amount of molecular chain involved in intercalation also increases, resulting in the PU molecular chains being blocked and bound by the MMT intercalation, as well as hampering the movement of

Table 6.1: The relation between T_i and the content of MMT in PU/MMT [35].

MMT content/%	T_i/ °C
0	347
2	353
5	353
8	366
10	367

molecular chains (including rotation and translation). When the content of MMT in PU/MMT is up to 8% to 10%, the T_i of PU/MMT increases greatly for the bound PU molecular chain that enters into the intercalation of MMT have increased.

2. Organic modifier of MMT is usually ammonium halides, which can perform Hofmann elimination reactions at temperatures below the decomposition temperature of PU, when the olefin and quaternary amine are generated, leaving acid protons on the surface of MMT. These acid sites can promote the early stages of organic matter decomposition within MMT, (this position may have catalytic to organic matter within the MMT at an early stage of the acidic decomposition), which is not conducive for improving the T_i of the PU/MMT.

   According to actual measurements, the impact modifier shows a limited impact on PU/MMT. This may be because of the low contact within the modifier of the PU/MMT, the decrease of T_i offset which even surpasses the increase of MMT to T_i. However, there are also examples of T_i of the PMN below the T_i of the resin substrate.

3. The weight loss of PU/MMT is close to PU when the MMT content is 2% to 5% of the PU/MMT, at or slightly below T_i. However, above T_i, the former is lower than the latter.

6.5.2 Fire resistance

Heat release rate(HRR) influences the time of ignition, the fire hazard environment, the speed of fire spread, etc. If HRR is small, the material will be difficult to burn, and vice versa. HRR tested in a dual cone calorimeter and the heat flow is 35 kW.m^{-2} indicates that the PHRR of PU/MMT (4.5%) decreases to 44% as shown in Figure 6.11. If the nanocomposite comprises MMT (4.5%) in terms of phosphoric acid ester PU, PHRR can drop to 70% as illustrated in Figure 6.12.
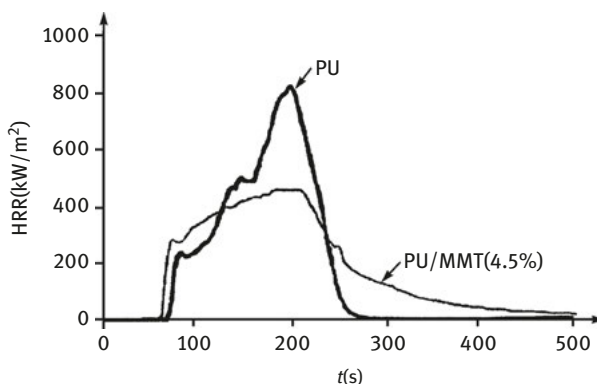

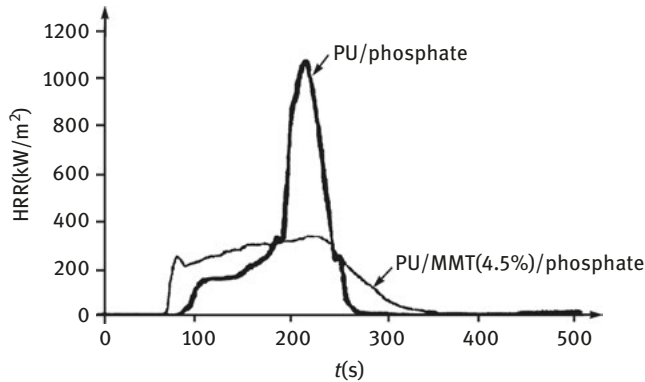**Figure 6.11:** The HRR curve of PU (1) and PU/MMT (4.5%) [38].

Figure 6.12: The HRR curve of PU/ phosphate (1) and PU/MMT phosphate (4.5%) (2).

The fire performance index

Fire performance index (FPI) is the ratio of TTI and PHRR, i.e., FPI = TTI/PHRR, and is considered to be more capable of showing the flame retardant property index compared to PHRR as it consider TTI such that the FPI can be associated with the flashover time. The higher the FPI, the lower the rate of fire hazard for materials. When PU and MMT form nanocomposite materials, FPI increases significantly. The FPI of PU is 0.073, that of PU/MMT (4.5%) is 0.130; the FPI of phosphate flame-retardant PU is 0.071, that of phosphate flame-retardant PU/MMT (4.5%) is 0.199. Thus, MMT (4.5%) can increase FPI value of PU by approximately 80%, whereas phosphate has no impact on the FPI of PU; however, if you add MMT (4.5%) in the PU of phosphate, the FPI value increases to 2.8 times of its original value.

Mass loss rate

Mass loss rate (MLR) affects the fire environment temperature of materials and the fire spread rate. The smaller the MLR, the more difficult it is to combust the material, and vice versa. Figure 6.13 shows the MLR curve of PU and its corresponding PU/MMT (measured in the cone calorimeter and heat flow 50 $kW.m^{-2}$); the MLR peak of PU/MMT is 40% of its preceding PU, but the peak is achieved in advance.

In PU/MPP (Melamine polyphosphate), the dispersion of MMT plays a significant role in reducing MLR. The MLR of PU/MMT (5%) is 60% of PU, whereas the PU/MMT (5%)/MPP (6%) is only 35%.
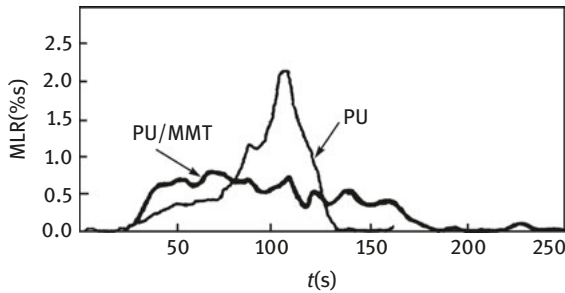
Figure 6.13: The MLR curve of PU and its corresponding PU/MMT [34].

Oxygen index

The MMT in PMN cannot effectively improve the limiting oxygen index (LOI) of materials, such as the LOI (20.5) of PU/MMT with MMT (5%), which could only improve 1.5 units than PU (19.0). However, when MMT is used in conjunction with conventional flame retardants such as MPP, dispersing 5% of MMT in PU/MPP (6%), the LOI of materials could reach 27.5% and could improve 3.5 units of the LOI (24.0) in PU/MPP (6%). This shows that, to improve the LOI of PU/MPP, MMT may have synergistic effect with MPP. Therefore, adding certain conventional flame retardants in polymers/MMT may be able to improve the flame retardant performance.

In summary, thermal stability and flame retardancy of PU/MMT nanocomposites can be attributed to the following three points:

1. When there is approximately 5% MMT in PU/MMT, compared with the original PU, PHRR can decrease by approximately 40%~60%, and the FPI can increase by approximately two times, significantly improving the fire safety of materials.
2. When MMT content in PU/MMT is below 5%, T_i and PU are similar, but if it reaches 8%~10%, T_i increases. Hofmann elimination reaction occurs at a certain temperature after the application of modifier alkyl ammonium halide in MMT, which is not conducive for increasing T_i and TTI in PU/MMT.
3. At the same time, using conventional flame retardants with a synergistic effect with MMT in PU/MMT, such as phosphate, can further improve the PHRR, FPI and LOI of materials.

6.6 Polymer/carbon nanotubes nanocomposites

6.6.1 Carbon nanotubes (CNT) and their features

CNT is a typical fullerene (cage atom clusters) which is actually a seamless nanotube composed of curling graphite sheets. The wall thickness is only a

few nanometers, the diameter ranges from a few nanometers to tens of nanometers, axial length of microns can reach centimeter magnitude, and the ratio of length to diameter reaches 100~1000. The structure of CNT is similar to fullerene and graphite, with curved crystal surface made of SP^2 hybridized carbon and the shortest C-C length of 0.142 nm. CNT could be divided into single layer and multilayer (SWCNT and MWCNT) with both having varied shapes. CNT has a very high specific surface area; the specific surface area of CNT currently is 15~400 m^2/g, which is far less than the theoretically predicted value. CNT has a very high tensile strength reaching 50~200 GPa, 100 times more than that of steel, while its density is only one-sixth of steel. The Young's modulus and shear modulus of CNT are equal to that of diamond, with a failure strain of 5%~20%. In addition, with a strong anti-distortion capability, CNT also shows good flexibility and elasticity in the axial direction, and can be resistant to oxidation and corrosion. Therefore, CNT will be an ideal reinforcement of advanced materials. Composite materials made of CNT and polymers have a high specific strength along with a series of other valuable properties.

The research concerning the polymer/CNT nanocomposites focuses on treating CNT as reinforcement to significantly improve the strength and toughness of the materials or using their good electrical properties to improve the conductivity of the materials. Using MWCNT as flame retardants have a series of advantages: (1) with a large ratio of length to diameter (more than 1000) materials with MWCNT as the dispersing agent can easily form a protective char layer with a continuous network structure, few surface cracks, and does not shrink, resulting in good flame retardant effects; (2) MWCNT do not need to undergo surface modification such as LS and can be compatible with numerous polymers; (3) TTI of the polymer/MWCNT nanocomposites does not decrease, while the organic surface modification agent of LS often reduces TTI; (4) When MWCNT content in polymers is 2.0%~5.0%, it works better in reducing HRR and MLR than LS; (5) MWCNT have synergistic effects with other nanoscale inorganic compounds (such as MMT) and some conventional flame retardant.

6.6.2 The thermal stability of the nanocomposites of polymer/MWCNT

Some thermal parameters of PA6 and PA6/MWCNT (5%) are shown in Table 6.2 [42] measured by thermal analysis (TGA and DTA). The table shows that, compared with PA6, the mass loss of PA6/MWCNT (5%) decreases when the temperature is lower than 330 ℃. When the temperature is lower than 600 ℃, the residual char in air increases, but the peak thermal decomposition temperature and melting temperature remain unchanged.

Table 6.2: The thermal parameter of PA6 and PA6/MWCNT (5%) measured by TGA and DTA.

Thermal parameter	PA6	PA6/MWCNT (5%)
The mass loss when the temperature is lower than 330 °C/%	2.1±1.0	1.1±1.0
Thermal decomposition peak temperature/ °C	459±1.0	459±1
Melting temperature/ °C	227±1.0	225±1.0
The amount of residual char(600 °C, air)/%	0.0±1.0	5.2±1.0

❖ The condition of TGA: air, 10 °C/min, 12 mg

6.6.3 The flame retardation of nanocomposites of polymer/MWCNT

Heat release rate

1. The heat release rate of PP/MWCNT

   The HRR curve of PP/MWCNT with different amounts of MWCNT (0.5%~4%) (measured by 50 kW/m^2 cone calorimeter) is shown in Figure 6.14.
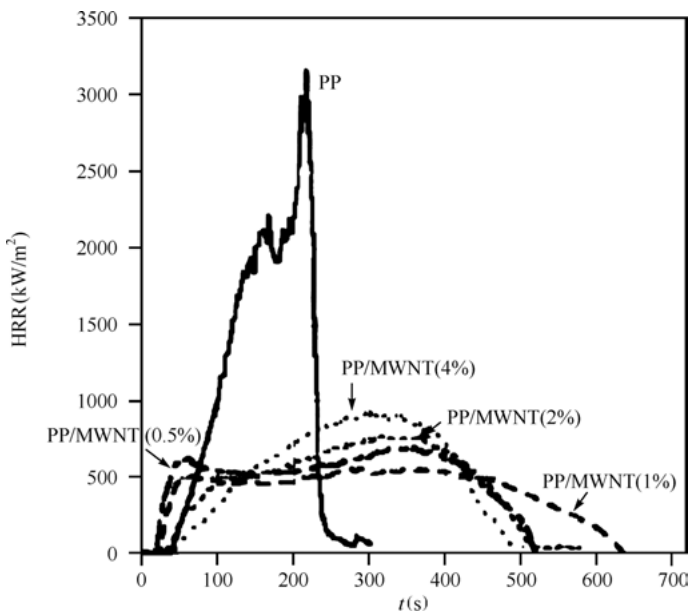

Figure 6.14: The HRR curve of PP and PP/MWCNT [43, 44].

Figure 6.14 shows that the PHRR of PP/MWCNT is the lowest (only one-sixth of PP) when the MWCNT content is 1%. On increasing or decreasing the MWCNT content, the PHRR increases. It is caused by the balance between thermal

conductivity and barrier quality of the char layer formed during combustion. When MWCNT content in PP/MWCNT is 0.5%, TTI is lower than PP, while it increases with increase in MWCNT content.

2. The heat release rate of EVA/MWCNT

    Figure 6.15 [45–47] is the HRR curve of the nanocomposite material comprising EVA (2%VA) with MWCNT, MMT and MWCNT+MMT (heat flow 35 kW.m^{-2} measured in the cone calorimeter). The purity of MWCNT is 99%, with the remaining 1% constituting inorganic compounds (Fe, Al_2O_3 and CO). The MMT modifier is dimethyldi(octadecyl) ammonium halide. Each sample has been measured three times, and the measured deviations are within ±5%.
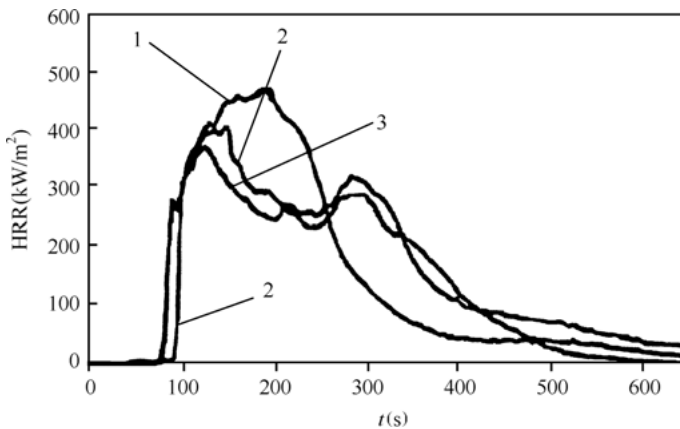
Figure 6.15: The three HRR curves of EVA/inorganic nanocomposite materials.

Figure 6.15 shows that, when we reduce HRR, MWCNT is more effective than MMT; and when the nanofiller dosage is 5%, with MWCNT and MMT for 50%, PHRR value significantly reduces than the single MWCNT. This shows that there is a certain degree of synergism between MMT and MWCNT. However, it is worth noting that MWCNT plays a less important role in reducing the HRR of EVA compared with PP.

3. The heat release rate of PA6/MWCNT

    Figure 6.16 [48] is the HRR curve of PA6/MWCNT (5%) measured in the cone calorimeter where the heat flow is 30 kW/m^2. According to the figure, the PHRR values of PA6/MWCNT (5%) decreases by approximately 40% in terms of pure PA which is equal to the average decrease of HRR of PA6/ MWCNT (5%).
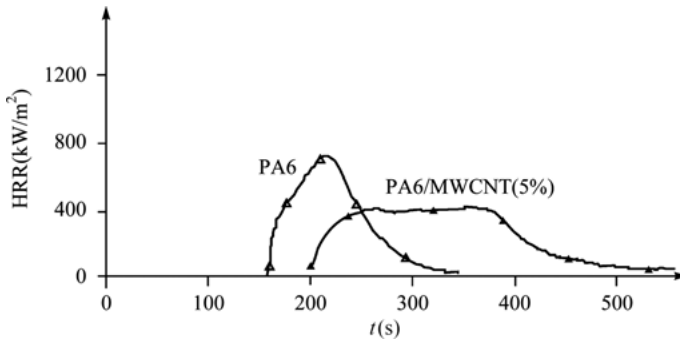
Figure 6.16: The HRR curve of PA6 and PA6/MWCNT (5%) [48].

Mass loss rate

Using a radiation gasification device wherein the heat flow was 50 kW/m^2 (N$_2$, no combustion), the MLR curves of PP and PP/MWCNT are shown in Figure 6.17 [43]. The MLR measured using the cone calorimeter is higher than that measured using the radiation gasification device. This is because in the cone calorimeter experiments oxidation of the material is intense, such that the material consumption rate is higher. However, when the content of MWCNT in PP is increased from 0.5% to 1%, it shows limited effects on the MLR of the materials, with similar effects seen in air and N$_2$.

Figure 6.17: The MLR curve of PP and PP/MWCNT [43].

PP/MWCNT can form a network structure of char layer which is relatively uniform across the surface of the combusted materials without any cracks and voids. The

char layer can prevent the loss of mass and heat, and a significant part of the incident energy and reflection flow to the gaseous phase, thus reducing the amount of heat in the char layer matrix, thereby slowing the rate of thermal degradation of the matrix and reducing the MLR to improve the efficiency of the flame retardancy.
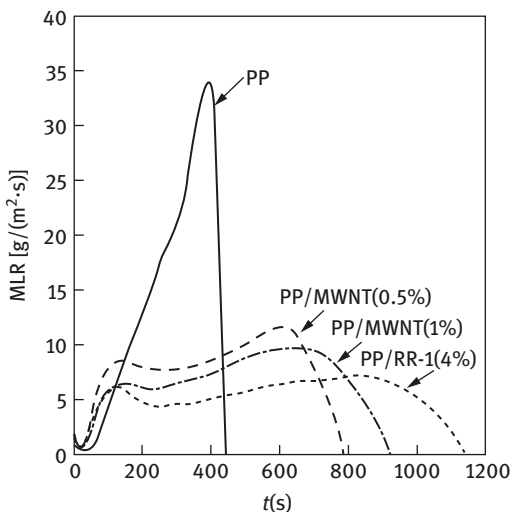
Time to ignition

As is well known, when the polymer/inorganic nanocomposite material with MMT is used as a flame retardant to improve the compatibility between the polymer MMT and substrate, the surface of the MMT must be modified. The modified agent is alkyl quaternary ammonium salt because the latter can undergo Hofmann elimination reaction at certain temperatures, hence sometimes the TTI of the polymer/inorganic nanocomposites decreases slightly. However, when MWCNT is used as a flame retardant of the polymer/inorganic nanocomposite (including EVA/MWCNT), such a problem does not exist because it can retain the original TTI value of the substrate. Table 6.3 is the testing TTI value of EVA nanocomposite [49].

Table 6.3: The testing TTI value of EVA nanocomposite.

Sample	TTL / s
EVA	84
EVA/LS (2.5%)	70
EVA/LS (5.0%)	67
EVA/MWCNT (2.5%)	85
EVA/ MWCNT (2.5%)	83

The limiting oxygen index and UL94 flame retardancy

The LOI of PA6 is (26.4% ± 1%), however, the limiting oxygen index of PA6/MWCNT (5%) decreases to (23.7% ± 1%) [48]. Because the PA6 produced droplet in the experiment, the material flew away from the droplet of the hot crack zone, taking away the heat and reducing the material supply. Consequently, the material is burnt only in a small fire, and the LOI ratio is high. While for PA6/MWCNT (5%), due to the formation of a network structure of char layer during combustion and increase in the viscosity of the material, it will block the material removed from the cracking area. Therefore, the materials are burnt in a big fire burn, and the LOI declines.

Figure 6.18 [50] demonstrates that, with regard to the UL94 vertical burning test, there is a similar situation of testing LOI compared with PA6. PA6/MWCNT is easy to produce droplets, so PA6 is very close to the UL94V-2 level, and PA6/MWCNT (5%) showed no capability of self-extinguishing and cannot go through any flame retardant grade of UL94V.
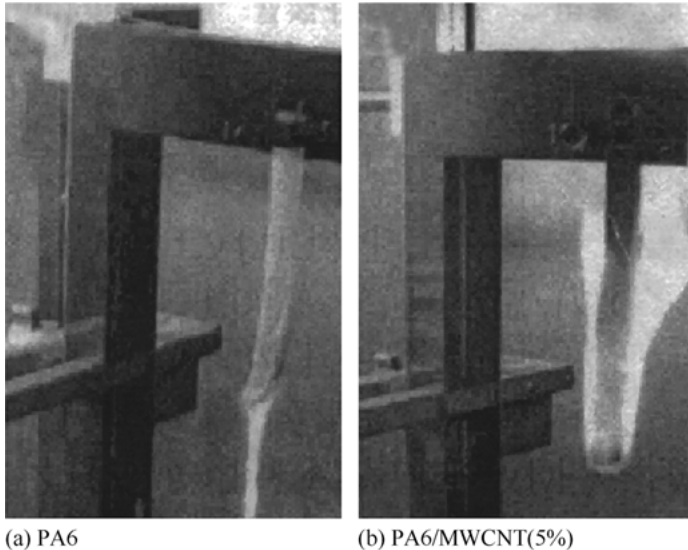
(a) PA6   (b) PA6/MWCNT(5%)

Figure 6.18: The general burning situation of UL94V of PA6 (a) and PA6/MWCNT (5%) (b) UL94V [50].

Synergistic effect of MWCNT and other inorganic fillers and conventional flame retardants

The dispersion of two or more than two kinds of inorganic nanomaterials, which can play a synergistic effect, is an effective way to improve the flame retardant performance (and other properties) of the non-composite. The cooperation of MMT and MWCNT of the EVA results in better flame retardant properties (Figure 6.15).

In addition, adding CNT in a series of conventional flame retardant can reduce the dosage of conventional flame retardants and improve the properties of flame retardant materials. For example, when we disperse 2%~5% CNT in the EVA/ATH (aluminum hydroxide) system, the amount of ATH needed which makes the material go through the V-0 degree can be decreased from 60% to 50%. Meanwhile, the EVA/ATH/CNT system is a flame retardant sheath/dual-use material which is low in smoke, halogen-free and low voltage cable with the oxygen index reaching 31%, and the temperature index reached 235 °C. Smoke density conformed to the IEC601034 standard, and the toxicity index of NES713 was 3.0 [1].

6.6.4 Char and char layer structure of polymer/MWCNT nanocomposites

EVA/MWCNT and EVA/MWCNT/MMT

EVA/MWCNT and EVA/MWCNT/MMT, two nanocomposite materials were burned in a cone calorimeter (heat flow 35 kW.m^{-2}) and Bunsen burner (the height of the

fire was 6 cm, the surface temperature of the sample was 45 °C, and the time of burning was 1 min; the sample size was 30 mm × 30 mm × 3 mm); the shape of the char layer are shown in Figures 6.19 and 6.20, respectively [7].

(a) EVA/MWCNT(4.5%)   (b) EVA/MWCNT(2.5%)+MMT(2.5%)
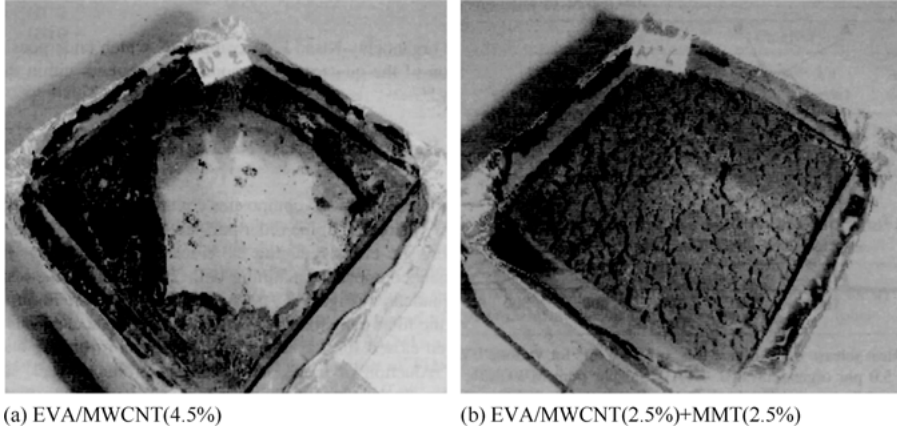
Figure 6.19: EVA/MWCNT (4.5%) (1) and EVA/MWCNT (2.5%) + MMT (2.5%) (2) The char layer formed in the cone calorimeter test [47].

(a) EVA/MWCNT(4.5%)   (b) EVA/MWCNT(2.5%)+MMT(2.5%)
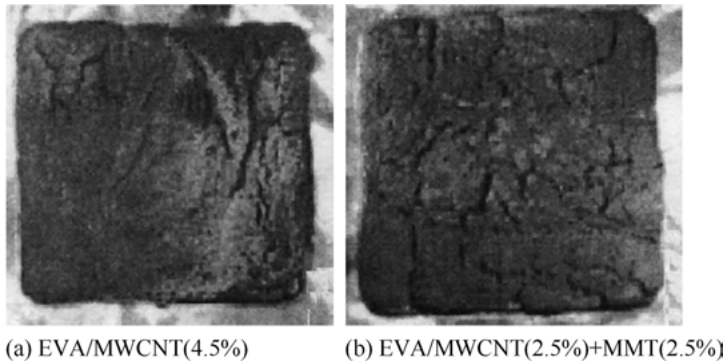
Figure 6.20: EVA/MWCNT (4.5%) (1) and EVA/MWCNT (2.5%) + MMT (2.5%) (2) The char layer formed in Bunsen burner test [47].

In the cone calorimeter test, char residue of EVA/MWCNT will be burned; whereas in Bunsen burner test, the overall structure of the char layer can be formed on the surface. In terms of EVA/MMT+MWCNT, a good smooth char layer can be generated in the cone calorimeter test, however, the cracks in the char layer grow more in Bunsen burner test.

On comparing the cone calorimeter test and Bunsen burner test, the combustion in the former is milder and the char oxidation degree is low, which is equivalent to

the early stage of the cone calorimeter test. In the Bunsen burner test, EVA/MWCNT generates a smooth char layer with small cracks, and hence, the PHRR value of EVA/ MWCNT is low. As mentioned above, the Bunsen burner test conditions are equal to the early stages of the cone calorimeter. In the Bunsen burner test, the char layer formed by EVA/MWCNT is more effective than those formed by EVA/MMT b blocking the combustible volatile compounds escape from gas phase and the oxygen penetrating into the condensed phase. However, the antioxidant effect of the char layer of the former may be worse than the latter. Hence, if the sample is exposed to a high temperature for a long time (such as in the cone calorimeter test), due to the worse stability of char layer oxidation of EVA/MWCNT, most of the char residue will be burned. Instead, EVA/MWCNT+MMT contains MMT with better resistance to oxidation, and hence, in both the cone calorimeter and Bunsen burner test, they can form a integral char layer, such that the PHRR value is low.

MWCNT has the properties of graphite nucleation during combustion when making the material burn and it will lead to the formation of graphite carbon and turbulence carbon. If the materials contains both MWCNT and MMT, the abovementioned effect can be strengthened. If the char layer contains graphite carbon, the value of PHRR can be considerably reduced. In addition, MWCNT can also reduce the number of cracks on the surface of the char layer.

Oxidation resistance of the char layer also plays an important role in flame retardant properties. The oxidative activity of the char layer is generally higher than that of pure graphite, and usually depends on the graphitization degree of the char layer. Adding MMT to the polymer/MWCNT helps improve the oxidation resistance of the material.

Figure 6.21 shows the cracks formed on the surface of char layers when EVA/ MWCNT (4.5%) combusts for 4 min at 600 °C, as measured by a scanning electron microscope [47]. The precipitated MWCNT can be distinguished from the crack surface. It is clear from the Figure that MWCNT can play an important role in preventing the formation of cracks on the surface of char layer. Because fiber-shaped
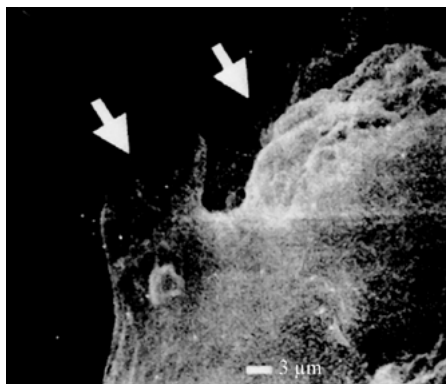

Figure 6.21: The surface crack of the char layer of EVA/MWCNT (4.5%) at 600 °C for 4 min [47].

MWCNT can connect with the EVA matrix and enable the material to not generate excessive cracks during the combustion process, smooth-faced char layer can be formed during the early stages of combustion.

The diffraction results of EVA/MWCNT (4.5%), as measured by X-ray, (burning for 4 min at 600 °C) are shown in Figure 6.22 [47]. The specimen did not have a graphite structure before combustion, and the char residue as per the XPD diagram had a strong and broad peak at 0.3445 nm, which is characteristic of turbulent char. It proves that EVA/MWCNT forms a turbulent carbon structure during the combustion of char. In such a structure, a series of aromatic layers stack together with each layer being parallel and equidistant, but at the same time being fully disordered.
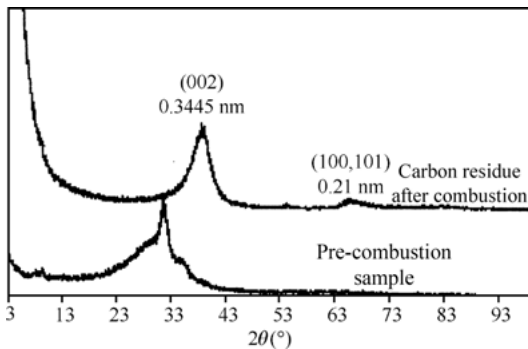
Figure 6.22: The combustion of EVA/MWCNT (4.5%) (at 600 for 4 min) [47].

When MWCNT is used as a flame retardant for polymer/inorganic nanocomposite materials, the effectiveness is prominent in terms of reducing HRR and MLR, which is better than MMT for some polymers. In particular, it may have synergistic effects with other inorganic fillers and conventional flame retardants, highlighting the application prospects of MWCNT in the flame-retardant polymeric materials. However, the polymer/inorganic nanocomposite materials containing MWCNT are still in the early stages of development, being from industrial application. Further research is needed for the flame retardation mechanism of MWCNT (such as failure mode, effect of nanomaterial combustion and heat on the char impact, condensed form and phase barrier layer of the layer of physical performance).

PMMA/SWCNT

With a heat flow in the cone calorimeter of 50 kW.m^{-2}, we tested the HRR of three different samples [well dispersed PMMA, PMMA/SWCNT (0.5%) and poorly dispersed PMMA/SWCNT (0.5%)]. Although well dispersed samples burnt more slowly

than the poorly dispersed ones, the two samples were almost completely burned out at a heating rate of 50 kW.m^{-2}. However, in the process of thermal cracking gasification, the same PMMA/SWCNT in N$_2$ (external radiation heat flow 50 kW.m^{-2}) could form the char residue. Regarding the well dispersed samples of SWCNT, during the thermal cracking process, they first formed a large number of splash vesicles on the surface of the material, followed by solid matter (without any liquid characteristics), and finally a black char covering the entire sample container. Regarding the poorly dispersed sample, first, it formed a large number of vesicles on the surface of the material, followed by many black islands, which finally connected into a whole structure (Figure 6.23 [44, 51]). The MLR curve for of the two samples (thermal cracking gasification) and HRR curve (cone calorimeter) displayed the same trend. On comparing poorly dispersed samples of SWCNT (dosage of 0.5%) with well dispersed samples, PHRR and PMLR of the former was much lower, while for the latter was almost as the same as a single PMMA. SWCNT with a good dispersion of 0.5% in PMMA could reduce PHRR by approximately 60%, whereas 3% of the MMT could only reduce approximately 30% [52].

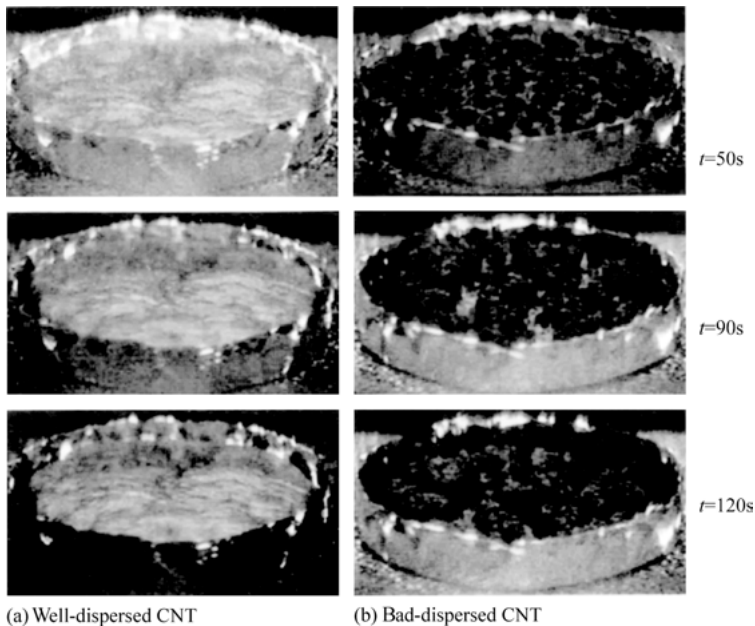(a) Well-dispersed CNT   (b) Bad-dispersed CNT

Figure 6.23: PMMA/SWCNT (consumption of 0.5%) vaporization residue [44, 51].

PMMA/SWCNT with the consumption of 0.2% of SWCNT is similar to that with the consumption of 0.5% of SWCNT in nitrogen. In the process of thermal cracking gasification, PMMA/SWCNT comprising 0.5% and 1% of SWCNT is similar to a solid in

terms of hot cracking behavior. The sample surface is always covered with a mesh-shaped protective layer, eventually forming a solid residue layer, with no perceivable cracks (see Figure 6.24 c and d [44, 51]).

(a) PMMA (b) PMMA/SWCNT(0.2%) (c) PMMA/SWCNT(0.5%) (d) PMMA/SWCNT(1%)
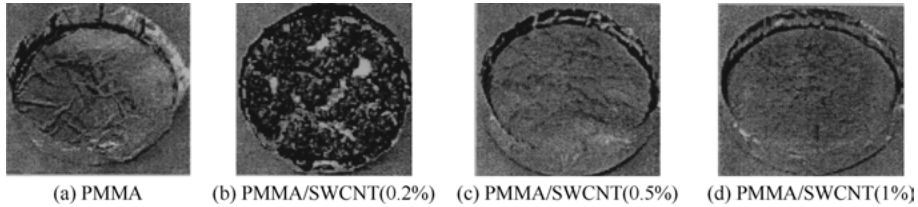
Figure 6.24: Gasification and hot tearing (50 kW/m^2, phenol nitride) PMMA/SWNT sample's residue [44, 51].

PMMA/SWNT (consumption of 1%) mesh structure of the hot tearing residue comprises bunches of CNT which are coiled with each other. The residue is so hard that it cannot be damaged easily. CNT can only slightly increase the rate of char residue rate of PMMA by collecting and weighing the residue.

6.7 Polymer/layered double hydroxyl compounds nanocomposite

The anions in layered double hydroxyl compounds have greater exchange capability than the cations in MMT (approximately 3–4 times higher). However, the electrostatic attraction between the layers increases with the growth of ion exchange capability, which is not conducive to the formation of exfoliation nanocomposites. Thus, it could only form LDH-containing nanocomposites with smaller interlayer spacing. However, regarding flame retardant and thermal stability, EP/LDH (EP is an abbreviation for epoxy resins) has more advantages over EP/MMT (e.g., extremely large self-extinguishment). The following sections discuss the EP/LDH nanocomposite as per a previous study [53].

6.7.1 Characteristics of LDH

An anionic clay, LDH is a layered mixed metal hydroxide with the chemical formula of $(Mg_6Al_2(OH)_{16}CO_3^{2-} \cdot nH_2O)$. It is composed of coplanar octahedron unit with a cation at the center which coordinates with six hydroxyl units at the peak (Figure 6.25); chemical formula of the octahedron unit is usually denoted as:

$[M_{1-x}M^{III}_{x}(OH)_2]^{q}$
layer formation

$[A_{q/n}^{\,n-} \bullet m\,H_2O]$
interlayer formation

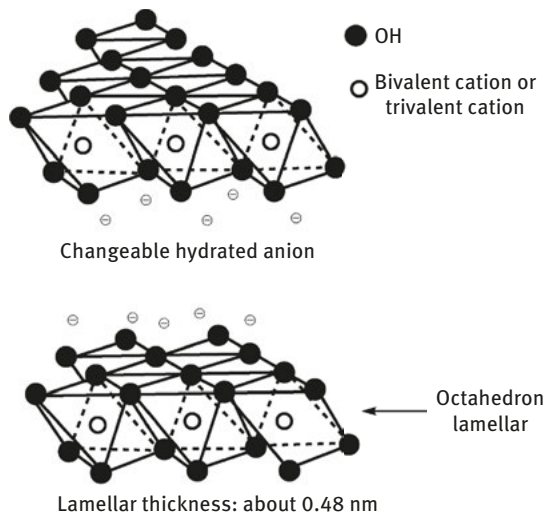● OH

○ Bivalent cation or trivalent cation

Changeable hydrated anion

Octahedron lamellar

Lamellar thickness: about 0.48 nm
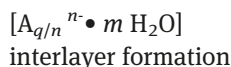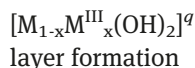
Figure 6.25: Structure of layered double oxyhydrogen compound.

Where M is a bivalent cation (e.g., Mg^{2+}, Zn^{2+}, Ca^{2+}, Co^{2+}, Cu^{2+}, Mn^{2+}) or an univalent cation (e.g., Li^+) (Li-Al LDH is the only well-known M^+-M^{3+} LDH, where Li^+ is inserted in the octahedron interspaces of gibbsite [y-Al(OH)$_3$]); MⅢ is a trivalent cation (Al^{3+}, Cr^{3+}, Fe^{3+}, Co^{3+}, Ni^{3+}, Ga^{3+}, Mn^{3+}); A^{n-} is an exchanged interlayered anion; q is the quantity of electric charge of octahedron unit (when M is divalent cation, $q = x$, when M is univalent cation, $q = 2x - 1$). An important characteristic of LDH is that the forms of internal layer and the interlayer can be adjusted. By changing the ratio of univalent cations, divalent cations and trivalent cations with $p = (1 - x)/x$, electric charge q and anion exchange capacity (AEC) can be adjusted. Usually, the exchange capacity of LDH is 200~470 meq• (100 g), which is higher than the cation exchange capacity (CEC); e.g., the CEC of sodium montmorillonit is 80~145 meq• (100 g). The diameter of the anionic clay is similar to that of the cationic clay, and may even be larger. By changing the synthesis conditions, the lamellar thickness of LDH can reach 0.48~0.49 nm and the layer size of LDH can be 0.06~20 um [53].

6.7.2 Thermal decomposition of EP/LDH

In the air, by using synchronous thermal analysis (STA), the thermal stability of cured EP/LDH (4-cis-tritosylate) of polypropylene oxide diamine (JeffamineD230), sole EP and EP/MMT (double (2-hydroxyethyl) modified ammonium) (30B) were

compared. The additive volume of the two nanocomposites is 5%. According to the DTA curve [53], sole EP has a main endothermic peak at approximately 550 °C; EP/LDH has two endothermic peaks so that HRR is reduced and heat release is delayed; the heat release conditions of EP/MMT are the same as that of sole EP.

As can be seen from the TGA curve [53] of sole EP (two amino and two phenyl sulfone-cured DGEBA) and EP/LDH (5%, 3-amino benzene sulfonic acid ester modified), initial decomposition temperature of nanocomposite reduced about 15 °C compared with sole EP. Meanwhile, at approximately 550 °C, the amount of residue increases by approximately 36%. In addition, the charring amount of EP adding phosphorus-based flame retardant chemical (e.g., ammonium polyphosphate) increases and its thermal stability reduces. This is because ammonium polyphosphate (APP) degrades into polyphosphate and ammonia at approximately 200 °C. At the first stage of EP/APP degradation, EP undergoes a dehydration reaction and polyphosphate acts as an important catalyst in this reaction. Polyphosphate can also promote promote the formation of unsaturated matter and char [54, 55]. Phosphorus compound is the usual charring precursor agent of the expansion system; in most cases the agent is APP, but can also be a sulfur compound. When heated, the sulfonic acid ester decomposes into a strong mineral acid, whereas the latter acts as a catalyst for the dehydration reaction [56]. Thus, it can be considered that the surface active agent of organic sulfonic acid ester of EP/LDH can prompt char formation. Char formation reaction is related to the nature of the surfactant, but has nothing to do with LDH. EP/LDH, produced by Hsueh and Chen [57], uses amino carboxylic ester (12-amino laurate) to modify LDH. The study results show that, because of the blocking effect of typical LDH, thermal stability of the nanocomposite is improved compared with sole EP; however, the amount of residue did not increase at high temperatures. Meanwhile, Chen and Qu [58] observed that the thermal stability of PP-g-MA/LDH (using dodecyl sulfate to modify LDH) was reduced, but the amount of char residue was increased. According to the mechanism of char formation, intercalated anion, especially acidity, seems to be the key factor influencing the decomposition progress.

6.7.3 Flame retardancy of EP/LDH

As a kind of additive, when decomposing, LDH can form refractory oxides on the surface of the material, while releasing water vapor and carbon dioxide, resulting in improved flame retardation of the matrix. During combustion, it extends TTI and reduces the total quantity of heat required [53] by absorbing considerable amount of heat and attenuating flammable gases produced by pyrolysis. When LDH presents nanoscale dispersion in the matrix, it has the typical effect of nanocomposites.

The results of UL94 level of EP/LDH, EP/MMT, EP/ATH and EP/APP are listed as follows: EP/LDH1 (modified 3-amino benzene sulfonic acid ester) and EP/LDH2

(modified 4-toluene sulfonic acid ester) are superior to EP/MMT1 (double (2-hydroxyethyl) modified ammonium), EP/MMT2 (C_{14}~C_{18} modified ammonium), EP/ATH and EP/APP [53]. Factually, in the horizontal flame test of UL94, only LDH nanocomposite has self-extinguishing performance. The flame retardancy of LDH nanocomposite is related to the dispersion of the modified LDH and its internal features. EP/LDH is the first nanocomposite which can self-extinguish without the need for adding additives. Hence, the anion clay of LDH can improve materials' flame retardancy and substitute the common cation clay. In the horizontal flame test of UL94, although EP/LDH has unique self-extinguishing properties, the previous nanocomposites do not exhibit such characteristics. When anionic clay materials burn, consecutive and expanded ceramic coating is formed on the polymer surface, leading to a larger reduction amplitude of HRR than that of MMT nanocomposites. Furthermore, anionic clay can effectively compound with phosphorus flame retardants to improve expansibility and reduce the amount of HRR released and smog.

When LDH radical nanocomposites burn, they formed mixed metal oxides (formed during the thermal decomposition of LDH) and intercalated nanocomposites. On burning UL94, there is a diffraction peak at 1.28 nm in the XRD pattern of EP/LDH1 and EP/LDH2. Consistent with this, Gilman and others [60] reported that intercalated structure of char produced by montmorillonite nanocomposites has the same interlayer distances between char intercalation (1.3 nm), which is not related with the types of polymer (thermosetting or thermoplastic) and their nanostructure (intercalation or layer). This implies that the interlayer distances between char intercalation are unrelated with the nature of the layered crystal.

As listed in Figure 6.4 and Table 6.4 [53], data of cone calorimeter tests involving EP radical sample further prove that flame retardancy of LDH radical nanocomposite is superior than that of montmorillonite nanocomposite. Compared with sole EP, PHRR of EP/LDH1and EP/LDH2 reduced by 51% and 40%, respectively, which were obviously superior to EP/MMT2, with the latter only reducing by 27%. After testing by cone calorimeter, EP/LDH1and EP/LDH2 formed expended, dense and successive residue, whereas the residue produced by EP/MMT2 was cracked, as shown in Figure 6.26 [53, 59]. Residue of EP/LDH1 has a shell-like structure, whose protective layer is approximately 1 mm thick with a maximum thickness of up to 5 cm. The residue has superior mechanical strength and integrity, as well as consistency and adhesiveness. After burning, the protective layer formed on the surface of sample has a bilayer structure – the white and porous inner layer is formed by metallic oxide, whereas the black and compact outer layer is formed by the remaining char (some may be formed by smog in the air).

As mentioned above, residue of LDH radical nanocomposite has an intercalated structure with an interlayer distance of 1.28 nm as per the UL94HB test. On testing by cone calorimeter, diffraction peak cannot be observed in the XRD pattern of the
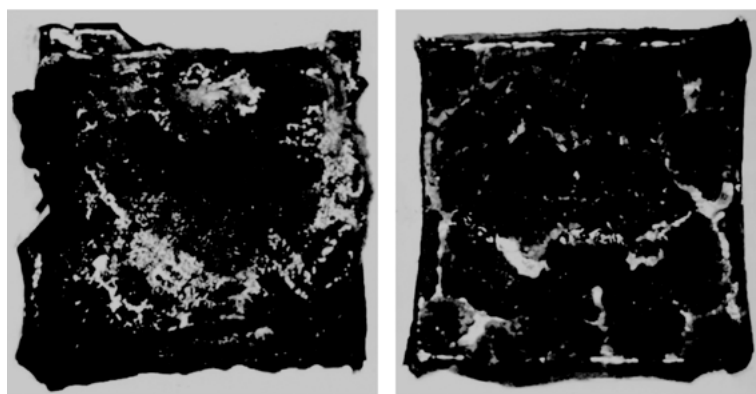
(a) Closed char layer formed by EP/LDH1 with expansibility and the thickness of 50 mm

(b) Broken char layer formed by EP/MMT2

Figure 6.26: Char residue after testing by cone cal:orimeter.

Table 6.4: Data of cone calorimeter of EP-based nanocomposites [53].

Sample	Amount of residue (%)	PHRR (kW·m^{-2}) (% dropping)	mHRR (kW·m^{-2}) (% dropping)	mHc (mJ·kg^{-1})	mMLR (g·m^{-2}·s^{-1})	mSEA (m^2·kg^{-1})	TTI (s)
EP	3.3	1181	533	26	23	750	109
EP/MMT2	8.6	862(27)	477(11)	23	21	773	110
EP/LDH1	8.4	715(40)	382(28)	23	17	724	98
EP/LDH2	9.5	584(51)	347(35)	22	15	743	112
EP/APP	90.1	491(62)	105(80)	17	6	720	78

(external radiant power is 35 kW•m^{-2}; error of PHRR, MLR and SEA is ±10%; error between Hc and TTI is ±15%; all data are the average values of the same three samples; sample is a 100 mm square plate with a thickness of 8 mm)

residue. In fact, the test conditions between UL94HB and cone calorimeter are different. In UL94, the flame used in the sample test is the only heat source, and hence, the char residue cannot be oxidized after the flame self-extinguishes. Conversely, the residue was exposed to external radiation until the sample removed the devices (about 2 min) during burning and self-extinguishing in the cone calorimeter. After the flame self-extinguished, EP/LDH radical nanocomposite still has a strong incandescence light which oxidizes the char residue to CO and CO$_2$. This is because the degradation products of LDH (magnesium-aluminum oxide catalyst) catalyze the oxidizing reaction, which forms sparks [61, 62]. Therefore, in the burning progress, LDH radical nanocomposite first formed an intercalated structure

between the metallic oxide and the char, and then the intercalary char-containing residue is oxidized to CO and CO_2 in a reaction catalyzed by the metallic oxide.

Figure 6.27 [53, 59] shows the HRR curve of the EP radical nanocomposite. After 160 s, HRR of EP/LDH1 and EP/LDH2 clearly reduced, which is related to intercalary rapid expansion. Therefore, EP/LDH (organic sulfonate modified) is an expansion system, where EP is the carbon source, sulfonic acid ester is the charring agent and water and CO_2 (produced by hydroxide radical thermal decomposition) are the foaming agents [53].
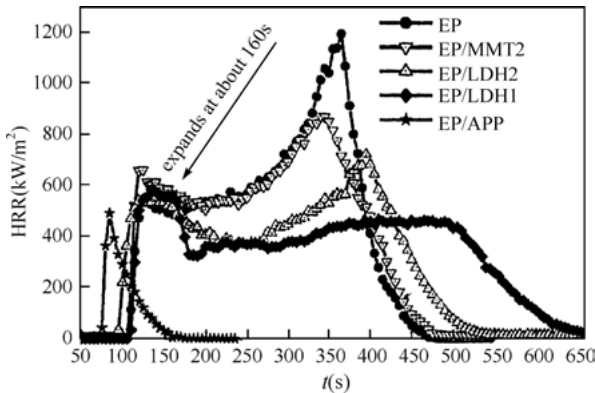
Figure 6.27: HRR curve of sole EP, EP/LDH1, EP/LDH2, EP/MMT2, EP/APP material (LDH radical nanocomposite expands at about 160 s) [53, 59].

For reducing weightlessness and heat release, nanocomposites are less effective than EP/APP, but APP reduces the thermal stability of materials and reduces the TTI by 29%. However, TTI of EP/LDH1 and EP/LDH2 are almost the same. In addition, APP reduces the mechanical property of EP, whereas the tensile strength, Young modulus and breaking elongation of LDH radical nanocomposite improve, while at the same time both the penetrating quality and thermal expansion reduce [25, 26].

Although the flame retardant effect of LDH is worse than APP, there is a synergistic effect between LDH and APP. In fact, for a 3 mm sample, to reach the standard of UL94 V-0, 30% of APP should be added into epoxy resin; while if 4% of 3-amino benzene sulfuric acid ester modified LDH is added, the additive amount of APP only needs to range 16%~20% [53].

References

[1]   Morgan A B, Wilkie C A. Flame Retardant Polymer Nanocomposites[M]. Hoboken: John Wiley & Sons, Inc., 2007.
[2]   Jiang D D. Polymer Nanocomposites[A]//Wilkie C A, Morgan A B. Fire Retardancy of Polymeric Materials. 2nd edition[M]. Beca Raton: CRC press, 2009: 261–300.

[3]   Lopez-Cuesta J-M,Laoutid F. Multicomponent Flame Retardant Systems.Polymer Nanocomposites Combined with Additional Materials[A]//Wilkie C A, Morgan A B. Fire Retardancy of Polymeric Materials. 2nd edition[M]. Beca Raton: CRC press, 2009:301–328.

[4]   Yang Rongjie,Wang Jianqi.Polymer Nano Composites Processing, Thermal Behavior and Flame Retardant Performance[M].Beijing: Sciencepress,2010.

[5]   Yuan Hu, Song Lei and so on.Flame Retardant Polymer Nanocomposites[M].Beijing: ChemicalIndustry Press,2008: 58–88.

[6]   Yuxiang Ou.Polymer/The Research and Development of Montmorillonite Nanocomposites Flame Retardant Mechanism[J].Polymer Materials Science and Engineering,2009,25(3): 166–174.

[7]   Zammaran M. Thermoset Fire Retardant Nanocomposites[A]//Morgan A B,Wilkie C A.Fire Retardant Polymer Nanocomposites[M].Hoboken: JohnWiley & Sons,Inc.,2007: 235–284.

[8]   Berta M, Lindsay C, Pans G, et al. Effect of Chemical Structure on Combustion and Thermal Behaviour of Polyurethane Elastomer Layered Silicate Nanocomposites [J]. Polymer Degradation and Stability, 2006,91(5):1179–1191.

[9]   Gilman J W, Kashiwagi T, Lichtenhan J D. Nanocomposites. A Revolutionary New Flame Retardant Approach [J]. SAMPE Journal, 1997,33(4):40–46.

[10]   Utrakil A. Clay-Containing Polymeric Nanocomposites[M]. Shrewsburg: Woodhead Publishing Limited, 2005:615.

[11]   Mai Y, Yu Z. Polymer Nanocomposites[M]. Shrewsburg: Woodhead Publishing Limited, 2006:256–272.

[12]   Zanetti M, Costa L. Preparation and Combustion Behaviour of Polymer/Layered Silicate Nanocomposites Based upon PE and EVA [J]. Polymer, 2004,45(13):4367–4373.

[13]   Levchik S, Wilkie C A. Char Formation [A]//Grand A F, Wilkie C A. Fire Retardancy of Polymeric Materials [M]. New York: Marcel Dekker Inc., 2000:171–215

[14]   Benson S W, Nangia P S. Some Unresolved Problems in Oxidation and Combustion [J]. Accounts of Chemical Research, 1979,12(7):223–228.

[15]   Zanetti M, Camino G, Reichert P. Thermal Behaviour of Polypropylene Layered Silicate Nanocomposites [J]. Macromolecular Rapid Communications, 2001,22(3):176–180.

[16]   Zanetti M, Camino G, Mulhaupt R. Combustion Behaviour of EVA/Fluorohectorite Nanocomposites[J]. Polymer Degradation and Stability, 2001,74(3):413–417.

[17]   Shuqing He,Yuan Hu,Song Lei.Flame Retardant Polypropylene/The Combustion Performance of Montmorillonite Nanocomposites[J].Journal of University of Science and Technology of China,2006,36(4):408–412.

[18]   Zanett I M, Camino G, Thomann R, et al. Synthesis and Thermal Behaviour of Layered Silicate EVA Nanocomposites [J]. Polymer, 2001,42(10):4501–4507.

[19]   Bourbigot S, Gilman J W, Wilkie C A. Kinetic Analysis of the Thermal Degradation of Polystyrene-Montmorillonite Nanocomposite [J]. Polymer Degradation and Stability, 2004,84 (3):483–492.

[20]   Zanetti M, Kashiwagi T, Falqui L, et al. Cone Calorimeter Combustion and Gasification Studies of Polymer Layered Silicate Nanocomposites[J]. Chemistry of Materials, 2002,14(2):881–887.

[21]   Ma H Ｙ, Tong L Y,Xu Z B, etal.Clay Network in ABS Graft MAH Nanocomposite.Rheolog and Flammability[J].Polymer Degradation and Stability,2007,92:1439–1445.

[22]   Lewin M. Some Comments on the Modes of Action of Nanocomposites in the Flame Retardancy of Polymers [J]. Fire and Materials, 2003,27(1):1–7.

[23]   Wang J, Dua J, Zhu J, et al. An XPS Study of the Thermal Degradation and Flame Retardant Mechanism of Polystyrene-Clay Nanocomposites [J]. Polymer Degradation and Stability, 2002,77(2):249–252.

[24]   Kashiwagi T, Harris R H, Zhang X, et al. Flame Retardant Mechanism of Polyamide 6 Clay Nanocomposites [J]. Polymer, 2004,45(3):881–891.

[25] Zhu J, Uhl F, Morgan A B, et al. Studies on the Mechanism by Which the Formation of Nanocomposites Enhances Thermal Stability [J]. Chemistry of Materials, 2001,13(12): 4649–4654.

[26] Xie W, Gao Z, Pan W P, et al. Thermal Degradation Chemistry of Alkyl Quaternary Ammonium Montmorillonite [J]. Chemistry of Materials, 2001,13(9):2979–2990.

[27] Xie W, Gao Z, Liu K, et al. Thermal Characterization of Organically Modified Montmorillonite [J]. Thermochimica Acta, 2001,367:339–350.

[28] Zanetti M, Camino G, Canavese D, et al. Fire Retardant Halogen-Antimony-Clay Synergism in Polypropylene Layered Silicate Nanocomposites [J]. Chemistry of Materials, 2002,14(1):189–193.

[29] Gilman J W, Kashiwagi T, Morgan A B, et al. NISTIR 6531 Flammability of Polymer Clay Nanocomposites Consortium.Year One Annual Report [R]. Gaithersburg: NIST(National Institute of Standards and Technology), 2000.

[30] Qin H, Zhang S, Zhao C, et al. Thermal Stability and Flammability of Polypropylene/ Montmorillonite Composites [J]. Polymer Degradation and Stability, 2004,85(2):807–813.

[31] Gilman J W. Flame Retardant Mechanism of polymer-Clay Nanocomposites[A]// Morgan A B, Wilkie C A(editors). Flame Retardant Polymer Nanocomposites[M]. Hoboken: John Wiley & Sons, Inc., 2007:67–87.

[32] Cipiriano B H, Kashiwagi T, Raghavan S, et al. Effects of Aspect Ratio of MWNT on the Flammability Properties of Polymer Nanocomposites [J]. Polymer, 2007,48(20):6086–6096.

[33] Morgan A B, Harris R H, Kashiwagi T, et al. Flammability of PS Layered Silicate (Clay) Nanocomposites. Carbonaceous Char Formation [J]. Fire and Materials, 2002,26(6):247.

[34] Ou Yuxiang.Polyurethane/Thermal stability and Flame Retardancy of Modified Montmorillonite Nanocomposites[J].Polyurethane Industry,2006,21(6):6–9.

[35] Chenggang Liang,Ruiying Zhang,Shujuan Wu .Polyurethane/Montmorillonite Nanocomposites [J]. Polyurethane Industry,2005,20(1):13–16.

[36] Beyer G. Progress with Nanocomposites and New Nanostructured FRs [A]//Proceedings of Conference of Flame Retardants 2006's [C]. London (UK): Interscience Communications Ltd., 2006:123–133.

[37] Wang Jianqi.Nanostructures with Hot Polymer Flame Retardant[A].The Thesis Collection of the Third Synposium on the latest Research and Development of Flame Retardant Technology and Materials[C].Beijing: Beijing Institute of Technology,2006. 45–64.

[38] Kashiwagi T, Grulke E, Hilding J, et al. Thermal and Flammability Properties of Polypropylene/ Carbon Nanotube Nanocomposites [J]. Polymer, 2004,45(12):4227–4239.

[39] Kashiwagi T. Progress in Flammability Studies of Nanocomposites with New Types of Nanoparticles [A]. Morgan A B, Wilkie C A. Flame Retardant Polymer Nanocomposites [M]. Hoboken: John Wiley & Sons, Inc., 2007:285–324.

[40] Beyer G. Carbon Nanotubes as Flame Retardants for Polymers [J]. Fire and Materials, 2002,26:291–293.

[41] Beyer G. Flame Retardant Properties of Organoclays and Carbon Nanotubes and Their Combinations with Alumina Trihydrade [A]//Morgan A B, Wilkie C A. Flame Retardant Polymer Nanocomposites [M]. Hoboken: John Wiley & Sons, Inc., 2007.163–190.

[42] Fengge Gao, Gunter Beyer, Qingchun Yuan. A Mechanistic Study of Fire Retardancy of Carbon Nanotube/EVA and Their Clay Composites [J]. Polymer Degradation and Stability, 2005,89 (3):559–564.

[43] Yuxiang Ou, Tingjie Han, Jianjun Li .The Manual of Flame Retardant Plastic[M].Beijing : NationalDefense Industry Press,2008:653.

[44] Yuxiang Ou, Xin Fei, Zhao Yi and so on. Polymer/The Manufacturing, Thermal Stability and Flame Retardancy of Carbon Nanotube Composite Materials[J].China Plastic, 2006,20(8):1–6.

[45] Schartel B, Pottschke P, Knoll U, et al. Fire Behaviour of Polyamide 6/Multiwall Carbon Nanotube Nanocomposites [J]. European Polymer Journal, 2005,41(5):1061–1070.

[46] Kashiwagi T, Du F, Winey K I, et al. Flammability Properties of Polymer Nanocomposites with Single-Walled Carbon Nanotubes. Effects of Nanotube Dispersion and Concentration [J]. Polymer, 2005,46(2):471–481.

[47] Zhu J, Start P, Mauritz K A, et al. Thermal Stability and Flame Retardancy of Poly(methyl methacrylate)–Clay Nanocomposites [J]. Polymer Degradation and Stability, 2002,77(2):253–258.

[48] Zammarano M .Thermoset Fire Retardant Nanocomposites[A]//Morgan A B, Wilkie C A.Flame Retardant Polymer Nanocomposites[M].Hoboken: JohnWiley& Sons,Inc.,2007.235–284.

[49] Levchik S V, Camino G, Costa L, et al. Mechanistic Study of Thermal Behaviour and Combustion Performance of Carbon Fibre–Epoxy Resin Composites Fire Retarded with a Phosphorus-Based Curing System [J]. Polymer Degradation and Stability, 1996,54(2–3):317–322.

[50] Hörold S. Phosphorus Flame Retardants in Thermoset Resins [J]. Polymer Degradation and Stability, 1999,64(3):427–431.

[51] Lewin M, Brozek J, Marvin M M. The System Polyamide/Sulfamate/Dipentaerythritol.Flame Retardancy and Chemical Reactions [J]. Polymers for Advanced Technologies, 2002,13(10–12):1091–1102.

[52] Hsueh H B, Chen C Y. Preparation and Properties of LDHs/Epoxy Nanocomposites [J]. Polymer, 2003,44(18):5275–5283.

[53] Chen W, Qu B J. Structural Characteristics and Thermal Properties of PE-g-MA/MgAl-LDH Exfoliation Nanocomposites Synthesized by Solution Intercalation [J]. Chemistry of Materials, 2003,15(16):3208–3213.

[54] Zammarano M, Franceschi M, Bellayer S, et al. Preparation and Flame Resistance Properties of Revolutionary Self-extinguishing Epoxy Nanocomposites Based on Layered Double Hydroxides [J]. Polymer, 2005,46(22):9314–9328.

[55] Gilman J W, Kashiwagi T, Nyden M, et al. Flammability Studies of Polymer–Layered Silicate Nanocomposites.Polyolefin, Epoxy, and Vinyl Ester Resins [A]//Ak-Malaika S, Colovoy A, Wilkie C A. Chemistry and Technology of Polymer Additives [M]. Malden: Blackwell Science, 1990.249–265.

[56] Delfosse L, Baillet C, Brault A, et al. Combustion of Ethylene Vinyl-Acetate Copolymer Filled with Aluminum and Magnesium Hydroxides [M]. Polymer Degradation and Stability, 1989,23 (4):337–347.

[57] Rychly J, Vesely K, Gal E, et al. Use of Thermal Methods in the Characterization of the High-Temperature Decomposition and Ignition of Polyolefins and EVA Copolymers Filled with $Mg(OH)_2$, $Al(OH)_3$ and $CaCO_3$ [J]. Polymer Degradation and Stability, 1990,30(1):57–72.

7 The mechanism of smoke suppression

When materials undergo combustion under certain conditions and their components are dispersed in the air in the form of solid particles (diameter ranging 1~50 μm) forming a dispersed system, smoke is generated. However, smoke is not merely dust in the air, uncombusted carbon particles, liquid particles and aerogels but also includes mist from industrial emissions, where solid smoke is considered to be the nucleus of condensation.

7.1 The relationship between the molecular structures and smoke of polymers

On combustion, a host of polymers, such as PVC, PS and PU, produce a considerable amount of smoke. Moreover, some flame-retardant polymers containing halogen flame retardants and antimony generate significantly more smoke. Even in the 1970s, people were aware that smoke was one of the hazards leading to deaths in a fire accident, severely delaying the time to rescue people's lives and property. Understandably, smoke suppression has become one of the basic requirements for flame-retardant polymers since 1980s [1, 2].

It is universally acknowledged that the mechanism of flame retardancy in the gas phase mainly includes trapping the free radicals that assist flame propagation (such as H·, OH· and O·), as well as suppressing the oxidation reaction of smoke precursors formed during combustion, which increases the amount of smoke generated by such flame-retardant materials. Unfortunately, flame retardancy in the gas phase is influenced by smoke suppressing agents that play the role of chemical smoke suppression. Therefore, flame retardant mechanism in the gas phase and smoke suppression are often contradictory.

The amount of smoke generated in the process of combustion is not an intrinsic characteristic of a material but is closely related to the measured smoke density of the material, combustion conditions (e.g., heat flux, shape of the material, presence or absence of flames, etc.) and experimental environment (e.g., temperature, volume of the combustor, ventilation, etc.) [3–5]. In addition, the molecular structure of a polymer also affects the amount of smoke generated in the process of combustion.

The amount of smoke generated during combustion varies from polymer to polymer. Polymers that can be depolymerized into monomers (acetal, PMMA, nylon 6, etc.) can undergo complete combustion and generate little smoke, whereas aromatic polymers that can produce high polymers with aromatic rings (such as PVC) generate more smoke on combustion.

Polymers with aliphatic hydrocarbons on the main chain, particularly those containing oxygen atoms in the main chain, produce relatively small amounts of

smoke, whereas polymers containing benzene rings on the main chain produce relatively large amounts of smoke. Polyenoid polymers containing benzene rings on the side chains generate significantly more smoke. This is possibly because the polyenoid carbon chains can produce graphitized carbon microparticles through cyclization and polycondensation, whereas polymers which have benzene rings on the side chains, such as polystyrene, can easily form conjugated double bond unsaturated hydrocarbons; these carbon chains then carbonize through cyclization and polycondensation, producing large amount of smoke.

Polymers containing halogen produce considerable smoke, however, the amount of smoke generated is out of proportion to the amount of halogen.

With increasing thermal stability of polymers, smoke generation tends to decrease. Consider polycarbonate and polysulfone, for example, which produce relatively small amounts of smoke during pyrolysis because volatile products reduce as a result of the formation of bulk carbon residue in the condensed phase, thus reducing the amount of smoke generated.

The introduction of heteroatoms into polymers results in reducing the flammability and increasing the smoke generation properties, which may be related to the incomplete oxidation of the volatile decomposition products of the polymer.

Interestingly, PVC and polyvinylidene chloride (PVDC) are significantly different in terms of smoke generation. The smoke density of the former is seven times than that of the latter, which may be due to different decomposition mechanisms. PVC forms an aromatic nucleus after dehydrochlorination, whereas PVDC does not. The maximum specific optical density (Dm) of different polymers listed in Table 7.1 [6] explains the abovementioned phenomenon. The maximum specific optical density of a few other polymers is listed in Table 7.2 [8]. However, the data presented in the two tables and the testing mechanisms used are different, which results in no strict comparison between them.

Table 7.1: Smoke generation properties of different polymers (determined according to the XP smoke box of Rohm Hass Company).

High polymer	Dm	High polymer	Dm
Acetal	0	PVDC	98
PA6	1	PET	390
PMMA	2	PC	427
LDPE	13	PS	494
HDPE	39	ABS	720
PP	41	PVC	720

In particular, the amount of smoke generated by flame-retardant polymers (by adding flame retardants) is usually high. For instance, gas-phase flame retardants promote smoke production as a result of inhibited oxidation effect. Some smoke

Table 7.2: Smoke generation properties of different polymers (determined according to the NBS smoke box).

High polymer	Dm	
	Combusting	**Smoldering**
PS (The sheet thickness is 6.35 mm)	780	395
PTFE	53	0
PVC (The sheet thickness is 6.35 mm)	780	315
ABS (The sheet thickness is 6.35 mm)	780	780
RUPF (Flame retardant)	500	170
PC (The sheet thickness is 6.35 mm)	324	48
UP (Glass fiber reinforced, the sheet thickness is 2.80 mm)	720	420

suppressants that are conducive to oxidation interfere with the flame retardancy of smoke suppressors, indicating that the functions of flame retardants and smoke suppressors are often contrary to each other. However, some fillers (e.g., Al(OH)$_3$, Mg(OH)$_2$, etc.) possess both flame retardancy and smoke suppression properties. The replacement of Sb$_2$O$_3$ in the halogen/antimony system with zinc borate can also reduce smoke generation without the restrictions of flame retardancy of deterioration of materials. In addition, materials with intumescent coating materials also boast of the double functions of combustion retardancy and smoke suppression.

There are two ways to reduce the amount of smoke. One is using polymers with relatively low smoke generation (achieved by the structural design of the polymers as well as structural modification). The other is using chemical methods or incorporating smoke suppressors (or fillers) into plastics. For example, the combustion of phenol-formaldehyde resin produces a high amount of carbon with low smoke generation, and some heat-resistant thermoplastics (mainly polyether and polysulfone) also produce little smoke. However, even though some commonly used plastics generate a high amount of smoke, they cannot be replaced by other less smoke generating materials on account of a series of advantages. Therefore, the first way to reduce the amount of smoke is rather limited; and the application of a chemical method is also hardly employed due to the associated high cost. Thus, it has become a practical method to add smoke suppressants (or fillers) as additives (or fillers) into plastics to reduce the amount of smoke generated. The formation of a porous carbon layer with isolation function on the surface of polymers also results in smoke suppression. Table 7.3 lists the various smoke suppression methods and examples of applications and possible mechanisms. This section is limited in the discussion of the smoke suppression mechanisms of smoke suppressor additives.

**Table 7.3:** Smoke suppression methods and applications.

Methods	Examples	Suitable polymers	Possible Mechanism
Adding smoke suppressors	Ferrocene	PVC	Promote carbonization and soot combustion
Adding smoke suppressors	Fumaric acid	PU Foam Plastics	Change PU dissociation modes
Adding inert fillers	Silica	Various thermoplastics and elastomers	Dilution of incombustibles
Adding active fillers	Aluminum hydroxide	Various thermoplastics and elastomers	Promote carbonization and reduce mass combustion rate and dilution
Surface treatment	Intumescent coating	Various plastics	Surface isolation and reduce the mass combustion rate
Structural modification	Polyurethane/ polyisocyanurate		
Structural modification	CPVC (chlorinated polyvinyl chloride)		

7.2 Smoke suppression mechanism of molybdenum compounds

Molybdenum in molybdenum trioxide and ammoniummolybdat is hexavalent, and its oxidation state and coordination number can be easily changed, which makes molybdenum trioxide and ammoniummolybdat possible flame retardants and smoke suppressors functioning in the solid phase instead of the gas phase. The smoke suppression mechanism of molybdenum compounds are most likely through the Lewis acid (LA) mechanism that promotes the formation of a carbon layer and in turn reduces the amount of smoke. It has been proved that the flame-retardant properties of molybdenum trioxide are not affected by oxidation medium during combustion, and 90% or more of the molybdenum is present in the char residue in the condensed phase during the combustion of the PVC of ammonium molybdate. In addition, the amount of char retained in the test samples is more than double after adding two phr of molybdenum trioxide into the semi-rigid PVC. This is consistent with the flame-retardant mechanism in the solid phase. It is proposed that the addition of molybdenum compounds into PVC catalyzes the dehydrochlorination of PVC to form trans-polyenoid, which cannot be cyclized into aromatic rings that are the main components of smoke. Some hold that molybdenum compounds can form crosslinked polymer chains by metal bonding or reductive coupling of the carbon-chlorine bond to reduce the contribution of combustibles to the fire. It is also suggested that molybdenum compounds can form the nucleus of aromatic smoke, which are firmly bonded into the

metal/aromatic polymer composites. The exact smoke suppression mechanism of molybdenum compounds is still uncertain. [9–11].

The smoke suppression of MoO_3 to PVC is considered to be carried out mainly in the condensed phase, and its mechanism is shown by eq. (7.1) [9]

(7.1)
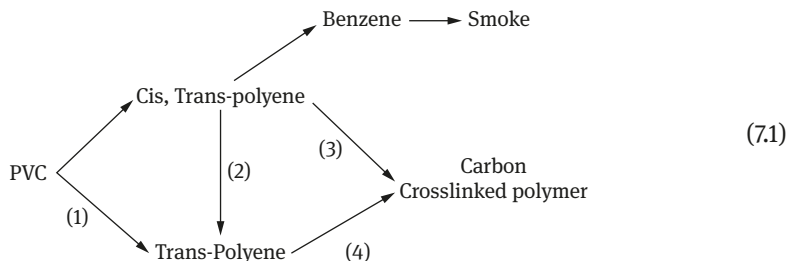
Hence, smoke suppression of hexavalent molybdenum may be because of the catalytic effects of the following three reactions, (1) PVC dehydrocholorides to form trans-polyenoid; (2) cis-form polyenoid isomerizes to form trans-polyenoid (3) Polyenes crosslink through Friedel-Crafts alkylation reaction or a Diels-Alder cyclization reaction. When PVC dissociates to form a large number of trans-polyenoids, the amount of benzene can be reduced because it needs at least 1 Mol of cis-form diene to form 1 Mol benzene.

The crosslinking of carbocation led by Friedel-Crafts reaction can be described by the following reaction: the Lewis acid captures chlorine from PVC to form a carbocation which is then alkylated to polyenes (eq7.2) [9]

(7.2)
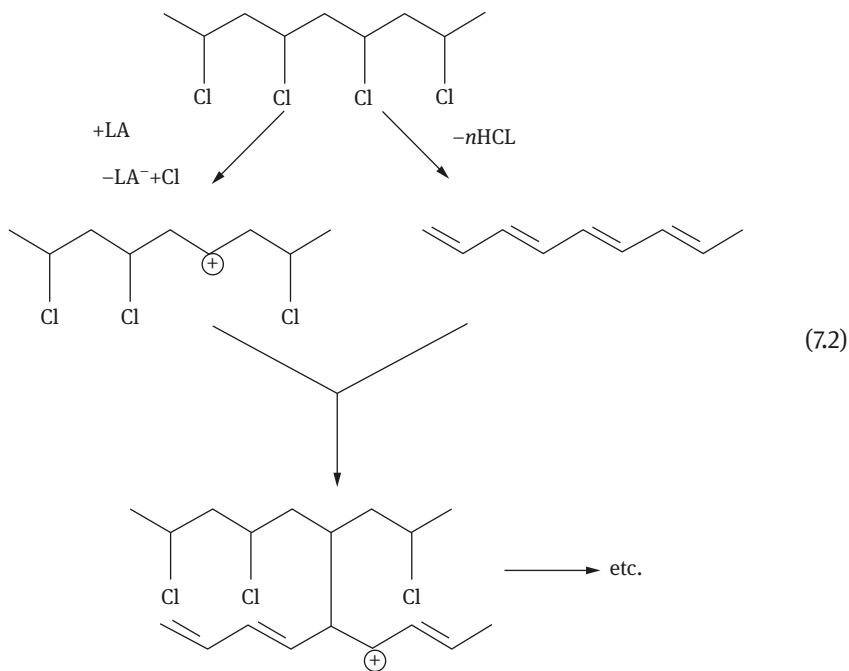
Hexavalent molybdenum compound mainly promotes the isomerization of polyene at approximately 200 °C (changed from the cis form to trans form). At high temperature, the cracking reaction of cationic of polyene occurs which increases the amount of fuels that can be combusted in the gas phase, hence reducing the amount of smoke while improving the flame propagation. Therefore, if the acidity of Lewis acid is weak, it is useful for the smoke suppression of PVC, however if the acidity of Lewis acid is strong, it may have a negative impact on flame retardancy.

MoO_3 mainly acts as a coupling agent of the Lewis acid, while its role of acting as a reductive coupling agent is not important. There is significant evidence to prove this. First, the reductive coupling agent should be able to suppress the dehydrochlorination of PVC, but MoO_3 can significantly increase the speed of dehydrochlorination of PVC, which is the function of the Lewis acid. Second, Mo (IV) is not easily oxidized and cannot directly promote reductive coupling. For reductive coupling, Mo (IV) must have thermal reducibility.

Finally, any PVC treated by MoO_3 or MoO_2Cl_2 has failed to provide reliable evidence of reductive coupling reactions. Similarly, some high-valence iron compounds and certain metal salts are also Lewis acid smoke suppressors.

7.3 Smoke suppression mechanism of iron compounds

Currently, ferrocene is a frequently used smoke suppressor, which is a type of iron compound. Ferrocene has no impact on the flammability and char yield of PVA, but in the case of PVC, it increases the char yield by 20%–60% and relatively improves the oxygen index by 15%–19%. Ferrocene, however, considerably reduces the amount of visible smoke during the combustion of both polymers (PVA and PVC). The influence of ferrocene on the amount of visible smoke is also related to the molecular weight of PVC. Ferrocene can accelerate the loss of thermal mass and crosslinking of PVC in its primary stage based on thermal analysis.

Ferrocene can suppress smoke in both the gas phase as well as condensed phase. The mechanism of smoke suppression is related to the structure of the polymer, in particular, smoke suppression is related to whether polymers contain halogen. For example, for ABS, ferrocene suppresses smoke mainly in the gas phase; on the contrary, for styrene-acrylonitrile-chloroprene terpolymer containing chlorine, it suppresses smoke in the condensed phase [9].

The role of ferrocene and two other organic iron compounds in halogen-containing and halogen-free ABS polymers is shown in Table 7.4 [9]. The data in Table 7.4 shows that, for the halogen-free ABS, there is a good correlation between the amount of reduced smoke and the amount of volatilized metal compounds; whereas for styrene-acrylonitrile-chloroprene terpolymer (ACS) containing chlorine, the situation is just the opposite. This proves that, for halogen-containing polymers,

Table 7.4: Smoke suppression effect of organic iron additives [9].

Polymers	additives		Dm	Dm reduction amount /%	The amount of volatile metal /%
	Category	Addition amount (according to iron)/g $(100g)^{-1}$			
ABS	None		440		
	Ferrocene	5.0	130	70	100
	Benzoyl ferrocenes	2.5	175	60	60
	Iron acetylacetonate	2.5	310	30	20
ACS	None		500		
	Ferrocene	5.0	380	24	100
	Benzoyl ferrocenes	5.0	310	38	60
	Iron acetylacetonate	5.0	225	55	20

iron compounds suppress smoke in the condensed phase, whereas for halogen-free polymers, iron compounds suppress smoke in the gas phase.

One of the smoke suppression mechanisms of ferrocene and its derivatives of PVC (below is the same) is the formation of highly-active free radicals triggered in the gas phase (such as OH·); these free radicals then oxidize the smoke particles into CO, see reaction eq. (7.3) [11]

$$C(s) + OH^{\cdot} \xrightarrow{CO} H^{\cdot} \qquad (7.3)$$

In addition, ferrocene and some metallic compounds (such as V_2O_5 and CuO) can convert some decomposition products formed by PVC into CO, thus reducing smoke generation.

Moreover, ferrocene and some other metallic compounds can also passivate the nuclear center and growth steps of the ionization, thus distracting the nucleation reaction in the formation of soot. In this case, the metal which is heat ionized or catalyzed ionizabled that firstly attacks nucleation centers, the nucleation centers are subsequently passivated. Meanwhile, the function of ferrocene or metallic compounds that can occur during the early stages of combustion and lead to the formation of OH, i.e., soot precursor that is the fused ring aromatic compounds will be reduced or disappeared, if oxidized. Hence, ferrocene and some metallic compounds may restrict the formation of benzene and other aromatic compounds in the gas phase.

Smoke suppression effect of ferrocene and several metal oxide compounds in the condensed phase is to promote PVC surface dehydrochlorination and crosslinking carbonization reaction [13]. In the presence of HCl and trace amounts of oxygen, ferrocene can form ferrocene positive ions, which may be used as Lewis acid to catalyze the dehydrochlorination, crosslinking and carbonization reactions.

FeCl$_3$, a strong Lewis acid, is also considered to be an effective smoke suppressor system and a carbonization agent containing PVC. FeCl$_3$ is a catalyst of Friedel-Crafts-type reaction, and it can be coupled with alkyl chloride (eq. 7.4) and the remaining aromatic compounds in the condensed phase to reduce smoke generation and improve char yield [11]. The formed reactive char residues may also eliminate H· and ·OH radicals formed during the continuous combustion reaction. Lewis acids such as FeCl$_3$ have also been used in a range of high polymers, including polyesters, polyurethane and PS, resulting in reducing the materials' flammability and increasing the char yield.

$$(7.4)$$
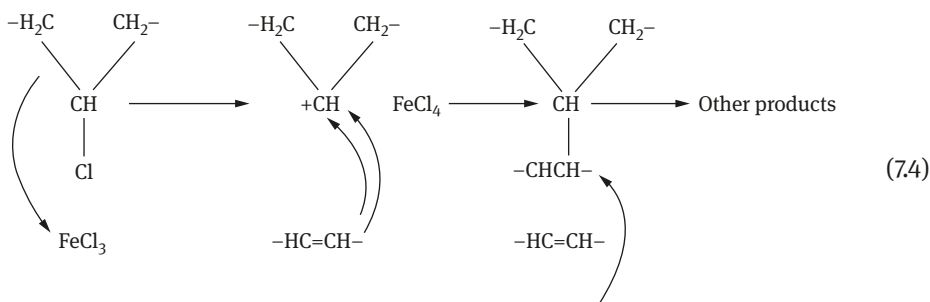
7.4 Reductive coupling smoke suppression mechanism

Some additives containing low-valence transition metals can promote PVC crosslinking for smoke suppression through the reductive coupling mechanism of polymer chains. Smoke suppressors that can facilitate this coupling process are zerovalence metal compounds formed during the pyrolysis of PVC, including phosphite esters and other clathrates of monovalent copper, a series of low-valence transition metal carbonyl compounds, formates and oxalates, monovalent copper halides, etc. Because of the low acidity of the reductive coupling, they do not lead to cracking of cations in the char residue. Therefore, using this kind of low-valence transition metal coupling agent instead of Lewis acid crosslinking agent for PVC smoke suppression is attractive.

Some divalent transitional metal oxalates and formates which are decomposed at temperatures ranging from 200 °C to 300 °C are usually effective crosslinking agents of PVC, and hence can be used as smoke suppressors [15, 16]. Zero-valence metal is formed through reductive reaction, see reaction eqs (7.5) and (7.6)

$$MC_2O_4 \rightarrow M + 2CO_2(g) \tag{7.5}$$

$$M(O_2CH)_2 \rightarrow M + CO_2(g) + H_2O(g) + CO(g) \tag{7.6}$$
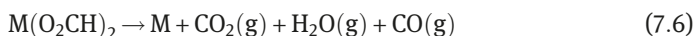
A series of transition metals such as oxalates and formates have been used as smoke suppressors for PVC. At temperatures of 200 °C–300 °C, decomposed oxalates and formates are usually more effective crosslinking agents.

When additives with transition metals suppress smoke through polymer chains reductive coupling mechanism promoting crosslinking, the crosslinking can occur below 200 °C in the solid PVC. When the coupling agent is Cu (0), reductive coupling of allyl chlorides is most likely to occur. However, other collateral couplings cannot be completely ruled out. Clear evidence of reductive coupling are fast jelling of polymers while the overall mass loss rate is reducing (tested by TGA), formation of double bonds (tested by FTIR) and the release of HCl (tested by acid-base titration) [15, 17, 18]. Reduction reaction and coupled reaction of simple allylhalides and benzyl halides promoted by low-valence organic metal clathrates proceed according to the eqs. (7.7) to (7.9) [14, 15].

$$2 \quad \overset{\text{CuOAc}}{\underset{H_2NCH_2CH_2NH_2}{\longrightarrow}} \quad (7.7)$$

$$2 \quad \overset{\text{CoCl(PPh}_3)_3}{\longrightarrow} \quad (7.8)$$

$$2 \quad \overset{\text{Fe}_3(CO)_{12}}{\underset{\text{Pyridine nitrogen oxide}}{\longrightarrow}} \quad \text{Isomer} \quad (7.9)$$
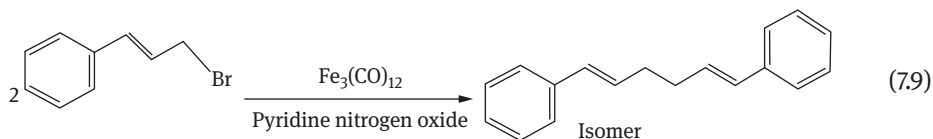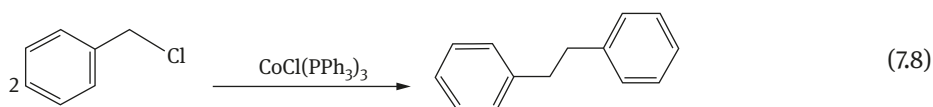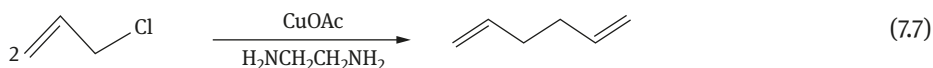
Some suspended solids of high-reactivity metal powders with zero-valence can promote reductive coupling of allylhalide and benzyl halides. Sometimes it can promote the reductive coupling of alkyl halide and aryl halide (eq. 7.10).

The mechanism of the abovementioned coupled reaction perhaps involves the oxidative addition of organic halides to metal centers, which changes the oxidation state of the metal from 0 to II or from I to III, forming dihalide and dialkyl group metallic compounds. The initial metals and C-C bonds are easily formed through reduction elimination reaction by the latter. However, the abovementioned reaction involves the mechanism of free radical intermediate.

The following reaction proposes that reductive coupling of PVC occurs under the condition of dissociation. Therefore, the products of degraded PVC possibly contain allylhalides groups, which are the reactive center of dehydrochlorination and the formation of polyenoids. Reductive coupling of allylhalide on the chains of the neighboring polymers leads to a crosslinking reaction.

(7.10)
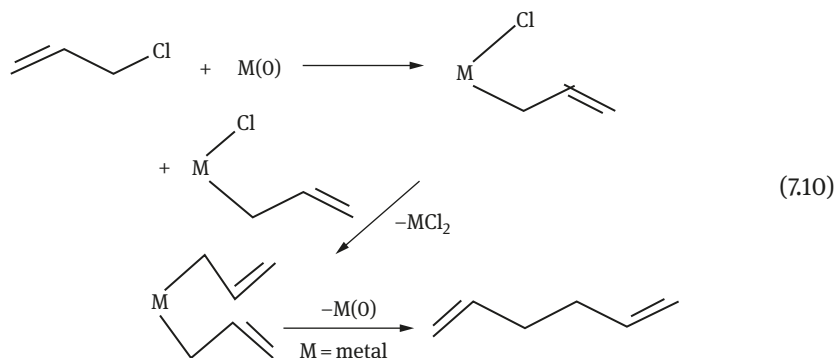
Furthermore, the coupling can make the allyl halide unreactive, thus terminating the transmission of dehydrochlorination along with the polymer chains (eq. 7.11) [9, 15].

(7.11)
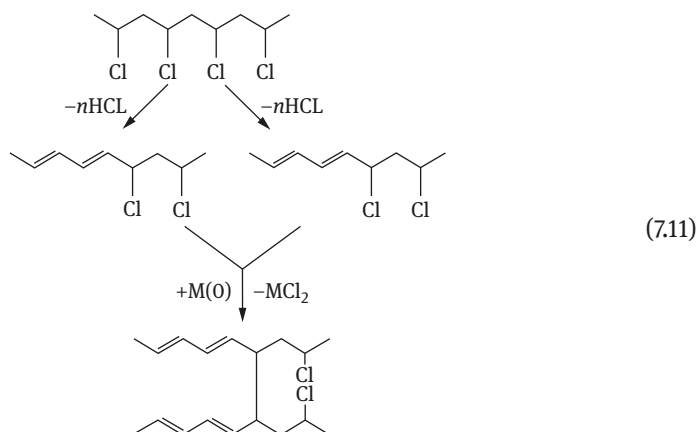
Compared with the Lewis acid, the smoke suppression as a result of reductive coupling has the following advantages. First, each reductive coupling crosslinking can terminate the growth of two polyene chains at the same time, which can slow down the degradation of polymer. Especially for the reaction at the allyl position, reductive coupling crosslinking can inhibit thermal degradation in the early stages. Second, to some extent, coupling might possibly happen at the position of a non-allyl group, which can delay the dehydrochlorination of PVC. The relatively short polyene chains formed by the allyl coupling can restrict the amount of benzene and other arenes generated during the pyrolysis of PVC. The easily reductive metallic additives are not only reductive coupling agents but are also typical weak Lewis acids, therefore, these metallic additives can also catalyze the crosslinking of some Friedel-Crafts reactions, which are beneficial to flame retardancy and smoke suppression, but cannot promote the cracking of carbon layers.

A reductive coupling agent should have the following capabilities: ① Metallic ions can be easily reduced to zero-valent metals; ② In metallic compounds, metals should be at a relatively low oxidation state; or metal clathrates have oxidizable ligands which can be eliminated by thermal reduction, thus forming low-valence or zero-valence metals; ③ Metallic ions can only be reduced at temperatures considerably higher than the polymer processing temperature; ④ The reductive coupling agents should be inexpensive, colorless and should have no adverse effects on the polymer formulas; ⑤ Over-crosslinking should not be caused within the processing temperature and time of PVC.

Copper is one of the most effective additive agents for PVC smoke suppression employing the reductive coupling mechanism. For example, copper compounds can dramatically reduce the amount of benzene formed during PVC dissociation. However, when the temperature is within 200 °C–300 °C and Cu_2O is present in PVC, the crosslinking degree of PVC is greatly improved and the amount of smoke generated is largely reduced. In addition, cuprous and cupric compounds can be used as weak acid catalysts to promote the alkylation of Friedel-Crafts reactions.

Cuprous clathrate is a coupling smoke suppression agent which has the most potential applicable value because of its excellent color and thermal stability that can be adjusted through ligand selection. The phosphate esters and clathrates of copper as smoke suppression agents have better impact on the crosslinking of PVC.

The active zero-valent copper can also catalyze the reductive coupling reactions of interchains of PVC, which results in the crosslinking of polymers; the active zero-valent copper then boasts of smoke suppression property. Even at a temperature of 66 °C, the active zero-valent copper can cause intense crosslinking of PVC. However, zero-valent metals which are simply blended with polymers can not only improve the processing difficulty of polymers but can also not serve as good smoke suppression agents because such a metal powder will be oxidized by the surrounding air, which is detrimental to smoke suppression. Therefore, PVC smoke suppressants with good application prospects should be metal compounds that can produce free metals during thermal decomposition.

7.5 The smoke suppression mechanism of Mg-Zinc compounds

The effects of flame retardancy and smoke suppression of Mg-Zinc compounds in semi-rigid PVC are mainly worked in the solid phase by catalyzing solid phase decomposition, promoting the formation and restructuring of the char layer, such that it can reduce the formation of benzene and volatile hydrocarbons (lower 1/3–2/3), more part (70%) remains in the carbon layer. The formation of dense and low fragile carbon layers and the decrease in total organic volatile compounds can account for the flame-retardant properties of the additive, whereas the remarkable reduction in the release of benzene is the main reason for the high

smoke suppression efficiency of the additive. It is supposed that the reactions between Mg-Zinc compounds and HCl released from PVC form solid metal chlorides, which can suppress smoke by interrupting the recombination reaction between the chlorine atom and polyene (formed during the initial phase of the thermal decomposition of PVC). The recombination of chlorine atom and polyene largely depends on the irregularity of bonding structures, which can affect the decomposition of polyene bonds and change the smoke generation ability of PVC.

7.6 The smoke suppression mechanism of other smoke suppressors

Some metallic (Ba, Sr, Ca) oxides can also clear soot because they can catalyze hydrogen molecules and decompose water molecules to produce H·. H· can further react with water to form OH·, which can turn soot into CO by oxidation of coal according to eq. (7.3) [see eqs. 7.12–7.15] [11].

$$MO + H_2 \rightarrow MOH + H \cdot \qquad (7.12)$$

$$MOH + H_2O \rightarrow M(OH)_2 + H \cdot \qquad (7.13)$$

$$M(OH)_2 + (X) \rightarrow MO + H_2O + (X) \qquad (7.14)$$

$$H \cdot + \ H_2O \rightarrow OH \cdot + H_2 \qquad (7.15)$$
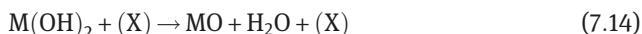
The abovementioned mechanism of smoke suppression can also account for the smoke suppression effect of transition metals and oxides formed by dicyclopentadienyl iron (as α-Fe_2O_3).

ZS and ZHS are efficient flame retardants and smoke suppressants for many synthetic high polymers because they undergo synergistic reactions with halogenated polymers and halogen-containing polymers. ZHS and ZS can diminish the generation of smoke, CO_2 and CO during combustion. In addition, they are less toxic, safe and effective at low dosages.

Although the mechanism of ZHS and ZS remains unknown, they may act in two possible ways: ① accumulate char formation from the crosslinking reaction in the condensed phase resulting in the reduction of combustible volatile products. ②form volatile tin compounds which act as gas phase catalyst to promote the transformation of CO and soot inflame zone. The accurate effect of tin compounds hinge on their dosage, other additives within the system and the structures and properties of flame-retardant high polymers [20].

Substituting PS bond with non-aromatic bonds (such as methyl methacrylate or ethyl acrylate) to crosslink unsaturated polyesters can substantially lower smoke density [21]. Using carboxylic acids (such as fumaric acid and maleic acid) to

crosslink unsaturated polyesters is also effective in smoke suppression. Substances that can promote carbonization can also be used as smoke suppressors of unsaturated polyesters. For example, organophosphate can dehydrate resins and produce polyphosphoric acid, and when heated, the latter can form a protective layer for resins to suppress smoke.

For some chlorine-containing unsaturated polyesters, Fe_2O_3 can be used as smoke suppressing agent because with the chlorine source, for example, in unsaturated polyesters acted on by HET acid as flame retardant, if Fe_2O_3 is added, the latter changes into $FeCl_3$. $FeCl_3$ is a known strong Lewis acid, which is conducive to crosslink unsaturated polyesters and promote carbonization. Meanwhile, $FeCl_3$ is also a catalyst for Friedel-Crafts reaction because it can accelerate the coupling reaction between alkyl chloride and aromatic compounds to keep aromatic compounds inside, thus the amount of smoke released is reduced [21].

The use of isocyanuric acid ester, imide and carbodiimide can intensify the degree of crosslinking of polyurethane foam plastics during production, and this kind of crosslinking structure is beneficial to carbonization and smoke suppression. Solid dicarboxylic acid, such as maleic acid, m-phthalic acid and HET acid, have similar effects [22, 23]. It has been reported that some alcohols, such as furfuryl alcohol, is also a good smoke suppressing agent for polyurethane foam plastics [24], the mechanism of which perhaps is that this kind of alcohol can clear off polyisocyanate caused by polyurethane's thermal decomposition and polyisocyanate is the precursor of dense smoke. Moreover, after alcohol has been oxidized to aldehyde, aldehyde through a Schiff alkali reacts with polyisocyanate and isocyanate, forming a crosslinking structure in the condensed phase. Many phosphorus compounds can also be used for promoting carbonization and smoke suppression of polyurethane foam plastics. In addition, dicyclopentadienyl iron, some metal chelates and potassium tetrafluoroborate or ammonium tetrafluoroborate are also effective smoke suppressing agents for polyurethane foam plastics because all of them have similar effect as Lewis acid in the condensed phase.

Some inorganic and organic iron compounds also can be used as smoke suppressing agents for PVC and PVC blends. For example, ferric oxide hydrate is effective in suppressing the smoke of PVC-C/ABS blends. Because, on the one hand, FeOCl and/or $FeCl_3$ formed originally can catalyze the crosslinking of Lewis acid and then produce large amount of carbon; on the other hand, $FeCl_3$ reacts with benzene produced during the decomposition of PVC and PVC-C and then produce chlorinated aromatic compounds [25, 26].

8-quinolinol heavy metallic (Fe, Mn, Cr) salt, copper salts, lead salt and free radical initiator of phthalocyanine (for instance tetraphernl-lead) can react with aromatic compounds in the gas phase, and therefore, all can be used as smoke suppressing agents for styrene plastics [27]. Recently, the properties and smoke

suppression mechanisms of a new metal hydroxides [28] and thermal decomposition silica gel [29] in styrene plastics were reported.

Adding some polymers produced by the crosslinking of silane into PE/metal hydroxides can substantially improve the flame retardancy and smoke suppression properties of materials, which is also applicable to other plastics [30]. As a smoke suppressing agent, zinc borate is applicable to a series of plastics such as PVC, polyolefin, polysiloxane and fluoroplastics. Apart from suppressing smoke, zinc borate also possesses properties such as flame retardancy, anti-smoldering, electric arc resistance and promoting carbonization.

Smoke suppression of plastics is a complicated issue that requires understanding the mechanism of smoke formation and methods of controlling the combustion of materials. Some achievements have been made in this field, for example, relevant comprehensive theses have been issued concerning the mechanism of smoke suppression for molybdate [4], achievable approaches for suppressing smoke, mechanisms of smoke suppression and combustion [5], the impact of fillers to the amount of smoke and toxic gases generated [31].

Nowadays, flame retardancy and smoke suppression have been given equal importance because a flame-retardant material with large smoke generation has little applicable value. Therefore, smoke suppressing agents and their mechanisms have been given high importance in recent years. Currently, several smoke suppressing agents and their mechanisms mainly aim at PVC, but more and more are being applied to other plastics. Effective smoke suppressing agents include molybdenum compounds (AOM, MOM and MoO_3), iron compounds (dicyclopentadienyl iron), metal compounds, zinc stannate and Mg-Zinc compounds. Approximately 2%–4% of such smoke suppressing agents can reduce the amount of smoke generated by PVC and styrene plastics by 30%–50%, while improving the flame retardancy of plastic.

The low-valence transitional metal compounds being researched and developed are reductive coupling smoke suppressing agents and new flame retardants, some of which can be used in smoke suppression of PVC as a substitute for some Lewis acid smoke suppressing agents.

References

[1]   Ou Yuxiang. The Flame Retardants[M]. Beijing: WeaponIndustry Press, 1997: 219–226.
[2]   Whitman P A. Ammonium Polyphosphate and Melamine Phosphate Flame Retardants [A]// The Seminar Proceedings of the Latest Research Progress of the Second Flame-Retardant Technologies and Materials [C]. Beijing: Beijing Institute of Technology, 2004: 14–31.
[3]   Stec A A, Hull T R, Lebek K, et al. The Effect of Temperature and Ventilation Condition on the Toxic Product Yields from Burning Polymers [J]. Fire and Materials, 2008, 32(1): 49–60.
[4]   Innes J D, Cox A W. Smoke: Test Standards, Mechanisms, Suppressants [J]. Journal of Fire Sciences, 1997, 15(3): 227–239.
[5]   Green J. Mechanisms for Flame Retardancy and Smoke Suppression.A review [J]. Journal of Fire Sciences, 1996, 14(6): 426–442.

[6]   Ou Yuxiang, Chenyu, Wang Xiaomei. The Flame-Retardant Polymers Materials [M].Beijing: National Defence Industry Press, 2001: 26–27.

[7]   Ou Yuxiang. Applied Flame-Retardant Technologies [M]. Beijing: Chemical Industry Press, 2003: 39–40, 169.

[8]   Ou Yuxiang, Li Jianjun. The Flame Retardants [M]. Beijing: Chemical Industry Press, 2006: 37–39.

[9]   Li Jianjun, Huang Xianbo, Cai Tongmin. Flame-Retardant Polystyrene Plastics[M]. Beijing: Science Press, 2003: 84.

[10] Troitzsch J. Interntional Plastics Flammability Handbook [M]. Munich: Hanser Publishers, 2004: 197–205.

[11] Lawson D F. Investigation of the Mechanistic Basis for Ferrocene Activity During the Combustion of Vinyl Polymers [J]. Journal of of Applied Polymer Science, 1976, 20(8): 2183–2192.

[12] Ou Yuxiang, Wu Junhao, Wang Jianrong. The Reductive Coupling and Smoke Suppression Agents of Polyvinyl Chloride [J]. Polymer Materials Science and Engineering, 2003, 19(4): 6–9.

[13] Al–Malaika S. Chemistry and Technology of Polymer Additives [M]. New York: Blackwell Science Publishers, 1999.195–216.

[14] Gorski A, Krasnicka A. Formation of Oxalates and Carbonates in the Thermal Decompositions of Alkali Metal Formats [J]. Journal Thermal Analysis, 1987, 32(6): 1895–1904.

[15] Hegedus L S, Thompson D H P. Reactions of π-Allylnickel Halides with Organic Halides. A Mechanistic Study [J]. Journal of the American Chemical Society, 1985, 107: 5663–5669.

[16] Yanagisawa A, Hibino H, Habaue S, et al. Highly Selective Homocoupling Reaction of Allylic Halides Using Barium Metal [J]. Journal of Organic Chemistry, 1992, 57(24): 6386–6387.

[17] Wang Jianrong, Tang Xiaoyong, Ou Yuxiang. The Effects of Flame Retardancy and Smoke Suppression of Zinc Stannate and Polyvinyl Chloride [J]. China Plastics, 2003, 17(4): 76–78.

[18] Selley J E, Vaccarella P W. Controlling Flammability and Smoke Emissions in Reinforced Polyesters [J]. Plastics Engineering, 1979, 35(2): 43–47.

[19] Lawson D F, Kay E L. New Developments in HFC-245fa Appliance Foam [J]. JFF/Fire Retardant Chemistry, 1975, 2: 132–137.

[20] Doerge H P, Wismer M. Polyurethane Foams with Reduced Smoke Level [J]. Journal of Cellular Plastics, 1999, 35(2): 118–125.

[21] Ashida K, Ohtani M, Yokoyama T, Ohkubo S. Epoxy-Modified isocyanurate foams [J]. Journal of Cellular Plastics, 1972, 8(3):160–167.

[22   Carty P, White S. A Review of the Role of Basic Iron(III) Oxide Acting as a Char forming/smoke Suppressing/Flame Retarding Additive in Halogenated Polymers and Halogenated Polymer Blends [J]. Polymer Composites, 1998, 6(1): 33–38.

[23] Carty P, Metcalfe E, White S. A Review of the Role of iron Containing Compounds in Char Forming Smoke Suppressing Reactions During the Thermal Decomposition of Semirigid Poly (vinyl chloride) Formulations. [J]. Polymer, 1992, 33(13): 2704–2708.

[24] Lawson D F, Kay E L, Roberts D F. Mechanism of Smoke Inhibition by Hydrated Fillers[J]. Rubber Chemistry and Technology, 1975, 48(1): 124–131.

[25] Horn W E Jr, Stinson J M, Smith D R. A New Class of Metal Hydroxide Flame Retardants. I. FR/SS Performance in Engineering Thermoplastics [A]//Proceedings of the 50th Annual Technology Conference Society Plastics Engineering [C]. 1992: 2020–2023.

[26] Chalabi R, Cullis C F, Hirschler M M. Mechanism of Action of Pyrogenic Silica as a Smoke Suppressant for Polystyrene [J]. European Polymer Journal, 1983, 19(6): 461–468.

[27] Yeh T J, Yang H M, Huang S S. Combustion of Polyethylene Filled with Metallic Hydroxides and Crosslinkable Polyethylene [J]. Polymer Degradation and Stability, 1995, 50: 229–246.

[28] Rothon R. Particulate-Filled Polymer Composites [M]. New York: John Wiley, 1995: 203.

8 Technical means on flame retardation mechanism

8.1 Cone calorimetry

8.1.1 Principles and measurable parameters

Cone calorimeter was successfully developed by Dr. Babrauskas of the U.S. National Bureau of Standards (NBS), now called the U.S. National Institute of Technology and Standards (NITS) [1] in 1982. At present, cone calorimeter has become one of the widely used equipment to determine the flame retardancy and flame retardation mechanism of materials. Figure 8.1 shows the basic structure of a cone calorimeter [2]. The working principle of a cone calorimeter is to calculate the heat released from the test samples when they undergo combustion under different external radiant heat sources by measuring the required amount of oxygen, because when high polymers consume 1 kg of oxygen during combustion, they release 13.1 mJ of heat [3]. For most plastics and rubbers, this value is almost the same, such that following flame retardancy parameters [3], including heat release rate (HRR), can be measured: ① the maximum HRR or peak heat release rate (PHRR) is the peak value of the HRR-time curve which reflects the maximum intensity of combustion, characterizing the spread and extent of combustion; HRR is regarded as the most important parameter to predict the combustion risk; ② the average heat release rate (mHRR), mHRR often refers to the average HRR from the ignition of the sample to combustion for 3 min; ③ the combustion thermal effects – effective heat of combustion (EHC), total heat release (THR); ④ the mass loss rate (MLR); ⑤ the amount of smoke generation (specific extinction area (SEA), smoke parameter (SP) = SEA × PHRR); ⑥ the combustion performance index (FPI), the ratio of time to ignition (TTI) to PHRR – the higher the ratio is, the smaller the combustion; ⑦ the generation volume of CO and CO_2; ⑧ the char yield; ⑨ the TTI, time required for the entire surface to produce sustained flame combustion, usually observed by visual determination.

8.1.2 Operation

In a cone calorimeter, the test sample under the heater is ignited. The surface area of the test sample is 10 cm × 10 cm, and the thickness can be up to 5 cm. If the surface is not very irregular, the test requirements can be satisfied. The radiation intensity of the heater is controlled by three evenly distributed thermocouple thermometers, which are usually set at 25 kWm^{-2}, 50 kWm^{-2}, 75 kWm^{-2} or 100 kWm^{-2} [3]. During measurement, the distance between the sample and heater is 25 cm, and the igniter should be placed 13 cm above the sample. After spark ignition, the
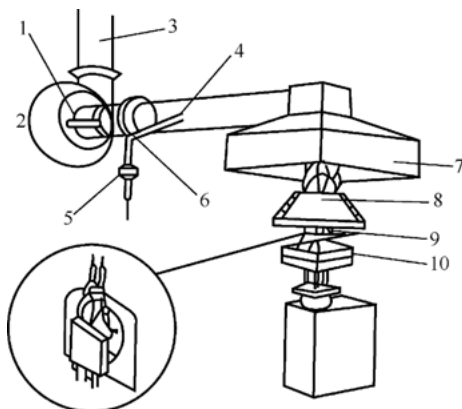
Figure 8.1: Basic structure of Cone Calorimeter [2]. 1 – Laser smoke meter and thermometer; 2 – Exhaust blowers; 3 – Thermometer and differential manometer; 4 – Ash sampling tube; 5 – Soot collector; 6 – Exhaust gas sampling tube; 7 – Exhaust hood; 8 – Cone heater; 9 – Electric igniter; 10 – Test sample.

combustion gas generated during the pyrolysis process will be dispersed through the exhaust system. By continuously measuring the oxygen concentration and flow rate of the exhaust system, the relationship between the HRR and time can be calculated. On choosing a sample in the exhaust system, the oxygen, carbon monoxide and carbon dioxide content in the exhaust gas can be analyzed using a gas analyzer. Test samples can be placed horizontally or vertically; however, the test samples and their brackets should be placed on a very sensitive balance to measure weight loss rate during combustion. However, samples with an uneven surface, very thin samples, as well as some composite materials do not fit in the cone calorimeter. The sampling system, oxygen analyzer and temperature controller of the cone calorimeter should be regularly calibrated.

Cone calorimeters are equipped with sophisticated and advanced testing systems (such as laser photometer) and data processing systems, which can automatically record the changes in the abovementioned flame retardancy parameters during the testing process; moreover, cone calorimeters can be combined with a variety of chemical measuring instruments as per the user demand, for example, the online Fourier transform infrared spectroscopy (FTIR), the latter can identify a variety of products generated during the combustion of materials. Exhaust gas samples can also be collected using an exhaust gas sampling tube, following which oxygen, carbon monoxide and carbon dioxide can be measured by a gas analyzer. Some previous studies have recorded the HRRs of many materials measured by the cone calorimeter. A previous study also proposed a simplified cone calorimeter, which measures the weight loss rate of materials and temperature instead of measuring oxygen consumption. The typical HRR and MLR curve measured by cone calorimeter is discussed in Chapter 6.

8.1.3 Features

Cone calorimeters have the following features [4]: (1) they do not require heat insulation while determining the heat release, and can conduct combustion in open conditions; the reaction can also be visually observed; (2) the design of the cone calorimeter can balance the heat distribution of samples on the surface; (3) monochromatic light is adopted to measure the smoke generation property; (4) horizontal placement of the sample is good for heat distribution. In addition, cone calorimeters can also be used to assess the overall performance of materials related to combustion hazards, such as the smoke parameter (Sp) (the product of maximum HRR and average specific extinction area or the product of HRR and the specific surface area) of materials and smoke factor (Sf) (the product of the total amount of smoke and HRR). Previous experiments have proven that Sp measured using a cone calorimeter has a certain relationship with the extinction coefficient (Ce) measured using a large-scale combustion test (Formula 8.1) [2]:

$$\lg S_p = 2.24 \lg C_e - 1.31 \tag{8.1}$$

There are at least four additional correlations for the test results of a cone calorimeter [4]: (1) the specific peak extinction area is parallel to the peak measured by the calorimeter; (2) the specific extinction area of simple fuels combusted in a conical calorimeter can be well connected to that of similar fuels combusted at a similar rate in large-scale experiments; (3) the maximum HRR predicted by cone calorimeter data correlates well to the results of the corresponding large-scale combustion test; (4) the function of the total heat release and ignition time can accurately predict the flash time of some wall lining materials large-scale experiments.

Cone calorimeter can also be used to study the pyrolysis and the related kinetics of polymers during combustion, and the result is more consistent with the behavior of the polymers during the combustion stage than that using the thermogravimetric method because the cone calorimeter can provide better heat, heating rate and heat transfer mode, which is close to the real fire hazard.

8.2 Radiation gasification assembly

Radiation gasification assembly (RGA) was developed at the end of the 20th century in the U.S. to provide evidence for the deduction of flame retardation mechanism, and can be used to simulate the thermal decomposition of polymer materials of the

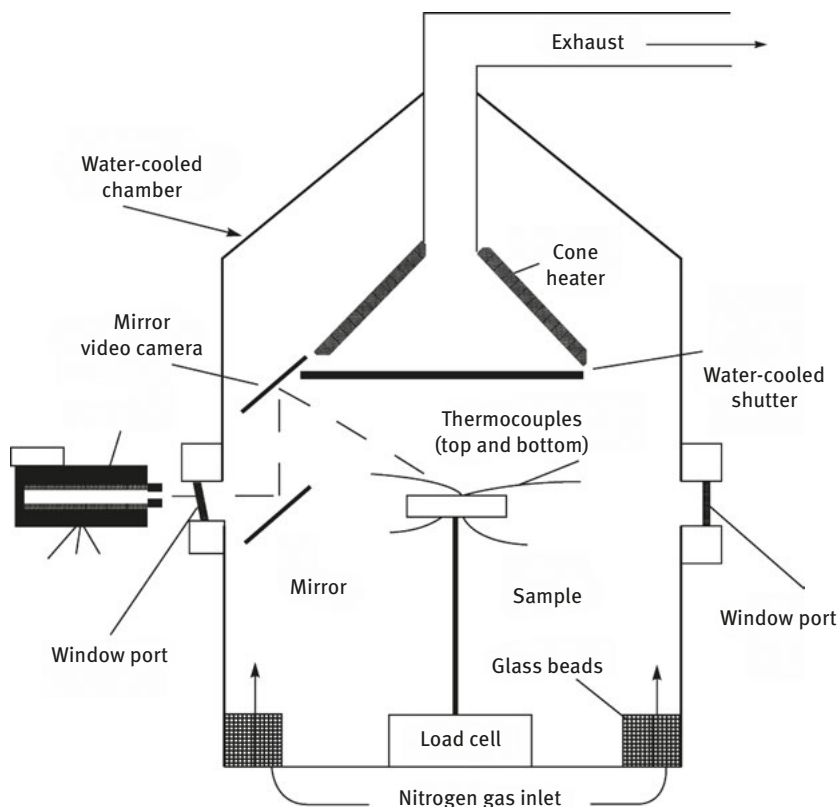solid phase in combustion heat radiation. The schematic of the structure's device is shown in Figure 8.2 [5].

Figure 8.2: Schematic drawing of RGA [5].

For RAG measurements, materials placed in a single inert gas atmosphere (e.g., N_2, air excluded) only undergo single pyrolysis rather than oxidation pyrolysis and combustion, thus preventing interference in pyrolysis in the solid phase of materials from combustion flame. However, in an oxygen atmosphere, RGA may cause combustion reaction.

RGA is equipped with a water cooling device that can stop the pyrolysis or combustion at any time. Thus, it can help to get a series of solid phase residues from pyrolysis or combustion, which is very helpful to understand the process of pyrolysis or combustion as well as analyze the flame retardation mechanism.

RGA can be used to determine the MLR of the samples during pyrolysis or combustion and the bottom surface temperature of the samples. The measured MLR can be associated with the HRR measured by the cone calorimeter because MLR is

caused by volatile gases produced during pyrolysis or combustion; further, the combustion of gaseous products releases heat during combustion with oxygen.

Similar to the cone calorimeter, RGA also has a cone heater, with temperature measured by a thermocouple, providing heat flux close to combustion conditions. RGA also has a visible window and camera that can observe the morphology of the samples at different stages of pyrolysis or combustion.

The gaseous products produced during pyrolysis or combustion in RGA can be sent separately and identified by the online detector. Solid phase residues are often observed by wide-angle X-ray diffraction (XRD) and transmission electron microscopy (TEM). The MLR curves measured by a radiation gasification device have been discussed in Chapter 6.

8.3 Laser pyrolysis device

Laser has the characteristics of large energy density and short heating time (100 μm~500 μm), which fits the pyrolysis speed of high polymers. In addition, fewer secondary reactions occur in the laser pyrolyzer (LP), and hence, the graph is relatively simple. However, the shape, color and dosage of samples used in LP affect the results. To obtain better reproducibility, the amount of samples should not be too much due to the limited depth of penetration of the laser. Furthermore, the temperature of LP can neither be measured nor be accurately controlled. Figure 8.3 shows an LP device that can be used to study the flame retardation mechanism of polymer nanocomposites.
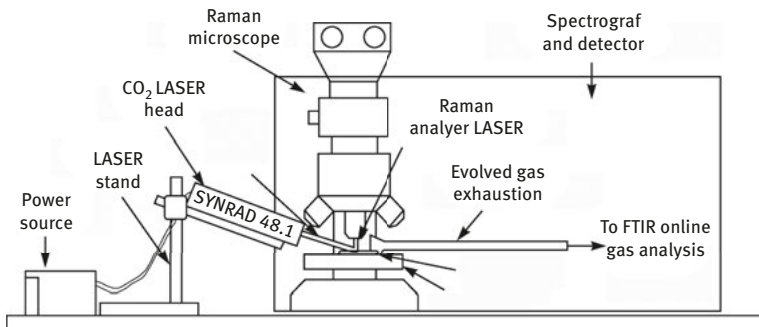
Figure 8.3: Laser pyrolysis device [6].

The LP shown in Figure 8.3 is equipped with a CO_2 laser and Raman-infrared microscope. When the CO_2 laser beam is incident on the samples, it is still within the infrared range and can simulate combustion effects on the samples. LP is installed with a universal laser controller, which can control laser power by pulse width modulation (PWM). For lasers, the standard frequency is 5 kHz, and its power can be changed.

The cycle of the samples irradiated by the laser can be modulated through grid control. The pyrolyzer is installed on the chassis. With the help of a special reflector, CO_2 laser beam can be focused on the surface of the samples. The samples are placed on top of the probe before irradiated by the laser, namely when they are; the probe is located under a Raman-attenuated total reflection infrared (ATR) microscope.

The gaseous products generated by the pyrolysis of the samples are analyzed using an online infrared spectrometer, and the chemical changes and morphology on the surface of the samples are monitored using Raman microscopy technology or ATR technology. Raman microscopic analysis helps characterize the structure of the solid phase of the samples and the interaction in multicomponent.

Microthermal deformation on the surface of the samples and thermal conductivity of the samples are measured using microthermal analyzer. The measuring temperature range is from 25 °C to 250 °C, and the heating rate is 5 °C/s [6]. Scanning electron microscope (SEM) is used to analyze the additives in the samples.

8.4 Differential thermal analysis and differential scanning calorimeter

8.4.1 Fundamental principles

The differential thermal analysis (DTA) measures the temperature difference (ΔT) between the samples and the reference materials at temperature (T) or change in time (t), that is, when the samples and the reference materials (a-Al_2O_3, silicone) are heated or cooled under the same temperature, the temperature difference (ΔT) with the change in temperature (T) or time (t) are measured in DTA; further, a DTA curve is plotted to analyze the thermal behavior of the sample.

There are two kinds of differential scanning calorimeters (DSC), namely, heat flux differential scanning calorimeter and compensatory differential scanning calorimeter. The principle of the former is similar to that of DTA, but is more accurate than DTA in quantitative analysis. The latter determines the relationship between the required heat and temperature (T) when maintaining the temperature difference between the samples and the reference materials as zero. The samples and reference materials (or the use of an empty vessel without a reference material) of the compensatory DSC require respective heaters and detectors, and regardless of the endothermic or exothermic nature of the samples, both the samples and reference materials can maintain the same temperature during the temperature programing (or cooling/constant temperature) as the compensator can increase or decrease heat. Only while measuring the compensation power can the curve of the relation between the heat flow rate (dH/dt) and temperature (T), namely the DSC curve, can be obtained. Heat flux DSC and compensatory DSC are illustrated in Figure 8.4 [7], and typical DTA and DSC curves are shown in Figure 8.5 [9, 10].
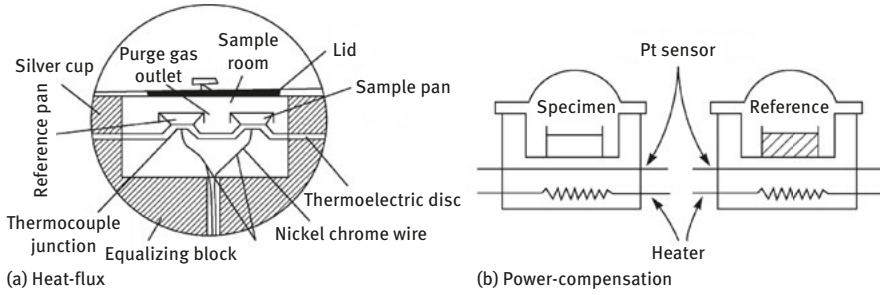
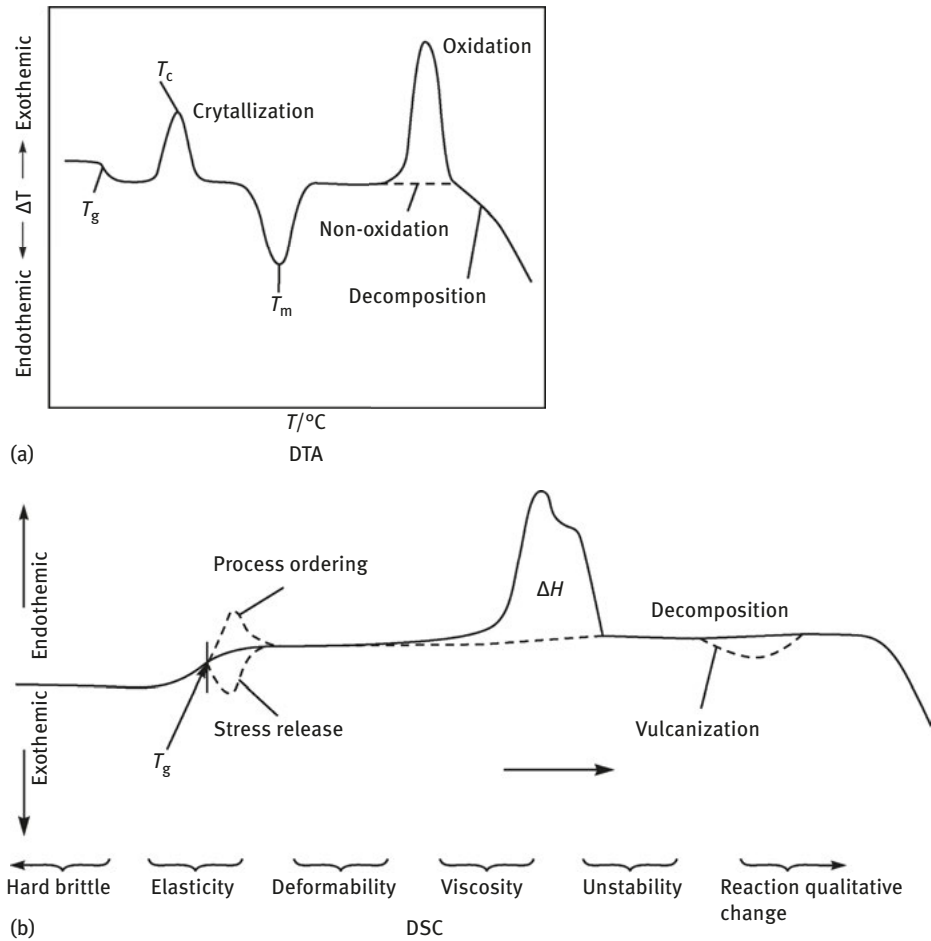**Figure 8.4:** Schematic diagram of DSC [7, 8].

Figure 8.5: DTA and DSC curve of typical polymers [9, 10].

DTA usually qualitatively determines the transformation temperature of the samples according to the position of the peak. As the accuracy of the quantitative processing is poor, it is frequently used in inorganic analysis. On the other hand, the resolution, reproducibility and accuracy of DSC are better than that of DTA, and hence can be used for quantitative processing and are also suitable for polymer determination.

DTA is suitable to measure high temperatures (up to 1500 °C~1700 °C, ultrahigh temperature furnace can be up to 2400 °C), whereas DSC only reaches 700 °C. The position of the peak of the DTA and DSC curves can decide the corresponding temperature change. The area of the peak can help determine the changing thermal effect, and the shape of the peak can help understand the dynamic characteristics of transformation.

8.4.2 Operation

Both solid and liquid samples can be for DTA and DSC. Solid samples should be paved in vessels as densely and uniformly as possible to increase the packing density and reduce the thermal resistance between the samples and the vessels. For volatile liquids, a pressure-resistant sealed plate should be used. An aluminum dish should be used in DTA and DSC; however, when the temperature is above 500 °C, plates resistant to high temperatures should be used (such as platinum, aluminum oxide, graphite).

Before or after using the thermal analyzer, the baseline temperature and heat should be calibrated. The baseline should be straight, without any curves or slopes, and should not exhibit endothermic or exothermic peaks. The temperature and heat should be calibrated according to the melting point and melting heat of standard pure substances within the temperature range.

The main factors that affect the measurement, including sample volume, heating rate and atmosphere, need to be marked out in the measurement result.

The sample volume is generally 3 mg~5 mg (changes with thermal effects), and the heating rate is generally in the range of 5 °C min^{-1}~20 °C min^{-1}, however, both these parameters affect the sensitivity, resolution and measuring temperature. Low heating rate and large sample volume can lead to better resolution and sensitivity. The DTA and DSC curves of high polymers determined under different heating rates are different – the faster the heating rate, the higher the peak temperature and the wider the peak shape. It is better for the atmosphere to be N_2, Ar, H_2 (or air sometimes), and the flow rate is generally 10 mL • min^{-1} (preferably constant); oxidation and corrosion can be avoided in an inert gas atmosphere. The measured results in an air atmosphere and inert atmosphere are not the same, and the difference between the two can explain the oxidation reaction of certain high polymers.

8.4.3 Application

DTA and DSC are commonly used to measure melting/crystalline transition temperature [melting point (T_m) and the equilibrium melting point (T_m^0)], glass transition temperature (T_g), specific heat capacity and composition of multicomponent polymers.

When testing T_m of polymers using the DSC curve, the accuracy can be up to ±1 °C. In general, T_m can be determined by the intersection (B) of the tangent of the maximum slope of the peak and the baseline or by directly making the temperature of peak point A (Figure 8.6) [11]. However, both the sample volume and heating rate can affect the peak temperature. Fast heating rate and large sample volume can increase the measured T_m.
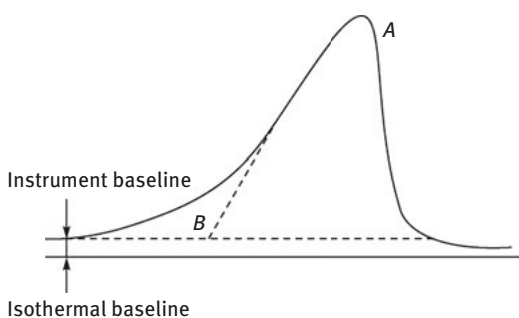

Figure 8.6: Calculation of T_m using the DSC curve [11].

T_m^0 is the melting temperature of high polymers with a perfect crystal structure, and is generally extrapolated by Hoffman – Weeks equation from T_m (as it cannot be directly measured) (eq. 8.2).

$$T_m = T_m^0(1 - \eta) + \eta T_C \tag{8.2}$$

In the above equation, η is the thermal stability of the crystal, whose value is between 0 and 1 (the smaller the η value, the higher the thermal stability of the crystal), and T_c is the temperature of the crystal sample.

When measuring T_g using DSC, it is preferable to determine the temperature at point B, where the extension of the glass baseline and the extension of the transition region intersect, or to determine the temperature at point C, which corresponds to half of the specific heat variation as T_g (Figure 8.7) [8].

Glass transition is not an equilibrium process, implying that the higher the heating rate (usually within 10 °C•min^{-1}~20 °C•min^{-1}) becomes, the higher the measured T_g will be.

For multicomponent polymers, DSC can be used to measure the compatibility of all the components. The compatibility is determined by T_g if the measured T_g of
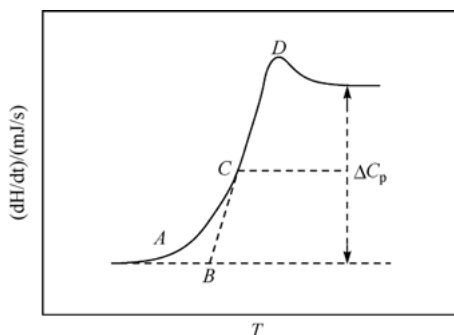
Figure 8.7: Measuring T_g using DSC curve [8].

multicomponent polymers is between the T_g of two pure components, implying that the multiple components of the polymer are compatible.

If a high polymer displays two T_g values, then its components can be considered incompatible. In addition, if the polymers contain one or more crystalline polymers, their compatibility can be determined by the changes in T_m, T_c (crystallization temperature), X_c (crystallinity) and X_v (crystallization rate) compared to the pure state. For example, the T_m of some crystalline components for multicomponent polymers clearly decreases when it is in a relatively pure sate; this system is then termed compatible system. The composition of multicomponent polymers can be confirmed by the conditions of high polymers (eqs. 8.3 to 8.5).

(1) Incompatible, amorphous multicomponent polymers in an amorphous phase

$$x_i = c_{pi}/\Delta c_{pi} \tag{8.3}$$

Where x_i represents the i content (%); c_{pi} is the increase in the specific heat capacity of the constituent i in multicomponent polymers in the glass transition region; Δc_{pi} is the increase in the specific heat capacity of pure components in the glass transition region.

The specific heat capacity (C) can be obtained by the sample heat absorption rate or HRR (dH/dt) and heating rate (dT/dt) using the DSC method. Heat capacity can be expressed as dH/dt = cm·dT/dt (where m is the mass of the sample).

(2) Compatible, amorphous multicomponent polymers in an amorphous phase

$$1/T_g = x_1/T_{g1} + x_2/T_{g2} \tag{8.4}$$

Where T_g, T_{g1} and T_{g2} represent the T_g (°C) of multicomponent polymers, component 1 and component 2, respectively; and x_1 and x_2 represent the content (%) of component 1 and component 2, respectively.

(3) Incompatible, crystalline multicomponent polymers containing crystal components

$$x_i = \Delta H_{mb}/\Delta H_m \qquad (8.5)$$

where ΔHmb and ΔHm represent the melt enthalpy of crystal components and multicomponent polymers, respectively; and xi is the content of component i.

8.5 Thermogravimetric analysis

TG analyzer is used to test the change in weight with change in temperature or time when a material is heated. Weight is usually measured using a thermal balance; it actually measures the change in electric current to determine the change in weight.

TG analyzer consists of a heater, thermostat, microthermal balance (a core part), amplification and recording device. Figure 8.8 present a schematic of an electromagnetic microthermal balance
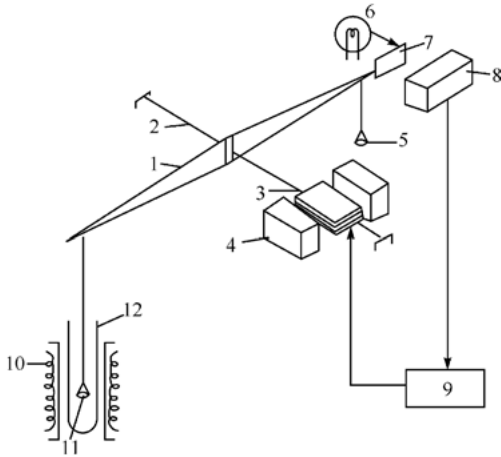
Figure 8.8: Schematic of an electromagnetic microthermal balance [11]. 1 – beam; 2 – stent; 3 – induction coil; 4 – magnet; 5 – scale pan; 6 – light source; 7 – baffle; 8 – sylvatron; 9 – weak current amplifier; 10 – heater; 11 – sample pan; 12 – reaction tube.

Different sample utensils for thermogravimetric analysis can be made of aluminum, glass, platinum, ceramic, etc. Based on the sample properties and testing temperature, such as DSC, some factors may influence the results of thermogravimetric analysis, including sample weight, heating rate and atmosphere. Fine particles weighing between 2 mg and 5 mg can be appropriate samples and should be paved evenly in the utensil (Exact measurement can reach 0.1 μg using a thermobalance). If the quantity of the sample is more than the required amount, the mass transfer resistance and internal temperature gradient increases. The heating rate should be

maintained between 1 °C/min and 10 °C/min. Fast heating rate increases the temperature hysteresis and reduces resolution. Atmosphere has significant effects on thermogravimetric curve, especially under conditions that it interferes with the thermal decomposition of the samples. Common atmospheres include air, nitrogen and vacuum. In general, the gas flow rate is 40 ml/min, and larger gas flow rate benefits both mass and heat transfer. In addition, deviation of the sample weight loss is due to recondensation, revolatilization and buoyancy of volatile components generated during the thermal decomposition of the sample by thermogravimetric analysis. TG and DTG curve can be measured by thermogravimetric analysis.

In general, initial decomposition temperature and weight loss temperature at 1%, 3%, 5%, 10% and the termination decomposition temperature of 50% can be noted in the TG curve (Figure 8.9). Initial decomposition temperature refers to the temperature of point A, where the TG curve starts to deviate from the baseline (epitaxial initial decomposition temperature refers to the temperature shown at intersection B). Termination decomposition temperature is the temperature at point D, the highest weight loss of samples. At the temperature of point E, point F and point G, as shown in Figure 8.9, the sample weight loss is 5%, 10% and 50%, respectively.
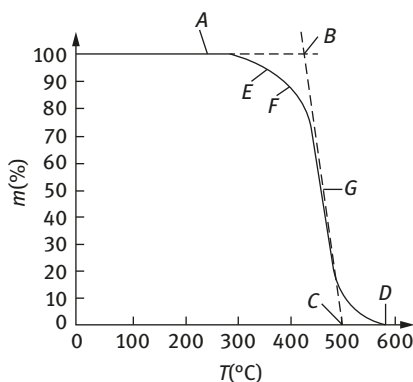

Figure 8.9: Determining the decomposition temperature of the samples using TG curve. A – The initial decomposition temperature; B – Extension of the initial decomposition temperature; C – Termination decomposition temperature epitaxy; D – Termination decomposition temperature; E – 5% decomposition temperature; F – 10% decomposition temperature; G – 50% decomposition temperature (half-life temperature).

DTG curve has a trapezoidal form when denoting the mass change rate of samples at different temperatures and different times. Some parameters can be calculated by the DTG curve, such as the initial decomposition temperature, temperature of the maximum decomposition rate (peak temperature) and the termination decomposition temperature. All these parameters can be used in quantitative analysis (peak area

corresponds with mass change) and differing reaction stages, which helps in analyzing decomposition mechanism. Typical DTG curves can be found in Chapter 6.

Thermogravimetric analysis is commonly used to evaluate the thermal stability, component analysis and kinetics of thermal decomposition of polymers. It can also be used to study some chemical reactions in high polymers.

The most common and simplest method to analyze the thermal stability of different high polymers is to compare their TG and DTG curves and then evaluate their weight loss rate and weight loss temperature.

When the TG curve is used to analyze the composition of high polymers, the inflection points of the TG curve (because of the different decomposition of multiple components) are frequently used. For example, on comparing the TG curves of single PP and PP comprising fillers (as shown in Figure 8.10), we can observe that at temperature ranging 480 °C–500 °C single PP undergoes complete decomposition, whereas PP with fillers retains 45% of its initial mass; thus, confirming that the initial filler content in PP was approximately 45%. At temperature ranging 750 °C–800 °C, PP with fillers undergoes 3.5%–4.0% mass loss, which may be caused by another filler in the sample.
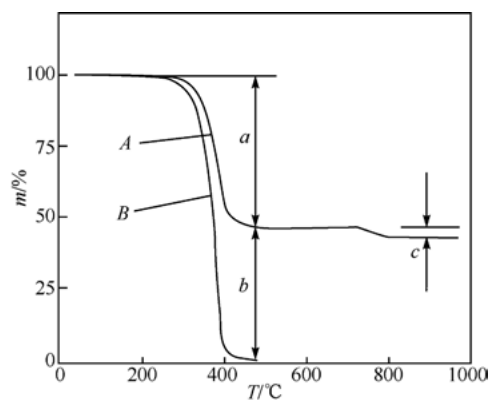
Figure 8.10: Determining the filler content of PP composite by TG curve [10].

When TGA is used to study the kinetics of the thermal decomposition of high polymers, multiple heating methods are usually adopted; that is, testing the TG or DTG curves of polymers under different heating rates, and then applying the integral method (Ozawa) or calculus method (Kissinger) according to the basic kinetic formula. The activating energy (E), reaction order (N) and pre-exponential factor (A) of the thermal decomposition can be obtained by plotting curves.

8.6 Thermodynamic analysis

Thermodynamic analysis (DMA) is used to study the changes in the dynamic mechanical properties of high polymers under vibrating conditions (under the effect of

alternating stress). The essential parameters governing the dynamic mechanical properties are storage modulus E', energy loss E'' and loss factor tanδ. Dynamic mechanical properties of materials are used to measure the impact of various factors (intrinsic and extrinsic) on E', E'' and tanδ.

DMA can be used to determine the elastic and viscous properties of polymers, as well as the transition temperature (e.g., T_g), with an accuracy better than that of DSC, and can also work continuously in the range of transitional heat or frequency. In addition, the dynamic mechanical properties of high polymers in DMA, compared to static properties, is closer to the reality. Deformation modes of DMA include stretching, bending, compression, torsion and shear. The vibrating modes of DMA include self-vibration damping, forced resonance, forced non-resonant and acoustic propagation.

Consider forced resonance as an example which imposes periodically varying forces or moments to the samples to test their amplitude. When the applied force frequency is the same as the resonance frequency of the samples, the sample shows the maximum amplitude. When the resonance frequency of the maximum amplitude of the sample is measured, modulus and damping can be calculated using existing formulas. One of the fixed free vibration instrument of forced resonance method is the vibrating reed instrument illustrated in Figure 8.11.
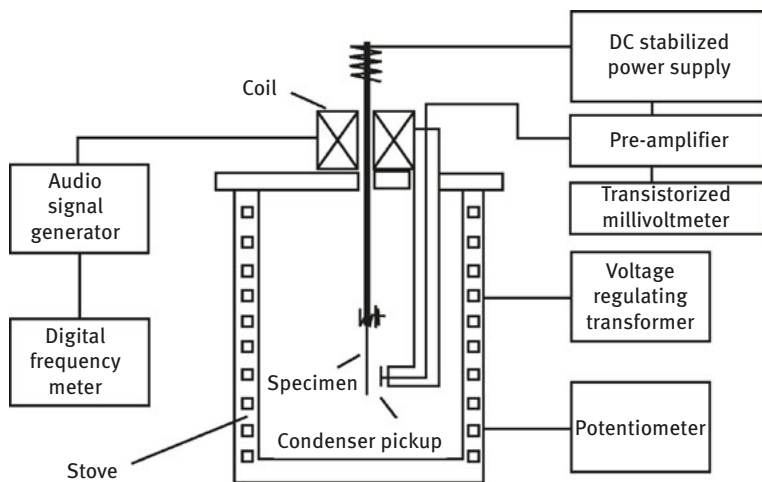
Figure 8.11: Schematic diagram of the dynamic vibrating reed instrument [7].

One end of the vibrating reed instrument is held to the vibrator while the other end is free. When oscillator frequency is the same as the fixed frequency of the samples, the amplitude of the samples reaches its maximum. The resonance frequency at the maximum amplitude of the samples can be tested using a detector; eqs. 8.6 to 8.8 can be used to calculate E', E'' and tanδ, respectively.

$$E' = (38.24 \rho L^4 f_r^2)/h^2, E'' = (38.24 \rho L^4 f_r \Delta f_r)/h^2 \tag{8.6}$$

$$\tan \delta = \Delta f_r / f_r = E''/E' \tag{8.7}$$

$$E'' = E' \tan \delta \tag{8.8}$$

where E' is storage modulus (Pa); ρ is density of the samples (gcm^{-3}); L is the free end of the sample length (cm); F_r is the resonance frequency (Hz); h is the thickness of the samples (cm); E'' is the loss modulus; Δf_r is half-width of the frequency, which is the difference between the frequencies at $1/\sqrt{2}$ or $1/2$ of the biggest amplitude; Tanδ is the loss tangent.

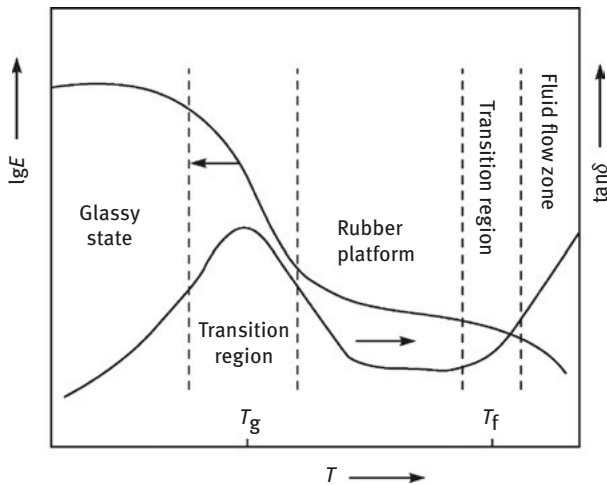Figure 8.12 shows the dynamic mechanical spectroscopy of linear amorphous polymers [11].

Figure 8.12: Dynamic mechanical spectroscopy of linear amorphous polymers [11].

DMA samples can have different shapes and different sizes, however, their sizes should be measured as accurately as 0.1%. Moreover, the samples should be uniform, smooth and free of any impurities and bubbles. DMA can undergo temperature (T) scanning and time (t) scanning because its basic parameters (E', tanδ and E'') are associated with T, f and t. Characteristic temperatures of T_g, T_f (temperature at transition from high elastic state to viscous flow state), T_m, T_β, T_γ, T_δ, etc. of high polymers as well as modulus and damping can be obtained through the temperature spectra of DMA. The temperature spectra of DMA can be used to study the transition temperature, impact of temperature resistance (high and low temperature), low temperature toughness, effects of structural parameters on the performance of polymers, along with the investigations of process (such as curing) and quality control. For example, T_g can be determined

according to the E'-T curve or Tanδ-T curve. DMA can determine T_g more accurately and intuitively. In addition, it can also test the changes in high polymer E' and damping in a wider temperature range to provide more comprehensive and scientific evaluation of material properties by combining T_g and E'.

8.7 Electron microscopy

Electron microscopy (EM) images the interaction between an electron beam and the samples under investigation. EM has a high magnification (approximately 106 times) and high resolution, which helps in determining the minimum distance of two neighboring particles (even at the scale of 0.1 nm to 0.2 nm). Optical microscopes cannot be compared with EM, which is a powerful tool to study the structure of polymers.

Only two types of EM are discussed in this article, namely the transmission electron microscopy (TEM) and scanning electron microscope (SEM) which are illustrated in Figure 8.13 and 8.14, respectively.

8.7.1 Transmission electron microscopy

TEM functions by projecting electron imaging (by directly projecting electron and elastic or non-elastic scattering) and diffraction. TEM mainly consists of a light source, an objective lens and a projection lens. It is similar to an optical microscope, with the major difference being that it uses an electron beam to replace a light beam, while also using magnetic lenses to replace glass lenses.

Resolution, magnification and contrast are the three basic elements of TEM. The larger the aperture, the shorter is the electron wavelength (depending on the acceleration voltage), ultimately resulting in higher resolution. The magnification of TEM is the ratio of visual resolution (approximately 0.2 mm) to EM resolution (0.2 nm), i.e., of the order of 10^6. Further, its contrast is related to imaging the electrons of samples undergoing imaging, as well as the thickness and density of samples. If the sample is thicker and denser, its image will be darker.

TEM can only measure solid samples; the samples should be clean and without any volatile components, and are not damaged by the electron beam within the observation time.

The thickness of TEM sample is generally less than 100 nm. The samples are placed on a metal mesh during the test. In case of some small samples, the samples must be used with a transparent supporting film (such as a plastic film). For a nonconductive polymer, it is better to have a metal film on the surface to reduce surface charge accumulation. To increase contrast, the samples need to be stained (such as OsO_4) at times. To obtain a clear image, the samples sometimes need special treatment.

8.7.2 Scanning electron microscopy

Compared with TEM, SEM has a wide magnification ranging from 20 to 100 thousand times featuring better focus, three-dimensional image, simple sample preparation and lesser damage to the samples. SEM is particularly suitable to study the morphology of the polymer surface; even samples with a rough surface can be tested using SEM. Therefore, it is an important method to study the three-dimensional structure of polymers. SEM is electronic imaging detected by secondary electron and background scattering. The three basic elements of SEM are resolution, magnification and contrast.

SEM samples only need to be stuck to an aluminum seat by a double-sided adhesive, however, the bonding technique must be paid attention to so that the surface charge of samples can be conducted.

The basic requirement for the samples of SEM is the same as that of TEM. However, not only the preparation of SEM sample is simple but there are also some modern SEM instruments, for example, the so-called environmental scanning electron microscopy (ESEM) that can simulate environmental working situation, without metallization film for a non-conductive polymer. This can aid the observation of watery and oily samples, and perform dynamic variation research on the sample by thermal and mechanical simulation.
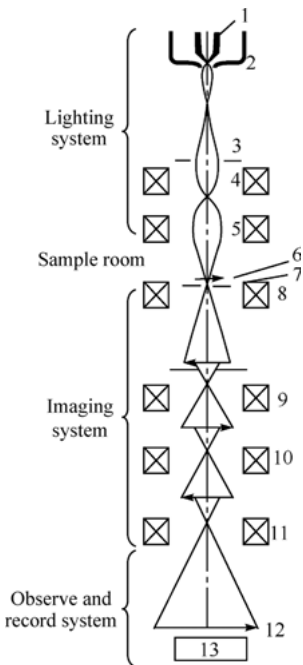

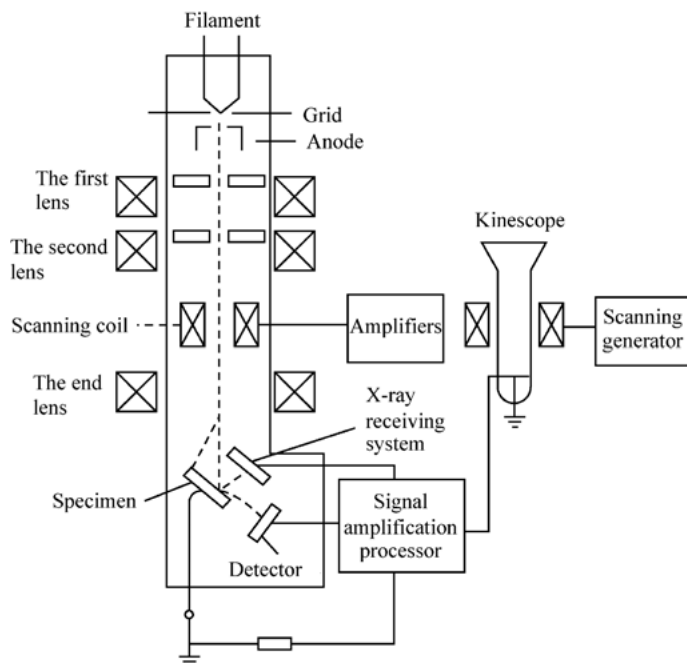**Figure 8.13:** Structure of a TEM [8].

Figure 8.14: Structure of an SEM [9].

8.7.3 Application in polymer research

EM is used to study the morphological structure of crystalline and amorphous high polymers and composite systems of multiphase materials (blends, composites, etc.), as well as toughening mechanism of two-phase systems.

EM is widely applied for flame-retardant polymers. When combined with XRD, EM can provide more information on the structure of the material. As for high polymers acted on by flame retardants/inorganic nanocomposite, when inorganic fillers (e.g., montmorillonite) are inserted by polymer macromolecules, intercalated or exfoliated composite material will be present among lamellas, which can be clearly seen in the TEM images A typical EM diagram has been shown and discussed in Chapter 6.

Further, optical microscope can be used for observing the surface of carbon layer. Figure 8.15 is the optical microscopy image of residual carbon of the coatings: PU, PU/EG and PU/APP processed for 15 min at a temperature of 800 °C [12].

There are cracks in the residual char surface of the PU coating; in the residual char of the PU/EG coating, EG fragments are observed mainly; a large area of the char carbon surface of the PU/APP coating has deformed, but there are no visible cracks.
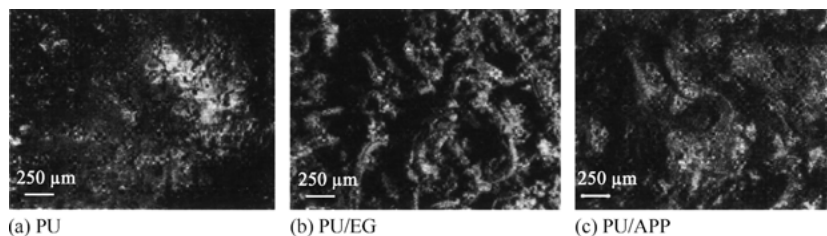
(a) PU   (b) PU/EG   (c) PU/APP

Figure 8.15: Optical microscopy image of the three coatings processed for 15 min at a temperature of 800 °C [12].

8.8 Wide-angle X-ray diffraction method

8.8.1 Principle and equipment structure

X-ray methods are divided into wide-angle ($2\theta = 5°\sim165°$) X-ray diffraction method (WAXD) and small-angle ($2\theta = 5°\sim7°$) X-ray scattering method (SAXS). Only WAXD method is discussed in this book.

When X-ray irradiates the crystal, atoms can scatter X-rays in different directions (with atoms becoming the secondary X-ray source), but only when the scatter direction is in the direction of the optical path difference of the scattered rays equaling the incident X-ray wavelength, the intensity of scattered rays can be enhanced due to the superposition, which can be observed experimentally. In other directions, scattered rays are reduced or eliminated. The beam of the maximized intensity is called X-ray diffraction ray, while its direction is termed diffraction direction. X-ray diffraction follows Bragg's law (eq. 8.9).

$$2d\sin\theta = n\lambda \tag{8.9}$$

where n represents diffraction order, which is an integer; λ is the wavelength of the X-ray, which is a known number; θ is the diffraction angle, which can be experimentally measured. Interplanar spacing d can also be computed according to Bragg's law.

X-ray used for polycrystalline materials should be monochromatic. For testing high polymers, a copper target is commonly used.

During experiments, a photographic method (making photographic negatives) and counter method are adopted to record X-rays. A proportional counter is based on the proportion of the current intensity generated by the ionized gas and X-ray intensity. A scintillation counter is based on the photoelectric conversion of the fluorescence generated by X-rays striking on the crystal.

Polycrystalline diffraction of X-ray diffraction refers to WAXD analysis of crystalline or crystalline aggregate samples, which can be divided into polycrystalline photographic method and polycrystalline diffraction method.

Polycrystalline photographic method is also termed powder photography, which uses a special camera with a special film to record the diffraction intensity and diffraction direction of the sample. Photographic negative features can be used to directly determine sample crystallization, grain orientation, orientation degree, etc. Polycrystalline diffraction method utilized the gas ionization effect of X-ray and undergoes conversion, amplification and selection to derive the relevant diffraction orientation and the diffraction degree graph. According to the peak, spike and intensity of the graph, the phase, crystallinity, grain size, grain orientation of the sample can be analyzed. Polycrystalline diffraction instrument consists of X-ray tube, goniometer and counter. A typical diffraction graph has been illustrated in Chapter 6.

At present, polycrystalline diffraction method has replaced polycrystalline photographic method in many aspects. The X-ray diffraction structure is presented in Figure 8.16 [8].

Polycrystalline X-ray diffraction method can be used for ① qualitative identification (compared with the reference spectrum); ② phase analysis (crystallization and type of crystallization); ③ crystallinity (crystallization orientation, grain size, polymorphs) of the polymers.

8.8.2 Role of X-ray diffraction in studying flame retardation mechanism

X-ray diffraction is used to analyze ordered structures as illustrated in Figure 8.16, while the char layer formed by IFR is mainly unordered. However, to study some of carbonization processes of the IFR system with layered additive (EG, MNT), X-ray diffraction is still a useful method.
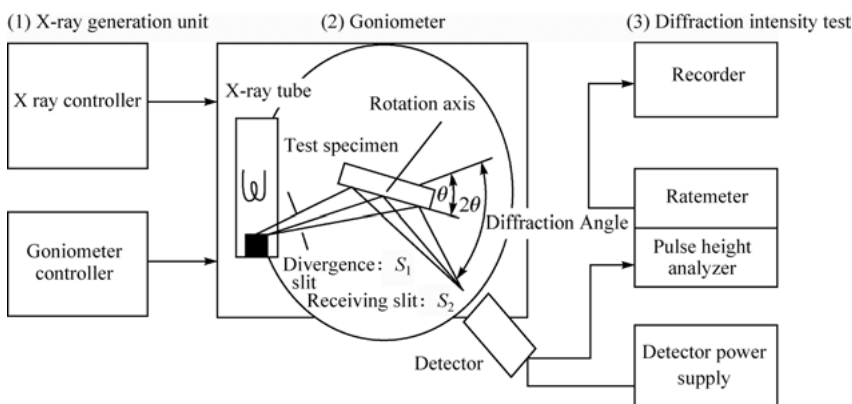

Figure 8.16: The X-ray diffraction structure [8].

X-ray diffraction curve of the residue can be obtained under four different stages of mass loss in radiation gasification plant (N_2 atmosphere, heat flow 50 kW/m^2) for PA6, clay (unmodified), PA6/clay (5%) and PA6/clay [13] (as presented in Figure 8.17) [13].
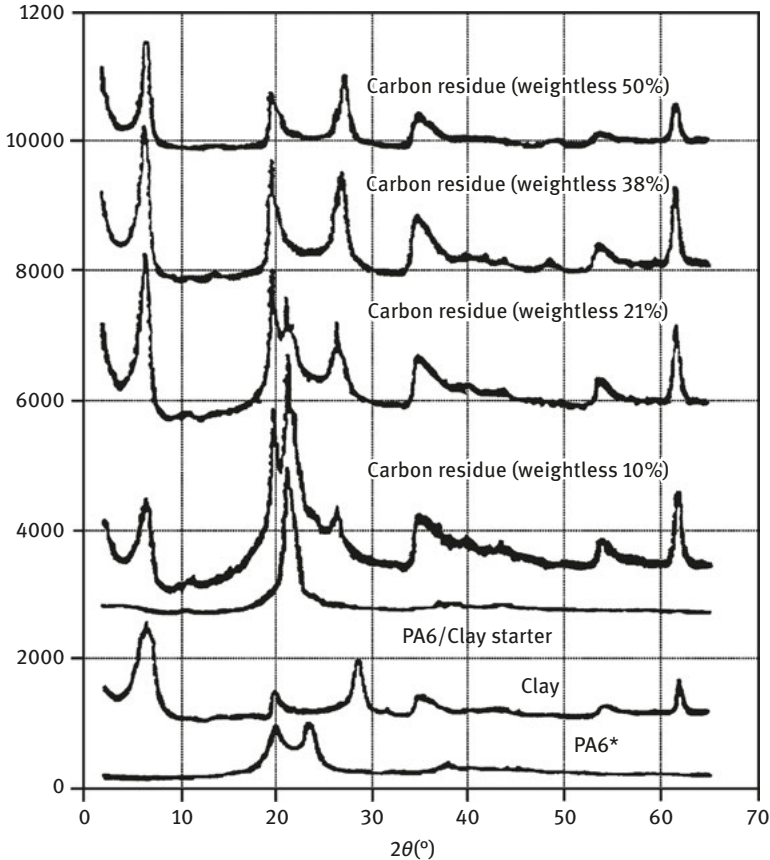
Figure 8.17: X-ray diffractogram of various materials [13] The intensity of PA6 and PA6/clay is only 10% of the measured value.

On comparing the abovementioned X-ray diffraction curves for the samples, we can observe that PA6/clay contains γ crystalline phase (PA6 has a crystalline α phase), possibly because silicate is helpful in the formation of phase γ, that is, the clay has changed the crystal structure of the substrate PA6. The comparison between the combustion residues of PA6/clay and original PA6/clay shows that the crystalline phase and the clay layer spacing in the original PA6γ have been reduced. As for the residues with weight loss of 38%, PA6 disappears. However, the clay layer spacing in the residues is still larger than the original clay layer spacing, demonstrating

that the clay layer may capture some organic in the residues. X-ray diffraction curve of the residue also shows that, under high temperatures, PA6/clay can generate a small number of extremely heat-resistant graphite structured materials (2θ is at the peak of 26.5° and 27.38°).

8.9 X-ray photoelectron spectroscopy

8.9.1 General principles and equipment structure

X-ray photoelectron spectroscopy (XPS), also known as electron spectroscopy for chemical analysis, is a useful method applied to analyze material surface. It is also one of the important methods to study the fire retardation mechanisms of polymers.

XPS measures energy; when the monochromatic X-rays act on the sample, the sample can emit photoelectrons. Therefore, electronic energy photoelectron spectrometer can measure the data by responding to the energy of the photoelectrons. On plotting intensity (usually expressed as a count or counts/second) and electron energy, we can get the XPS spectrum (Figure 8.18).
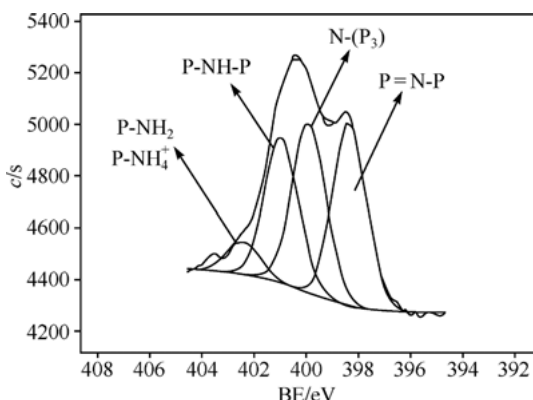
Figure 8.18: XPS spectra of residual char N1s of phosphorus/nitrogen compounds after combustion [14].

Electron kinetic energy (E_k) is a physical parameter that can be measured by energy disperse spectroscopy, but is relevant with the photoelectron energy of the used X-rays. Thus, E_k cannot reflect the intrinsic properties of the test substance, while electron binding energy (E_B) is better at identifying electrons.

Indeed, $E_B = h\nu - E_k - W$ ($h\nu$ is the photon energy and W is the work function of spectrometer). As the three values on the right side of the equation are already known or can be measured, it is easy to calculate electron binding energy through spectrometer's monitoring systems and data processing systems. Therefore, XPS

electronic energy was E_B. Because of the different chemical environments of atoms (ions, molecules), the E_B also changes, which is the so-called chemical shift phenomenon in XPS. That is to say, XPS atomic energy in different chemical environments have small differences, and hence, almost all elements in the Periodic Table are presented in the chemical shift (from less than one electron volt to several electron volts). Chemical shift is the cornerstone technology for XPS analysis.

All electrons with electron binding energy less than photon energy can be displayed in XPS spectra, hence, the XPS spectra can accurately reproduce the electronic structure of atoms. XPS can detect all elements except H and He. Figure 8.18 [14] shows an XPS spectra of residual carbon N1s of phosphorus/nitrogen compounds after combustion.

The main information provided by full-scan XPS spectra relate to the elements and their chemical bonds (element's chemical states), which can be used for the qualitative and quantitative analysis of metals, semiconductors, ceramics and organic matter. The samples can be solids (powders, fibers, etc.) or viscous liquids, however, the surface of the samples should not be polluted. The analyzing depth varies 3 nm~10 nm, and the resolution depth is approximately 1 nm.

XPS device consists of ultrahigh vacuum system, injection system, X-ray source, energy analyzer, scanning and recording system, etc. (Figure 8.19) [8].
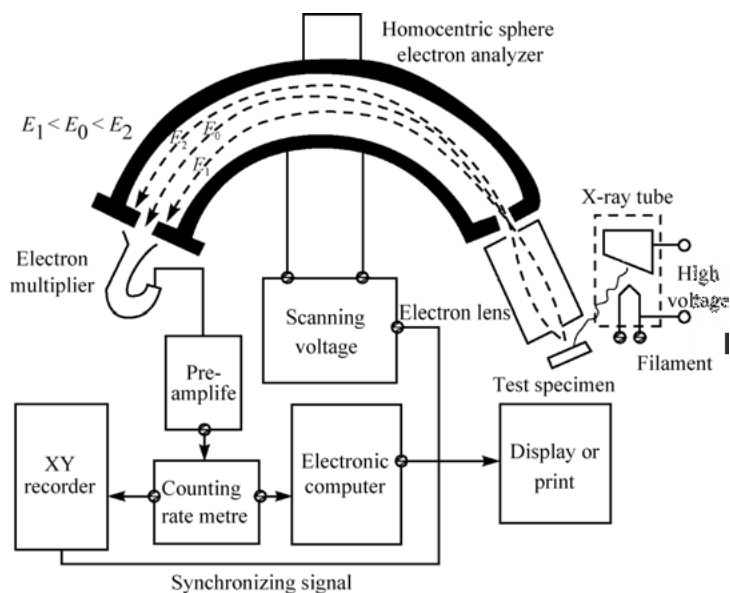

Figure 8.19: The XPS structure [8].

XPS can be used to study the conditions of material surface including element species, element existence state and the condition of chemical bonds. It can also be used to study the geometric construction (crystalline, amorphous) of the material surface, the surface atomic motion (diffusion, vibration) and surface electrons structure (spatial distribution and energy distribution).

8.9.2 Application in flame retardation mechanism

Furthermore, XPS is a useful tool to study the chemical composition of the carbon layer formed after the combustion of flame-retardant materials, as well as to understand the function of fire-retardant systems in the condensed phase [15]. Being similar to ssNMR, XPS can not only provide information regarding certain elements but can also provide information regarding carbon layer elements; thus, it can be used as a supplement to ssNMR. For example, in nitrogen compounds, its hard for ^{15}N ssNMR to identify the surrounding environment of the N because the abundance of ^{15}N is only 0.4%; thus, the signal is in general very weak. IR, ^{13}CNMR and ^{1}HNMR cannot be directly used to identify nitrogen-based substances in char layers. However, XPS is a convenient analytical tool to study nitrogen compounds in carbon layers. Meanwhile, information from XPS can also be used to identify intermediates oxidized during the degradation of the protective char layer [16].

For the epoxy resin/APP/polyethylene polyamide system, some research [17] has investigated additives in the system through XPS studies. The results show that, if the system uses manganese dioxide and calcium borate, an inorganic structure can be formed on the surface of the intumescent coating, and the metal-containing carbon tubes can be conducive to the formation of foam coke with certain structure. Because of improved thermal properties (such as heat capacity) and mechanical performance, the efficiency of the flame retardancy of the system also improves.

Using XPS to analyze char layer containing EG [18], the elements of the char layer, carbon concentration and oxidation of char layer can be obtained. Table 8.1 [18] lists the elements of the carbon layer formed by the intumescent coating with EG and without EG (coating raw consists of acrylic resin/APP/PER/MA). In the char layer containing EG, the char enrichment degree is very high, and the antioxidant activity in the flame is very strong.

Table 8.1: Elements formed by the char layer coated with EG and without EG [18].

Sample	O%	C%	P%
Coating with EG	18.8	74.7	6.4
Coating without EG	40.2	51.8	8

8.10 Infrared spectroscopy and Raman spectroscopy

8.10.1 Infrared spectroscopy

Infrared spectroscopy (IR) is a molecular vibrational spectroscopy, whose radiation energy is much less than that of ultraviolet radiation. Infrared can only stimulate vibration and transition of rotation levels among nucleus in molecules to study molecular structure by measuring the energy level transition. Infrared wave has a wavelength of 0.75–100 μm, which can be divided into the near infrared, middle infrared and far infrared. Because the mid-infrared radiation can identify the molecular structure and chemical composition of organic compounds, it is most widely used. When we mention IR, it generally refers to the mid-infrared range, with wavenumber ranging 4000 cm^{-1}~400 cm^{-1}.

The scan rate of the traditional infrared spectrometer is rather slow with low sensitivity; however, the newly developed Fourier transform infrared spectroscopy (FTIR) can determine all frequencies with a short scan time, high sensitivity and resolution, and hence, is widely used currently.

The ordinate of infrared spectra is linear transmittance or linear absorbance, and the abscissa is the wavenumber of light (cm^{-1}).

In general, an automatic dual-beam scanner consists of a light source, sample cell, monochromator, detector, amplifier and recorder. Its working principle and structure are illustrated in Figure 8.20 [19].

The infrared light emitted from the light source (S) can split into convergent light beams of equal strength after being reflected – one beam goes through the sample cell (test beam), and the other goes through a bunch of reference cells (reference beam). Subsequently, the two beams go through the monochromator entrance slit S_1 alternately after dispersion by the grating (G), and then they pass the slit S_2; finally, they focus on the detector (D) by the light filter. If the sample does not absorb infrared radiation, the two light beams are of equal intensity; if the sample absorbs infrared radiation, intensity of the two beams becomes different, whereas the signal of the reference beam is much stronger than the other. However, after covering a part of the light by an optical comb A, the energy of the two beams equals that of the test beam. When it reaches equilibrium, the detector does not give alternating signals.

Rotation of the monochromator grating changes the wavelength of the monochromator continuously in the infrared region, and the speed of the recording matches with the rotation speed of the monochromator grating. Therefore, as the intensity of infrared radiation absorbed by the samples are different, and the degree of shading by the optical comb in the reference beam changes, the linkage between the optical comb and recording pen helps draw the transmittance of special wavelength on the spectra.
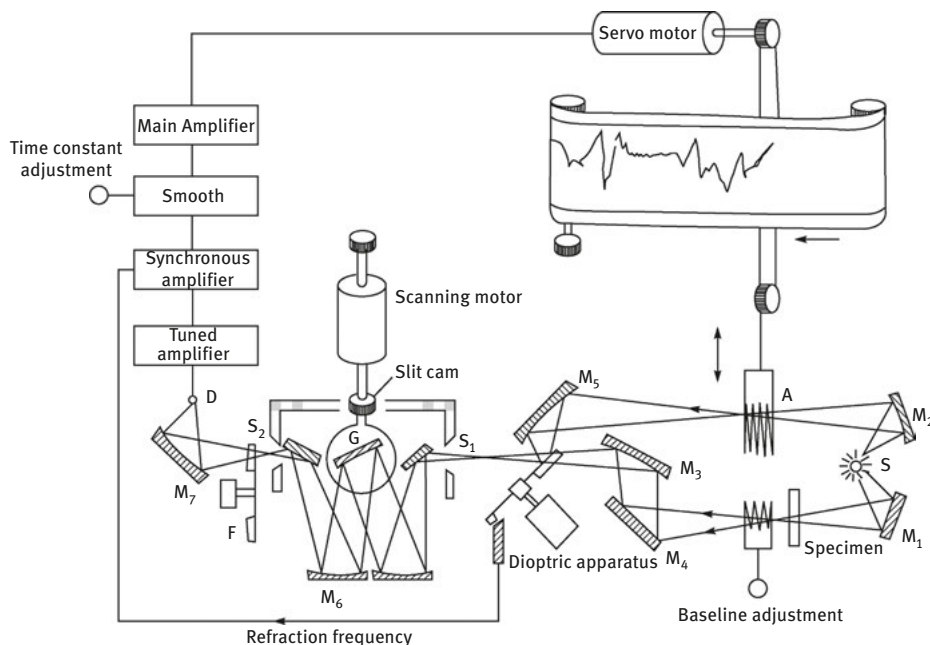
Figure 8.20: Working principle and structure diagram of dual-beam infrared spectrometer [19].

Spectral analysis

Before spectral analysis, it is helpful to investigate odor, solubility, thermal analysis, elemental composition (qualitative identification), as well as the other features of unknown samples.

The three elements of infrared spectral analysis are the spectrum peak position, shape and intensity. Figure 8.21 is the FTIR spectra of flame-retardant HIPS [11].

The spectrum peak position refers to the characteristic vibrational frequency of the band, which can determine specific functional groups in samples, while the fingerprint region can determine the fine structure of the compounds. Band shape can be used to study the molecular association, molecular symmetry, rotational isomeric, tautomerism, etc. On the other hand, band intensity is associated with molecular content and the variation rate of the dipole moment during molecular vibration, which forms the foundation of quantitative analysis. In fact, when analyzing infrared spectra, although usually information provided by certain bands is enough to judge the molecular structure of the samples, the influence of the substituent functional groups on the frequency and interference of the impurities due to water bands should be taken into consideration.
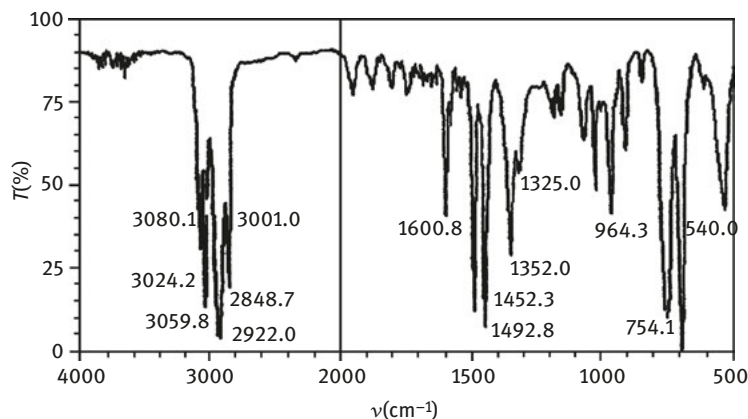
Figure 8.21: The FTIR spectra of flame-retardant HIPS[10].

The easiest approach for spectral analysis is to compare the sample spectra with the known spectra of standard samples, although different conditions of sample preparation affect the position, shape and intensity of the band. The category of test samples can be determined according to the characteristics of group frequency; the negative and positive method can also be used to determine which groups exist in the unknown samples.

Sample preparation technique

1. Solid sample
    (1) KBr compression method is the most commonly used method. This method involves smooth grinding of the sample (approximately 1 mg) with dry potassium bromide (approximately 100 mg) in an agate mortar, and then pressing it into an almost transparent sheet.
    (2) Grinding method. In this method, 2–5 mg of the sample is grinded into a powder, and 1–2 drops of paraffin oil (Nujol) or fluorinated kerosene or chlorine 1,3-butadiene are added, followed by grinding the sample and placing between sodium chloride chips.
    (3) Powder method. In this method, after grinding the sample into a powder, the sample is spread onto the surface of a volatile solvent. The solvent is then evaporated on the salt window, thus giving a uniformly thin layer of the sample.
2. Liquid sample
    Drop the sample onto two polished salt windows to form a liquid film for testing.

During the measurement of infrared spectra of the polymer, thin samples should be prepared due to their strong absorption capacity. For polymers that can be dissolved, appropriate solvents can be chosen as liquid samples.

Infrared spectroscopy is used to qualitatively determine the polymer type, separation and analysis of the polymer mixture; moreover, it can be used to quantitatively determine the chain structure of the polymer (the proportion of each structure, grafting, etc.) according to the law of light absorption rate, as well as studying the reaction mechanism and polymer kinetics.

Polarized infrared, infrared attenuated total reflection (ATR), photoacoustic spectroscopy (PAS) and other modern technologies have extended the application range of infrared spectra. ATR is applied to achieve the figure by recording the intensity of light reflected multiple times (30–50 times) and the corresponding wavelength (the peak and its position only slightly differ than those of FTIR). ATR is also a powerful tool to analyze the surface of the materials (such as surface grafting modification), and the variable angle ATR-FTIR can also be used to study the regional structure of different layers.

8.10.2 Laser Raman spectroscopy

General principles

Raman spectroscopy is a scattering spectrum. When a monochromatic light is incident on a sample (in gas, liquid or a transparent crystal state), the light gets scattered. If the frequency of the scattered light is the same as the incident light, the phenomenon is termed as Rayleigh scattering. If the frequency of the scattered light is on both sides to the frequency of the Rayleigh light (their strength is 10^{-4} of Rayleigh light, 10^{-8} of the incident light), the phenomenon is termed as Raman scattering. In Raman scattering, if the wavelength is longer than that of Rayleigh light, it is termed Stokes line, and if it is shorter, it is termed anti-Stokes line. The frequency difference between Stokes lines and anti-Stokes line and the incident light is termed Raman shift. Because the Stokes line has much greater intensity than the anti-Stokes line, the Raman spectrum always sets the former to investigate the Raman frequency shift (Δv).

Raman spectroscopy measures the Δv (Δv has nothing to do with the frequency of the incident light). During Raman spectroscopy, Δv is the abscissa and the scattering intensity is the ordinate. Figure 8.22 shows the Raman spectra of PP, along with the infrared spectra of PP for comparison [11].

Because Raman spectroscopy is weak, it is appropriate to use strong lasers as light sources to enhance the intensity of the Raman scattered light, namely, laser Raman spectroscopy. Because lasers have great strength, strong direction, small emission angle, and small focusing area, a few samples (0.5 μm) can obtain the Raman spectra, thus limiting qualitative identification and quantitative analysis.
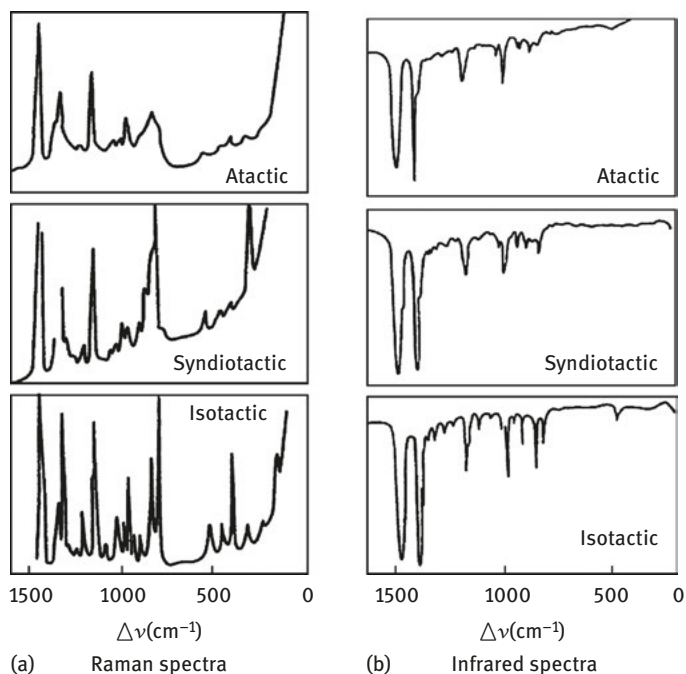
Figure 8.22: Raman spectra of PP (left) and infrared spectroscopy (right) (less than 1600 cm) [11].

Although the intensity of Raman scattering can estimate the molecular concentration of the tested sample, there are many influencing factors that require internal standard method or contrast method for quantitative analysis.

Of course, Raman spectroscopy can also use Fourier transform technology to form Fourier transform Raman spectroscopy (FT-Raman), improving signal-to-noise ratio by accumulation.

Raman spectrometer is similar to infrared spectrometer, consisting of light source (laser), sample cell, monochromator and detector/recorder.

Raman spectra and infrared spectra are both molecular vibration spectra, providing similar information; their qualitative factors are the same, namely the frequency, intensity and peak shape. However, in Raman spectroscopy, the depolarization ratio (the degree of removing polarization) characterizes the level of molecular symmetry vibration modes. There are both similarities and differences between the infrared and Raman spectra; the absorption frequency of infrared is equivalent to Δv of Raman, and multiple bands in both correspond to the vibration of some functional groups in the molecule. For most functional groups, stretching vibration frequency in the infrared are fairly close to the Δv value of Raman, however they arise due to different mechanisms, such as infrared absorbtion, Raman scattering. While infrared is generated because of changes in the dipole moment generated by molecular vibrations,

Raman is generated by the induced dipole moment changes. Therefore, infrared is sensitive to polar groups whereas Raman is sensitive to non-polar groups. Both infrared and Raman can provide complementary information. Some groups can be detected by infrared easily, while other groups are easily detected by Raman, hence, they are often compared with each other (Figure 8.21).

Raman spectroscopy can be used for qualitative identification of polymers and structural analysis (structure, conformation, crystallinity, etc.); it can also be used for quantitative analysis and investigating the reaction and thermal degradation of polymers.

Applications in flame retardant mechanism
Laser Raman (LR) can also be used to identify different carbon layer structures. In this aspect, it can be a complement with ssNMR. The literature [20] provides a good overview of LR regarding the flame-retardant mechanism. LR in graphite can provide lots of defects of the information about defects in the internal structure and the electronic graphite, which finally complements the carbonization process [21, 22].

A previous study [23] applied LR to investigate the structure of the expanded carbon layer formed by LLDPE Halogen IFR. Researchers placed several samples in a tube furnace for thermal degradation in air stream. The generation of the residue LR shows that, if expandable graphite (EG) is present in the materials, a peak can be seen at approximately 1575 cm^{-1}. For the LLDPE/NP28 system (a P/N compound), there will be two broad peaks at approximately 1575 cm^{-1} and 1350 cm^{-1}. Therefore, the former has an ordered structure of C-C vibration with no internal defects in graphite. Different IFR forms different carbon layers after combustion, which may be ordered graphite or a disorder system.

A previous study [24] applied LR to investigate the thermal stability of untreated and silane-treated cotton fiber. For the silane-treated cotton fiber LR, in the range of 3200 cm^{-1} to 3500 cm^{-1}, the peak is much stronger and narrower in the ordered phase; with increasing OH concentration, crystallinity also increases. In the crystalline phase, silane reaction does not occur. The improvement in the degree of crystallinity is due to the mobile segment, which decreases secondary chemical bonds in the amorphous phase. The structural change shows that the silane treatment improves the thermal stability of cotton fiber because the amorphous phase of OH on thermal degradation was more sensitive than OH in the ordered phase.

ssNMR can only be used in *in-situ* applications, whereas LR can be used for testing the changes on heating specimen surface. For example, a previous study [25] applied LR by adding nano-MMT and silane (BSil) into the APP (75)/polyol(25) system for PP to check its impact on the material surface and interface modification. The result shows that the synergistic effect of MMT is limited, but the effect of BSil is good.

Figure 8.23 [25] shows LR after heating and treating by two systems, namely, a PP/MMT (4%) and PP/MMT (4%)/BSil (2%). For the former, LR does not change after heat treatment; while for the latter, the peak of BSil coated with MMT can be clearly seen (enriched on the surface) after heat treatment. When MMT is coated with BSil, its surface energy can be significantly reduced, which makes it easy to
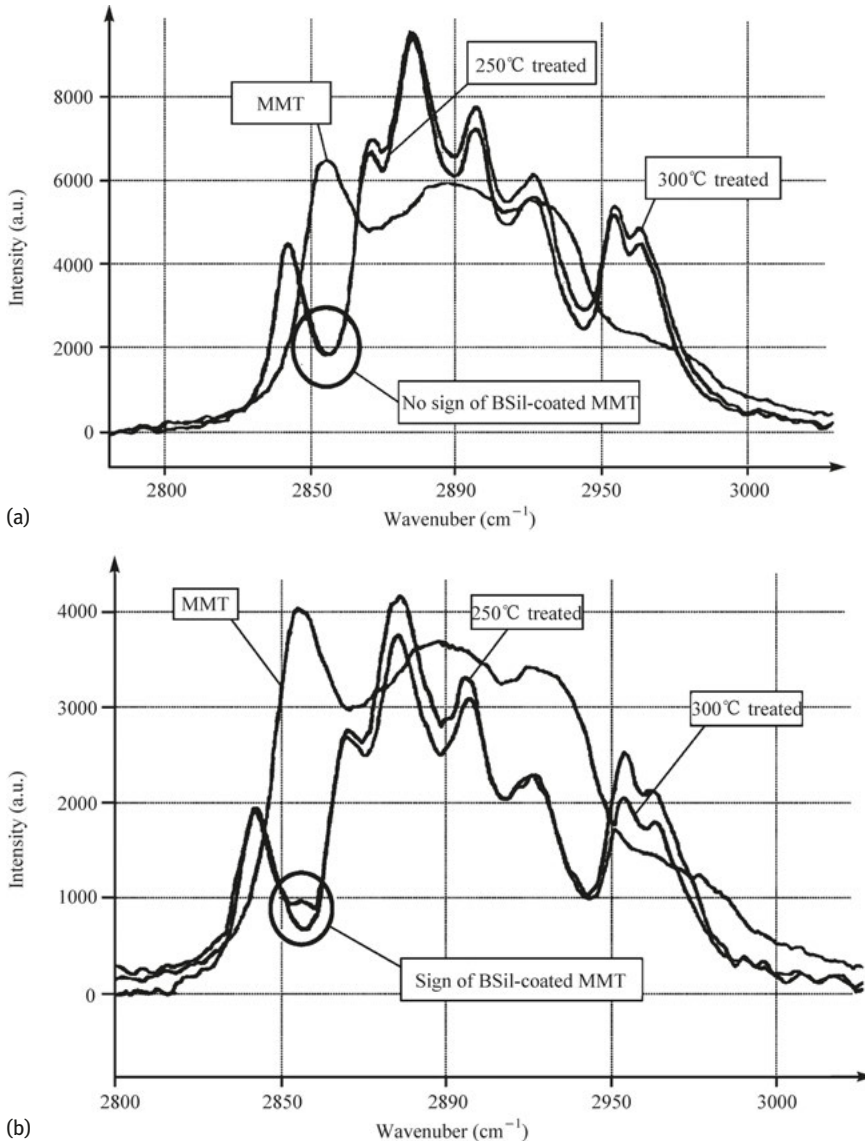

Figure 8.23: PP/MMT (4%) and PP/MMT (4%)/BSil (2%) Raman spectroscopy [20, 25]. (After 2 min treatment at 250 °C−300 °C).

migrate to the surface and stabilize it, forming a flexible protective layer on the surface to improve the flame retardant efficiency.

8.11 Nuclear magnetic resonance spectroscopy

Nuclear magnetic resonance spectroscopy uses molecular irradiation with electromagnetic waves with MHz frequency, long wavelength and low energy. Electromagnetic interaction with magnetic nuclei exposed to a strong magnetic field results in resonance transitions of the latter in an external magnetic field, thereby producing absorption signal. This absorption is termed nuclear magnetic resonance spectroscopy (NMR).

NMR is one of the most useful tools for the identification of molecular structure and composition. NMR can directly obtain quantification results from the spectrum peak area without using a known standard sample as long as there is sufficiently high resolution. The ordinary NMR using liqiud sample, solid state NMR can determine the solid sample.

NMR used for organic samples is usually a proton and carbon-13 NMR, denoted as ^{1}HNMR (or PNMR) and ^{13}CNMR.

8.11.1 Nuclear magnetic resonance

Figure 8.24 shows the pulse Fourier-nuclear magnetic resonance (PFT-NMR) [26] composed of a magnet (permanent magnet or an electromagnet), radiofrequency emission system, signal receiving system and signal control, processing and display system, probe and sample holder.

8.11.2 Proton nuclear magnetic resonance spectrum

The main information of ^{1}HNMR spectrum includes ① chemical shift values (δ) that confirms the chemical environment and nuclear magnetic environment of hydrogen atoms; ② coupling constants (*J*), inferring the relationship and structure of atoms around hydrogen; ③ absorption peak area (*S*), determining the number ratio of hydrogen atoms in various molecules. Figure 8.25 is the ^{1}HNMR spectrum [10] of syndiotactic PS pattern.

Chemical shift (δ)
δ is used to show the distance between the resonance peak in different chemical environments and the resonance peak of other reference materials (tetramethylsilane is
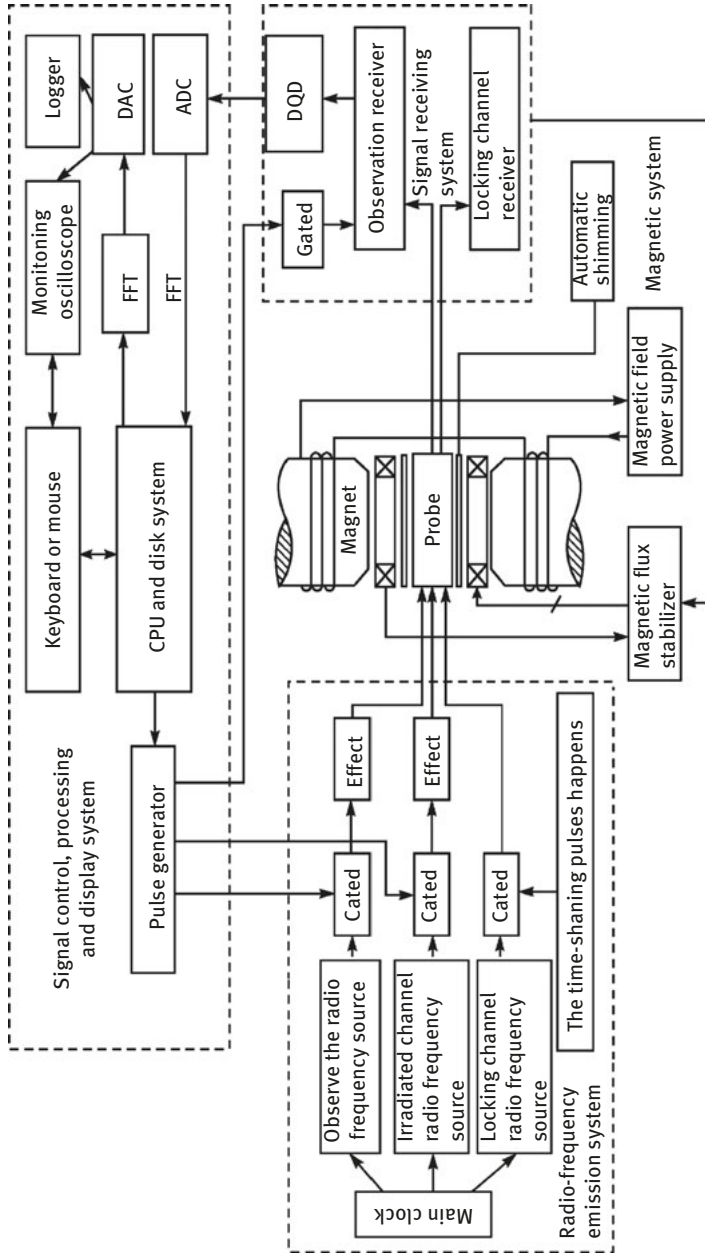
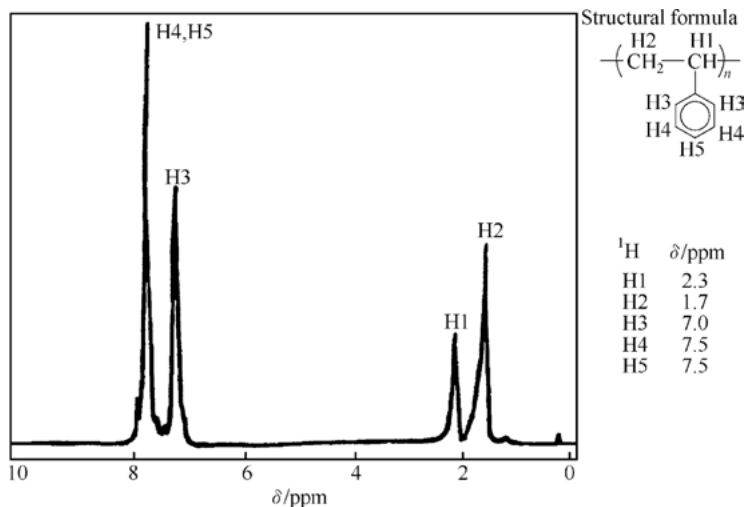**Figure 8.24:** Working principle of PFT-NMR [26].

Figure 8.25: ^{1}HNMR spectrum [10] of syndiotactic PS pattern.

usual) in ^{1}HNMR spectrum. We cannot accurately determine the absolute value of δ, and hence, the relative value is often applied, which is determined by the resonance peak of the reference material as the origin point and the relative distance between the origin point and other ^{1}H peak as δ (ppm).

The value of δ in various ^{1}H in organic compounds depends on their electronic environment. If the effect of magnetic field on ^{1}H is shielded by an electron cloud, the resonance signal appear in a high field; with shielding effect on ^{1}H, resonance signals appear in the low field.

Coupling constant (J)

J measures the spin-spin coupling generated due to the effect of the external magnetic field and the electromagnetic field caused by the spin of the neighboring proton. Through spin-spin coupling, NMR single peak is split into multiple peaks, and the distance between the split lines is called J. Using J, the relative position of coupling nuclei can be speculated.

Peak area (S)

S indicates NMR signal intensity which is the area under the peak absorption. S value is proportional to the number of protons generating this set of signals. Comparison of S values can determine the relative number of various proton types. NMR signal area is measured by the electronic scoring, and is usually expressed by ladder curve in the spectrum. When the line starts from low to high field, it implies that the step height is proportional to S value. If the formula of the

compounds is known, the actual number of protons can be calculated through S (or step height).

Analysis of spectrum

Using the three aspects mentioned above, especially the relationship between δ and J and its molecular structure, the spectrum of ^{1}HNMR can be analyzed. The following constitutes the general procedure for spectral analysis: ① calculate the ratio of the hydrogen atoms in different groups according to the relative area of each peak signal; ② calculate the single peak first through δ, followed by coupling peak; ③ using other experimental techniques further define the structure. For example, the addition of deuterium oxide can determine the location of hydrogen.

For some complex spectra, it is difficult to determine the molecular structure only by relying on ^{1}HNMR, and meanwhile, they need mutual cooperation with other analytical tools.

Further, a more common and convenient method is to compare the unknown sample with the standard pattern of known compounds to determine the unknown sample.

8.11.3 Carbon-13 NMR spectroscopy

^{13}CNMR is very useful in studying the carbon backbone structure and carbon affiliation.

Compared with ^{1}HNMR, ^{13}CNMR has lower sensitivity because the gyromagnetic ratio of ^{13}C is only 1/4 of the ^{1}H, and the natural isotopic abundance of ^{13}C is only about 1.1%, making the sensitivity of ^{13}C NMR only 1/6000 of the proton spectra. In addition, the chemical shift range of ^{13}CNMR is about 300 ppm, 20 times higher than that of ^{1}HNMR, with a higher resolution. Further, ^{13}CNMR can directly determine molecular skeleton and obtain information such as C=O, C≡N and quaternary carbon atoms that cannot be detected in ^{1}HNMR spectra.

Similar to hydrogen spectrum, carbon spectrum can also determine the structure of the compounds by the intensity of the absorption peak, peak position, peak spin-spin splitting and coupling constants. However, because of the decoupling technique, the peak area is affected, which is different from the hydrogen spectrum in that the carbon peak area cannot be accurately determined by carbon number, while the most important factor is the chemical shift.

In the carbon spectrum, the chemical shift of each group is broadly consistent with the sequence of the hydrogen spectrum. Figure 8.26 is a syndiotactic PS of ^{13}CNMR spectrum [10].
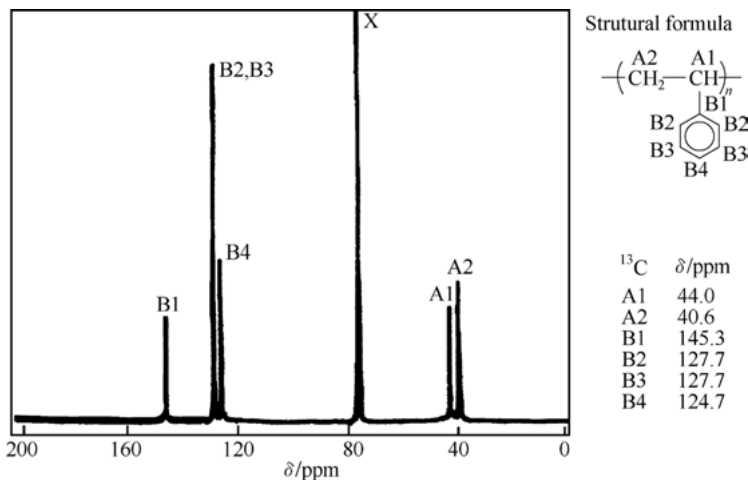
Figure 8.26: PS (syndiotactic) ^{11}C NMR spectrum [10].

8.11.4 NMR spectra determination

Sample should be of sufficient purity, and solid samples must match the solution (except solid NMR). The sample solution is generally 0.4 ml (10% concentration), with 1%~2% TMS as the internal standard. For liquid samples with low viscosity, NMR can be measured directly.

A 4 mm sample tube is commonly used; if the sample volume is very small, a 0.025 ml microtube can be adopted. The solvent should be free of protons with a low boiling point, should not react with the sample, and should have sufficient solubility to the sample. Some commonly used solvents include D_2O, $CDCl_3$ and CD_3SOCD_3. Non-solvents are also used such as CCl_4 and CS_2.

8.11.5 Solid-state nuclear magnetic resonance

For information about the function of ssNMR in the flame retardation mechanism, please refer to literature [20].

Because the flame retardant system involves many materials (including combustion residues) that are generally insoluble in the solvent used in NMR measurement, we can only use ssNMR to measure its spectra. ssNMR is a powerful analytical technique especially to study the formation of IFR carbon layer along with its composition and structure, and can also determine the relationship between the chemical structure of the material and the time and temperature during combustion. For example, APP derivatives with boric acid (HBO_3) for epoxy resin coating, that thermal degradation mechanism have been researched through [11]BssNMR and [31]PssNMR. Figure 8.27 is a

spectrum [27] of ^{11}BssNMR when the mixture of single HBO$_3$ and APP/HBO$_3$ was heated to 450 °C. Similar patterns can be observed for boron oxide and phosphate. On comparing the four lines we can see that heating APP/HBO$_3$ to 450 °C generates boron phosphate, with an NMR peak of δ = −30 ppm. Figure 8.28 is an atlas of ^{31}PssNMR measured when APP/HBO$_3$ at different temperatures is compared with boron phosphate [27]. Boron phosphate showed strong peaks of B-O-P bond in δ = −30 ppm in the spectra of APP/HBO$_3$, at temperature under 95 °C or 150 °C, there is no peak at δ = −30 ppm, implying that at this point there is no formation of boron phosphate; whereas for spectra at 300 °C and 450 °C, in the peak of δ = −30 ppm is very strong, but the other peaks are weak. This implies that the phosphorus in APP has been converted into boron phosphate. Therefore, when APP/HBO$_3$ is used for coating epoxy resin, because of the presence of boron phosphate, the char layer displays high mechanical strength and excellent heat resistance, as well as good adhesion to the substrate and flame retardancy.
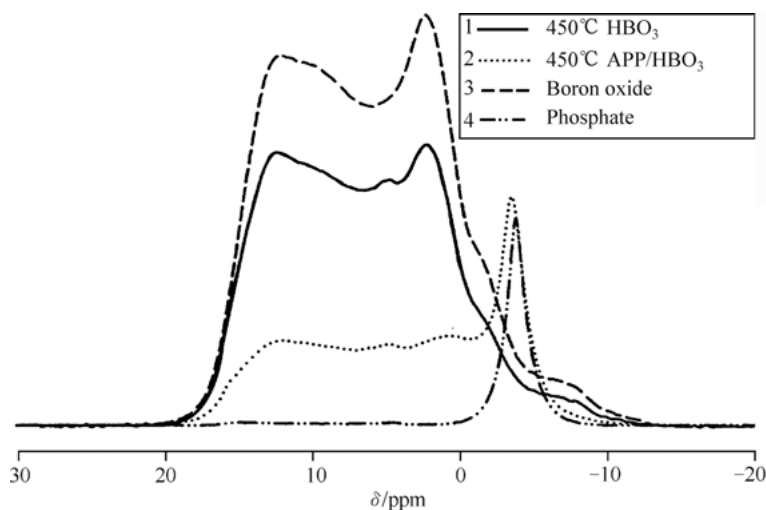
Figure 8.27: ^{11}B ss NMR spectrums [20, 27]. 1 – HBO$_3$ under 450 °C; 2 – APP/HBO$_3$ under 450 °C; 3 – Boron oxide; 4 – Borophosphate.

^{1}H ssNMR can also be used to investigate the structure of the char layer. Because the char layer generated during combustion is heterogeneous containing different areas of mobility, we can obtain relevant information through molecular kinetics studies. For example, we found that for the APP/PER system applied for polyolefins, with or without molecular sieve, self-spinning, namely relaxing time of network (t1), and rule of alteration differs vastly at different heat treatment temperatures (HTT) (Figure 8.29).
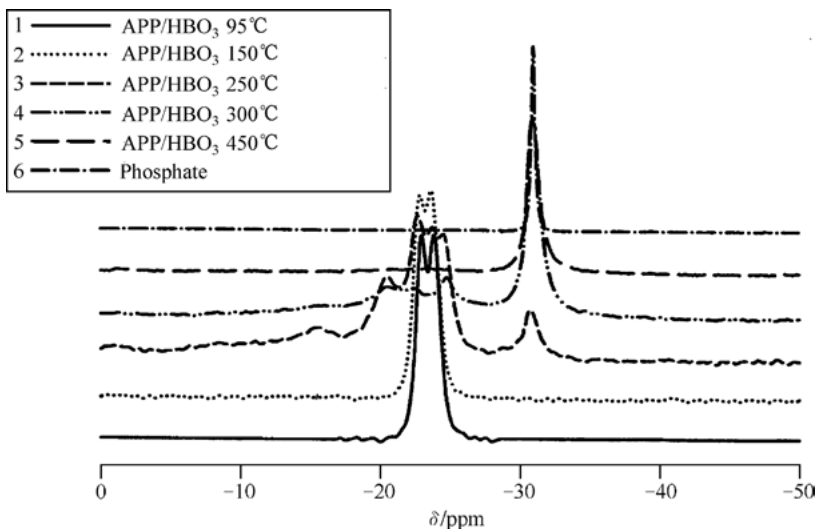
Figure 8.28: [11]P ssNMR atlas [20, 27]. 1 – APP/HBO$_3$ sub-zero 95 °C; 2-APP/HBO$_3$ sub-zero 150 °C; 3 – APP/HBO$_3$ sub-zero 250 °C;4 – APP/HBO$_3$ sub-zero 300 °C; 5 – APP/HBO$_3$ sub-zero 450; 6 – Borophosphate.
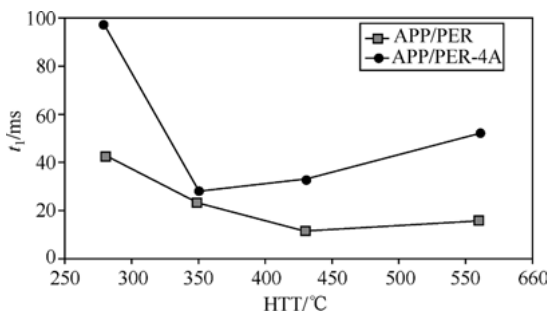
Figure 8.29: Relationship between t_1 values of PO/APP/PER along with PO/APP/PER/4A and HTT [20].

Figure 8.29 shows that curves of relations of the two abovementioned systems are different. The t_1 value in APP/PER/4A system, with its HTT at 280 °C, is double than that in APP/PER system, possibly because different structures are formed at this temperature. Low value of t1 shows that the molecular motion of matter is blocked, causing a rigid structure. When HTT in the range of 280 °C to 350 °C, T1 value in the two systems increase as the HTT decreases, but drops more in the system with 4A; at 350 °C, T1 values of the two systems are almost the same. This is because the two systems mainly contain stacked polycyclic aromatic compounds at high temperature, and hence have a similar structure. However, at higher

temperatures, the t_1 value of a system containing 4A always exceeds that of a system without 4A. The carbonization processes of these two IFRs are different; a molecular sieve is helpful in molecular motion, making the carbon layer more mobile. Comparing APP/PER/4A with APP/PER, the temperature at which the former can maintain the mobility of the carbon layer is higher than that of the latter, which is convenient for the former to form a char layer with better flame retardant properties. It is not easy for them to generate and propagate cracks, and they are more able to withstand stress.

8.12 Mass spectrometry

On exposure to strong current, organic molecules in vacuum can generate molecular ions (isotope ions) and various fragment ions in chemical bond fracture. On separating these ions, recording their quality and strength and arranging them by mass ratios, a mass spectrogram (MS) can be obtained, which can be applied to analyze the composition and structure of the materials. This method is termed mass spectrometry.

MS instrument is widely applied because of its high sensitivity (up to 50 μg), high analysis efficiency (multicomponent detection at the same time), and small sample requirement in the range of micrograms (solid, liquid and gas can be used as samples).

Mass spectrometer mainly consists of vacuum system, inlet system, ion source, analyzer and detector and recorder.

The key technique of MS is the ionization of the sample. There are many ionization techniques such as electron impact ionization (EI), electrospray ionization (ESI) and matrix-assisted laser desorption/ionization (MALDI), which have been developed in recent years. The combination of MALDI-TOF mass spectrometry and MALDI-TOF-MS can be applied without any standard sample; this technique was able to accurately determine the molecular weight of the polymer, structural units, end group, molecular weight distribution, etc. The principle is shown in Figure 8.30 [9].

Resolution is an important parameter of MS instrument to characterize the separation degree between the two adjacent peaks. When the peak of the two intersecting adjacent peaks comprises 10% of the peak height, it can be considered that these two peaks are separated. Mass of low-resolution ion peaks can only be integers, whereas mass of high resolution can be as accurate as upto four digits after the decimal point.

MS results can be shown as spectra or tables. When expressed as spectra, abscissa is mass ratio (m/e) and ordinate is ionic strength (mainly relative abundance). Figure 8.30 shows the MS spectra of PMMA [11]. As Figure 8.31 is scanned from the point of m/e = 33, it does not display the fragment peak of m/e = 31.
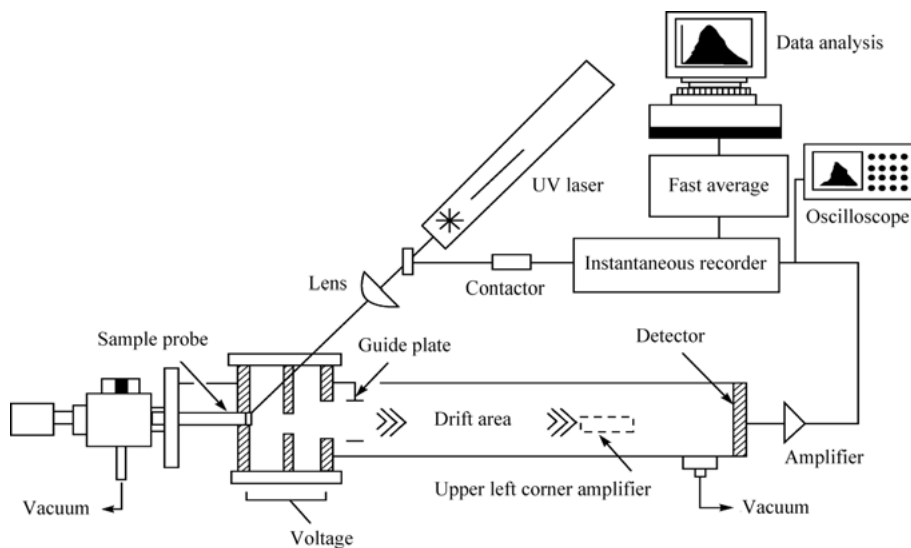
Figure 8.30: Working principle diagram of MALDI-TOF-MS instrument [9].
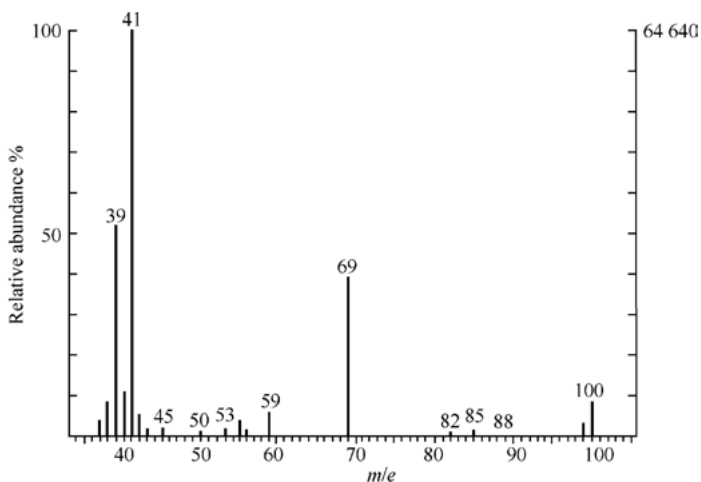
Figure 8.31: MS spectra of PMMA [11].

The most important MS spectra information is the relative molecular mass of the compound (the molecular ion peak in the spectra). The peak must be for the ion with the highest m/e and odd number electronics, and the ion that can generate significant fragment ions is not the only method. There are other reliable methods to identify the molecular ion peak (such as the nitrogen rule, and mass difference between the adjacent peaks) with evidence. If the molecular ion peak cannot

detected or its intensity is too low, the experimental technique can be changed (such as lower the energy of bombarding electron, increase the amount of samples) to improve the results.

MS spectra can be used to determine the molecular weight and composition of the compounds, identify the substituent group of compounds, propose the structure formula of compounds (with the help of other spectra), as well as study the degradation mechanism of compounds.

GC-MS is a powerful technique for the separation and identification of organic compounds. However, for polymers, its first better to conduct pyrolysis, followed by separation using GC and dissociation using MS, and finally, identification can be achieved by analyzing the fragment ions.

8.13 Chromatography

8.13.1 Principles

Chromatography is a physical-chemical separation method, with sample separation carried out in the stationary and the mobile phase.

Samples enter into the stationary phase with the mobile phase. Because of the different differentiating characteristics of each group, their interactions with the stationary phase are also different, thus the two phases (the stationary and the mobile phase) have different roles. When the component achieves a balanced level, the concentration of the component in the stationary phase and the mobile phase is named as the partition coefficient K. When components with different k-values are repeatedly allocated between the two phases, separation occurs (Figure 8.32) [10].

Figure 8.32: Schematic of chromatographic separation [10].

During measurement, with different concentrations (or mass) in the sample out-flow, the detection systems can be transformed into electrical signals, giving a chro-matogram, as shown in Figure 8.33 (for the physical meaning of gas chromatography see Section 8.13.4) [10].

Figure 8.33: Gas chromatography.

Abscissa of chromatogram analysis is mobile phase flow volume, and ordinate is detector response signal, which is a representation of sample post outflowing con-centrations (mass). Outflow component provides a response signal as a differential curve called a chromatogram.

Chromatogram analysis can be carried out using the following three aspects: ① The position of chromatographic peaks, which relates to the components of the molecular structure, is based primarily on qualitative analysis, and reflects the thermodynamic process of chromatography. ② The size and shape of chro-matographic peaks, which represents the level of each component in the sample, based primarily on quantitative analysis, and reflecting the kinetics process of chromatography. ③ Chromatographic separation, which shows whether sample components can be separated

8.13.2 Thin-layer chromatography

Thin-layer chromatography (TLC) analysis separates material chromatography on a glass board dotted with the stationary phase. In other words, after placing the sample on one side of the glass board and inserting it into a certain kind of solvent (devel-oper), each component will migrate for a particular distance along the fixed phase, giving Rf values. Rf is the base of TLC qualitative identification (Figure 8.34) [29].

After dropping samples on TLC plates and placing into different solvents types, the samples can be identified by accurately determining the location of the sample

(a) Tilt up the law to start   (b) Down method to start
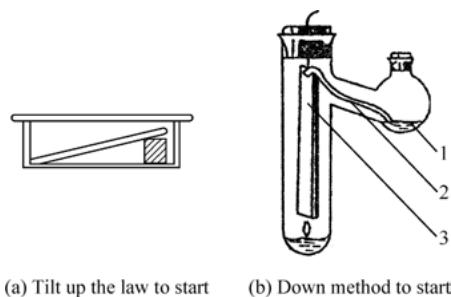
Figure 8.34: TLC schematic diagram [29] 1 – Solvent; 2 – The filter paper strip; 3 – Thin layer plate.

dots. If the sample has two or more Rf values, the sample can be confirmed as a mixture or as impure.

TLC is a quick method which can simultaneously analyze multiple samples within a few minutes without sophisticated devices.

TLC is normally only used for qualitative identification, but it can also make precise quantitative analysis, if required, with the help of sample replication equipment and ultraviolet detectors that quantitatively analyze the sample dots.

The disadvantage of TLC is that the number of theoretical plates is less than the precise chromatograph with a very low resolution, hence compounds with similar Rf values cannot undergo efficient separation

The choice of TLC solvent mainly depends on the chemical structure of the sample, with two or more kinds of solvents chosen sometimes.

Chromogenic technology such as ultraviolet light and chemical reactions can locate points on the TLC plate quickly. The commonly used ultraviolet color-developing method involves applying certain ultraviolet wavelengths to irradiate thin-layer plates, which can be applied to color lots of plastic additives. Iodine, potassium iodoplatinate and 2,6-Dichloroquinone-4-chloroimide spraying chromogenic agents can also be used to react with samples to generate specific color points for locating the sample's position on the thin-layer plate, as well as calculating the Rf value.

8.13.3 High-performance liquid chromatography

High-performance liquid chromatography (HPLC) involves transferring the sample solution into a chromatographic column filled with a fixed phase. Because of the different affinity and partition coefficients of the sample components in the mobile and stationary phase, the samples are separated.

HPLC device is relatively complex, expensive and often requires professionals to operate and maintain.

HPLC conditions

For HPLC, appropriate stationary phase and eluent (mobile phase) should be chosen. For reversed-phase chromatography, non-polar stationary phase and polar solvent mobile phase are applicable. While for normal-phase chromatography, polar material should be chosen as the stationary phase and non-polar material should be chosen as the mobile phase. In addition, selection of the columns and mobile phase should be based on the chemical properties of the sample. Although normal-phase HPLC was more often used previously, reverse-phase HPLC has now become the preferred mode.

Most reversed-phase chromatography methods adopt gradient elution method, which demonstrates the polarity changes of the mobile phase as a function of time. This method has the advantage of increasing separation resolution to obtain relatively sharp peak, so that the measurement can be completed in a relatively short time.

Another important parameter of HPLC is the flow rate of the mobile phase. The flow rate of the eluent has a significant impact on the results of the separation. For example, for some components normal phase chromatography and constant current chromatography are hard to separate and can only be completely separated by using flow programing.

HPLC device

HPLC device consists of infusion system, sample injection system, chromatography column and detector (Figure 8.35) [29]. If using gradient elution method, infusion system must be capable of supplying two or more solvents. Maintaining the chromatographic column at a constant temperature can improve reproducibility. Short and thin connecting pipes minimize dead space and improve the resolution of chromatography. Moreover, reducing the particle diameter of the stuffing to 3 μm can improve the resolution of chromatography.
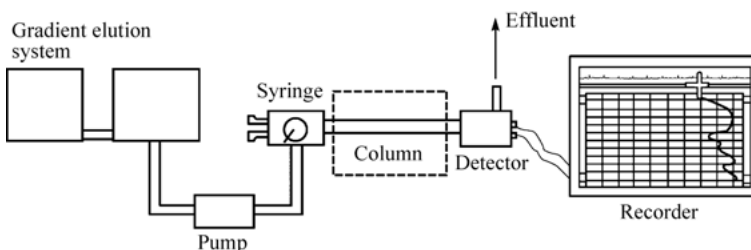

Figure 8.35: Schematic diagram of an HPLC system [29].

Detection technology

Ultraviolet detector is still the most suitable and often-used detection device for HPLC because many samples can absorb ultraviolet light. Even when the concentration is

as low as 1~10 mg/L, ultraviolet detector still functions well. Photodiode array detectors can also be used to detect ultraviolet/visible spectrum absorption peaks of the sample. In addition, refractive index and light scattering detector can be used to analyze molecules without employing a chromophore.

The HPLC analyzer presently used adopts external standard method for quantitative analysis. Without taking into account variables during extraction, the average analytical error is not more than 2%. The internal standard method can be adopted when more accurate results are needed.

8.13.4 Ordinary gas chromatography

Structures and separation conditions

HPLC or GC can be used to separate samples. GC is widely used because many samples are volatile and application of GC chromatographic column at high temperature is a well-known method. However, GC cannot identify each separated component and can only analyze vapor samples capable of gasification at certain temperatures. GC is efficient and quick, and because of the development of a hollow capillary column over the past few years, it can separate compounds containing dozens of or even hundreds of components within a short period of time, which remains unmatched by other separations methods.

Contrary to HPLC, GC employs gas as the mobile phase. Because there are no gradient infusion pumps and solvents, GC is simpler than HPLC. Moreover, the number of theoretical plates in a GC column is greater than that in HPLC, which results in better separation of samples.

Because GC only requires helium (or hydrogen) as a carrier gas to transfer the gasified samples to the detector, its cost is lower. Moreover, GC devices do not have moving parts and hence are durable.

GC consisting of flame ionization detector (FID), high efficiency capillary columns and solution concentration of 20 mg/L can be used for regular sample analysis. By adjusting the injection volume of the sample, the sensitivity of GC detection becomes superior to that of HPLC. FID is sensitive to almost all organic compounds, but other detectors can also be used in GC. Figure 8.36 is a schematic diagram of a GC system [26].

A limitation of GC is that after the introduction of volatile samples, the peak areas decline and even fade away. In addition, GC gives more peaks than HPLC, which makes their identification difficult. Further, the continuous use of chromatographic columns of GC results in loss of coating inside the columns and appearance of rising amount of active centers. Consequently, the speed of analysis reduces, even resulting in failure of chromatographic columns.

Similar to HPLC, because of the different polarities of coatings inside the chromatographic columns, the species that can be separated are also different. Nowadays,
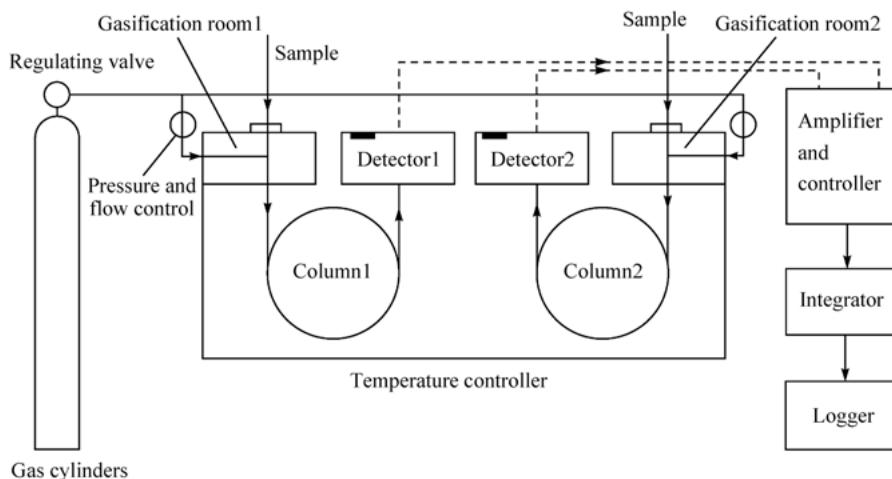
Figure 8.36: Schematic diagram of a GC system [26].

we are able to produce capillary chromatographic columns with extremely large number of theoretical plates and high resolution. At present, inner diameters of chromatographic columns produced are only 0.3 mm to 0.5 mm, and the thicknesses of their coatings are only 0.10 μm, which have considerably reduced the loss of chromatographic columns under high temperatures, thus, realizing the analysis from intermediate speed to high speed.

In general, GC is frequently used to analyze impurities of monomers and volatile substances of high polymers. It is also used to measure the changes in the concentration of raw materials and the amount of volatilized substances during polymerization reactions; in this manner, reaction kinetics can be studied.

Chromatogram analysis

In general, the following two parameters can be used to describe GC peaks: ① The peak height (h). The distance between the maximum to the bottom of the peak, shown as BE in Figure 8.33. ② Peak width (w). In Figure 8.33, peak width (w) refers to the distance between the two intersections (IK in Figure 8.33) formed by drawing tangents from two inflection points on both sides of the peak (F, G) and intersecting with peak base. Sometimes to facilitate measurement, it can also be shown by peak width at half height that is the width of half peak ($w_{1/2}$, JH in Figure 8.33). Peak height is an important parameter related to column efficiency and reflects the movements of components in chromatography columns. It is related to the diffusion of components in the gas phase and mass transfer of components in the stationary phase. Moreover, it is also influenced by chromatographic manipulation conditions.

The primary basis of quality analysis in GC is the retention value of components. When chromatographic conditions are invariant, retention value of the component is fixed. Therefore, the simplest and most reliable method is to compare with the retention values of known and unknown components at the same chromatographic conditions (including the amount of sample introduction). If the retention values are not consistent, the components are not the same; if the retention values are consistent, they are likely to be the same components. In addition, we can also contrast the quality analysis according to the retention value of components in the literatures, but this method is a necessary condition and not a sufficient one.

Another method is to use GC, MS and FTIR qualitative analysis. Such a method can not only bring into play their respective advantages but also complement their respective weaknesses, making the quantitative analysis more accurate.

GC used in quantitative analysis is accurate and convenient. Based on the chromatographic peak heights or areas, it determines the content of the test sample. However, because the same detector has different response values to different substances, when two components with the same amount are tested by the same detector, the signal strengths may vary. Therefore, we must introduce the relative response (s) or the correction factor (f) to correct the response values. There are several quantitative calculation methods such as normalization method, superposition method, internal standard method and external standard method. Each method has its own specific application conditions and special instrumental requirements. Hence, we can use different methods or a combination of methods based on different analysis objectives.

8.13.5 Other gas chromatography methods

Inverse gas chromatography

Inverse gas chromatography (IGC) is a method that uses high polymers as stationary phase and inert gases (with probe molecules) as mobile phase. It measures the distribution of probe molecules (volatile low molecules) in the two phases, thus determining the properties of high polymers, as well as the effects of the probe molecules and high polymers.

Any type of GC can be applied in IGC, with the packing and selecting probe molecules being the crucial point. There is only one peak in the spectrum of IGC. (Retention time t_R or retention volume V_R, generally is specific retention volume Vg). In general, IGC measures the changes of Vg with change in temperature (or flow); a retention graph can be drawn in accordance to lgVg to I/T (Figure 8.37) [30]. The straight line in the graph refers to low molecular weight compound and the zigzag line indicates high polymers. Therefore, some properties of polymers can be analyzed.
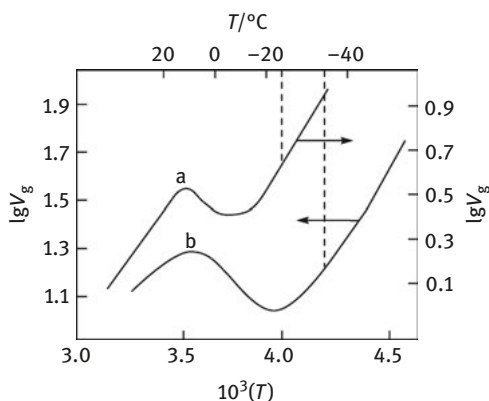
Figure 8.37: IGC retention graph of polyethylene [30] A – HDPE (probe molecule: n-pentane); b – LDPE (probe molecule:2-isopentane).

IGC can not only be used to determine the T_g, T_m and crystallinity of high polymers as well as the relative molecular weight of oligomer, it can also be applied to study the thermokinetics of high polymer solution and the surface property of the polymer.

Reaction gas chromatography

Reaction gas chromatography (RGC) refers to the decomposition of polymers into volatile products or generation of volatile products through reactions between specific compounds and functional groups on bonds. Following the decomposition, analysis of the products can be done by GC and some certain properties of the high polymers, such as the monomers distribution in the polymers chains. Some polymers which can be decomposed easily, such as polyester and polyamide, are suitable for GRC analysis.

Pyrolysis gas chromatography

Pyrolysis gas chromatography (PGC) refers to the pyrolysis of polymers into volatile macromolecular products. Subsequently, the composition, structure and properties of polymers can be determined by GC analysis. PGC, together with IR, NMR and MS, can accurately identify products after pyrolysis, and hence, is a prominent and widely used approach to study polymers.

PGC comprises a pyrolyzer, including tubular, filament or zonal, laser pyrolyzers, etc., to an ordinary GC at the place of sample introduction.

PGC can not only be used to identify polymers from the perspective of qualitative analysis and differentiate copolymers from blends, it can also be applied for the quantitative determination of copolymers (for example, the content of link structure, the tacticity, the assessment of relative molecular weight, and so on).

8.13.6 Gel permeation chromatography

Gel permeation chromatography (GPC), or column liquid solid chromatography, is a fast and effective way to determine the relative molecular weight and molecular weight distribution of polymers.

The classification of GPC is based on the volume exclusion principle, that is, the macromolecular chains in the polymers are first eluted in the mobile phase from the columns followed by medium and small molecules, and finally the smallest molecules of some additives in high polymers. In doing so, separation occurs and the spectra of GPC is achieved through the detector.

GPC instrument mainly comprises high pressure pump, sample injector, temperature controlling system, separation column (chromatographic column) and data processing device.

GPC samples should be pure, without any impurities and moisture, otherwise they interfere with the chromatographic peaks of the sample. The concentration of the test liquid is generally 0.05%~0.3% (no requirement of accurate determination). Filtration is required before entering the sample injector (some GPC instruments are equipped with an in-line filter).

The GPC spectra is a curve drawn by concentrations of various levels of high polymers to the corresponding maintained time (Figure 3.38) [30]. According to this curve and the calibration curve [Usually the standard sample PS (PS with dispersity of less than 1.05) are used to establish the calibration curve, but only for universal calibration], the relative molecular weight and the molecular weight distribution of the polymers can be calculated using formulas. Also through integral of chromatographic peak areas, GPC integral curve can be drawn to determine the total content when the sample reaches certain relative molecular weight.
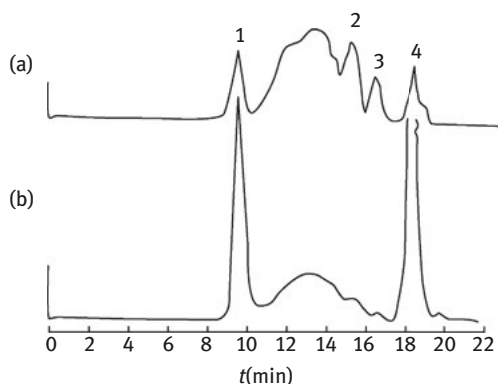

Figure 8.38: GPC curves of styrene butadiene rubber adhesive [30] (a) UV monitoring; (b) refractive index (RI) monitoring1 – High molecular weight resin; 2,3 – Additive; 4 – Solvent (tetrahydrofuran).

GPC is usually used for the determination of relative molecular weight and molecular weight distribution of polymer, detection of auxiliary (because its relative molecular weight is very small, it can be separated from the polymers in the GPC figure) and impurities, quantitative determination of multicomponent sample and preparation of high polymers with narrow molecular weight distribution. GPC can also be used to track polymerization reaction or study reaction kinetics according to changes of relative molecular weight of resultant or reactant in the reaction process.

8.14 Methods to determine the degree of intumescence and strength of char layers

It is very important to characterize and determine the characteristics of the char layer formed during combustion of materials in details because the char layer is closely linked with the flame retardant properties of the material. However, for flame retardancy, there is no comprehensive summary of methods used for determination of structure and properties of char layers. Moreover, there are many fundamental question that yet remain unanswered such as why some polymers carbonize while some do not, how to increase the amount of carbonization, how to improve the quality of char layers, what is the carbonization condition of polymer nanocomposites, etc. This is obviously related to the lack of appropriate measurement techniques.

Much of the technologies mentioned in this chapter can be used to determine the structure and composition of char layers. This section will describe the methods of the determination of the degrees of intumescence and strength of char layers [20]

8.14.1 The degree of intumescence

For the IFR system, the formation of char layer is an indispensable condition and the intumescence of char layer has an important effect on the flame-retardant properties. However, a high degree of intumescence does not necessarily imply excellent flame resistance, because the char layer structures (such as the size of the bubbles and its distribution) are also related to the thermal properties of the intumescent char layer [12, 31]. In some reports describing the methods of the determination of the degree of intumescence and its relationship with temperature, the device used is parallel-plate rheometer [20], where the samples can or cannot be loaded.

Figure 8.39 [20, 31] presents the relationship between the degree of intumescence and temperatures of four kinds of epoxy resin-based flame-retardant intumescent coatings (IF1, IF2, IF3 and IF8) and the same coatings without flame retardant properties. Boric acid and derivatives of APP are used as the two main flame
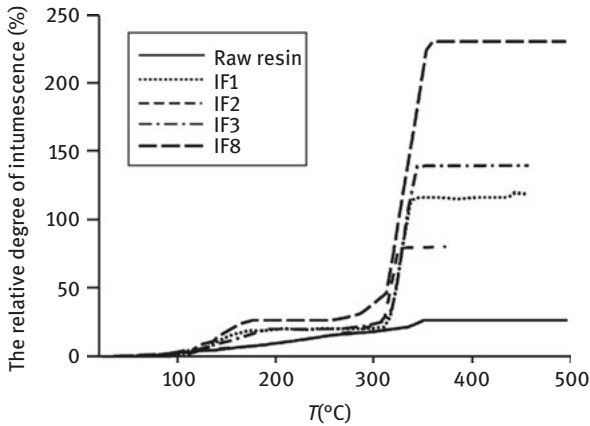
Figure 8.39: The degree of intumescence of four kinds of intumescent coatings at different temperatures tested by rheometer [20, 31].

retardants in the four kinds of fire-retardant coatings, where the latter contains 20% phosphorus.

Boric acid can be used as an intumescent agent, as it forms boron trioxide after dehydration, which contributes to the formation of glass intumescent layer and increases material viscosity, and delays gases into flames.

For non-flame-retardant coatings, there is almost no intumescence in high temperatures. Four kinds of flame-retardant coatings reaches the maximum intumescence at 300 °C~350 °C, which is because the capture of gases released from the degradation of resins and IFR in the materials.

Table 8.2 [31] reflects the relationship between the degree of intumescence of coating and their flame retardancy. The better the intumescent flame-retardant

Table 8.2: The flame retardant properties of the four types of intumescent flame-retardant coatings [31].

Sample		UL1709		
		Time of losing efficacy /min	Relative degree of intumescence	degree of intumescence measured by the rheometer /%
Non-flame-retardant coatings		5	0	26
Flame-retardant coatings	IF1	11.3	500	99
	IF2	18.2	550	116
	IF3	30	730	139
	IF4	38.1	1164	190

coating, the longer it lasts before it fails; thus, the one with the longest time of losing efficacy has the best protection effect.

The relative degree of intumescence of the UL1709 experiment in Table 8.2 is based on the sample's thickness ratio before and after the experiment.

According to previous studies [32], the degree of intumescence is measured using cone calorimeter by employing infrared photography instrument (through imaging analysis); the experimental apparatus shown in Figure 8.40 [32]. For epoxy-base resin intumescent flame-retardant coatings coated on the surface of the plate, when it is experimented in cone calorimeter (thermal 35 kWm^{-2}), the degree of intumescence of the coating is the largest.
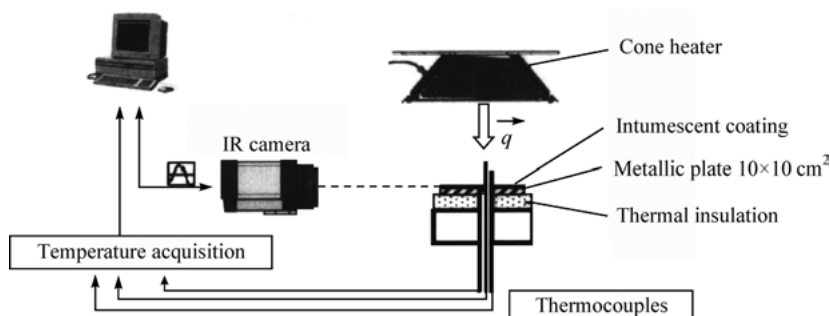

Figure 8.40: The experimental apparatus using infrared instrument that determines the degree of intumescence in cone calorimeter [32].

If the intumescence of materials is even, the degree of intumescence of IFR can be quantitatively determined using imaging and analysis under dynamic conditions.

For epoxy-based flame-retardant coatings on the surface of the plate, when experimented in cone calorimeter, the degree of intumescence increased rapidly at the initial stage (before 400 s), and then tended to be approximately stable during the subsequent relatively long time (400~800 s) [32]

For the epoxy-based intumescent flame-retardant coating coated on the surface of the plate, when its relationship between time and temperatures is measured in cone calorimeter (external heat flux 35 kW/m^2) using an electric thermocouple, the temperature under the bottom of the sample after 600 s is slightly above 2000 °C. However, the critical temperature of heated steel plates is generally about 500 °C. At the initial stage (before 200s), due to the unformed intumescence protection layer, temperature rises fast. While at the subsequent stage (200~400 °C), temperature rises relatively slowly. When temperature is within 400~800 °C, it nearly keeps invariable, at this moment, it has formed intumescence protection layer.

8.14.2 Intensity

The property of the char layer, especially for its intensity, is one of the major factors to affect the protection of carbon layer. When exposed to fire, the char layer will be under pressure from the inside and outside, and if it becomes fragile and cracked, or even collapsed, the fire resistance of the carbon layer will be damaged or lost. Thus, to measure the technique of the carbon layer's intensity is also a topic worthy of studying. [20]

Using rheometer is one of ways to measure the intensity of the char layer under pressure (Figure 8.41[31, 32]). The working principle is as follows: put the sample in the rheometer oven and heat it to the required temperature, thus, enabling expansion without interference. After intumescence, make the upper plate of the rheometer to come in contact with the sample and push the upper plate down directly to press the sample. The pressure needed to push the upper plate is changed with the space between the top plate and the bottom plate and the pressure varies directly with the distances between the two plates. Before the cracking of the char layer, the downward force of top plate depends on the intensity of a single bubble inside of the char layer. Once the carbon layer is cracked, the downward force increased dramatically, because the carbon layer is being pressed. [34]
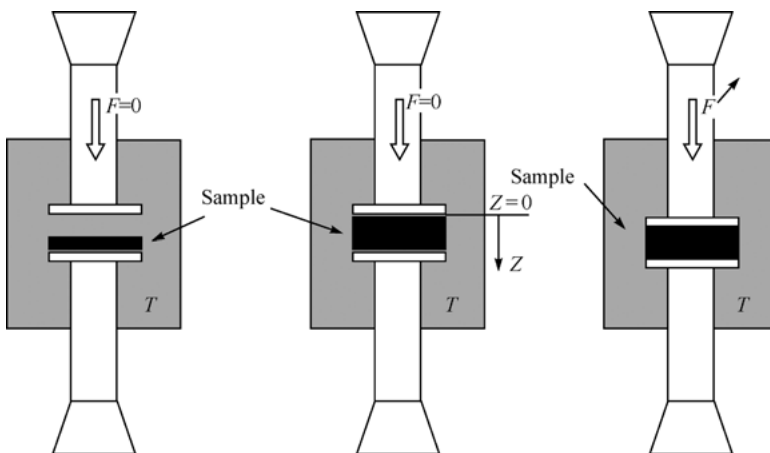

Figure 8.41: Schematic diagram of the determination of carbon layer intensity [31,32].

Adding spherical SiO_2 nanoparticles to polymers containing IFR (EVA/PA6/APP) does not change the intensity of the char layers, however, adding laminar organic-modified MMT and LDH can increase the intensity of the char layer. If the intensity of the char layer is higher, the probability of cracks will be lower, and the capacity of reducing heat transmission, mass transfer and flame retardance

of the carbon layer will be better. In addition, as discussed earlier, there are two endothermic peaks on a typical HRR curve of IFR-containing polymers. The first peak can be attributed to the formation of the intumescent protective carbon layer. The second peak corresponds to the thermal degradation of the intumescent carbon layer. If the intensity of the char layer is higher, the efficiency of flame retardancy is better, and the duration of second peak will be longer. For example, the duration of a polymer containing SiO_2 for the second peak is 300 s, while for a polymer containing MMT the second peak increases to 500 s. [20, 34]

References

[1]   Xiuwei Jia. Nanometer Flame-Retardant Materials [M]. Beijing: Chemical Industry Press, 2005: 161.

[2]   Yuxiang Ou, Tingjie Han , Li Jianjun.The Manual of Flame-Retardant Plastics [M]. Beijing: National Defence Industry Press, 2008: 726–727.

[3]   Yuxiang Ou, Jianjun Li . The Determination Methods of Flame-Retardantcy of Materials [M]. Beijing: Chemical Industry Press, 2007: 139–142.

[4]   Zhang Jun, Kuijiang Ji, Yanzhi Xia.The Combustion and Flame-Retardant Technoloy of Polymer [M]. Beijing: Chemical Industry Press, 2005: 431–438.

[5]   Gilman J W. Flame Retardant Mechanism of Polymer-Clay Nanocomposites [A]//Morgan A B, Wilkie C A. Flame Retardant Polymer Nanocomposites [M]. Hoboken: John Wiley & Sons, Inc., 2007: 67–87.

[6]   Szabo A, Marosfoi B B, Anna P, et al. Complex Micro-Analysis Assisted Design of Fire-Retardant Nanocomposites.Contribution to the Nanomechanism [A]//Hull T R, Kandola B K. Fire Retardancy of Polymers. New Strategies and Mechanisms[M]. Cambridge: The Royal Society of Chemistry, 2009: 74–91.

[7]   Haiyang,Yang, Pingping Zhu , He Pingsheng. High Polymer Physics Experiment [M].Hefei: Press of University of Science and Technology of China, 2008: 101, 144.

[8]   Xingying Zhang, Qifang,Li. Scientific Experiment of High Polymer (Second Edition)[M]. Beijing: Chemical Industry Press, 2007: 45, 46, 60, 68, 73.

[9]   Manjun He , Hongdong Zhang , Weixiao Chen, etc. High Polymer Physics (Third Edition)[M]. Shanghai: Fudan University Press, 2008: 291, 327, 334.

[10]   Jianjun Li, Xianbo Huang, Tongmin,Cai. Flame-Retardant Polystyrene Plastics[M]. Beijing: Science Press, 2003: 223, 224, 287, 293.

[11]   Yangrui, Zhouxiao, Luo Chuanqiu, ect. Modern Instrumental Analysis on Polymers (Third Edition)[M].Beijing: Tsinghua University Press, 2010: 40, 57, 167, 174, 187.

[12]   Duquesne S, Delobel R, Le Bras M, et al. A Comparative Study of the Mechanism of Action of Ammonium Polyphosphate and Expandable Graphite in Polyurethane [J]. Polymer Degradation and Stability, 2002, 77(2): 333–344.

[13]   Kashiwagi T, Harris Jr R H, Zhang X, et al. Flame Retardant Mechanism of Polyamide 6-Clay nanocompsites [J]. Polymer, 2004, 45(3): 881–891.

[14]   Gaan S, Sun G, Hutches K, et al. Flame Retardancy of Cellulosic Fabrics. Interactions Between Nitrogen Additives and Phosphorus-Containing Flame Retardants [A]//Hull T R, Kandola B K. Fire Retardancy of Polymers. New Strategies and Mechanisms [M]. Cambridge: The Royal Society of Chemistry, 2009.294–306.

[15] Duquesne S, Le Bras M, Jama C, et al. X-ray Photoelectron Spectroscopy Investigation of Fire Retarded Polymeric Materials. Application to the Study of an Intumescent System [J]. Polymer Degradation and Stablity, 2002, 77(2): 203–211.

[16] Thomas K M. The Release of Nitrogen Oxides During Char Combustion [J]. Fuel, 1997, 76(6): 457–473.

[17] Kodolov V I, Shuklin S G, Kuznetsov A P, et al.Formation and Invistygation of Epoxy Intumescenet Compositions Modified by Active Additives [J]. Journal of Applied Polymer Science, 2002, 85(7): 1477–1483.

[18] Wang Z, Han E, Ke W. Influence of Expandable Graphite on Fire Resistance and Water Resistance of Flame-Retardane Coatings [J]. Corrosion Science, 2007, 49(5): 2237–2253.

[19] Jincheng Feng. The Analysis and Identification of Organic Compounds Structures [M]. Beijing: National Defence Industry Press, 2003: 21.

[20] Duquesne S, Bourbigot S. Char Formation and Characterization [A]. Wilkie C A, Morgan A B. Fire Retardancy of Polymeric Materials. 2nd Edition[M]. Beca Raton: CRC Press, 2009: 239–299.

[21] Dresselhaus M S, Dresselhaus G, Saito R, et al. Raman Spectroscopy of Carbon Nanotubes [J]. Physics Reports, 2005, 409(2): 47–99.

[22] Reich S, Thomsen C. Raman Spectroscopy of Graphite [J]. Philosophical Transcations of the Royal Society A, Mathematical, Physical and Engineering Science, 2004, 362(1824): 2271–2288.

[23] Qu B. Xie R. Intumescent Char Structures and Flame-Retardant Mechanism of Expandable Graphite-Based Halogen-Free Flame-Retardant Linear Low Density Polyethylene Blends [J]. Polymer International, 2003, 52(9): 1415–1422.

[24] Anna P, Zimonyi E, Márton A, et al. Surface Treated Cellulose Fibres in Flame Retarded PP Composites [J]. Macromolecular Symposia, 2003, 202: 245–254.

[25] Marosi Gy, Márton A, Szép A, et al. Fire Retardancy Effect of Migration in Polypropylene Nanocomposites Induced by Modified Interlayer [J]. Polymer Degradation and Stability, 2003, 82(2): 379–385.

[26] Peirong Chen, Jinghong Li, Dengbo. The Experiment and Technology of Modern Instrumnets (Second Edition)[M].Beijing: Tsinghua University Press, 2011: 177, 233.

[27] Jimenez M, Duquesne S, Bourbigot S. Intumescent Fire Protective Coating.Toward a Better Understanding of Their Mechanism of Action [J]. Thermochimica Acta, 2006, 449 (1–2): 16–26.

[28] Yuxiang Ou, Jianjun Li. Flame Retardants [M]. Beijing: Chemical Industry Press, 2006: 450–451.

[29] Dong Yanming. The Practical Dissection Techniques of High Polymers [M]. Beijing: China Petrochemical Press 1997: 261, 264.

[30] Jimenez M, Duquesne S, Bourbigot S. Multiscale Experimental Approach for Developing High-Performance Intumescent Coatings [J]. Industrial and Engineering Chemistry Research, 2006, 45(13): 4500–4508.

[31] Boutbigot S, Duquesne S. Intumescence-Based Fire Retardants [A]//Wilkie C A, Morgan A B. Fire Retardancy of Polymeric Materials(2nd editon)[M]. Beca Raton: CRC Press, 2009: 129–162.

[32] Duquesne S, Lefebvre J, Bourbigot S, et al. Nanoparticles as Potential Synergists in Intumescent Systems [A]//Paper Presented at the ACS 228th Fall National Meeting, Division of Polymeric Materials, Science and Engineering Session----Fire and Materials [C]. Philadelphia: 2004.

Appendix

Appendix 1 Abbreviations and names of common polymers

Abbreviation	Name
ABS	Acrylonitrile-butadiene-styrene copolymer
ACS	Terpolymer of acrylonitrile-chlorinated polyethylene-styrene
ALK	alkyl resin
ASA	Acrylic-styrene-acrylonitrile copolymer
BA	Butadiene-acrylonitrile copolymer
BS	Butadiene-styrene copolymer
CA	Cellulose acetate
CAB	Cellulose acetate butyrate
CB	Cellulose butyrate
CN	Cellulose nitrate
COP	Copolyester
CP	Cellulose propionate
CPE	Chlorinated polyethylene
CPVC	Chlorinated polyvinyl chloride
CSPER	Chlorosulfonated polyethylene rubber
CTA	Cellulose triacetate
CTFE	Chlorotrifluoroethylene polymer
CV	Viscose rayon
EAA	Ethylene-acrylic acid copolymer
EBA	Ethylene-butyl acrylate copolymer
EC	Ethyl cellulose
EEA	Ethylene-ethyl acrylate copolymer
EMA	Ethylene-methyl acrylate copololymer
EMAA	Ethylene-methacrylic acid copolymer
EMAAI	Ethylene-methacrylic acid ionomer
EPDM	Ethylene propylene terpolymer rubber
EP, EPR	Epoxy resin
EPS	Expandable polystyrene
ETFE	Ethylene-tetrafluoroethylene copolymer
EVA	Ethylene-vinyl acetate copolymer
EVOH	Ethylene-vinyl alcohol copolymer

(continued)

(continued)

Abbreviation	Name
FEP	Fluorinated ethylene-propylene copolymer
FPUF	Flexible polyurethane foam
GPS	General purpose polystyrene
HDPE	High-density polyethylene
HMW-HDPE	High-molecular-weight high-density polyethylene
IBIP	Copolymer of isobutylene and isoprene
IR	Isoprene rubber
LCP	Liquid crystal polymer
LDPE	Low-density polyethylene
LLDPE	Linear low-density polyethylene
LPE	Linear polyethylene
MF, MFR	Melamine formaldehyde resin
MIPS	Medium-impact polystyrene
MOD	Modacrylic fiber
NBR	Acrylonitrile-butadiene rubber
NR	Natural rubber
PA	Polyamide
PAA	Polyarylamide
PAI	Polyamide-imide
PAN	Polyacrylonitrile
PAR	Polyarylate
PAS	Polyarylsulfone
PB	Polybutene or polybutylene
PBD	Polybutadiene
PBDR	Polybutadiene rubber
PBI	Polybenzimidazole
PBMA	Poly-n-butyl methacrylate
PBN	Polybutylene naphthalate
PBSF	Polybutene sulfone
PBT	Polybutylene terephthalate
PC	Polycarbonate
PCR	Polycholoroprene rubber
PDMS	Polydimethylsiloxane
PE	Polyethylene
PEEK	Polyether ether ketone

Abbreviation	Name
PEI	Polyetherimide
PEK	Polyetherketone
PES	Polyethersulfone
PET	Polyethylene terephthalate
PF, PFR	Phenol formaldehyde resin
PHB	Poly-*p*-hydroxy benzoic ester
PHSF	Polyhexene sulfone
PI	Polyimide
PIB	Polyisobutene
PMP	Poly(4-methylpentene-1)
PMS	Poly methylstyrene
PO	Polyolefin
POE	Polyethylene oxide
POM	Polyformaldehyde, polyoxymethylene
POP	Polypropylene oxide
POR	Phenoxy resin
PP	Polypropylene
PPE	Polyphenylene ether
PPO	Polyphenylene oxide
PPS	Polyphenylene sulfide
PPSF	Polypropene sulfone
PR	Phenolic resin
PS	Polystyrene
PSF, PSU	Polysulfone
PSI	Polysilicone
PTFE	Polyterafluoroethylene
PTHF	Polytetrahydrofuran
PU	Polyurethane
PUF	Polyurethane foam
PUR	Polyurethane rubber
PVA	Polyvinyl alcohol
PVAL	Polyvinylacetate
PVB	Polyvinylbutyral
PVC	Polyvinyl chloride
PVCA	Polyvinyl chloride-acetate

(continued)

Abbreviation	Name
PVDC	Polyvinylidene chloride
PVDF	Polyvinylidene fluoride
PVF	Polyvinyl fluoride
PVFO	Polyvinyl formal
PX	Poly-*p*-xylylene
RP	Reinforced plastics
RPUF	Rigid polyurethane foam
SAN	Copolymer of styrene-acrylonitrile
SANR	Styrene-acrylonitrile-resin
SBE	Styrene-butadiene elastomer
SBP	Styrene-butadiene copolymer
SBR	Styrene-butadiene rubber
SBS	Styrene-butadiene-styrene block copolymer
SI	Silicone
SIR	Silicone rubber
SMA	Styrene-maleic anhydride copolymer
SMMA	Styrene-methyl methacrylate copolymer
TEO	Thermoplastic elastomeric olefin
TFEVDF	Copolymer of tetrafluoroethylene-vinylidene fluoride
TFEP	Copolymer of tetrafluoroethylene and propylene
TPE	Thermoplastic elastomer
TPU	Thermoplastic polyurethane
UFR	Urea formaldehyde resin
UHMWPE	Ultrahigh-molecular-weight polyethylene
ULDPE	Ultralow-density polyethylene
UP, UPE	Unsaturated polyester
XLPE	Crosslinking polyethylene
XLPO	Crosslinking polyolefin

Appendix 2 Important terms of flame retardation

Actual calorific value	Fire hazard
Afterflame	Fire hazard assessment
Afterflame time	Fire hazard testing
Afterglow	Fire-induced environment
Afterglow time	Fire initiation
Area burning rate	Fire integrity
	Fire load
Burned area	Fire load density
Burned length	Fire model
Burning behavior	Fire parameter
Burning dripping	Fire performance
	Fire protection
Calorific potential	Fire resistance
Charring	Fire risk
Combustibility	Fire safety engineering
Combustibility class	Fire safety regulation
Combustion	Flame
Combustion characteristic	Flame combustion
Combustion product	Flame propagation
Combustion toxicity test	Flame retardancy
Critical radiant flux	Flame retardant
	Flame retardant chemical
Damaged area	Flame retarded
Damaged length	Flame spread
Deflagration	Flame spread rate
Dose-response and time-response relationship	Flame spread time
Dynamic method	Flameless combustion
	Flammability
Early fire hazard	Flash temperature
Ease of ignition	Flash temperature (flash point)
Evaluation of toxicity	Flash
	Flashover
Field model	Full-scale room test
Fire	Fully developed fire

(continued)

(continued)

Actual calorific value	Fire hazard
Fire behavior	Furniture fire model
Fire classification	
Fire danger	Glowing combustion
Fire effluent	Gross calorific value
Fire growth	
Heat emission	Self ignition
Heat release	Self propagation of flame
Heat release rate	Small-flame action
Heat transfer	Smoke
Heat of combustion	Smoke developing behavior
Horizontal burning	Smoke generation
	Smoke obscuration
Incandescence	Smoke production
Ignitable	Smoke production rate
Ignition	Smoke release
Ignition source	Smoke toxicity
Ignition temperature	Smouldering
Ignition time	Soot
Laboratory-scale test (bench test)	Specific extinction area (SEA)
Large (full)-scale test (real-scale test)	Specific optical density
Light absorbance	Spontaneous combustibility
Light transmission	Spontaneous ignition temperature
Liner burning rate	Static method
Low combustibility	Surface combustion
	Surface flashover
Mass burning rate	Surface spread of flame
Minimum ignition time	
Modeling fire growth	Thermal decomposition
	Thermal degradation
Non-combustibility	Thermal insulation
Optical density of smoke	Time-temperature curve standardized
Oxygen consumption combustion heat	Time to ignition (TTI)
Pyrolysis	Total heat release
Radiant flux	
Radiation	Vertical burning

Actual calorific value	**Fire hazard**
Reaction to fire	
Secondary effects of fire	Zone model
Self heating	